Development of a Livestock Odour Dispersion Model

A Thesis Submitted to the College of

Graduate Studies and Research

in Partial Fulfillment of the Requirements

for the Degree of Philosophy

in the Division of Environmental Engineering

University of Saskatchewan

Saskatoon

By

Zimu Yu

PERMISSION TO USE

In presenting this thesis in partial fulfillment of the requirements for a Postgraduate degree from the University of Saskatchewan, I agree that the Libraries of the University may make it freely available for inspection. I further agree that permission for copying of this thesis in any manner, in whole or in part, for scholarly purposes may be granted by the professors who supervised my thesis work or, in their absence, by the Head of the Department or the Dean of the College in which my thesis work was completed. It is understood that any copying or publication of use of this thesis or parts thereof for financial gain shall not be allowed without my written permission. It is also understood that due recognition shall be given to me and to the University of Saskatchewan in any scholarly use which may be made of any material in my thesis.

Requests for permission to copy or to make any other use of the material in this thesis in whole or in part should be addressed to:

Chair of the Division of Environmental Engineering

University of Saskatchewan

Saskatoon, Saskatchewan, S7N 5A9, Canada

ACKNOWLEDGEMENTS

First of all, I would like to thank my supervisors, Dr. Huiqing Guo and Dr. Claude Laguë, for their invaluable mentoring and encouragement. Without their constant guidance and encouragement, I would never have completed my thesis. I would like to express my appreciation to my advisory committee chairs, Dr. Yen-Han Lin, Dr. Charles Maule, Dr. Ian Fleming, and the committee members, Dr. Qiang Zhang, Dr. Bernardo Predicala and Dr. Oon- Doo Baik for their valuable assistance and guidance and for their precious time on my Ph.D program.

I would like to acknowledge College of Graduate Studies and Research, University of Saskatchewan and Natural Sciences and Engineering Research Council (NSERC) of Canada for funding this research. I would also like to thank the Division of Environmental Engineering, Department of Agricultural and Bioresource Engineering for providing great assistance. My gratitude and acknowledgement go to University of Manitoba and University of Minnesota for providing field odour plume measurement data. Many thanks are given to Dr. Xue Li, Yanan Xing, and Dr. Yongxin Li for their help both in my study and life.

Finally, I would like to thank my family and friends for their support. Special thanks are given to Zhaoqin Li, my wife, for her encouragement and unconditional support.

ABSTRACT

Livestock odour has been an obstacle for the development of livestock industry. Air dispersion models have been applied to predict odour concentrations downwind from the livestock operations. However, most of the air dispersion models were designed for industry pollutants and can only predict hourly average concentrations of pollutants. Currently, a livestock odour dispersion model that can consider the difference between livestock odour and traditional air pollutants and can account for the short time fluctuations is not available. Therefore, the objective of this research was to develop a dispersion model that is designed specifically for livestock odour and is able to consider the short time odour concentration fluctuations.

A livestock odour dispersion model (LODM) was developed based on Gaussian fluctuating plume theory to account for odour instantaneous fluctuations. The model has the capability to predict mean odour concentration, instantaneous odour concentration, peak odour concentration and the frequency of odour concentration that is equal to or above a certain level with the input of hourly routine meteorological data.

LODM predicts odour frequency by a weighted odour exceeding half width method. A simple and effective method is created to estimate the odour frequency from multiple sources. Both Pasquill-Gifford and Hogstrŏm dispersion coefficients are applied in this model. The atmospheric condition is characterized by some derived parameters including friction velocity, sensible heat flux, M-O length, and mixing height. An advanced method adapted from AERMOD model is applied to derive these parameters. An easy to use procedure is generated and utilized to deal with the typical meteorological data input as ISC met file.

LODM accepts and only requires routine meteorological data. It has the ability to process individual or multiple sources which could be elevated point sources, ground level sources, livestock buildings, manure storages, and manure land applications. It can also deal with constant and varied emission rates. Moreover, the model considers the relationships between odour intensity and odour concentrations in the model. Finally, the model is very easy to use with a friendly interface.

Model evaluations and validations against field plume measurement data and ISCST3 and CALPUFF models indicate that LODM can achieve fairly good odour concentration and odour frequency predictions. The sensitivity analyses demonstrate a medium sensitivity of LODM to the controllable odour source parameters, such as stack height, diameter, exit velocity, exit temperature, and emission rate. This shows that the model has a great potential for application on resolving odour issues from livestock operations. From that perspective, the most effective way to reduce odour problems from livestock buildings is to lessen the odour emission rate (e.g. biofiltration of exhaust air, diet changes).

TABLE OF CONTENTS

PERMISSION TO USE i
ACKNOWLEDGEMENTS ii
ABSTRACT iii
LIST OF FIGURES ix
LIST OF TABLES xiii
LIST OF ABBREVIATIONS xv
LIST OF SYMBOLS xvi
Chapter 1. INTRODUCTION 1
1.1 Literature Review 2
1.1.1 Livestock Odour and Its Measurement 2
1.1.2 Livestock Odour Sources and Emission Rates 6
1.1.3 Odour Plume Measurement 9
1.2 Odour Dispersion Modeling 11
1.2.1 Gaussian Plume Model 11
1.2.2 Puff Model 15
1.2.3 Meandering/Fluctuating Model 18
1.2.4 Other Models 21
1.3 Adapting and Validating Odour Dispersion Models – Some Issues 22
1.3.1 Scaling Factors 23
1.3.2 Peak to Mean Ratio 24
1.3.3 Relationship between Odour Concentration and Intensity 25
1.4 Research Gaps in Odour Dispersion Modeling 30
1.5 Summary 33
1.6 Objectives 34
1.7 Contributions to Knowledge 35
Chapter 2. MODEL THEORIES AND METHODS 36
2.1 Mean Odour Concentration 36
2.2 Gaussian Fluctuating Plume Model 37
2.2.1 Instantaneous Odour Concentrations 39
2.2.2 Odour Frequency 40

2.2.3 Peak Odour Concentration 43
2.3 Stack-tip Downwash and Plume Rise 44
2.4 Dispersion Coefficients 44
2.4.1 Pasquill-Gifford Mean Dispersion Coefficients 44
2.4.2 Pasquill-Gifford Short Time Dispersion Coefficients 45
2.4.3 Hogstrŏm Dispersion Coefficients 46
2.5 Parameters Used to Characterize PBL 47
2.5.1 Surface Energy Budget and Net Radiation 47
2.5.2 Identification of CBL or SBL 48
2.5.3 Parameters Derived for CBL 49
2.5.4 Parameters Derived for SBL 50
2.6 Vertical Wind Speed Profile 51
2.6.1 P-G Scheme 51
2.6.2 Hogstrŏm Scheme 52
2.7 Vertical Gradient of Potential Temperature 52
2.8 Treatment of ISC Met File 53
2.9 Adapting the Model for Livestock Odour Dispersion 56
2.9.1 Odour Emission from Elevated Stack 56
2.9.2 Odour Emission from Animal Building 56
2.9.3 Odour Emission from Manure Storage 57
2.9.4 Multiple Sources 57
2.9.5 Persistence of Different Odours 60
2.10 Case Study 61
2.10.1 Derived Parameters and Profiles of Wind Speed and Potential Temperature Gradient 61
2.10.2 Effective Plume Height and Hogstrŏm Stability 66
2.10.3 Dispersion Coefficients 69
2.10.4 Hogstrŏm Dispersion Coefficients from Ground Release 78
2.10.5 Odour Concentration and Frequency from an Elevated Point Source 79
2.10.6 Multiple Sources 89

2.10.7 Odour Concentration and Odour Frequency from an Area Source and an Building Source 90
2.10.8 Summary of Case Study 95
2.11 Summary 95
Chapter 3. MODEL DEVELOPMENT PROCEDURE AND MODEL INTRODUCTION 97
3.1 Model Development Procedures 97
3.2 Downwind and Crosswind Distance 101
3.3 Model Introduction 102
3.3.1 Main Interface 102
3.3.2 "File" Menu 103
3.3.3 "Edit" Menu 104
Chapter 4. MODEL EVALUATION AND VALIDATION 117
4.1 Data from University of Manitoba 117
4.1.1 Site Description and Odour Emission Rates 117
4.1.2 Downwind Odour Plume Measurement 118
4.1.3 Model Configuration 119
4.1.4 Relationship between Odour Intensity and Concentration 120
4.1.5 Comparison between LODM and ISCST3 and CALPUFF 120
4.1.6 Comparisons between LODM Predictions and Field Measurements 123
4.2 Data from University of Minnesota 127
4.2.1 Site Description and Odour Emission Rates 127
4.2.2 Downwind Odour Plume Measurement 128
4.2.3 Relationship between Odour Concentration and Odour Intensity 129
4.2.4 Comparisons between LODM Predictions and Field Measurements 129
4.3 Discussions 130
4.4 Conclusions 131
Chapter 5. SENSITIVITY ANALYSIS 133
5.1 Source Parameters 135
5.1.1 Stack Height 135
5.1.2 Stack Diameter 137

5.1.3 Exit Velocity 139
5.1.4 Exit Temperature 141
5.1.5 Emission Rate 143
5.2 Meteorological Parameters 145
5.2.1 Wind Speed 145
5.2.2 Stability class 149
5.2.3 Wind Direction 151
5.2.4 Ambient Temperature 153
5.2.5 Mixing Height 155
5.2.6 Radiation 156
5.2.7 Cloud Cover 156
5.3 Surface Roughness, Albedo, and Bowen Ratio 157
5.4 Discussion and Conclusion 158
Chapter 6. SUMMARIES AND CONCLUSIONS 161
6.1 The Model Theory, Assumption, and Function 161
6.2 The Model Evaluation and Validation 162
6.3 The Model Sensitivity Analysis 163
6.4 Application of the Model 163
6.5 Advantages and Disadvantages of the Model 163
6.6 Future Direction 165
REFERENCE 166
APPENDIX A: STACK-TIP DOWNWASH AND PLUME RISE 181
APPENDIX B: HOGSTRŐM DISPERSION COEFFICIENTS 185
APPENDIX C: SOLAR ELEVATION ANGLE 190

LIST OF FIGURES

Figure 1.1 Relationships between odour intensities and odour concentrations of swine odour from different researchers (0-8 scale and 0-5 scale)..... 29
Figure 1.2 Relationships between odour intensities and odour concentrations of swine odour from different researchers (0-8 scale and 0-6 scale)..... 30
Figure 2.1 (a) Areal view of Gaussian plume model; (b) areal view of fluctuating plume model; (c) standard deviations of crosswind distances in the fluctuating plume model (adapted from Mussio et al., 2001). 39
Figure 2.2 Schematic diagrams of cross sections of the odour exceeding part of the instantaneous plume at different heights (h_i) and the associated instantaneous odour exceeding half width (y_i) (adapted from Bree and Harssema,1988) 41
Figure 2.3 Schematic diagrams of the portion of time for the different odour exceeding widths (a) and the odour frequency (b)..... 43
Figure 2.4 Wind profile for each stability class at height less than $7z_0$ (Hereafter, SC(1), SC(2)…SC(6) refer to stability class A, stability class B… stability class F.) 64
Figure 2.5 Wind profile for each stability class at height greater than $7z_0$..... 64
Figure 2.6 Potential temperature gradient profile for each stability class at height less than 100 m..... 65
Figure 2.7 Potential temperature gradient profile for each stability class at height greater than 100 m..... 66
Figure 2.8 Plume height with downwind distance for stability class E..... 67
Figure 2.9 Plume height with downwind distance for stability class F 67
Figure 2.10 Hogstrŏm stability (s) and the plume height (PH) at different downwind distance for stability class E and F..... 69
Figure 2.11 Pasquill-Gifford mean horizontal dispersion parameters for different stability classes..... 69
Figure 2.12 Pasquill-Gifford mean vertical dispersion parameters for different stability classes..... 70
Figure 2.13 Pasquill-Gifford short time horizontal dispersion parameters for different stability classes..... 70
Figure 2.14 Pasquill-Gifford short time vertical dispersion parameters for different stability classes..... 71
Figure 2.15 Hogstrŏm mean horizontal dispersion parameters for different stability classes..... 71
Figure 2.16 Hogstrŏm mean vertical dispersion parameters for different stability classes 72
Figure 2.17 Hogstrŏm short time horizontal dispersion parameters for different stability classes..... 72

Figure 2.18 Hogstrŏm short time vertical dispersion parameters for different stability classes..... 73
Figure 2.19 Hogstrŏm mean and short time dispersion parameters for stability class D . 74
Figure 2.20 Comparisons of mean dispersion coefficients between P-G method and Hogstrŏm method for stability class A 75
Figure 2.21 Comparisons of mean dispersion coefficients between P-G method and Hogstrŏm method for stability class B..... 75
Figure 2.22 Comparisons of mean dispersion coefficients between P-G method and Hogstrŏm method for stability class C..... 76
Figure 2.23 Comparisons of mean dispersion coefficients between P-G method and Hogstrŏm method for stability class D 76
Figure 2.24 Comparisons of mean dispersion coefficients between P-G method and Hogstrŏm method for stability class E..... 77
Figure 2.25 Comparisons of mean dispersion coefficients between P-G method and Hogstrŏm method for stability class F 77
Figure 2.26 The instantaneous odour concentrations, computed mean odour concentration and modeled odour concentration for stability class D at a receptor 1 km downwind of a point source 80
Figure 2.27 Layout of 231 downwind receptors (each symbol represents a receptor with a height of 1.5 m)..... 85
Figure 2.28 Odour plume predicted by the model from an elevated point source for unstable condition 85
Figure 2.29 Odour plume predicted by the model from an elevated point source for neutral condition 85
Figure 2.30 Odour plume predicted by the model from an elevated point source for stable condition..... 86
Figure 2.31 Odour frequency predicted by the model from an elevated point source for unstable condition 86
Figure 2.32 Odour frequency predicted by the model from an elevated point source for neutral condition 86
Figure 2.33 Odour frequency predicted by the model from an elevated point source for stable condition 87
Figure 2.34 Modeled mean odour concentrations and peak concentrations for the example point source..... 88
Figure 2.35 Peak to mean ratios with downwind distances from ground level release 89
Figure 2.36 Plot of computed odour frequencies and modeled odour frequencies 90
Figure 2.37 Layout of an area source and a volume source..... 91
Figure 2.38 Centerline mean odour concentrations from two sources 91
Figure 2.39 Centerline odour frequencies from two sources..... 92

Figure 2.40 Mean odour concentration plume from two sources at unstable condition... 93
Figure 2.41 Mean odour concentration plume from two sources at neutral condition..... 93
Figure 2.42 Mean odour concentration plume from two sources at stable condition..... 93
Figure 2.43 Mean odour frequencies from two sources at unstable condition (SC = C).. 94
Figure 2.44 Mean odour frequencies from two sources at neutral condition (SC = D).... 94
Figure 2.45 Mean odour frequencies from two sources at stable condition (SC = E)..... 95
Figure 3.1 Schematic procedure of calculating mean odour concentration by LODM.... 98
Figure 3.2 Schematic procedure of calculating instantaneous odour concentration by LODM 99
Figure 3.3 Schematic procedure of calculating peak odour concentration by LODM ... 100
Figure 3.4 Schematic procedure of calculating odour frequency by LODM 101
Figure 3.5 Schematic of calculating downwind and crosswind distance..... 102
Figure 3.6 Main interface of LODM..... 103
Figure 3.7 File menu of LODM..... 104
Figure 3.8 Edit menu of LODM 105
Figure 3.9 Simulation window of LODM..... 106
Figure 3.10 Format of input meteorological data file 106
Figure 3.11 Point source window of LODM 107
Figure 3.12 Variable emission rate window of LODM 108
Figure 3.13 Area source window of LODM..... 109
Figure 3.14 Schematic of the treatment of an area source..... 110
Figure 3.15 Volume source window of LODM..... 111
Figure 3.16 Gridded receptors of LODM 112
Figure 3.17 Discrete receptors of LODM..... 113
Figure 3.18 Surface parameters of LODM 114
Figure 3.19 Model output window of LODM 115
Figure 3.20 Intensity window of LODM..... 116
Figure 4.1 Comparisons of the predicted mean odour concentrations by LODM (P-G) and ISTSC3 models 121
Figure 4.2 Comparisons of the predicted mean odour concentrations by LODM (P-G) and CALPUFF models..... 122
Figure 4.3 Comparisons of the predicted mean odour concentrations by LODM (Hogstrŏm) and ISTSC3 models..... 122
Figure 4.4 Comparisons of the predicted mean odour concentrations by LODM (Hogstrŏm) and CALPUFF models 123
Figure 4.5 Fractial bias (FB) for LODM predicted odour intensities and measured odour intensities 125
Figure 4.6 Comparisons of the model predicted frequencies and observed odour frequencies 130
Figure 5.1 Centerline odour concentrations for different stack heights (SH)..... 136

Figure 5.2 Centerline odour frequencies for different stack heights (SH)..... 136
Figure 5.3 Centerline odour concentrations for different stack diameters (SD)..... 138
Figure 5.4 Centerline odour frequencies for different stack diameters (SD)..... 138
Figure 5.5 Centerline odour concentrations for different exit velocities (EV)..... 140
Figure 5.6 Centerline odour frequencies for different exit velocities (EV)..... 140
Figure 5.7 Centerline odour concentrations for different exit temperatures (ET)..... 142
Figure 5.8 Centerline odour frequency for different exit temperatures (ET) 142
Figure 5.9 Centerline odour Concentrations for different emission rates (ER)..... 144
Figure 5.10 Centerline odour frequencies for different emission rates (ER)..... 144
Figure 5.11 Centerline odour concentrations for different wind speeds (Ws) under unstable conditions (SC = C) 146
Figure 5.12 Centerline odour frequencies for different wind speeds (Ws) under unstable conditions (SC=C)..... 146
Figure 5.13 Centerline odour concentrations for different wind speeds (Ws) under neutral conditions (SC = D) 147
Figure 5.14 Centerline odour frequencies for different wind speeds (Ws) under neutral conditions (SC = D) 147
Figure 5.15 Centerline odour concentrations for different wind speeds (Ws) under stable conditions (SC= E)..... 148
Figure 5.16 Centerline odour frequencies for different wind speeds (Ws) under stable conditions (SC = E)..... 148
Figure 5.17 Centerline odour concentrations for different stability classes (SC)..... 150
Figure 5.18 Centerline odour frequencies for different stability classes (SC)..... 150
Figure 5.19 “Centerline” odour concentrations for different wind directions (WD)..... 152
Figure 5.20 “Centerline” odour frequencies for different wind directions (WD)..... 152
Figure 5.21 Centerline odour concentrations with different ambient temperatures (AT) 154
Figure 5.22 Centerline odour frequencies with different ambient temperatures (AT) ... 154

LIST OF TABLES

Table 1.1 Odour intensity referencing scale 5
Table 1.2 Constants in weber-Fechner models and odour scales used by different researchers 29
Table 2.1 Parameters to determine wind speed profile with P-G stability class 51
Table 2.2 Key to the Pasquill stability categories (USEPA, 2000) 54
Table 2.3 Key to SRDT method for estimating P-G stability categories (US EPA, 2000) 54
Table 2.4 Representative solar radiation or cloud cover values for different P-G stability class 55
Table 2.5 Parameters derived for CBL 62
Table 2.6 Parameters derived for SBL 62
Table 2.7 P-G stability class, conditions, wind speeds and M-O length by Hanna et al. (1996) 63
Table 2.8 Hogstrŏm stability(s) and the plume height (PH) at different downwind distance for stability class E and F 68
Table 2.9 Hogstrŏm mean and short time vertical dispersion parameters for different heights for unstable condition (SC = C) 78
Table 2.10 Hogstrŏm mean and short time vertical dispersion parameters for different heights for stable condition (SC = E) 79
Table 2.11 Modeled and computed mean odour concentration and odour frequency for different P-G stability classes at a receptor 1 km downwind of a point source 81
Table 2.12 Modeled mean odour concentrations and odour frequencies for ground level point release without plume rise at a receptor 1 km downwind of a point source 81
Table 2.13 Mean odour concentration and odour frequency ranges for unstable P-G stability class at a receptor 1 km downwind of a point source 83
Table 2.14 Mean odour concentration and odour frequency ranges for stable P-G stability class at a receptor 1 km downwind of a point source 84
Table 2.15 Peak to mean ratios at different downwind distances 88
Table 2.16 Odour frequencies from computed and modeled methods 89
Table 4.1 Odour emission rates of the farms (Zhang et al., 2005) 118
Table 4.2 Comparisons in odour concentrations between LODM and ISCST3 and CALPUFF 123
Table 4.3 Agreements between predicted mean odour intensities and measured mean intensities using equation (1.16) 124
Table 4.4 Agreements between predicted mean odour intensities and measured mean intensities using equation (1.17) 124

Table 4.5 FAC2, Ran0.2, and Ran0.1 of the model predicted odour frequency with observed odour frequency 127
Table 4.6 Measured odour emission rates for different farms in Minnesota 128
Table 4.7 FAC2, Ran0.2 and Ran0.1 values of the model predicted odour frequency with observed odour frequency 130
Table 5.1 Sensitivity analysis of odour concentration and frequency to stack height with a control value of 10 m 137
Table 5.2 Sensitivity analysis of odour concentration and frequency to stack diameter with a control value of 3 m 139
Table 5.3 Sensitivity analysis of odour concentration and frequency to exit velocity with a control value of 3 m s^{-1} 141
Table 5.4 Sensitivity analysis of odour concentration and frequency to exit temperature with a control value of 300 k 143
Table 5.5 Sensitivity analysis of odour concentration and frequency to emission rate with a control value of 5E5 OU s^{-1} 145
Table 5.6 Sensitivity analysis of odour concentration and frequency to wind speed with a control value of 4 m s^{-1} 149
Table 5.7 Sensitivity analysis of odour concentration and frequency to stability class . 151
Table 5.8 Sensitivity analysis of odour concentration and frequency to wind direction with a control value of 90° 153
Table 5.9 Sensitivity analysis of odour concentration and frequency to ambient temperature with a control value of 20 ℃ 155
Table 5.10 Sensitivity analysis of odour concentration and frequency to mixing height with a control value of 1000 m 155
Table 5.11 Sensitivity analysis of odour concentration and frequency to cloud cover with a control value of 0.5 in SBL (Stable Boundary Layer) 157
Table 5.12 Sensitivity analysis of odour concentration and frequency to surface roughness with a control value of 0.1 m 158

LIST OF ABBREVIATIONS

ADMS	**A**tmospheric **D**ispersion **M**odelling **S**ystem
AERMOD	**A**MS/**E**PA **R**egulatory **MOD**el
AODM	**A**ustrian **O**dour **D**ispersion **M**odel
AREMET	**A**MS/EPA **R**egulatory **MET**eorological preprocessor
AT	**A**mbient **T**emperature
AUSPLUM	**AUS**tralian **PLUM**e dispersion model
CBL	**C**onvective **B**oundary **L**ayer
CFD	**C**omputational **F**luid **D**ynamics
EMS	**E**arthen **M**anure **S**torage
ET	**E**xit **T**emperature
EV	**E**xit **V**elocity
FB	**F**ractional **B**ias
INPUFF	Gaussian **IN**tegrated **PUFF** model
ISC	**I**ndustrial **S**ource **C**omplex
LODM	**L**ivestock **O**dour **D**ispersion **M**odel
MAE	**M**ean **A**bsolute **E**rror
M-O	**M**onin-**O**bukhov
OC	**O**dour **C**oncentration
ODODIS	**ODO**ur **DIS**persion software
OU	**O**dour **U**nit
PBL	**P**lanet **B**oundary **L**ayer
PH	**P**lume **H**eight
P-G	**P**asqiull-**G**ifford
RMSE	**R**oot-**M**ean-**S**quare **E**rror
SBL	**S**table **B**oundary **L**ayer
SC	**S**tability **C**lass
SD	**S**tack **D**iameter
ST	**S**tack **H**eight
WS	**W**ind **S**peed

LIST OF SYMBOLS

FR	Air flow rate of the exhaust air, $m^3\ s^{-1}$
OB	Average of the observed values
PR	Average of the predicted values
$\bar{u}$	Average wind speed, $m\ s^{-1}$
R_0	Clear sky radiation, $W\ m^{-2}$
n	Cloud cover
K_{w1}, K_{w2}	Constants of Weber-Fechner law
y_i	Crosswind distance from the center of the fluctuating plume to the receptors, m
σ_{yi}, σ_{zi}	Dispersion coefficients referring to the i^{th} strip of the area source, m
$\sigma_x, \sigma_y, \sigma_z$	Dispersion parameters in the three orthogonal directions, m
C	Downwind concentration, $g\ m^{-3}$ or $OU\ m^{-3}$
x, y, z	Downwind receptor location, m
H_e	Effective emission height, m
OU_E	European odour unit
y_0	Fluctuating plume half width when the height of the plume is zero, m
θ_*	Friction temperature, k
u_*	Friction velocity, $m\ s^{-1}$
H	Height of a building, m
s	Hogstrŏm stability parameter
C_i	Incoming supply air odour concentration, , $OU\ m^{-3}$
σ_{y0}, σ_{z0}	Initial lateral and vertical dimensions of a volume source, m
Q_{ip}	Instantaneous point source emission rate, g
t_m, t_p	Integration time, s
λE	Latent heat flux, $W\ m^{-2}$
h_i	Local plume height, m

y_c , h_i	Locations of the center of the instantaneous plume (horizontal and vertical), m
C_m	Mean concentration, OU m^{-3}
z_i	Mixing height, m
L_{mo}	Monin-Obukhov length, m
R_n	Net radiation, W m^{-2}
$\Phi(x, y, z)$	Normalized concentration
WDO	Observation of wind direction (WDO) which is the direction wind is blowing from
ODC_b	Odour concentration of n-butanol at its detection threshold, ppb
ODT	Odour detection threshold (ratio) of the sample, ppb
C_o	Odour concentration of the exhaust air, OU m^{-3}
ER	Odour emission rate, OU s^{-1}
I	Odour intensity
C_p	Peak concentration, OU m^{-3}
R_p	Peak to mean ratio
$p(x)$	Probability of x
T_{ref}	Reference air temperature, K
z_{ref}	Reference height, m
S_{av}	Sensitivity index
G	soil heat flux, W m^{-2}
φ	Solar elevation angle, rad
$\boldsymbol{\varphi_t}$	Solar elevation angle, rad, at transition point between CBL and SBL
R	Solar radiation, W m^{-2}
Q	Source emission rate, g s^{-1} or OU s^{-1}
R^2	Square of correlation coefficient
σ_{SB}	Stefan Boltzmann constant (5.67 $\times 10^{-8}$ W m^{-2} K^{-4})
H_s	Surface heat flux, W m^{-2}
z_0	Surface roughness, m

FAC2	The percentage of the predictions within a factor of 2 of the observed values
Ran0.1	The percentage of the predictions within the range of ±0.1 of the observed values.
Ran0.2	The percentage of the predictions within the range of ±0.2 of the observed values
P_i	The portion of time that the local plume height h_i confined to a given interval, $h_i \in \left[h_i - \frac{\Delta h}{2}, h_i + \frac{\Delta h}{2} \right]$
P_0	The portion of time that the local plume height h on ground level
$\sigma, \sigma_p, \sigma_c$	The standard deviations and the subscript p denotes instantaneous or short term-averaged plume and c denotes the meandering component, m
$\mathrm{u_{ref}}$	The wind speed at reference height, m s^{-1}
k	van Karman constant (0.4)
$\frac{\partial \theta}{\partial z}$	Vertical gradient of potential temperature, k m^{-1}
V	Vertical term of Gaussian plume model equation
x_y, x_z	Visual lateral and vertical distance, m
$\bar{y}$	Weighted odour exceeding half width
X , Y	Width and length of the areal source, m
W	Width of a building, m
WD	Wind direction which is the direction to which wind is blowing
u_f	Wind speed at the top of friction layer, m s^{-1}

Chapter 1. INTRODUCTION

Livestock farming is increasingly confronted with questions of environmental protection because of different kinds of airborne pollutants emitted into the atmosphere. One of them is odour because the acceptance of livestock farming in the neibourghhood can decrease due to an increase in odour sensation (Martin and Schauberger, 1999). Leonardos (1996) reported that over 60% of the air pollution complaints to regulators were related to odours. In USA, about 70% of all complaints on air quality concerned odour (Watts and Sweeten, 1995). In UK, about 25% of all 3700 complaints received by the Environmental Health officers were about odours from farms in the years 1989 and 1990 (Skinner et al., 1997). It was reported in 1998 in Thüringen, Germany that 16% of all complaints in the year 1996 were odour related, 34% of these stemmed from agricultural sources (Schauberger et al., 2001). Schauberger et al., (2001) pointed out that the complaints caused by farms dominated with 89% compared to 11% by slurry spreading; however, Choinière et al. (2007) concluded that more than half of all complaints about intensive livestock facilities directly result from odour emissions following land application of manure. In addition, exposure to livestock odours is a potential health concern (Schiffman and Williams, 2005). Therefore, the diffusion of odours from livestock operations can be a very contentious issue between producers and neighbouring landowners and residents. With the increase of the size of livestock industry, the odour nuisance has become more and more important to livestock farm owners, their neighboring communities, and the government.

A number of approaches can be taken in order to avoid odour nuisance near the livestock operations. Setback distances are often specified as parts of local legislation or guidelines (Curran et al., 2002). These requirements are not always easy to achieve, particularly in which livestock operating units have existed. Another strategy is to assess the odour impact using field measurements by trained panellists (van Langenhove and van Broeck, 2001). This method is time consuming and expensive so that it cannot be implemented easily to account for a wide variety of local meteorological conditions.

Since the 1980's, researchers have been using industrial air dispersion models to predict livestock odours downwind from livestock operations, so as to determine where odour nuisance is likely to occur in the vicinity of livestock production facilities. However, most of models were originally designed for air contaminants from industrial sources and a number of studies have indicated that they cannot be directly used for livestock odour dispersion predictions (Zhu et al., 2000a; Guo et al., 2001; Zhang et al., 2005). Sources of industrial contaminants and of livestock odours usually differ in terms of source type, emitting height, emitting temperature, etc. In addition, contrary to air contaminants emitted by industrial sources, livestock odours are a complex and dynamic mixture of more than 300 compounds within which chemical or biological reactions may occur during its atmospheric transport (Schiffman et al., 2001). Odour is also measured differently compared to other air contaminants. Odour concentration, which is expressed in detection threshold with a unit of Odour Unit (OU or OU m^{-3}), is measured using an olfactometer and human panelists. Field odour plume can only be measured for odour intensity using human sniffers (Li et al., 1994; Hartung and Jungbluth, 1997; Zhu et al., 2000a; Guo et al., 2001; Zhang et al., 2005). Furthermore, most of the industrial air dispersion models calculate hourly average concentration, whereas a series of short detectable exposures to odours can cause nuisances and generate community complaints even though the long term (hourly) averaged concentration is lower than the detection level. Therefore, adapting industrial air dispersion models for odour dispersion and/or the necessity of developing an improved odour dispersion model need to be carefully evaluated.

1.1 LITERATURE REVIEW

1.1.1 Livestock Odour and Its Measurement

Livestock Odour

Odour is the human olfactory response to many discrete odorous gases (Sweeten et al., 2001). Odours from livestock operations are results of many different compounds and of their interactions; many of these compounds are present at very low concentrations. Schiffman et al. (2001) have identified a total of 321 different odorous compounds in

livestock buildings. The odorous compounds of livestock odour include ammonia (NH_3), amines, hydrogen sulphide (H_2S), volatile fatty acids, indoles, skatoles, phenols, mercaptans, alcohols, carbonyls, p−cresol and volatile carboxylic acids (Curtis, 1983; Yu et al., 1991; Zahn et al., 1997; Schiffman et al., 2001). The concentrations of some major compounds (H_2S, NH_3, volatile organic compounds (VOCs)) of livestock odour have been measured and large variations have been observed among different studies. The average H_2S concentrations measured in swine facilities were less than 2 ppm (Donham and Popendorf, 1985; Schiffman et al., 2001; Wang, 2007; Sun et al., 2008), although the peak concentrations were up to 100 ppm during agitation of manure and up to 220 ppm in the exhaust air from the pit fan of a deep-pit swine facility (Patni and Clarke, 1991). Koerkamp et al. (1998) reported average ammonia concentrations in cattle housing, swine housing, and poultry buildings to be less than 8 ppm, 5-18 ppm, and 5- 30 ppm, respectively. Donham and Popendorf (1985) measured higher mean NH_3 concentration of 34 ppm in 21 randomly selected swine producing farms in Iowa. Sun et al (2008) measured year-round NH_3 concentrations between 5 ppm and 32 ppm from two mechanically ventilated swine growing/finishing rooms. Wang (2007) reported NH_3 concentrations varying from 5 ppm to 26 ppm from swine nursery, farrowing and gestation rooms. The concentrations of VOCs in swine buildings ranged from 0.62 to 11.72 mg m^{-3} (Hartung and Phillips, 1994; Schiffman et al., 2001) and were much higher (up to 108.7 mg m^{-3}) in the case of emissions from slurry storages (Hobbs et al., 1997; Zahn et al., 1997).

Although the concentrations of many individual compounds responsible for livestock odours are below the standardized odour detection thresholds, the intensity of the total mixture may be very strong. Schiffman et al. (2001) pointed out that the intensity of odorous emission results not only from detectable individual compounds, but also from the aggregate effect of numerous odorous chemicals with concentration below detection threshold. It was also found that the concentrations of the most common specific odorous gases, such as hydrogen sulfide and ammonia, were not correlated well to livestock odour concentration (Spoelstra, 1980; Pain and Misselbrook, 1990; Jacobson et al., 1997; Zahn et al., 1997; Guo et al., 2000; Wang, 2007; Sun et al., 2008). Therefore, no individual

compound can be used to quantify the livestock odour intensity, rather, the overall odour strength or odour intensity of the air emitted from livestock facilities has to be measured.

Odour Characteristics and Measurements

There are various techniques for measuring and describing odour. Odour can be characterized by five attributes: concentration, intensity, persistence, hedonic tone and character descriptor (ASHRAE, 2005). Among the five, concentration and intensity are the most widely accepted and used characteristics.

Detection threshold and recognition threshold are usually measured to represent odour concentration. They are measured by an olfactometer (a dilution apparatus to dilute the odorous air sample by fresh air) and a panel of trained odour assessors and usually reported as odour units (OU). Odour unit for detection threshold or recognition threshold is defined as the dilution ratio of the odorous air sample by fresh air that must be achieved so that 50% of an odour panel can detect or recognize the odour after dilution (CEN, 2003). The geometric means of the panellists' individual detection or recognition threshold are taken as the detection or recognition threshold for the sample odour. If not specifically pointed out, the detection threshold is usually used as the odour concentration in most odour research such as air quality and odour emission and dispersion. The odour unit stated here is the same as European odour unit which is defined in terms of N-butanol (AWME EE-6, 2002). The European odour unit is calculated by the following equation:

$$OU_E = (ODT \cdot ODC_b) / 40\,ppb \quad (1.1)$$

In which, OU_E is European odour units; ODT is odour detection threshold (ratio) of the sample; ODC_b is odour concentration of n-butanol at its detection threshold, ppb; and 40 ppb is the "definition" of 1 OU_E in terms of n-butanol.

Another unit, OU m^{-3}, which will be discussed in section 1.1.2, is also widely used by odour researchers due to its consistency with mass concentration unit, g m^{-3}.

Odour intensity describes the strength of an odour sample. It is measured at concentrations above the detection threshold. Intensity changes with odour concentration.

It can be measured against a reference scale of n-butanol, a standard reference chemical (ASTM, 1998). Different n-butanol scales, i.e., various concentrations of n-butanol solutions in water that result in certain n-butanol concentrations in the head space of the container, each gives a certain level in odour strength, have been used by researchers. Guo et al. (2001) and Jacobson et al. (2000, 2005) used a 5-point scale, while Zhang et al. (2003, 2005) and Feddes (2006) used an 8-point scale. The comparison of these two scales is presented in Table 1.1. For the same n-butanol concentration in water, the intensity interpretation was different. For example, 240 ppm n-butanol in water was considered a little annoying on the 8-point referencing scale, while it was considered very faint when using the 5-point scale; therefore, the 5-point scale yields higher odour concentration (25 OU m^{-3}) than the 8-point scale (2 or 6 OU m^{-3}). This resulted in the different relationships between odour concentration and intensity that will be discussed later in this chapter.

Table 1.1 Odour intensity referencing scale

Odour Scale	Odour intensity	Odour Strength	n-butanol in water (ppm)	Odour concentration (OU m^{-3})	
				by Zhang et al. (2005)	by Feddes (2006)
0 to 8	0	No odour	0	0	1
	1	Not annoying	120	1	3
	2	A little annoying	240	2	6
	3	A little annoying	480	8	12
	4	Annoying	960	28	26
	5	Annoying	1940	101	57
	6	Very annoying	3880	365	123
	7	Very annoying	7750	1327	267
	8	Extremely annoying	15500	4824	580
0 to 5				By Guo et al. (2001)	
	0	No odour	0	0	
	1	Very faint	250	25	
	2	Faint	750	72	
	3	Moderate	2250	212	
	4	Strong	6750	624	
	5	Very strong	20250	1834	

Persistence indicates how easily the full-strength odorous air is diluted to below the detection threshold. It is the slope of the line representing the relationship between odour intensity and odour concentration on a log-log scale (ASHRAE, 2005). Hedonic tone describes the unpleasantness or pleasantness of an odour (ASCE, 1995; ASHRAE, 2005). It is typically rated using a scale that ranges from -10 (extremely unpleasant) to +10 (extremely pleasant) indicating unpleasant to pleasant. Character descriptors are used to describe the character of the odour (ASHRAE, 2005), for example, the odour smells like roses or rotten eggs. For livestock odour, character descriptors can be used by the panellists to identify different odour sources as indicated by such as swine manure odour or odour from cattle. Character descriptors are used when the samples' concentrations are at or above the recognition threshold concentration.

1.1.2 Livestock Odour Sources and Emission Rates

Odour emissions from animal production sites originate from three primary sources: manure storage unit, animal housing, and land application of manure (Zhang et al., 2005). Most odorous gases from livestock operations are by-products of the anaerobic microbial decomposition/transformation of livestock wastes including manure, spilled feed, bedding materials, wash water, and other wastes. Moisture content and temperature affect the rate of microbial decomposition. Microbial growth rates roughly double with each 10°C increase in temperature until the optimum temperature is reached (Metcalf and Eddy, 1991). Also, with increasing temperatures, the pollutants are more volatile and tend to transfer to the gas phase rather than remaining in the liquid phase. Hence, the odour production from these different odour sources varies diurnally and seasonally with the changing indoor and outdoor climatic conditions and animal conditions. Odour concentration inside the production building is of particular interest to researchers as it constitutes an important air quality parameter for both the workers and the animals present (Sun et al., 2008).

The physical factors of livestock odour sources that have direct impacts on odour dispersion including height of the emitting sources, temperature of the contaminated air, stack diameter, and exit velocity of the emission, were different from the industrial

sources. The exhaust air emitting height is at or lower than the ground level for outdoor earthen manure storages while for above ground concrete or steel storages that the emitting height can be up to 5 m above ground. In the case of animal buildings, exhaust air is vented through openings on the walls and roofs of the building. The emitting height for wall-mounted fans can be in the order of 1 to 2 m while it can increase to 6 m for ridge vents and ceiling-mounted fans. There are often a number of vertical or horizontal openings or fans for one building. For manure storages, the exhaust air temperature is the same as or closes to the ambient air temperature. In winter, when the manure storage is frozen, there will be no odour emission provided that the fresh manure is added to the storage facility under the ice cover and not on top of it. For livestock buildings, depending on the housing system, the exhaust air is typically kept at the required temperature range for animals during the winter, which may be as low as 0^{o}C for dairy and as high as 32^{o}C for young chicks. During summer, the temperature of the exhaust air will normally be 2 to 4^{o}C higher than ambient temperature (Guo et al., 2006b, 2007; Sun et al., 2008). Manure storage is often treated as an area source with very small exit velocity. Due to the complex structures of the openings and fans of livestock building, it is very difficult to consider individual stack diameter and exit velocity of the odour emission from a livestock building. Thus, it is can be treated as single or multiple point sources or area sources and very small exit velocity is assumed (Xing et al., 2006).

Odour emission rate from a livestock source measures the size of the air pollution source for the surrounding area and can be used in odour impact evaluation. As an essential input to an odour dispersion model, it is also important for the study and application of the odour dispersion model as well as the determination of setback distances. For a building source, odour emission rate is the product of the odour concentration of the exhaust air and ventilation rate of the building, if the incoming supply air odour concentration is neglected. For manure storages or land applied with manure, a wind tunnel or ventilated chamber with a certain air flow rate can be used to measure odour emission rate from the surface; and the odour emission rate is calculated as the product of the odour concentration of the exhaust air from this device and the air flow rate of the device (Pain et al., 1988; Ormerod, 1990; Pain and Misselbrook, 1990). If the supply air odour concentration is not negligible, the difference of the exhaust and supply air odour

concentrations has to be used in the calculation. The following equation can be used for odour emission calculation:

$$ER = C_o \cdot FR \quad (1.2)$$

Where, ER is odour emission rate, OU s^{-1}; C_o is the odour concentration of the exhaust air, OU m^{-3}; and FR is the air flow rate of the exhaust air, m^3 s^{-1}. C_o will be replaced by C_o-C_i if the incoming supply air odour concentration is not negligible; C_i is the incoming supply air odour concentration, OU m^{-3}.

When dealing with odour dispersion model, confusion may result from the particular units used to quantify emission rates because odour concentration, i.e. odour detection threshold, is expressed as OU rather than mass concentration such as g m^{-3}. Some researchers (Smith, 1993; Mahin, 1998) have used OU as the odour concentration unit and this caused confusion because the resulting odour emission rates have units of (OU)(volume)$(time)^{-1}$, which is not consistent with the units of (mass)$(time)^{-1}$ accepted by air dispersion models. If odour is to be treated as a specific matter in air dispersion modeling, the "mass" of odour should be expressed as OU. Under this assumption, odour concentration takes the unit of (OU)$(volume)^{-1}$ or OU m^{-3} and odour emission rate has the unit of (OU)$(time)^{-1}$ or OU s^{-1}, which is consistent with the format of mass concentration and emission rate. OU m^{-3} means the same as OU but specifies the dilution ratio is quantified on cubic meter basis. It thus is employed by most odour researchers in odour dispersion models (Williams, 1985; Carney and Dodd, 1989; Pain et al., 1991; Jacobson et al., 2005; Guo et al., 2005b).

Odour emission rates change constantly with changing animal mass and number and outside weather conditions. Odour emission rates have been measured more or less randomly during specific time periods (Klarenbeek, 1985; Verdoes and Ogink, 1997; Heber et al., 1998; Jacobson et al., 2000; Lim et al., 2001; Wood et al., 2001; Zhou and Zhang, 2003; Zhang et al., 2005). Great variations in odour concentrations and emission rates have been measured within each study and among different studies (Wood et al., 2001). The means or geometric means of the limited measured odour emission rates for each type of odour sources were used as representative values in odour dispersion and

setback modeling without considering the diurnal and seasonal variations (Jacobson et al., 2000; Lim et al., 2000; Zhu et al., 2000b). Guo et al. (2006a) found large variations in annual and diurnal odour emission rates from swine barns but no specific seasonal or diurnal patterns were observed. Sun et al. (2008) studied on a swine barn and revealed that odour and gas emission rates have significant fluctuations which presented different patterns as affected by observational time of day, season, animal growth cycles, room management and weather conditions. Wang (2007) observed that odour and gas emission rates from swine barn had both diurnal and seasonal variations. Significant or apparent diurnal pattern was found, while no specific seasonal pattern was observed. It was suggested that multiple measurements should be taken from an odour source to obtain the mean, maximum, and minimum odour emission rates for air dispersion modeling purposes.

1.1.3 Odour Plume Measurement

The accuracy of odour dispersion models needs to be evaluated by field odour plume measurement data, which is challenging. Although odour concentrations, i.e., odour detection threshold (OU m^{-3}), is used as input in dispersion models, air samples taken in the odour plume downwind from a source are generally below the sensitivity of olfactometory panels (Zhang et al., 2003), which excludes the use of an olfactometer for odour plume determination. Instead, odour intensity which measures odour strength by using number and word categories to describe an odour is widely accepted to measure downwind odour plumes (Li et al., 1994; Hartung and Jungbluth, 1997; Zhu et al., 2000a; Guo et al., 2001; Zhang et al., 2003, 2005).

There are two methods for measuring odour plume dispersion, which corresponds to the odour intensity at the observer's or receptor's location. The first method is to measure the odour plume using a panel of trained odour observers. The second method is to monitor odour occurrence at neighbouring residences using trained resident odour observers (Guo et al., 2005b).

For the first method, VDI (1993) provided detailed procedures for observers to record odour intensity of odour plumes downwind an odour source. Several studies have used

this method to measure odour plumes (Li et al., 1994; Hartung and Jungbluth, 1997; Kaye and Jiang, 1999; Jacobson et al., 2000; Zhu et al., 2000a; Zhang et al., 2003, 2005). Guo et al. (2005b) pointed out that this method is used because of its ability to control the quality of the data, however, it is only practical for short distances because little odour can be detected beyond 0.5 km downwind of the source. The high cost will prevent the use of this method to monitor the odour over a long time period in a certain area.

The second method, i.e., using trained voluntary resident odour observers to monitor odour also has its advantages and limitations (Guo et al., 2005b). This method is very useful for long term odour monitoring at the resident's location considering the low cost and durative observations. Jacobson et al. (2000) and Guo et al. (2001, 2003) used 19 trained resident odour observers to monitor odour in a 4.8 x 4.8 km grid of farmland that had 20 livestock farms within or adjacent to it in Minnesota, U.S.A. Nimmermark et al. (2003) also used a similar method and measured odours in five areas of Minnesota. Guo et al. (2005b, 2006a) monitored odour occurrences around three swine farms using 39 families living within 8.6 km (5 miles) from the swine farms for two separate years. These studies have proved that using resident odour observers for long term and long distance odour dispersion measurement to be practical and effective. However, measures need to be taken to increase the accuracy and credibility of the data. The possible options include implementing periodic nose calibration for odour intensity measurement, screening the observers for bias for or against the intensive livestock operations, and taking measurements at designated times (Guo et al., 2005b). Another drawback of this method is that odour monitoring can only be done at the volunteers' residence locations, which might not cover all desired locations (Guo et al., 2005b).

An alternative method by combining the above two was used by Guo et al. (2005c), which was using hired trained odour observers to travel on designated locations at designated time in a study area to monitor odours downwind of swine farms. High quality and unbiased data can be obtained by this method for short and long distances, and long term observations.

1.2 ODOUR DISPERSION MODELING

Atmospheric dispersion models have been proven to be very powerful tools for the prediction of odour concentration downwind from agricultural sources with an objective of determining whether or not odour nuisances are likely to occur near livestock production facilities. There are several models such as ISC3 (Industrial Source Complex), AERMOD (AMS/EPA Regulatory Model), ADMS (Atmospheric Dispersion Modelling System), AUSPLUME (AUStralian PLUME dispersion model), INPUFF (Gaussian INtegrated PUFF model), CALPUFF (A Lagrangian Puff model), and others, that are commercially available and have been applied for modeling agricultural odour dispersion. However, most of these models are originally designed for industrial pollution sources and may not be suitable for livestock odour dispersion modeling. Only a few models such as AODM (Austrian Odour Dispersion Model) and ODODIS (Odour DISpersion software) were developed specifically for odour dispersion from agricultural sources, however, these models need more validation to be confidently applied in livestock odour dispersion modeling.

1.2.1 Gaussian Plume Model

Traditionally, the Gaussian plume model is the most common air pollution model. Most regulatory models are based on this model for a continuous point source in a uniform flow with homogeneous turbulence. It can be expressed as (Arya, 1999):

$$C = \frac{Q}{2\pi\sigma_y\sigma_z\bar{u}}\exp\left(-\frac{y^2}{2\sigma_y{}^2}\right)\left\{\exp\left(-\frac{(z+H_e)^2}{2\sigma_z{}^2}\right)+\exp\left(-\frac{(z-H_e)^2}{2\sigma_z{}^2}\right)\right\} \tag{1.3}$$

where: Q is the source emission rate, g s^{-1}; C is the downwind concentration at the receptor location (x, y, z), g m^{-3}; $\bar{u}$ is the average horizontal wind speed, m s^{-1}; H_e is the effective emission height, m; and σ_y and σ_z are the dispersion parameters, or standard deviations (transversal and vertical) of the plume dimension, m, which are functions of downwind distance x and atmospheric stability.

ISC3 is the most commonly used air dispersion model based on the Gaussian plume dispersion theory. ISC3 model is designed to support the US EPA's regulatory modeling

programs and is widely used in North America and worldwide (US EPA, 1995a). It is a steady-state Gaussian plume dispersion model. The model can handle multiple sources, including point, volume, area, line and open pit sources. Source emission rates can be treated as constant throughout the modeling period, or may be varied by hour of a day, month, season, or other optional periods. Another US EPA model- AERMOD was developed to replace ISC3 with more advanced modeling techniques. Compared to ISC3, AERMOD contains new or improved algorithms including: dispersion in both convective and stable boundary layers, plume penetration into elevated inversions, computation of vertical profile of wind, turbulence, and temperature, advanced characterizations of the fundamental boundary layer parameters, the treatment of meander, etc. In the stable boundary layer the concentration distribution is assumed to be Gaussian in both the horizontal and vertical directions. However, in the convective boundary layer (CBL), the vertical distribution is described using a bi-Gaussian probability density function whilst the horizontal distribution is again considered to be Gaussian in nature (US EPA, 2004). ADMS is an advance air dispersion model used widely in UK and across the Europe. It includes almost all the features of AERMOD and ISC. Additionally, it has some new and advanced algorithms such as concentration fluctuation, plume chemistry and condensed plume visibility (CERC, 2004).

Considerable research has been implemented in simplifying and modifying the Gaussian plume model and applying it to livestock odour dispersion. Stoke (1977) applied the Gaussian plume model to predict odour dispersion from 10 pig barns. The model was used to calculate the distance at which the odour concentration would be reduced to 1 OU m^{-3} under a given emission rate and odour panels were employed to determine the downwind distance where odour concentration was equal to 1 OU m^{-3}. Agreement between predicted distance for 1 OU m^{-3} and measured distance at which half of a panel can detect odour was considered to be reasonable. Similar work had been done by Mejer and Krouse (1985), Williams (1985), and Carney and Dodd (1989) in modifying Gaussian plume model to predict odour concentration downwind from the livestock odour source. Mejer and Krouse (1985) considered the differences between the traditional air pollutant dispersion from industrial sources and odour dispersion from agricultural sources and argued that the Gaussian plume formula should be used only for

those downwind distances for which the empirical dispersion coefficients have been determined by standard dispersion experiments, which is a great point when trying to either adapt commercial air dispersion models into odour dispersion or to develop a new odour dispersion model. After reviewing the Gaussian plume methodology, the previous work and the existing problems with modeling agricultural odours, Gassman (1993) stated that the Gaussian method was adequate to compare differences between different scenarios, but could not be recommended for the determination of absolute odour concentrations.

Smith (1993) developed a Gaussian plume model (STINK) which predicts the dispersion of odours downwind area sources (such as feedlots) with specific shapes and orientations. The model is based on equation 1.4, which is derived from equation 1.3 first for finite line source and then for area source.

$$\Phi(x,y,z)=\sum_{1}^{n}\left\{\frac{1}{\sqrt{2\pi}\sigma_{zi}}\exp\left(-\frac{z^2}{2\sigma_{zi}^2}\right)\left[erf\left(\frac{y+Y/2}{\sqrt{2}\sigma_{yi}}\right)-erf\left(\frac{y-Y/2}{\sqrt{2}\sigma_{yi}}\right)\right]\right\}\delta X \qquad (1.4)$$

where: $\Phi(x,y,z)=\dfrac{C(x,y,z)\bar{u}}{Q}$ is a normalized concentration; The areal source is divided into n strips, σ_{yi} and σ_{zi} are dispersion coefficients referring to the i^{th} strip of the source, m; X and Y are the width and length of the areal source, m; other parameters have the same meaning as those of equation (1.3).

The odour concentration from a given area source is estimated by the numerical integration of the concentrations from the strips that the area source had been divided into. The advantage of the STINK model is to predict the dispersion considering an accurate description of the source geometry, which is important for the dispersion relatively close to large area sources. However, validations are needed to ensure this model can actually improve the accuracy of model predictions. This model had been adapted by ADMS to deal with area sources (CERC, 2004). It was also used to back-calculate the odour emission rates from relatively large area sources and has provided reasonable results as

compared with emission rates measured or estimated by other methods (Smith and Hancock, 1992; Smith, 1995; Smith and Kelly, 1996; Koppolu et al., 2002).

Odour researchers have been seeking approaches to adapt commercial models in odour dispersion modeling. Engel (1997) utilized the ISCST3 model to simulate odour dispersion from a composting facility. The resulting 1-hour concentrations were converted to 30-second peak concentrations with a peak-to-mean ratio (a ratio used to convert long time average odour concentrations into short time average odour concentrations) of 1.97. This methodology appeared to yield reasonable predictions of the frequency of nuisance conditions and the model results correlated with field measurements. Mahin (1997) summarized the selected case studies relative to the use of dispersion models to predict odour from composting facilities and wastewater treatment facilities. The ISCST3 model was used in most of the selected cases and different adjustment factors (peak-to-mean ratios) were applied to convert long time (1-hour) averaged concentration to short term peak concentration (2 min, 5 min or 10 min). Sheridan et al. (2004) selected ISCST3 as the most appropriate model to predict the odour dispersion from pig unit to obtain the setback distance and to access the odour control techniques such as biofiltration, feed manipulation and exhaust vent modification. The comparisons among ISCST3, other commercial Gaussian plume models (AERMOD, AUSPLUME and ADMS), puff models (CALPUFF, INPUFF) and numerical models on prediction of livestock odour can also be found in the literature (Curran et al., 2002; Zhou et al., 2005; and Xing et al., 2006, Wang et al., 2006).

Another Gaussian plume model needed to be mentioned is the Austrian Odour Dispersion Model (AODM) developed by Schauberger et al. (2000). The AODM first calculates the odour emission of the livestock building, and then predicts mean odour concentrations using the Austrian Gaussian regulatory dispersion model, and the last transforms the predicted mean odour concentration to instantaneous values depending on wind velocity and atmospheric stability. Using this model, Schauberger et al. (2001) calculated the separation distance between livestock buildings and residential areas and concluded that the AODM model is appropriate for regulatory purposes by comparing the model calculated setback distances with empirical guidelines. The model calculated odour

sensations (detectable odours) at the direction dependent separation were analyzed and compared with odour complaints statistics (Schauberger et al., 2006). It showed that the time pattern of the calculated odour sensations does not fit to the time pattern of the complaint statistics. A sensitivity study of separation distance calculated by AODM revealed the influence of cloudiness or net radiation on the determination of atmospheric stability and different peak-to-mean ratios on separation distance (Piringer et al., 2007). However, no direct field odour plume measurement data are used to validate this model.

1.2.2 Puff Model

The Gaussian puff model has been developed to model the dispersion of an instantaneous release of pollutants. The puff model offers advantages over steady-state plume model by accounting for spatial variability of meteorological and dispersion conditions, low wind speed dispersion, memory of previous hour's emissions, etc, The theoretical basis of this model is the same as the standard Gaussian plume model, with the difference that longitudinal dispersion is considered. The general expression of puff model is expressed as (Arya, 1999):

$$C = \frac{Q_{ip}}{(2\pi)^{3/2}\sigma_x\sigma_y\sigma_z}\exp\left[-\frac{x^2}{2\sigma_x^2}-\frac{y^2}{2\sigma_y^2}\right]\left\{\exp\left[-\frac{(z-H_e)^2}{2\sigma_z^2}\right]+\exp\left[-\frac{(z+H_e)^2}{2\sigma_z^2}\right]\right\} \qquad (1.5)$$

where: Q_{ip} is the instantaneous point source emission rate, g; σ_x, σ_y and σ_z are the standard deviations of the puff concentration in the three orthogonal directions, m; other parameters have the same meaning as those of equation (1.3).

Some models have been developed based on the puff theory, in which INPUFF2 model (Petersen and Lavdas, 1986) and CALPUFF model (USEPA, 1995b) are the most representative and most commonly used. INPUFF2, a Gaussian integrated puff model, was developed by the US EPA and marketed by Bee-Line Software Company (Asheville, N.C.). The Gaussian puff diffusion method is used to compute the contribution to the concentration at each receptor from each puff every time step. It can simulate dispersion of airborne pollutants from semi-instantaneous or continuous point sources. There is no treatment of area or volume sources. It may deal with non-reactive pollutants, deposition,

and sedimentation. It can deal with different time intervals with minimum of 1 s instead of 1 h required by the other models. This makes it suitable for simulating odours as measured by field odour assessors. This model has some consideration of terrain effects through the wind field but there is no explicit treatment of complex terrain.

CALPUFF air dispersion model was an US EPA regulatory model based on Lagrangian puff model designed to simulate continuous puffs of pollutants being emitted from a source into the ambient wind flow (US EPA, 1995b; US EPA, 1998). It consists of three sub-systems: CALMET, CALPUFF, and CALPOST. CALMET is a meteorological model that combines meteorological data and geophysical data to generate a wind field. CALPUFF model then combines the information provided by CALMET and source data to predict concentration, deposition flux, visibility impairment, etc., at each receptor for specified averaging time. CALPOST is a post-processor for the model. CALPUFF can accommodate point, volume, and area source emissions. CALPUFF can use the three dimensional meteorological fields developed by the CALMET model or the meteorological files used by ISCST3. CALPUFF contains algorithms for near-source effects such as building downwash, transitional plume rise, partial plume penetration, sub-grid scale terrain interactions as well as long range effects such as pollutant removal, chemical transformation, vertical wind shear, over water transport, and coastal interaction effects.

McPhail (1991) stated that puff models are more appropriate to be used to predict agricultural odours because odour moves more like a series of puffs rather flowing as a continuous stream. Gassman (1993) demonstrated that puff models might yield higher odour predictions and the peak concentrations will greatly exceed the mean concentrations for a short time period. Gaussian dispersion models are unable to account for the corresponding peak concentrations (Gassman, 1993).

Both CALPUFF and INPUFF2 models have been applied to odour dispersion modeling. Diosey et al. (2000) compared the ISCST3 and CALPUFF models for odour emission from a wastewater treatment plant with area and point sources, and found that, in general, the two models gave results in the same range. However, there were cases when the impacts predicted by the CALPUFF modeling system were either significantly lower or

higher. Bedogni and Sergio (2004) used the CALPUFF model in investigating the odour impact of a solid waste landfill in Italy and obtain satisfactory results in terms of the measured and predicted concentration of methane, which was used as an odour indicator. Wang et al. (2006) compared CALPUFF and ISCST3 models to predict downwind odour concentrations from a beef cattle feedlots farm. Their results indicated that CALPUFF model yielded better predictions of odour concentrations than ISCST3 which under predicted the odour concentrations.

Zhu (1999) used the INPUFF2 model to theoretically evaluate the influence of stability class on downwind odour concentration. The downwind odour concentrations at different distances from the odour source were investigated with respect to different stability classes and wind speed. According to his study, the unstable and neutral stability categories tended to govern the odour levels within 200 m range, while the stable categories yielded higher odour levels beyond that range. The odour plume width varies with the stability classes. He also pointed out that Gaussian models cannot predict odour for distances less than 100 m from the source and that stability class E and F are not suitable for use in Gaussian models to predict agricultural odour dispersion. Field data were used to evaluate the INPUFF2 model for predicting downwind odours from animal production facilities (Zhu et al., 2000a). Results from this study showed that the INPUFF2 model could predict downwind odour concentrations generated from animal production facilities within 300 m satisfactorily. At further distance, the accuracy of prediction by the model was significantly reduced. It was found that INPUFF2 cannot be directly applied for odour dispersion because the results obtained were much lower than the field measured results. Scaling factors of 35 for animal building sources and 10 for surface sources such as manure storage unit were used to amplify the odour emission rates by this study to adjust the model predicted concentration to the same numerical range as the field odour measurement (Zhu et al., 2000a). Following this work, Guo et al. (2001) calibrated the INPUFF2 model using odour monitoring data by resident odour observers for long-distance (up to 4.8 km) from animal production sites using the same scaling factors. Comparison between the modeled and measured odour intensity indicated that the model successfully estimated odour intensity 1 (faint odour) traveling up to 3.2 km under stable atmospheric conditions. However, the model underestimated moderate to

strong or very strong odours and odours that occurred during neutral and unstable weather. These results indicate that, after applying the scaling factors, this model could serve as a tool for agriculture odour dispersion estimation from animal production sources. The OFFSET model, a setback distance model for determination of odour-annoyance setback distances from animal production sites, was developed based on the INPUFF2 and the scaling factors (Jacobson et al., 2005; Guo et al., 2005a).

1.2.3 Meandering/Fluctuating Model

Changes in meteorological conditions have a direct impact on air pollution. However, even under apparently constant meteorological conditions, random concentration fluctuations may exist due to the turbulent motion of the atmosphere (Arya, 1999). The concentration fluctuations have been observed and measured by different researchers in wind tunnels and water channels (Fackrell and Robins, 1982; Deardorff and Willis, 1984; Hilderman and Wilson, 2007, 2008; Yee, 2009), full scale atmospheric measurements (Hanna 1984; Lewellen and Sykes, 1986; Dinar et al., 1988; Mylne and Mason, 1991; Mylne, 1992; Yee et al., 1993, 1994a, 1995; Mole and Jones, 1994; Mylne, et al., 1996; Yee and Biltoft, 2004). A wide range of models have been developed to model the concentration fluctuations. Hanna (1984) separated the existing models that are capable of calculating the concentration fluctuations into seven categories: K-models, empirical Gaussian models, similarity models, fluctuating plume models, PDF models, statistical models and advanced numerical models. The new developed models continued to fall into these categories. ADMS includes a fluctuations module by using a stochastic model and assuming a clipped normal distribution of concentration to account for the short time concentration fluctuations (CERC, 2004). Fluctuating plume models have been adapted and applied in odour dispersion modeling (Högström, 1972; de Bree and Harssema, 1987; Mussio et al., 2001; De Melo Lisboa et al., 2006).

The first fluctuating plume model was developed by Gifford (1959). The basic theory of the fluctuating plume model is that the total dispersion can be separated into two components, one that represents the relative dispersion within the instantaneous plume,

and the other that accounts for the variance of the centroid of the fluctuating plume. It can be expressed mathematically as (Arya, 1999):

$$\sigma^2 = \sigma_p^2 + \sigma_c^2 \tag{1.6}$$

where: σ is the standard deviations and the subscript p denotes instantaneous or short term-averaged plume and c denotes the meandering component.

The relative diffusion within the instantaneous plume is dominated by eddies which are smaller than the dimensions of the plume, whilst the meandering of the plume is caused by the eddies which are much larger than the plume dimensions (De Bree and Harssema, 1987; Yee et al., 1994b). The meandering of the plume is the dominant factor in the dispersion process for traveling times smaller than the Lagrangian time scale (Hanna 1984). The influence of the relative diffusion is increasing with the increasing traveling times. Since this model doesn't take the in-plume fluctuations into account, it was extended by many researchers to parameterize in-plume relative concentration fluctuations. Yee et al. (1994b) and Reynolds (2000) extended Gifford's model to include the in-plume fluctuations by assuming probability density functions (PDF). Luhar et al. (2000) and Franzese (2003) use Lagrangian stochastic models to account for the in-plume fluctuations. de Haan (2001) developed a puff-particle model to predict the concentration fluctuations by simulating a realistic 3-D meandering of the puffs.

Nevertheless, the current applications of meandering plume model are mostly derived from the original Gifford's model. The Hogström model (Högström, 1972) was proposed to predict odour with the capability of describing plume meandering based on the principles proposed by Gifford (1959). The model can estimate the odour frequency at a certain point downwind the source. The main point of the Hogström model is the determination of the weighted odorous width of the plume at ground level and its variation due to the meandering of the plume. The odorous width at a certain distance from the source is that part of the instantaneous plume within which the odour threshold (e.g. 1 OU m^{-3}) is exceeded at ground level. For certain threshold concentration, under certain meteorological conditions, the odorous width can be calculated by the fluctuating plume model, and then the frequencies of the odour threshold are calculated based on this

odorous width. From the comparison between calculated data and observed data from two field odour experiments, Hogström (1972) found that it was possible to make good estimates of odour frequencies near a point source with this method. In the distance range of 2 to 5 km from the source there was no systematic difference between the predicted and the observed frequencies. For the distance range of 10 to 20 km the calculated frequencies were significantly lower than the observed ones. However, the ability of this model to estimate the odour frequencies for different strength of odour has not been tested, and more field experimental work should be done in order to validate this method for more application.

A modified Hogström model was described by de Bree and Harssema (1987). The computation proceeded by calculating the weighted width of the detectable odour plume at ground level due to vertical meanderings, and integrating the predicted transverse distribution of the plume centerline over the interval of the weighted width, centered laterally at the receptor location. A field odour measurement was conducted by eight trained panel members who were placed along a line downwind of the source, perpendicular to the expected wind direction. The panellist made instantaneous observations of the detectability of the odour every 10 s during 10 min. Over all, the calculated and measured odour frequencies were strongly related (R = 0.90) under unstable and near neutral atmospheric conditions. However, this modified Hogström model was tested for relatively short traveling times only (10 min), for large distances the applicability was not tested and theoretically assumed to be low due to the less effects of the plume meandering on the concentration fluctuation.

Mussio et al. (2001) developed another dispersion model based on Gaussian fluctuating plume theory to facilitate the prediction of odour-impact frequencies in the communities surrounding elevated point sources. This model was tested by the field odour data collected from the residential areas surrounding the paint shop of an automotive assembly plant. The field odour measurements were conducted by observers every 12 s. Results showed that the simulation of the total frequency of occurrence was good for frequent odour (i.e. readily detectable more than 30% of the time). At low frequencies of occurrence, the model prediction was poor. The model also provided good predictions of

the maximum odour levels without being sensitive to either stability class or distance from the source. However, the testing field odour data was very limit, further calibration of the model is necessary to increase its accuracy and widen its applicability, especially for the long distance and wider variety of atmospheric conditions. De Melo Lisboa et al. (2006) developed a fluctuating model to estimate the odour impact. Nine approaches that explore several solutions within the Gaussian domain for the atmospheric dispersion problem are proposed in the software package ODODIS (ODOur DISpersion software). This model needs more validations with the odour field data, although a comparison with an existing database (the Prairie Grass database), which is a set of field experiments carried out in 1956 and was an important database for testing the Gaussian models, showed good agreement.

1.2.4 Other Models

There are many other models that have been developed to model air dispersion in the atmosphere including numerical gradient transport models, turbulence kinetic energy models, higher order closure models, Lagrangian stochastic models, large-eddy simulation models, and Computational Fluid Dynamics (CFD) models. However, the application of these models in odour dispersion modeling is very limited. A Lagrangian particle model-AUSTAL2000G has been developed in Germany as a regulatory dispersion model to deal with odour dispersion problems (VDI, 2000). However, there is little information on the validation and evaluation of this model by field measurement. Another Lagrangian particle model-WinTrax, developed by Thunderbeach Scientific (Nanaimo, BC, Canada) has been evaluated by Zhou et al. (2005). They concluded that the WindTrax dispersion model can predict odour concentrations with good agreement for distances of between 500 and 1000 m. Schiffman et al. (2005) used a model that combined an Eulerian higher order closure model and a Lagrangian stochastic model to simulate the dispersion of odour from a confined animal feeding operation (CAFO) under different meteorological conditions. The predicted odour dispersion distance was found to be greater at night-time than during daytime and was consistent with field reports from individuals living near the CAFO. Boeker et al. (2000) used a modified CFD model (NaSt3D) to carry out the time-resolved simulation of odourant dispersion. Bjerg et al.

(2004) conducted a study of using CFD model to investigate the possibilities to reduce odour concentrations by optimising the location and design of exhausts. The CFD model was validated against full scale tracer gas (SF6) measurements around a commercial growing-finishing pig building and showed that it was a suitable technique to predict the spreading of exhausted air 50 to 150 m from a livestock building. A comparison of odour dispersion prediction between CALPUFF and CFD models had been done by Li and Guo (2006). They stated that CFD model has the potential to characterize the instantaneous odour concentrations downwind but no validation was done using measured odour plume data. It requires refined meteorological data to process the short time modeling (Li and Guo, 2008).

1.3 ADAPTING AND VALIDATING ODOUR DISPERSION MODELS – SOME ISSUES

When either adapting existing industrial air dispersion model for odour dispersion modeling or using dispersion models developed specifically for odours, several important issues have to be addressed, including the difference between odour and specific air contaminant/gas, the instantaneous nature of odour, and the relationship between odour concentration and intensities in the validation of odour dispersion models. First, due to the inherent difference between odour and traditional air pollutant measurements, directly applying some industrial air dispersion models for odour dispersion has been proven incorrect and inappropriate (Zhu et al., 2000a; Guo et al., 2001; Zhang et al., 2005). Measures have to be taken to make the industrial air dispersion model usable for livestock odour dispersion. Second, odour can be perceived in very short time (a few seconds) when its concentrations exceed its detection threshold. Many industrial air dispersion models can only predict hourly average concentration which has little use for odour, because even the hourly average concentration is well below the detection threshold, short periods of high concentrations may occur and probably cause nuisance. Third, in evaluation of the accuracy of odour dispersion models, the ultimate method is to compare the model predictions with the field plume measurement data. As discussed previously, field odour plume is measured by estimating odour intensities at desired locations in the odour plume. To compare the field measured odour intensity with the model predicted odour concentration, the relationship between the odour concentration

and intensity has to be known. The first issue may be dealt with by using the "black box" concept by applying appropriate scaling factors to adjust the emission rate. The second issue may be dealt with by peak to mean ratios or scaling factors that transform the long term average concentration to a short term concentration. The third issue may be dealt with by selecting the appropriate relationship between odour concentration and intensity.

1.3.1 Scaling Factors

As discussed previously, Zhu et al. (2000a) and Guo et al. (2001) found that INPUFF2 cannot be directly applied for odour dispersion because the results obtained were much lower than the field measured results and scaling factors have to be used to amplify the odour emission rates in order to adjust the model predicted concentration to the same numerical range as the field odour measurement. Koppolu et al. (2004) reported that scaling factors in the range of 0.2 to 3900 may be needed to adjust AERMOD predictions to short-term odour measurements depending on the source type (point, area, volume) and the type of facility being modeled after comparison of measured odour intensities from livestock facilities to predicted ambient odour levels from AERMOD. Zhou et al. (2005) calibrated four air dispersion models, ISCST3, AUSPLUME, INPUFF2, and WindTrax using odour plume measurement data 100 to 1000 m from two swine farms. They concluded that these four models performed similarly and predicted downwind odour concentrations with good agreement with field measured results. Considering that 58.3% the measured odour concentrations were zero, this set data was re-examined by Xing et al. (2006) for ISCST3, AUSPLUME, INPUFF2, and CALPUFF models. It was found that although the agreement between the model predictions and measured odour intensities was between 37% and 50% for the four models considering all the measurements, however, if the measurements with intensity zero (no odour) were excluded, the agreement reduced to between 28 and 35%. No scaling factors were used by Zhou et al. (2005) and Xing et al. (2006). Xing et al. (2006) found that scaling factors could not improve the models' performances significantly because some model predictions were lower than measured values and some were higher, which is different than the findings by Zhu et al. (2000a) and Guo et al. (2001) that the model predictions of INPUFF2 were always lower than the measured values, which made the scaling factors

useful. The main reason for the difference between these studies might be that the odour intensity and concentration conversion equations are very different from each other (Xing et al., 2006). The odour intensity and concentration conversion equations are very important to ensure the accuracy of the comparison of the modeled and measured odour intensities as well as the effectiveness of improving model performance using scaling factors. This will be further discussed in sections 1.3.2 and 1.3.3.

1.3.2 Peak to Mean Ratio

Short term odours that exceed the odour detection threshold can cause odour nuisance, even the long time (hourly) average concentration is well below the odour detection. Although there are plenty of dispersion models which have been developed to account for concentration fluctuations, the current odour dispersion modeling is mainly based on Gaussian plume and puff models (e.g. ISCST3, AERMOD, and CALPUFF). Most of these Gaussian models can only predict the average concentration from 10 min to 1 h or longer and neglect the short term fluctuations.

The peak-to-mean ratio can be used as a correction factor to overcome this disadvantage of these kinds of dispersion models and estimate the maximum values in the field. Smith (1973) gives the following relationship (equation (1.7)) to transform the regulatory model calculated mean concentrations to peak odour concentration.

$$\frac{C_p}{C_m} = \left(\frac{t_m}{t_p}\right)^u \tag{1.7}$$

with the mean concentration C_m calculated for an integration time of t_m and the peak concentration C_p for a integration time of t_p. u is the stability dependent power law exponent. Smith (1973) gave the following values of the exponent u depending on the stability of the atmosphere: 0.65 (SC= B), 0.52 (SC= C) and 0.35 (SC= D) (Schaugerger et al., 2000). However, Duffee et al. (1991) reported different values for u: 0.5 (SC= A or B), 0.33 (SC= C), 0.20 (SC= D) and 0.167 (SC = E or F). Mahin (1997, 1998) stated that there was no agreement on the appropriate power law exponent (u) for different stability classes. One approach to convert averaging times to a shorter time is to assume a power

exponent of 0.2 for all stability classes. An odour dispersion model (AODM) developed by Schaugerger et al. (2000, 2001) transformed the half-hour average concentrations calculated by a Gaussian dispersion model to instantaneous values by an attenuation function decreasing the peak-to-mean ratio with increasing wind velocity, stability, and distance from the source.

1.3.3 Relationship between Odour Concentration and Intensity

Most of the odour dispersion models can predict odour concentrations downwind the sources, while the odour intensities are measured in the field plume measurement. This results in another problem to be solved in order to validate odour dispersion models, i.e., the odour detection threshold needs to be converted to the odour intensity in order to compare the result calculated by an air dispersion model to the field odour plume measurement .

There are three kinds of relationship between odour intensity and odour concentration that have been found by researchers including Weber-Fechner law, Stevens power law and Beidler model (Nicolai et al., 2000). The Weber-Fechner law can be expressed in a logarithmic form:

$$I = k_{w1}(\log_{10}C) + k_{w2} \quad (1.8)$$

where I is odour intensity; C is odour concentration, OU m^{-3}; and k_{w1} and k_{w2} are constants (Misselbrook et al., 1993).

Although all the researchers have agreements on the presence of the relationship between odour intensity and concentration, the best fit models are different and the constants in each model are different among the researchers. Misselbrook et al. (1993) related the odour detection threshold and odour intensity for emissions following land spreading of pig slurry and also emissions from broiler houses. The Weber-Fechner logarithmic model was applied to the both emissions and the relationships between odour concentration and odour intensity obtained were expressed as:

$$I = 1.61(\log_{10}C) + 0.45 \quad \text{for odours from pig slurries} \quad (1.9)$$

$$I = 2.35(\log_{10}C) + 0.30 \text{ for broiler house odours} \quad (1.10)$$

Chen et al. (1999) compared intensity and threshold from four different swine facilities (gestation, farrowing, nursery, and finishing). They concluded that the widely used Weber-Fechner model did not adequately fit the data as well as the Stevens power model. Nicolai et al. (2000) investigated the Weber-Fechner, Stevens, and Beidler models and found that the Weber- Fechner logarithmic model provided the best form to describe the relationship between odour concentration and intensity from the swine buildings:

$$I = 1.57(\log_{10}C) - 0.46 \quad (1.11)$$

For odour from manure storage, all three models were similar with the Weber- Fechner model indicating a slightly better fit:

$$I = 1.61(\log_{10}C) - 0.570 \quad (1.12)$$

For combined building and storage, Weber-Fechner model was selected as best model for low odour levels:

$$I = 1.59(\log_{10}C) - 0.528 \quad (1.13)$$

Zhang et al. (2003) investigated a total of 155 odour samples collected on four swine farms to determine the relationship between odour intensity and concentration. Odour intensity of bagged samples measured in laboratory correlated well with the odour concentration measured with olfactometers and the relationship could be adequately predicted by the Weber-Fechner model. The relationship they found can be expressed as:

$$I = 1.89(\log_{10}C) + 0.36 \quad (1.14)$$

Sheridan et al. (2004) collected 18 air samples over a 2-year period at finishing pig houses and at a 1000-sow integrated commercial pig unit and obtained a relationship between odour intensity and concentration following the Weber-Fechner model as:

$$I = 2.19(\log_{10}C) + 0.736 \quad (1.15)$$

Zhang et al. (2005) collected sixteen odour samples in Tedlar bags from two swine farm and presented to trained observers for odour intensity and concentration measurements in an olfactometer lab. The conversion equation from this study takes the form of:

$$I = 1.78(\log_{10}C) + 1.43 \quad (1.16)$$

Feddes (2006) studied the relationship between the perceived intensity of the headspace of standard 60 ml training jars containing n-butanol of the 8-point odour intensity referencing scale measured by odour sniffers and the corresponding n-butanol concentration (OU m^{-3}) determined by olfactometer. The resulting relationship was:

$$I = 2.97(\log_{10}C) - 0.21 \quad (1.17)$$

The concentrations for different intensity scales of equation (1.16) and equation (1.17) are listed in Table 1.1. When generating equation (1.16) by Zhang et al. (2005), 16 odour samples were used, while more n-butanol samples were used to generate equation (1.17) by Feddes (2006). From the point of view of sample numbers, equation (1.17) may be more reliable than equation (1.16). However, for equation (1.17) the concentration of high level intensity seems too low. In other word, for a given high level intensity of n-butanol the equivalent odour concentration (OU m^{-3}) is lower than that for the livestock odour (Feddes, 2006) as shown in Table 1.1. For example, odour concentration of 580 OU m^{-3} is at the moderate or low end of odour concentrations measured in swine barns and manure storages in warm seasons, and may not be considered strong comparing with odour measured in the manure storage or from the barns in winter. Xing et al. (2006) used equation (1.16) to evaluate four air dispersion models using the field odour plume data from the swine farm that Zhang et al. (2005) collected odour samples from to generate the equation (1.16). A similar equation as (1.17) (Seguar and Feddes, 2005) was also used to exam the agreement between measured and model predicted odour intensity (Xing et al., 2006). They concluded that using this equation cannot improve the agreement.

Guo et al. (2001) also obtained the relationships between odour concentration and intensity on a 5-point n-butanol scale. This is based on odour intensity and concentration measurements of 124 odour samples collected from 60 swine buildings and 66 swine

manure storage facilities, and 55 odour samples collected at 10 dairy and beef farms in Minnesota during 1998 and 1999. The Weber-Fechner model was the best fit for both swine and cattle data. The relationships between odour intensity on the 0 to 5 scale and concentration are expressed as:

$$I = 2.137(\log_{10}C) - 1.97 \quad \text{for swine odours} \tag{1.18}$$

$$I = 2.123(\log_{10}C) - 2.068 \quad \text{for cattle odours} \tag{1.19}$$

Equation (1.18) for swine odours is very different from equations (1.16) and (1.17). This results partly from the different intensity interpretation for the same n-butanol concentration-in-water for different odour scale as shown in Table 1.1. For example, intensity 1 on this 5-point scale is perceived as very faint odour and it is equivalent to intensity 2 for n-butanol concentration-in-water on the 8-point scale, but its swine odour concentration 25 OU m^{-3} is equivalent to intensity 4 on the 8-point scale represented by equations (1.16) and (1.17). Regarding swine odour concentration, intensity 2 on the 5-point scale is between intensity 4 and 5 in equation (1.16) and between intensities 5 and 6 in equation (1.17); intensity 3 is between intensities 6 and 7 in equation (1.17), and intensity 4 is equivalent to intensity 8 in equation (1.17).

The constants in Weber-Fechner models and odour scales used by different researchers were summarized in Table 1.2. The models that represented the relationship between odour intensity and concentration of swine odours were shown in Figure 1.1 and Figure 1.2. The intensity 8 on an 8-point scale, the intensity 6 on a 6-point scale, and the intensity 5 on a 5-point scale are considered the same. The odour intensity and concentration conversion equation is very important to ensure the accuracy of the comparison of the modeled and measured odour intensities as well as the effectiveness of improving model performance using scaling factors.

Table 1.2 Constants in weber-Fechner models and odour scales used by different researchers

Odour Source	Constants		Odour Scale	Reference
	K_{w1}	K_{w2}		
Pig slurries	1.61	0.45	0-6	Misselbrook et al., 1993
Broiler house	2.35	0.30	0-6	Misselbrook et al., 1993
Swine building	1.57	-0.466	0-5	Nicolai et al., 2000
Swine manure storage	1.61	-0.570	0-5	Nicolai et al., 2000
Swine building and manure storage	1.59	-0.528	0-5	Nicolai et al., 2000
Swine farms	1.89	0.36	0-8	Zhang et al., 2003
Finishing pig house pig unit	2.19	0.736	0-6	Sheridan et al., 2004
Swine farms and manure storages	1.78	1.43	0-8	Zhang et al., 2005
n-butanol	2.97	-0.21	0-8	Feddes, 2006
Swine buildings and manure storage	2.137	-1.97	0-5	Guo et al., 2001
Dairy and beef farms	2.123	-2.068	0-5	Guo et al. 2001

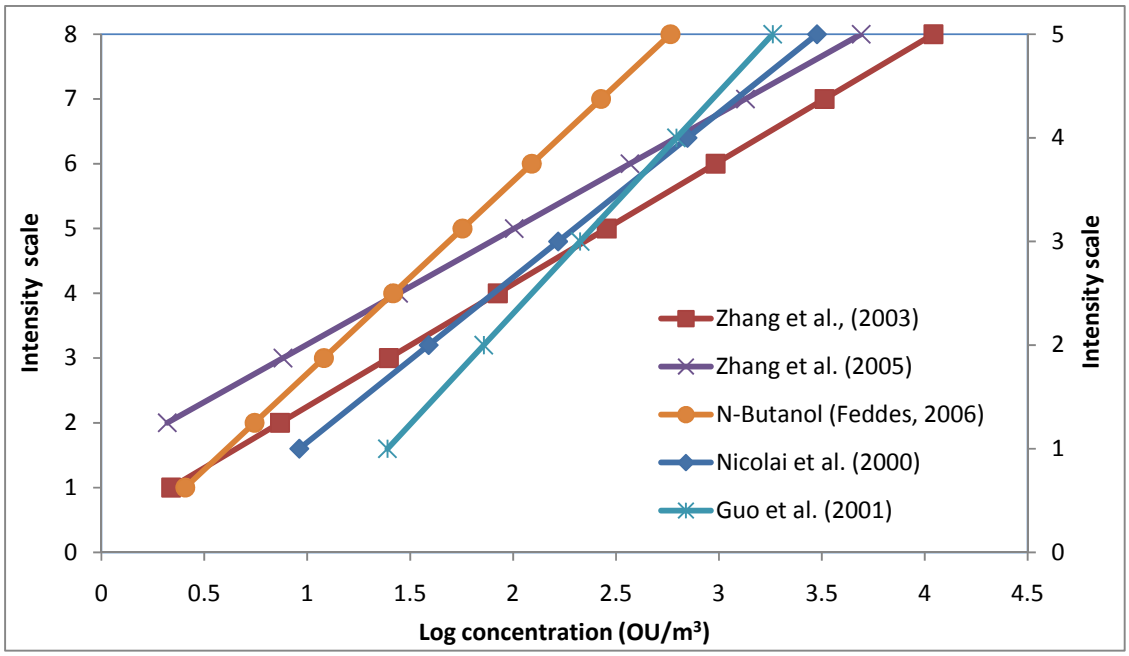

Figure 1.1 Relationships between odour intensities and odour concentrations of swine odour from different researchers (0-8 scale and 0-5 scale)

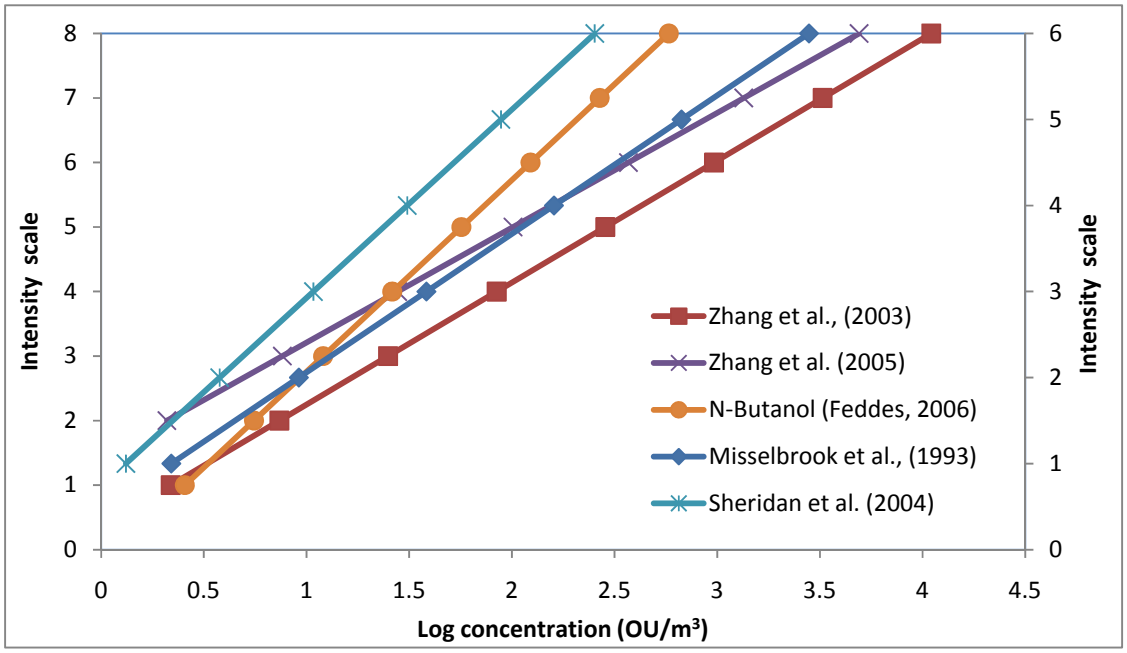

Figure 1.2 Relationships between odour intensities and odour concentrations of swine odour from different researchers (0-8 scale and 0-6 scale)

1.4 Research Gaps in Odour Dispersion Modeling

Currently, the application of model methods in odour dispersion modelling are mainly on adapting and applying the Gaussian plume or puff models (ISC3, AMERMOD, CALPUFF, INPUFF) that were originally developed for industrial sources. Although these air dispersion models have been used in predicting downwind odour concentrations from agricultural sources, several important factors which may challenge the use of air dispersion models in agricultural odours appear to have been ignored.

First, compared to industry air pollution, the travel distance of livestock odour is much less. Livestock odour can only travel less than 8 km distance (Guo et al., 2005b, 2006a). Hence the dispersion distance of interest for odour is much less than traditional industrial air pollutant. Therefore, the attempt to apply the established dispersion models based on industrial pollution to agricultural emission sources may lead to unreasonable results. There are also some other features of livestock odour that differ from industrial pollutants have to be taken into account. These features may include lower odour source, insignificant plume rise, large area source, relatively close receptor zone, uncertainty of measuring the odour emission rate, variations in emission rates, and the relatively low

intensity of emissions (Smith, 1993). Beside this, instead of the elevated stacks typical of many industrial sources, the odours coming from animal building are often emitted from openings on the walls and roofs of the buildings and from wall- or ceiling-mounted fans that have complicated structures. It is difficult to consider specifically each opening or fan. The current applications of dispersion models all have used assumptions to simplify the sources to single or multiple point sources or area sources based on the footprints of the sources.

Second, the Pasquill-Gifford dispersion parameters that have been used in the traditional Gaussian plume model were developed based on concentrations that were taken over smaller time increments, Fritz et al. (1997) stated that many models developed by US EPA could be misapplied to the estimation of odours downwind for one-hour or longer time period when using Pasquill-Gifford dispersion parameters. Guo et al. (2005b, 2006a) studied the impact of weather conditions including wind speed and atmospheric stability on odour occurrence with the data reported by resident observers living within 8.6 km from three intensive swine farms in Saskatchewan, Canada. From their study, most odour events (61.7%) were detected under neutral atmospheric stability class D while only 15% were detected under stable atmospheric conditions. Stable atmospheric conditions occurred the least in the period from May to August, yet this period had the highest number of odour events. They concluded that atmospheric stability class has little effect on odour occurrences in the vicinity of swine farms. This finding is important because it would be contrary to the basic air dispersion principle that stable weather stations would allow air to travel for farther distances than unstable conditions. Combined with the finding from Zhu (1999) that stability class E and F are not suitable for use to predict agricultural odour dispersion, this result could stem from two potential problems: a) the P-G stability class can not reflect the impact of weather stability conditions on odour dispersion at close distance from the source; b) the basic air dispersion principle is not suitable to odour dispersion for short distance within 8 km. Thus, in the future study of odour dispersion modeling, the stability class should be further evaluated. There are some models (such as AERMOD and ADMS) that treat PBL (Planetary Boundary Layer) properties in a different way from Pasquill-Gifford stability class that had been used in many traditional models like ISCST and AUSPLUME. ADMS described the boundary

layers by two parameters: the boundary layer depth and Monin-Obukhvo length (CERC, 2004). AERMOD represented turbulence based on PBL similarity theory and defined the stability by heat flux, Monin-Obukhov length, and mixing height (USEPA, 2004). More work need to be done on the application of these advanced Gaussian plume models on modeling odour dispersion from agricultural sources.

Third, a main drawback of Gaussian plume and puff models and some other models is that they can only predict average concentrations for long time period of 10 to 60 min; the short time concentration fluctuations were ignored. The peak to mean ratio cannot account for the concentration fluctuations which are important to odour impact assessment. Many models have been developed to deal with concentration fluctuations, among which the fluctuating plume models with sound theoretical basis and simple parameterizations have been used to model the odour fluctuations. However, most of these applications still ignore the in-plume fluctuations that will dominate the concentration fluctuations in far field. Models that can consider both fluctuating plume and in-plume fluctuation are also available. A fluctuations module has been included in ADMS by using a stochastic model and assuming a probability distribution function. Unfortunately, this fluctuations module and other advanced models such as higher order closure models, large-eddy simulation models, Lagrangian stochastic models, and CFD models were seldom applied in livestock odour dispersion. The application of these models needed to be seriously examined.

Also, odour concentration is measured using a totally different method from traditional air pollutant, thus, the air dispersion models are not applicable for odour dispersion predictions. To validate odour dispersion model using field odour plume measurement data, accurate relationship between odour intensity and concentration is needed to convert the modeled concentration to odour intensity.

In summary, because of the differences between industrial air pollution and livestock odour, the direct application of industry air dispersion models into livestock odour may cause unreasonable results. The traditional models that use Pasquill-Gifford stability categories may not be suitable for livestock odour. Instead, the advance Gaussian models (AERMOD and ADMS) should be considered. Very limited work has been done by

utilizing the fluctuating plume models and CFD models to deal with concentration fluctuations. The fluctuating plume models with in-plume fluctuations and other advanced models that can account for concentration fluctuations are not explored for livestock odour dispersion modeling. Since the field odour plume measurements are conducted in odour intensity, whilst the dispersion models predict odour concentrations. The conversion of odour intensity and concentration has to be considered by the model in order to validate it by field odour plume measurement data.

1.5 SUMMARY

Livestock odours come from three primary sources: manure storage unit, animal housing, and land application of manure. There are more than 300 compounds in the mixture of livestock odour. Odour concentration and odour intensity are the two most widely used measurement of livestock odour. The sensory method using olfactometry is most widely used to quantify odour concentration. Odour emission rate can be determined by odour concentration and airflow rate. Many commercial Gaussian models including Gaussian plume model (ISCST3, AERMOD), Gaussian puff model (INPUFF2 and CALPUFF) that have been originally designed for traditional industrial air pollutant dispersion have been used in odour dispersion predicting, while most researchers simplified and modified the Gaussian models to predict the odour dispersion from livestock operations. Due to the differences between industrial sources and livestock sources and the difference between the measurement methods of odour and traditional air pollutant, direct application of air dispersion models in livestock odour has been proved unreasonable. Very limited work has been done in applying the fluctuating models and other advanced models to account for odour concentration fluctuations. Scaling factors and peak to mean ratios have been used to adapt the air dispersion models in livestock odour dispersion. In order to validate the odour dispersion models, field odour plume measurements should be taken. The field odour plume is measured by intensity rather than concentration. Thus the conversion between odour intensity and odour concentration is critical in validating odour dispersion models.

Most of the air dispersion models currently applied in livestock odour dispersion can only predict hourly average concentration, the models that can predict odour

concentration fluctuations are required. However, the applications of advanced air dispersion models such as ADMS, fluctuating plume models, Lagrangian particle models, and CFD models in odour dispersion are very limited. More work need to be done in odour dispersion modeling research to fulfill the gap between air dispersion modeling and livestock odour dispersion modeling. Specific livestock odour dispersion model should be developed to include all the specific features of livestock odour dispersion such as short distance of transportation, multiple sources, variable odour emissions, and conversion between odour concentration and intensity. Most importantly, this model should have the ability to predict odour concentration fluctuations. For practical use, it should also accept routine meteorological data and should not have high computer requirements. A livestock odour dispersion model based on fluctuating plume theory that meets the above requirements is recommended.

1.6 OBJECTIVES

The general objective of this thesis was to develop and validate a livestock odour dispersion model based on the fluctuating plume theory. Specific objectives and/or characteristics of this model included:

•To calculate instantaneous concentration, mean odour concentration, the occurrence frequency of certain level odour, as well as the peak odour concentration using hourly routine meteorological data input.

• To use point, area, and volume odour sources having constant or variable emission rates.

• To validate the model using field odour plume measurement data.

• To use the model to complete a sensitivity analysis of the parameters (odour source characteristics, meteorological, dispersion surface characteristics) of the parameters that influence the dispersion of livestock odours.

• To design a user-friendly interface that will allow the model to be used by government officials, livestock producers and professionals.

1.7 CONTRIBUTIONS TO KNOWLEDGE

The main contributions of this thesis are:

- An odour dispersion model that considers the features of livestock odour was designed.
- The developed livestock odour dispersion model can predicted short time odour concentrations and odour frequency with the hourly routine meteorological data input.
- The model predicts odour frequency with an improved weighted odour exceeding half width method.
- The model uses an advance method to derive parameters to determine the Hogstrŏm stability index by routine meteorological data.
- A simple method was proposed to derive parameters (friction velocity, Monin-Obukhov length, etc.) that characterized PBL from ISC format meteorological data which does not include solar radiation or cloud cover.
- An effective method was created to obtain the odour frequency from multiple sources.
- Two new indices (Ran0.2 and Ran0.1) were carried out to assess the model performance on predicting odour frequency.
- The model sensitivities to input parameters are evaluated by an elasticity value, which results in great practical applications of the model.

Chapter 2. MODEL THEORIES AND METHODS

In this chapter, the model theories and main methods used to develop the livestock odour dispersion model (LODM) were presented. In LODM, the theory for calculation of mean odour concentrations is the basic Gaussian plume model, while for prediction of instantaneous odour concentrations, peak odour concentrations, and odour frequencies is the Gaussian fluctuating plume model. The method used for calculating odour frequencies is a weighted odour exceeding half width method. In addition, the algorithm of deriving the planet boundary layer (PBL) parameters and odour dispersion parameters were provided, and a case study was conducted to test the applicability of methods.

2.1 MEAN ODOUR CONCENTRATION

Mean odour concentrations or hourly averaged odour concentrations are calculated by the basic Gaussian plume model as described in equation (1.3). In order to account for effects of a restriction on vertical plume growth at the top of the mixing layer, the method of image sources is used to simulate the multiple reflections of the plume from the ground surface which is assumed to be totally reflective and at the top of the mixed layer. Therefore, the vertical term of equation (1.3) is modified as (Ayra, 1999):

$$V = \exp\left(-\frac{(z+H_e)^2}{2\sigma_z^{\,2}}\right)+\exp\left(-\frac{(z-H_e)^2}{2\sigma_z^{\,2}}\right) + \sum_{i=1}^{n}\left\{\exp\left(-\frac{(H_1)^2}{2\sigma_z^{\,2}}\right) + \exp\left(-\frac{(H_2)^2}{2\sigma_z^{\,2}}\right) + \exp\left(-\frac{(H_3)^2}{2\sigma_z^{\,2}}\right) + \exp\left(-\frac{(H_4)^2}{2\sigma_z^{\,2}}\right)\right\} \quad (2.1)$$

where:

$H_1 = z + \mathrm{H_e} - 2iz_i$

$H_2 = z - \mathrm{H_e} - 2iz_i$

$H_3 = z + \mathrm{H_e} + 2iz_i$

$H_4 = z - \mathrm{H_e} + 2iz_i$

z_i is the mixing height, m. Generally, it is enough to account for an effect of a mixing layer by setting n as five (Ayra, 1999).

2.2 GAUSSIAN FLUCTUATING PLUME MODEL

Researchers have been using industrial air dispersion models to predict livestock odours downwind of livestock operations since the 1980's. The main drawback of these industrial air dispersion models is that most of them can only calculate long time average concentration. However, a series of short detectable exposures of odours can cause nuisances and generate community complaints even though the hourly-averaged concentration is very low or undetectable (<1 OU m^{-3}). This drawback can be overcome by a fluctuating plume model proposed by Gifford (1959) due to its ability to account for short averaging time fluctuation.

Little research has been carried out to adapt and evaluate fluctuating plume models to predict odour dispersion. Hogström (1972) first proposed a fluctuating plume model to predict odour frequency based on the principles published by Gifford (1959). The comparisons between predicted and observed odour frequencies indicated that it is possible to make realistic prediction of odour frequencies near a point source. Bree and Harssema (1988) modified Hogström's model and evaluated it with field measurement around a point source, a building source, and an area source. They concluded that the modified model is superior for estimating odour exposures over Gaussian models based on hourly averages. Mussio et al. (2001) developed a fluctuating plume dispersion model to predict the odour-impact frequencies in the communities surrounding elevated point sources. The model provided good simulation of total frequencies of occurrence where the odour was frequent. Based on these countable studies, it appears that the fluctuating plume model even without considering in plume fluctuations could be an effective tool to predict odour dispersion at close downwind distance. At near source distance, the meandering of the plume has a greater effect on odour concentration fluctuations than the in-plume fluctuations (Bree and Harssema, 1988). Therefore, it will not result in large errors when used to predict odour frequency without considering in plume fluctuations. Moreover, the near source distances are where the odour researchers are mostly interested in because odour cannot travel to a far distance as industrial air contaminants. Hence, the

fluctuating plume model, that could provide better estimations of odour frequency compared to normally used Gaussian plume models, needs to be seriously considered as a tool to predict odour dispersion from livestock operations and more evaluations need to be done in order to eventually use it for regulatory purposes.

Gaussian plume dispersion model assumes that the average (hourly) concentration of a contaminant downwind of a source and perpendicular to the mean wind direction is normally distributed and centered along wind direction from a source (Figure 2.1(a)) (Mussio et al., 2001). However, a short averaging time plume has the appearance of a fluctuating plume in which plume meanders in the lateral and vertical directions are caused by the spatial distribution of large eddies in the flow (Figure 2.1(b)). The center of the instantaneous (short averaging time) plume fluctuates around the axis of the steady or long-term average plume in an irregular manner (Arya, 1999). The fluctuating plume model has been proposed to account for the presence of the instantaneous plumes.

The basic theory of the fluctuating plume model is that the total dispersion can be separated into two components, one represents the relative dispersion within the instantaneous plume, and the other represents the variance of the centroid of the fluctuating plume (Figure 2.1(c)) (Arya, 1999). The variation due to the fluctuations of local axis, σ_c^2, and the dispersion within the instantaneous plume, σ_p^2, are related to the dispersion of the long-term average plume, σ^2, which can be mathematically expressed as (Gifford, 1959):

$$\sigma_y^2 = \sigma_{yp}^2 + \sigma_{yc}^2 \tag{2.2a}$$

$$\sigma_z^2 = \sigma_{zp}^2 + \sigma_{zc}^2 \tag{2.2b}$$

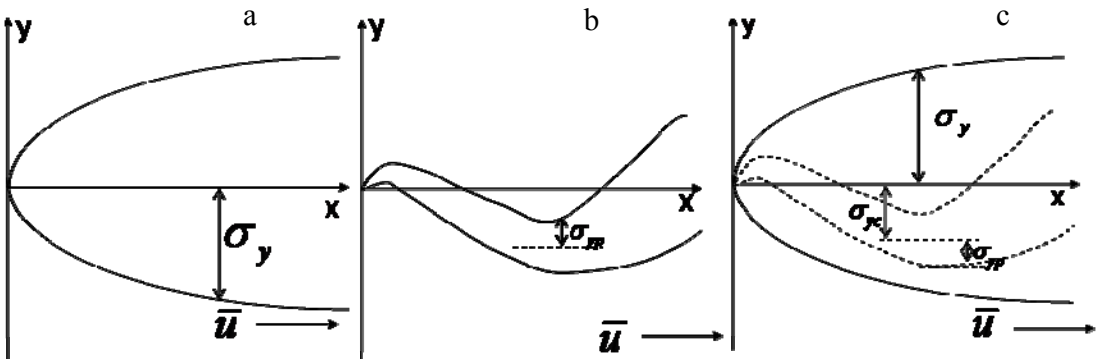

Figure 2.1 (a) Areal view of Gaussian plume model; (b) areal view of fluctuating plume model; (c) standard deviations of crosswind distances in the fluctuating plume model (adapted from Mussio et al., 2001).

2.2.1 Instantaneous Odour Concentrations

Gifford (1959) argued that it is reasonable to assume that the concentrations distribution within the instantaneous plume is also Gaussian. Considering the reflection of a ground level, the instantaneous or short averaging time odour concentration c in a receptor (x,y,z) downwind from an elevated point source can be calculated by the following equation from the fluctuating plume model:

$$C(x,y,z)=\frac{Q}{2\pi\bar{u}\sigma_{yp}\sigma_{zp}}\exp\left[-\frac{y_i^{\,2}}{2\sigma_{yp}^2}\right]\left\{\exp\left[-\frac{(z-h_i)^2}{2\sigma_{zp}^2}\right]+\exp\left[-\frac{(z+h_i)^2}{2\sigma_{zp}^2}\right]\right\} \tag{2.3}$$

where Q is the source odour emission rate (OU s^{-1}), $\bar{u}$ is the hourly average wind speed at effective stack height, m s^{-1}; σ_{yp} and σ_{zp} are the horizontal and vertical standard deviations of relative dispersion within the instantaneous plume, m; and y_i is crosswind distance from the center of the fluctuating plume to the receptors, m, and it can be calculated from $y - y_c$. y_c and h_i are the locations of the center of the instantaneous plume (m). They are also assumed to have a normal probability density function with the standard deviations of σ_{yc} and σ_{zc}, shown as (Arya, 1999):

$$p(y_c)=\frac{1}{(2\pi)^{1/2}\sigma_{yc}}\exp\left(-\frac{y_c^2}{2\sigma_{yc}^2}\right) \tag{2.4a}$$

$$p(h_i) = \frac{1}{(2\pi)^{1/2}\sigma_{zc}} \exp\left(-\frac{h_i}{2\sigma_{zc}^2}\right) \quad (2.4b)$$

In LODM, the restriction effect of mixing layer has been taken into account with all the calculations, which means that the vertical term in equation (2.3) will be modified as equation (2.1) with replacing H_e with h_i.

2.2.2 Odour Frequency

From equation (2.3), the instantaneous odour concentrations can be calculated given random generated values of y_c and h_i based on their respective standard deviations and the locations of receptors. Then the frequency of a certain odour level in an hour can be derived from the calculated sub-hour concentrations. This method was named as computed method. In the fluctuating plume model developed by Mussio et al. (2001), 200 random values were generated in an hour to calculate the frequency. Results showed that this method was effective at estimating the odour frequency. However, this frequency is based on random values, which increases its uncertainty. Hogström (1972) brought up the concept of weighted odorous half width to account for the vertical meandering of the plume and used an empirical formula to calculate the ground level odour frequency. This concept was followed by Bree and Harssema (1988). In their model, the ground level odour frequency was produced by consideration of the plume horizontal meandering. The method proposed in this study follows that of Bree and Harssema (1988), but it has been improved to account for more specified attributes of livestock odour dispersion. It can estimate the odour frequency for any odour level at any height of receptors (not only ground level) from any type of individual and multiple emission sources. The livestock odour dispersion model (LODM) developed in this study is specifically for livestock odour which emits from animal building sources and manure storage facilities sources.

Weighted odour exceeding half width

Under certain meteorological conditions, with certain odour emission rate and local instantaneous height h, equation (2.3) can be solved for y_i which describes the local, instantaneous half width of the area at z level that the odour is exceeding a certain level.

It is named as odour exceeding half width. This concept is adapted and improved from the odorous half width which was proposed by Hogström (1972) to indicate the local, instantaneous odorous area at the ground level. As shown in Figure 2.2(a), the local plume centroid is an ever differing height (h_i), and the odour exceeding half width is y_i. When the plume ascend or descend to some distant, the odour exceeding half width reaches zero as shown in Figure 2.2(b). With the aid of equation (2.3), the maximum height (h_{max}) and minimum height (h_{min}) can be determined with $y_i = 0$.

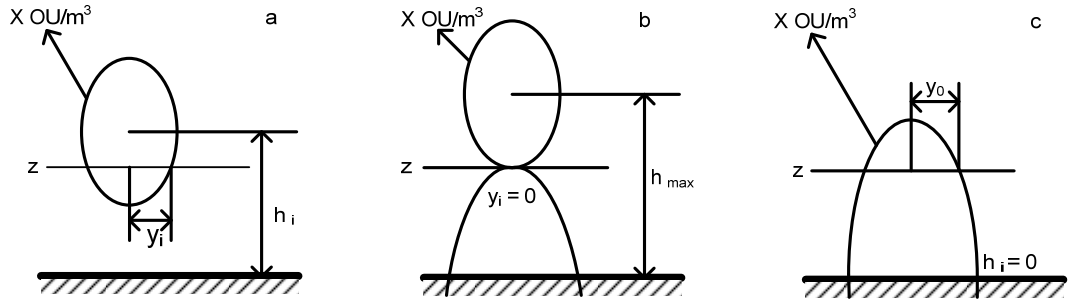

Figure 2.2 Schematic diagrams of cross sections of the odour exceeding part of the instantaneous plume at different heights (h_i) and the associated instantaneous odour exceeding half width (y_i) (adapted from Bree and Harssema,1988)

Taking into account the effect of ground level, the instantaneous height of plume can not fall under ground level, then a value of y_0 is gotten for $h_i = 0$, as shown in Figure 2.2(c). Now, the value of y_i is calculated for N equally spaced values (Δh) of h_i between $h_i = 0$ and $h_i = h_{max}$. In LODM, N is set to be 100. Then the weighted odour exceeding half width can be determined as the sum of the product of each y value and its probability:

$$\bar{y} = y_0 P_0 + \sum_{1}^{N} y_i P_i \tag{2.5}$$

where P_i can be defined as the portion of time that the local plume height h_i is confined to a given interval, $h_i \in \left[h_i - \frac{\Delta h}{2}, h_i + \frac{\Delta h}{2} \right]$. With the aid of the probability distribution of the value of h_i, given by the normal distribution defined by the hourly averaged vertical position of the plume centerline (the effective stack height, H_e) and the value of σ_{zc}, P_i is determined by the following expression:

$$p_i = \int_{h_i - H_e - \Delta h/2}^{h_i - H_e + \Delta h/2} \frac{1}{\sqrt{2\pi}\sigma_{zc}} \exp(-h^2/2\sigma_{zc}^2) dh \tag{2.6}$$

P_0 has the expression of:

$$p_0 = \int_{h_{\min} - H_e}^{-H_e} \frac{1}{\sqrt{2\pi}\sigma_{zc}} \exp(-h^2/2\sigma_{zc}^2) dh \tag{2.7}$$

Both P_i and P_0 can be shown as the shadow area beneath the normal distribution of the value of h_i (Figure 2.3(a)).

Odour frequency

In the fluctuating plume model, the crosswind horizontal position of the local instantaneous plume centroid meandering around the averaged horizontal position (hourly mean wind direction) of the steady plume axis. In a point R(x,y,z), the odour frequency is the portion of time that the horizontal position of the local instantaneous plume centroid locates in the range from $(y - \bar{y})$ to $(y + \bar{y})$. With the aid of the normal distribution of the value of the horizontal position of local plume, the odour frequency is shown as the shadow area in Figure 2.3(b), and is calculated by the following expression:

$$p = \int_{y - \bar{y}}^{y + \bar{y}} \frac{1}{\sqrt{2\pi}\sigma_{yc}} \exp(-y^2/2\sigma_{yc}^2) dy \tag{2.8}$$

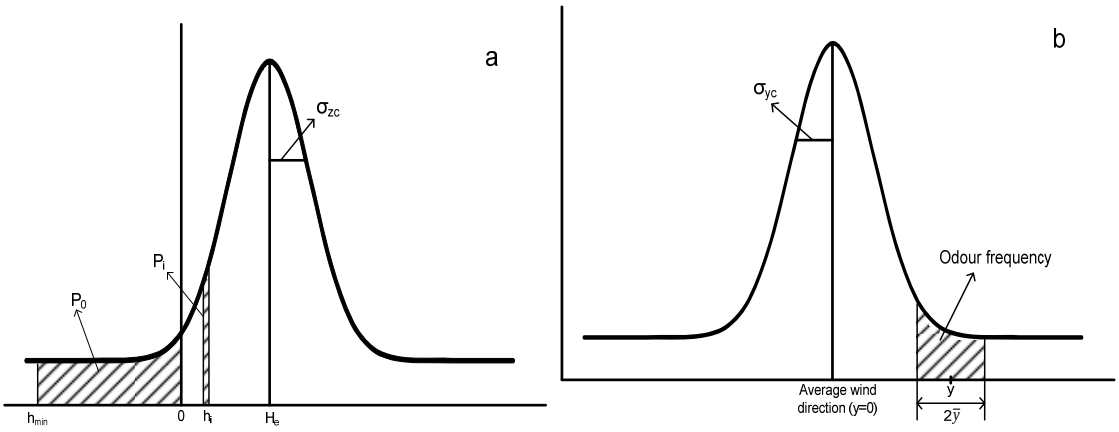

Figure 2.3 Schematic diagrams of the portion of time for the different odour exceeding widths (a) and the odour frequency (b)

2.2.3 Peak Odour Concentration

From equation (2.3), the maximum odour concentration occurs when y_i equals to zero and h equals to zero or z. It means that at a receptor, the maximum odour concentration occurs when the fluctuating plume centerline is at the location of the receptor horizontally and either at the ground level or at the receptor height vertically. Hence, the maximum odour concentration takes the form of:

$$C_p = \frac{Q}{\pi \bar{u} \sigma_{yp} \sigma_{zp}} \exp\left[-\frac{z^2}{2\sigma_{zp}^2}\right] \tag{2.9a}$$

or

$$C_p = \frac{Q}{2\pi \bar{u} \sigma_{yp} \sigma_{zp}} \left\{1 + \exp\left[-\frac{(2z)^2}{2\sigma_{zp}^2}\right]\right\} \tag{2.9b}$$

The peak odour concentration is the maximum value of C_p values calculated from equation (2.9a) and equation (2.9b).

Therefore, the peak to mean ratio that has a great application can be easily determined. This ratio depends on the short time dispersion coefficients, hourly dispersion coefficients, and location of the receptor. For the ground level receptors, without

considering the restriction effect of mixing layer, the peak to mean ratios can be described as:

$$R_p = \frac{\sigma_y \sigma_z}{\sigma_{yp} \sigma_{zp}} \tag{2.10}$$

Arya (1999) referred the ratio of the maximum centerline concentrations in fluctuating and steady plumes as the ratio of peak to average concentration, which takes the same form as equation (2.10).

2.3 STACK-TIP DOWNWASH AND PLUME RISE

If odour is emitted from an elevated point source, the stack tip downwash and plume rise will be calculated. The calculations follows the procedures described in ISC model (Bowers et al., 1979), which used the Briggs model to estimate the plume rise. The procedure of the calculations can be found in Appendix A, while readers can refer to the ISC Guiders (Bowers et al., 1979) for more details.

2.4 DISPERSION COEFFICIENTS

2.4.1 Pasquill-Gifford Mean Dispersion Coefficients

Equations that approximately fit the Pasquill-Gifford curves (Turner, 1970) are used to calculate σ_y and σ_z (in meters) for the rural area. The equations used to calculate σ_y are (Bowers et al., 1979):

$$\sigma_y = K \cdot x \cdot \tan\left(a - b \ln x\right) \tag{2.11}$$

The equation used to calculate σ_z is:

$$\sigma_z = c \cdot x^d \tag{2.12}$$

where, x is the downwind distance in kilometres. K is a constant. The parameters a and b depend on the stability class while c, d are not only related to stability class but also the downwind distance.

Buoyancy – induced dispersion

The method that used in ISC model (Bowers et al., 1979) is adopted to account for the initial dispersion of plumes caused by turbulent motion of the plume and turbulent entrainment of ambient air. Therefore, the effective dispersion is calculated as follows:

$$\sigma = \left[\sigma_0^2 + \left(\frac{\Delta h}{3.5}\right)^2\right]^{1/2} \quad (2.13)$$

where, σ is the dispersion due to ambient turbulence and Δh is the plume rise. This equation is used to account for both vertical and horizontal buoyancy-induced dispersion.

Adjusted P-G dispersion coefficient for surface roughness

The presence of topographic features and vegetation increase the ground surface roughness. For stable and neutral atmospheric conditions, the surface roughness increases vertical mixing of the plume, because the enhanced mechanical turbulence generates as the air moves over the ground (EPA, 2000).

The Pasquill-Gifford vertical dispersion coefficient was adjusted followed the suggestion of Smith (1972).

$$\sigma_{za} = \sigma_z[1.585 z_0^{0.1301}(0.001x)^B] \quad (2.14)$$

where :

$$B = 0.0777 + 0.0215 \ln(z_0) \quad (2.15)$$

X is the downwind distance, m; and Z_0 is the surface roughness, m.

2.4.2 Pasquill-Gifford Short Time Dispersion Coefficients

When Pasquill-Gifford dispersion coefficients are used, no existing formulas are related to the short time dispersion coefficients. Ratios of Hogstrŏm short time dispersion coefficients and one-hour mean dispersion coefficients are applied to get the P-G short time dispersion coefficients by the following formulas:

$$\frac{\sigma_{yp}}{\sigma_y}(P-G)=\frac{\sigma_{yp}}{\sigma_y}(Hogstr\ddot{o}m) \tag{2.16a}$$

$$\frac{\sigma_{zp}}{\sigma_z}(P-G)=\frac{\sigma_{zp}}{\sigma_z}(Hogstr\ddot{o}m) \tag{2.16b}$$

where, P-G indicates that the dispersion coefficients are following the Pasquill-Gifford's method; Hogstrŏm indicates that the dispersion coefficients are calculated using Hogstrŏm's method.

2.4.3 Hogstrŏm Dispersion Coefficients

Hogstrŏm (1968, 1972) developed a series of general formulas to carry out the calculation of both one-hour (mean) (σ_y and σ_z) and short time (σ_{yp} and σ_{zp}) dispersion parameters from the experiments conducted in Sweden for elevated point continuous release. At the same time, a method was proposed for ground level release. The Hogstrŏm dispersion coefficients depend on the distance and the stability condition. Their calculations can be observed in Appendix B and Hogstrŏm (1968, 1972). It needs to be noted that the stability used in the calculations is different from the Pasquill-Gifford stability. The Hogstrŏm stability parameter is defined as:

$$s=\left(\frac{\partial\theta}{\partial z}\Big/u_f^2\right)\cdot 10^5 \tag{2.17}$$

in which $\frac{\partial\theta}{\partial z}$ is the vertical gradient of potential temperature at the level of the plume centre, K m^{-1}; u_f is the wind speed at the top of friction layer, m s^{-1}. Both parameters cannot be obtained directly from routinely observed meteorological data. Therefore, the profile of vertical gradient of temperature and the profile of wind speed need to be characterized so that the Hogstrŏm stability parameter can be achieved.

2.5 PARAMETERS USED TO CHARACTERIZE PBL

The Monin-Obukhov similarity theory was used to estimate the vertical profile of wind speed and vertical gradient of potential temperature which determine the Hogstrŏm stability parameter (s). The Monin-Obukhov similarity theory has been widely accepted to characterize PBL (Ayra, 1999). It is based on the similarity hypothesis proposed by Monin and Obukhov (1954). The parameters used in the theory to represent the boundary layer are friction velocity (u_*), Monin-Obukhov length (L_{mo}), friction temperature (θ_*), mixing height (z_i), and surface heat flux (H_s). These parameters can be derived both in the convective boundary layer (CBL) and stable boundary layer (SBL). The methods used to derive the parameters as well as profile of vertical gradient of potential temperature and wind speed are following those used in AERMED model (US EPA, 2004).

2.5.1 Surface Energy Budget and Net Radiation

The surface energy budget relates the net radiation R_n to the various heat fluxes on the earth's surface (Oke, 1978):

$$H_s + \lambda E + G = R_n \tag{2.18}$$

Where, H_s is the sensible heat flux, W m^{-2}; λE is the latent heat flux, W m^{-2}; G is the soil heat flux, W m^{-2}. After making some simple parameterizations, that is $G = 0.1\, R_n$, and $\lambda E = H_s/B_0$, B_0 is the Bowen ratio of the surface, equation (2.18) becomes (Holtslag and van Ulden, 1983):

$$H_s = \frac{0.9\, R_n}{(1+\frac{1}{B_0})} \tag{2.19}$$

The net radiation can be estimated from the insolation and the thermal radiation balance at the ground following the method of Holtslag and van Ulden (1983):

$$R_n = \frac{(1-r)R+c_1 T_{ref}^6-\sigma_{SB} T_{ref}^4+c_2 n}{1+c_3} \tag{2.20}$$

In which c_1 = 5.31×10-13 W m^{-2} K^{-6}; c_2 = 60 W m^{-2}; c_3 = 0.12; σ_{SB} is the Stefan Boltzmann constant (5.67 ×10^{-8} W m^{-2} K^{-4}); T_{ref} is the reference air temperature, K; R is the solar radiation, W m^{-2}; and n is the cloud cover. If the solar radiation (R) is available, the cloud cover (n) is assumed to be 0.5, and then the net radiation can be easily obtained. If it is not available, it can be estimated from the cloud cover and clear sky radiation by the follows (Holtslag and van Ulden, 1983):

$$R = R_0(1 - 0.75n^{3.4}) \tag{2.21}$$

R_0 is the clear sky radiation for the certain location and certain date and time. It can be calculated from Holtslag and van Ulden (1983):

$$R_0 = 990 \sin\varphi - 30 \tag{2.22}$$

φ is the solar elevation angle, rad, which varies throughout a day. It also depends on the latitude of a particular location and the day of a year. The calculation of solar elevation angle can be found in Appendix C.

2.5.2 Identification of CBL or SBL

Since the methods for deriving parameters involving friction velocity and Monin-Obukhov length are different between CBL and SBL, it is necessary to distinguish the atmospheric conditions as convective or stable. When the PBL transits from convective to stable condition, the heat flux changes from positive to negative. Therefore, the net radiation will be zero, when the transition happens. By setting R_n equal to zero in equation (2.20), the solar elevation angle, $\boldsymbol{\varphi_t}$, which is the transition point between CBL and SBL, can be determined from

$$\boldsymbol{\sin\varphi_t = \frac{1}{990}\left[\frac{-c_1 T_{ref}^6 + \sigma_{SB} T_{ref}^4 - c_2 n}{(1-r)(1-0.75n^{3.4})} + 30\right]} \tag{2.23}$$

If the actual solar elevation angle is greater than $\boldsymbol{\varphi_t}$, the atmospheric condition is considered to be convective; While if the actual solar elevation is less than $\boldsymbol{\varphi_t}$, the atmospheric condition is stable. In AERMET (US EPA, 2004), if solar radiation measurements are available, $\boldsymbol{\varphi_t}$ is determined from an estimate of cloud cover (n_e), which

is shown as $\boldsymbol{n_e} = \left(\frac{(\mathbf{1}-\boldsymbol{R}/\boldsymbol{R_0})}{\mathbf{0.75}}\right)^{\mathbf{1/3.4}}$. This equivalent cloud cover is also adopted in LODM, when the solar radiation measurements are available.

2.5.3 Parameters Derived for CBL

The friction velocity u_* can be estimated by (Panofsky and Dutton, 1984):

$$u_* = \frac{k u_{ref}}{\ln(z_{ref}/z_0) - \psi_m\{z_{ref}/L_{mo}\} + \psi_m\{z_0/L_{mo}\}} \tag{2.24}$$

where k is the van Karman constant, k = 0.4; u_{ref} is the wind speed at the reference height, m s^{-1}; z_{ref} is the reference height, m; and z_0 is the roughness length, m. The stability term can be computed as:

$$\psi_m\{z_{ref}/L_{mo}\} = 2\ln\left(\frac{1+\mu}{2}\right) + \ln\left(\frac{1+\mu^2}{2}\right) - 2\tan^{-1}\mu + \pi/2 \tag{2.25a}$$

$$\psi_m\{z_0/L_{mo}\} = 2\ln\left(\frac{1+\mu_0}{2}\right) + \ln\left(\frac{1+\mu_0^2}{2}\right) - 2\tan^{-1}\mu_0 + \pi/2 \tag{2.25b}$$

and $\mu = (1 - 16\, z_{ref}/L_{mo})^{1/4}$, $\mu_0 = (1 - 16\, z_0/L_{mo})^{1/4}$

The Monin_Obukhov length (L_{mo}) can be defined as:

$$L_{mo} = -\frac{\rho c_p T_{ref} u_*^3}{k g H_s} \tag{2.26}$$

where g is the acceleration of gravity, g = 9.8 m s^{-2}; c_p is the specific heat of air at constant pressure, J g^{-1} K^{-1}; ρ is the density of the air, g m^{-3}.

In a convective layer, the sensible heat flux H_s can be obtained with equation (2.19) if net radiation and Bowen ratio are known. Knowing the value of H_s, it can be found from equation (2.24) and equation (2.26) that friction velocity and Monin_Obukhov length depend on each other. An iterative method is used to determine both u_* and L_{mo}. First, an initial value of u_* is calculated under the assumption of neutral conditions ($L_{mo} = \infty$, thus $\psi_m\{z_{ref}/L_{mo}\} = 0$ and $\psi_m\{z_0/L_{mo}\} = 0$), then L_{mo} and u_* can be iteratively recalculated until the value of L_{mo} changes by less than a tolerant value (e.g. 0.0001).

2.5.4 Parameters Derived for SBL

Venkatram (1980) suggested an empirical method to compute friction velocity (u_*) and Monin-Obuhkov length (L_{mo}) in the stable boundary layer from routine meteorological measurements. This method has been applied by US EPA AERMOD model (US EPA, 2004). It is also applied in LODM to derive the parameters for SBL.

The Monin_Obukhov length (L_{mo}) can also be defined as (Venkatram,1980):

$$L_{mo} = \frac{T_{ref}}{kg\theta_*} u_*^2 \tag{2.27}$$

where, θ_* is the friction temperature, and can be defined as (Arya, 1999):

$$\theta_* = -\frac{H_s}{\rho c_p u_*} \tag{2.28}$$

The wind speed profile in stable conditions takes the form of (Venkatram,1980):

$$u = \frac{u_*}{k}\left[\ln\left(\frac{z}{z_0}\right) + \frac{\beta_m z_{ref}}{L_{mo}}\right] \tag{2.29}$$

where β_m = 5. Substituting equation (2.27) into equation (2.29) and defining the drag coefficient, C_D, as $k/\ln(z_{ref}/z_0)$, after some algebraic transformation, results in;

$$u_*^2 - C_D u u_* + C_D u_0^2 = 0 \tag{2.30}$$

where $u_0 = (\frac{\beta_m z_{ref} g\theta_*}{T_{ref}})^{1/2}$.

This quadratic has a solution when the wind speed is greater than or equal to the critical value $u_{cr} = \left[4\frac{\beta_m z_{ref} g\theta_*}{T_{ref} C_D}\right]^{1/2}$, which has the form:

$$u_* = \frac{C_D u_{ref}}{2}\left[1 + \left(1 - \left(\frac{2u_0}{C_D^{1/2} u_{ref}}\right)^2\right)^{1/2}\right] \tag{2.31}$$

In stable conditions, the friction temperature can be calculated from the empirical form from cloud cover as (van Ulden and Holslag, 1985):

$$\theta_* = 0.09(1 - 0.5n^2) \tag{2.32}$$

where n is the fractional cloud cover.

For the wind speed less than the critical value, u_* and θ_* are parameterized by:

$$u_* = u_*\{u = u_{cr}\}\,(u/u_{cr}) \tag{2.33}$$

$$\theta_* = \theta_*\,(u/u_{cr}) \tag{2.34}$$

The surface sensible heat flux of stable conditions can be calculated by:

$$H_s = -\rho c_p u_* \theta_* \tag{2.35}$$

Since the maximum value of $u_*\theta_*$ cannot exceed 0.05 m s^{-1} K (Hanna et al., 1986), when it happens, u_* is recalculated by substituting $0.05/u_*$ into equation (15) for θ_*. The Monin-Obukhov length (L_{mo}) is calculated from equation (2.27).

2.6 VERTICAL WIND SPEED PROFILE

2.6.1 P-G Scheme

When Pasquil-Gifford scheme of dispersion parameters are used, the observed wind speed, u_{ref}, from a reference measurement height, z_{ref}, is adjusted to the stack or release height, H_e (Bower et al, 1979). If the stack height (H) is larger than z_{ref}, then:

$$u_s = u_{ref} * (\frac{H_e}{z_{ref}})^p \tag{2.36}$$

Else:

$$u_s = u_{ref} \tag{2.37}$$

The value of p depends on atmospheric stability class, shown as Table 2.1. If wind speed at stack height is less than 1 m s^{-1}, 1 m s^{-1} is assigned to it.

Table 2.1 Parameters to determine wind speed profile with P-G stability class (USEPA, 2000)

Stability Class	1	2	3	4	5	6
P	0.07	0.07	0.1	0.15	0.35	0.55

2.6.2 Hogstrŏm Scheme

The vertical profile equation for wind speed takes a logarithmic form (US EPA, 2004):

$$u = u\{7z_0\}\left[\frac{z}{7z_0}\right] \quad \text{for } z < 7z_0 \tag{2.38a}$$

$$u = \frac{u_*}{k}\left[\ln\left(\frac{z}{z_0}\right) - \Psi_m\left\{\frac{z}{L_{mo}}\right\} + \Psi_m\left\{\frac{z_0}{L_{mo}}\right\}\right] \quad \text{for } 7z_0 \leq z \leq z_i \tag{2.38b}$$

$$u = u\{z_i\} \quad \text{for } z > z_i \tag{2.38c}$$

For neutral conditions, $\Psi_m\left\{\frac{z}{L_{mo}}\right\}$ and $\Psi_m\left\{\frac{z_0}{L_{mo}}\right\}$ are zero; for unstable conditions, they are estimated by replacing z_{ref} with z in equation (2.25); for stable conditions, they are calculated from van Ulden and Holtslag (1985) and expressed as:

$$\Psi_m\left\{\frac{z}{L_{mo}}\right\} = -17\left[1 - \exp(-0.29\frac{z}{L_{mo}})\right] \tag{2.39a}$$

$$\Psi_m\left\{\frac{z_0}{L_{mo}}\right\} = -17\left[1 - \exp(-0.29\frac{z_0}{L_{mo}})\right] \tag{2.39b}$$

2.7 VERTICAL GRADIENT OF POTENTIAL TEMPERATURE

When P-G dispersion parameters are used, the vertical gradient of potential temperature need to be considered when estimating the plume rise under stable conditions (Stability class E and F). As a default approximation, for stability class E (or 5), $\partial\theta/\partial z$ is taken as 0.020 K m^{-1}, and for class F (or 6), $\partial\theta/\partial z$ is taken as 0.035 K m^{-1}.

When using Hogstrŏm dispersion parameters, the vertical temperature gradient was determined by the derived parameters of SBL (θ_*, L_{mo}) (US EPA, 2004). Below 100 m, the definition of the potential temperature gradient suggested by Dyer (1974) and Panofsky and Dutton (1984) can be used to estimate it. Combined with the methods from Stull (1983) and van Ulden and Holtslag (1985), the gradient of potential temperature can be calculated as,

$$\frac{\partial\theta}{\partial z} = \frac{\theta_*}{2k}\left[1 + 5\frac{2}{L_{mo}}\right] \quad \text{for } z \leq 2 \text{ m} \tag{2.40a}$$

$$\frac{\partial\theta}{\partial z} = \frac{\theta_*}{zk}\left[1 + 5\frac{z}{L_{mo}}\right] \quad \text{for } 2\text{ m} < z \leq 100\,m \tag{2.40b}$$

$$\frac{\partial\theta}{\partial z} = \frac{\partial\theta}{\partial z}\{100\}\exp\left[-\frac{(z-100)}{0.44z_{i\theta}}\right] \quad \text{for} \quad z > 100\,m \tag{2.40c}$$

where $z_{i\theta} = \max(z_i; 100)$. Paine and Kendall (1993) pointed out that $\frac{\partial\theta}{\partial z}$ is limited to a minimum of 0.002 K m^{-1}, therefore when the calculated $\frac{\partial\theta}{\partial z}$ is less than 0.002 k m^{-1}, it is assigned to be 0.002 k m^{-1}.

2.8 TREATMENT OF ISC MET FILE

From section 2.5, the atmospheric parameters in both CBL and SBL can be derived from surface meteorological data. Required inputs include wind speed, ambient temperature, solar radiation or cloud cover. However, LODM intends to be implemented with an input as simple as ISC met file which excludes the solar radiation and cloud cover. A method is proposed to derive the atmospheric parameters from the ISC met input by converting the P-G stability categories into solar radiations or cloud covers.

The P-G stability class is determined by surface wind speed, cloud cover or solar radiation. When the Pasquill stability categories are originally defined, Table 2.2 provides a key to determine them.

Another method used to determine P-G stability class is solar radiation/delta-T (SRDT). The method, outlined in Table 2.3, uses the surface layer wind speed in combination with measurements of total solar radiation during a day and a low-level vertical temperature difference (ΔT) at night.

Table 2.2 Key to the Pasquill stability categories (USEPA, 2000)

Surface wind speed (m/s)	Daytime Insolation			Nighttime cloud cover	
	Strong	Moderate	Slight	Thinly overcast or ≥ 4/8 low	≤ 3/8
<2	A	A-B	B	-	-
2-3	A-B	B	C	E	F
3-5	B	B-C	C	D	E
5-6	C	C-D	D	D	D
>6	C	D	D	D	D

Strong insolation corresponds to sunny, midday, midsummer conditions in England; slight insolation corresponds to similar conditions in midwinter. Night refers to the period from one hour before sunset to one hour after sunrise. The neutral category, D, should be used regardless of wind speed, for overcast conditions during day or night.

Table 2.3 Key to SRDT method for estimating P-G stability categories (US EPA, 2000)

Day time

Wind speed (m/s)	Solar Radiation (W m^{-2})			
	≫925	925-675	675-175	<175
<2	A	A	B	D
2-3	A	B	C	D
3-5	B	B	C	D
5-6	C	C	D	D
≫6	C	D	D	D

Night time

Wind speed (m/s)	Vertical Temperature Gradient	
	<0	≥0
<2.0	E	F
2.0-2.5	D	E
≥2.5	D	D

Combined these two methods, the P-G stability categories can be determined from cloud cover at nighttime and solar radiation in daytime. Using the average solar radiation or cloud cover to represent the values of each category, the relationship between P-G stability categories and wind speed, solar radiation or cloud cover can be achieved and listed in Table 2.4. In Table 2.4, R_0 is the clear sky solar radiation of the current hour. When R_0 is less than the upper bound of the range, the average is taken by R_0 and the lower bound of the range. For example, when wind speed is less than 2 m s^{-1}, for stability class B, the solar radiation should be in the range of 175 to 675 W m^{-2}. If R_0 is greater than 675 W m^{-2}, the average value will be 425 W m^{-2}; while if R_0 is less than 675 W m^{-2}, the average value will be $(R_0+175)/2$ W m^{-2} instead.

Table 2.4 Representative solar radiation or cloud cover values for different P-G stability class

Wind speed	Solar radiation, W m^{-2}			Cloud cover	
	A	B	C	E	F
<2	$(R_0+675)/2$	425 or $(R_0+175)/2$	-	-	-
2-3	$(R_0+925)/2$	800 or $(R_0+675)/2$	425 or $(R_0+175)/2$	6/8	3/16
3-5	-	$(R_0+675)/2$	425 or $(R_0+175)/2$	3/16	-
5-6	-	-	$(R_0+675)/2$	-	-
≫6	-	-	$(R_0+925)/2$	-	-

Based on these representative values of solar radiation and cloud cover for each wind speed and P-G stability class combination, the atmospheric parameters (friction velocity, Monin-Obukhov length, friction temperature) can be derived by the methods discussed in section 2.5. Hence, the vertical profile of wind speed and vertical gradient of potential temperature can be calculated by the methods in section 2.6 and 2.7.

For neutral conditions (D), the Monin-Obukhov length is assumed to be infinite (USEPA, 2004). The friction velocity can be defined as:

$$u_* = \frac{ku_{ref}}{\ln(z_{ref}/z_0)} \quad (2.41)$$

Therefore, the wind speed profile for neutral conditions can also be determined as described in section 2.6.

2.9 ADAPTING THE MODEL FOR LIVESTOCK ODOUR DISPERSION

The fluctuating plume model proposed above to estimate odour concentration and odour frequency is adapted into livestock odour dispersion with the considerations of different source characteristics and persistence of various odours.

2.9.1 Odour Emission from Elevated Stack

If the odour is emitted from an elevated stack, the source can be treated as a point source with a physical stack height. The plume rise will be calculated with Briggs plume rise formula.

2.9.2 Odour Emission from Animal Building

Odour emission from an animal building is from the exhaust air outlets which are the openings on the walls and roofs of the building and the wall or ceiling mounted fans. There are often a number of vertical or horizontal openings or fans for one building. Due to the complicated pattern of the openings and fans and the effect of building, it is reasonable to consider the building source as a whole volume source.

A virtual point source algorithm is used to model the odour released from volume sources. An imaginary or virtual point source is located at a certain distance upwind of the volume source (called the virtual distance) to account for the initial size of the volume source plume. Therefore, the equations used for a point source are also applied to calculate odour concentrations and odour frequency produced by volume source emissions.

The initial lateral (σ_{y0}) and vertical (σ_{z0}) dimensions should be assigned. Normally, it can be determined from the building dimension.

$$\sigma_{y0} = \frac{W}{4.3} \tag{2.42a}$$

$$\sigma_{z0} = \frac{H}{2.15} \tag{2.42b}$$

In which W is the width of building, m; and H is the height of building, m.

Then the visual lateral x_y and vertical distance x_z can be calculated with the aid of the initial dimensions and the formulas of dispersion coefficients' calculation. The concentrations or frequency in a downwind distance can be calculated by the same equations as used for a point source, with the modification of:

$$\sigma_y = \sigma_y(x + x_y) \tag{2.43a}$$

$$\sigma_z = \sigma_z(x + x_z) \tag{2.43b}$$

2.9.3 Odour Emission from Manure Storage

A source of manure storage can be treated as an area source. The same treatment will be used as a volume source with only consideration of lateral initial dimension.

2.9.4 Multiple Sources

The odour from livestock operations are often from by multiple sources. The impact of odours from multiple sources on a receptor is challenging. The odours from different sources have different persistences, which means after the same dilution, the odour strengths are different. Then the combined impact on receptors is very difficult to be evaluated. A simple and coarse method is used to account for multiple sources when dealing with odour concentrations, which should be improved with the further research on combining odour impact with different persistences. For an instant, two sources (Source 1 and Source 2) with emission rate of Q1 and Q2 have the odour impact on a receptor. Under certain meteorological conditions, the concentration of odour from source 1 is X_1, and X_2 from source 2. Assuming both odours have the same persistences,

then the odour concentration at the receptor is X_1+X_2. The contribution from these two sources is converted to be from only one source (for example, source 1) by combining an emission rate Q into this source (source 1) that has the same impact as the other (source 2), in which:

$$\frac{Q}{Q2} = \frac{X1}{X2} \tag{2.44}$$

However, this method is not applicable when calculating odour frequency from multiple sources. The odour frequency calculated by the weighted odour exceeding width method takes the form of:

$$p = \int_{y_i-\bar{y}}^{y_i+\bar{y}} \frac{1}{\sqrt{2\pi}\sigma_{yc}} \exp(-y^2/2\sigma_{yc}^2)dy \tag{2.8}$$

in which $\bar{y}$ is the function of the certain level of odour concentration.

If there are two sources that contribute to a receptor, the odour frequency from each source that exceeds a certain level (c_0) can be expressed as:

$$p(c_1 \geq c_0) = \int_{a(c_0)}^{b(c_0)} f(y)dy \tag{2.45a}$$

$$p(c_2 \geq c_0) = \int_{m(c_0)}^{n(c_0)} g(y)dy \tag{2.45b}$$

In which, f(y) and g(y) refer to the general forms of $(\frac{1}{\sqrt{2\pi}\sigma_{yc}}\exp(-y^2/2\sigma_{yc}^2))$, which are functions of crosswind distance y; $a(c_0)$ and $m(c_0)$ are the general forms of $(y_i - \bar{y})$, which are functions of certain level odour c_0; and $b(c_0)$ and $n(c_0)$ are the general forms of $(y_i + \bar{y})$, which are also functions of c_0.

To calculate the odour frequency of multiple sources, which is $p(c_1 + c_2 \geq c_0)$, the range of 0 to c_0 is separated into N equal pieces, each piece has a value of Δc. If the odour concentration from one source is equal or greater than c_0, then the total odour concentration from two sources will be equal or greater than c_0 regardless of the odour

concentration from the second source. Under this circumstance, the total odour frequency will be $p(c_1 \geq c_0) \cdot p(c_2 \geq 0)$ or $p(c_1 \geq c_0)$. If the odour concentration from one source is within the range from $(c_0 - \Delta c)$ to c_0, the total odour concentration will be equal or greater than c_0 only if the odour concentration from the second source is equal or greater than Δc. Therefore, the total odour frequency will be $p\big(c_0 \geq c_1 \geq (c_0 - \Delta c)\big) \cdot p(c_2 \geq \Delta c)$. By the same token, the total odour frequency can be obtained as:

$$p(c_1 + c_2 \geq c_0) = p(c_1 \geq c_0) \cdot p(c_2 \geq 0) + p\big(c_0 \geq c_1 \geq (c_0 - \Delta c)\big) \cdot p(c_2 \geq \Delta c) + p\big((c_0 - \Delta c) \geq c_1 \geq (c_0 - 2\Delta c)\big) \cdot p(c_2 \geq 2\Delta c) + p\big((c_0 - 2\Delta c) \geq c_1 \geq (c_0 - 3\Delta c)\big) \cdot p(c_2 \geq 3\Delta c) + \cdots + p\big((c_0 - (n-2)\Delta c) \geq c_1 \geq (c_0 - (n-1)\Delta c)\big) \cdot p(c_2 \geq (n-1)\Delta c) + p\big((c_0 - (n-1)\Delta c) \geq c_1 \geq (c_0 - (n)\Delta c)\big) \cdot p(c_2 \geq c_0) \quad (2.46)$$

Substituting $P_1(c)$ and $P_2(c)$ from equation (2.45) into equation (2.46), the total odour frequency can be expressed as:

$$P(c_1 + c_2 \geq c_0) = \int_{a(c_0)}^{b(c_0)} f(x)dx + \left(\int_{a(c_0-\Delta c)}^{b(c_0-\Delta c)} f(x)dx - \int_{a(c_0)}^{b(c_0)} f(x)dx\right) \cdot \int_{m(\Delta c)}^{n(\Delta c)} g(x)dx + \left(\int_{a(c_0-2\Delta c)}^{b(c_0-2\Delta c)} f(x)dx - \int_{a(c_0-\Delta c)}^{b(c_0-\Delta c)} f(x)dx\right) \cdot \int_{m(2\Delta c)}^{n(2\Delta c)} g(x)dx + \left(\int_{a(c_0-3\Delta c)}^{b(c_0-3\Delta c)} f(x)dx - \int_{a(c_0-2\Delta c)}^{b(c_0-2\Delta c)} f(x)dx\right) \cdot \int_{m(3\Delta c)}^{n(3\Delta c)} g(x)dx + \cdots + \left(\int_{a(c_0-(n-2)\Delta c)}^{b(c_0-(n-2)\Delta c)} f(x)dx - \int_{a(c_0-(n-3)\Delta c)}^{b(c_0-(n-3)\Delta c)} f(x)dx\right) \cdot \int_{m((n-2)\Delta c)}^{n((n-2)\Delta c)} g(x)dx + \left(\int_{a(c_0-(n-1)\Delta c)}^{b(c_0-(n-1)\Delta c)} f(x)dx - \int_{a(c_0-n(n-2)\Delta c)}^{b(c_0-(n-2)\Delta c)} f(x)dx\right) \cdot \int_{m((n-1)\Delta c)}^{n((n-1)\Delta c)} g(x)dx + \left(1 - \int_{a(c_0-(n-1)\Delta c)}^{b(c_0-(n-1)\Delta c)} f(x)dx\right) \cdot \int_{m(c_0)}^{n(c_0)} g(x)dx \quad (2.47)$$

After some algebraic transformations, it becomes:

$$P(c_1 + c_2 \geq c_0) = \int_{a(c_0)}^{b(c_0)} f(x)dx + \int_{a(c_0-\Delta c)}^{b(c_0-\Delta c)} f(x)dx \cdot \int_{m(\Delta c)}^{n(\Delta c)} g(x)dx + \int_{a(c_0-2\Delta c)}^{b(c_0-2\Delta c)} f(x)dx \cdot \int_{m(2\Delta c)}^{n(2\Delta c)} g(x)dx + \cdots + \int_{a(c_0-(n-2)\Delta c)}^{b(c_0-(n-2)\Delta c)} f(x)dx \cdot \int_{m((n-2)\Delta c)}^{n((n-2)\Delta c)} g(x)dx + \int_{a(c_0-(n-1)\Delta c)}^{b(c_0-(n-1)\Delta c)} f(x)dx \cdot \int_{m((n-1)\Delta c)}^{n((n-1)\Delta c)} g(x)dx + \int_{m(c_0)}^{n(c_0)} g(x)dx - \left(\int_{a(c_0)}^{b(c_0)} f(x)dx \cdot\right.$$

$$\int_{m(\Delta c)}^{n(\Delta c)} g(x)dx + \int_{a(c_0-\Delta c)}^{b(c_0-\Delta c)} f(x)dx \cdot \int_{m(2\Delta c)}^{n(2\Delta c)} g(x)dx + \cdots + \int_{a(c_0-(n-2)\Delta c)}^{b(c_0-(n-2)\Delta c)} f(x)dx \cdot \int_{m((n-1)\Delta c)}^{n((n-1)\Delta c)} g(x)dx + \int_{a(c_0-(n-1)\Delta c)}^{b(c_0-(n-1)\Delta c)} f(x)dx \cdot \int_{m(c_0)}^{n(c_0)} g(x)dx \Big) \quad (2.48)$$

It can be integrated as:

$$P(c_1 + c_2 \geq c_0) = \int_0^{c_0} \left(\int_{a(z)}^{b(z)} f(x)dx \cdot \int_{m(c_0-z)}^{n(c_0-z)} g(x)dx \right) dz - \int_{\Delta c}^{c_0} \left(\int_{a(z)}^{b(z)} f(x)dx \cdot \int_{m(c_0+\Delta c-z)}^{n(c_0+\Delta c-z)} g(x)dx \right) dz \quad (2.49)$$

Equation (2.49) is the general form of calculating the odour frequency from two sources.

In order to simplify the calculation, especially for more than 2 sources, we assume $\Delta c = c_0$ to get:

$$p(c_1 + c_2 \geq c_0) = \int_{a(c_0)}^{b(c_0)} f(x)dx + \int_{m(c_0)}^{n(c_0)} g(x)dx - \int_{a(c_0)}^{b(c_0)} f(x)dx \cdot \int_{m(c_0)}^{n(c_0)} g(x)dx$$

$$= p(c_1 \geq c_0) + p(c_2 \geq c_0) - p(c_1 \geq c_0) \cdot p(c_2 \geq c_0) \quad (2.50)$$

Equation (2.50) is equivalent to what we can get if we assume that c_1 and c_2 are independent. Then, the probability of $(c_1+c_2) \geq c_0$ is the probability of $c_1 \geq c_0$ or $c_2 \geq c_0$, which has the same form as equation (2.50).

If there are more than two sources, the following procedure can be taken to estimate the overall frequency. First, odour frequency from any two source is calculated using the method above, and then this calculated odour frequency is assumed to be the result from one source and is combined with the odour frequency from the third source to get odour frequency from these three sources. By this procedure, the overall odour frequency from multiple sources (n >2) can be estimated.

2.9.5 Persistence of Different Odours

A large difference between odour and traditional air contaminants is that various odours have different persistence. Then after the same dilution, the intensity is different for various odours that have the same initial intensity. Therefore, the persistence of odours is

an issue needed to be resolved when conducting odour dispersion modeling. Furthermore, the field measurement of odour plume is mostly recorded in intensity, while the model predicts odour concentrations or odour frequencies of certain odour concentrations.

Therefore, it is necessary to include the relationships between odour concentration and intensity into the model to consider the difference between odour and gas and to evaluate the model predicted concentration or frequency. Many existing relationships obtained by various researchers are provided in the model. Users can select one of the relationships or parameterize other specific relationships to do the conversion between odour intensity and concentration.

2.10 CASE STUDY

A case study was conducted to verify the model theories and methods. The derived parameters for PBL and the profile of wind speed and potential temperature gradient of some atmospheric conditions were estimated. The effective plume height and the Hogstrŏm stability for some stable conditions and an example point source were studied. Also, both the Pasquill-Gifford and Hogstrŏm dispersion coefficients for the example point source and the Hogstrŏm dispersion coefficients for a ground level release point source were investigated. Finally, the odour concentrations and odour frequencies from an elevated point source, multiple point sources, and an area source and a volume source were documented.

2.10.1 Derived Parameters and Profiles of Wind Speed and Potential Temperature Gradient

The derived parameters and the profiles of wind speed and vertical gradient of potential temperature for some hours were studied. The wind speed of these hours is 2.5 m s^{-1} at a reference height of 10 m. The ambient temperature is 20℃, and mixing height is 1000 m. The location of the source is at 52.167 N, 108.687 W and the time zone of this location is -6 hours. Surface roughness, albedo, and Bowen ratio of the source area are 0.1 m, 0.18, and 0.8 respectively. The simulating date and time is 12 PM for unstable conditions (A, B, and C) and 22 PM for stable conditions (E and F) on June 17, 2004. The parameters

derived for the hours with different P-G stability class (A, B, C, E and F) are listed in the Table 2.5 and Table 2.6.

Table 2.5 Parameters derived for CBL

Stability class	Radiation, W m^{-2}	Net radiation, W m^{-2}	Sensible heat (H_s), W m^{-2}	Friction velocity(u_*), m s^{-1}	M-O Length (L_{mo}), m
A	925	631	252.42	0.29	-9.02
B	726	485	194.14	0.28	-10.87
C	425	265	105.99	0.26	-16.95

Table 2.6 Parameters derived for SBL

Stability class	Cloud cover (n)	Friction temperature (θ_*), K	Friction velocity(u_*), m s^{-1}	M-O Length (L_{mo}), m	Sensible heat (H_s), W m^{-2}
E	6/8	0.06	0.16	28.68	-13.04
F	3/16	0.08	0.10	9.55	-11.28

In convective conditions, when the P-G stability changes from A to C, the sensible heat and friction velocity decrease from 252.42 to 105.99 W m^{-1} and 0.29 to 0.26 m s^{-1} respectively. The Monin-Obukhov length values change from -9.02 to -16.95 m with the increase of stability from A to C.

In stable conditions, with the increase of stability from E to F, the friction temperature increases from 0.06 to 0.08 K, while the friction velocity and Monin-obukhov length decrease from 0.16 to 0.10 m s^{-1} and 28.68 to 9.55 m respectively. The sensible heat is negative. Its absolute value decreases from 13.04 to 11.28 m when the P-G stability class changes from E to F. Hanna et al. (1996) related the Pasquill-Gifford stability class to Monin-Obukhov length as shown in the Table 2.7.

Table 2.7 P-G stability class, conditions, wind speeds and M-O length by Hanna et al. (1996)

Description	P-G Stability Class	Time of Day/Condition	Wind Speed U	M-O Length (L_{MO})
Very Unstable	A	Sunny Day	< 3 m/s	-10 m
Unstable	B or C	↓	2-6 m/s	-50 m
Neutral	D	Cloudy or Windy	> 3-4 m/s	|L| > 100 m
Stable	E	↓	2-4 m/s	+ 50 m
Very Stable	F	Clear Night	< 3 m/s	+10 m

Compared the values calculated by LODM to the values of Hanna et al. (1996), it can be concluded that the Monin-obukhov lengths derived from the model with P-G stability classes are reasonable.

The vertical wind profile is illustrated in Figure 2.4 and Figure 2.5 at the height less than $7z_0$ and greater than $7z_0$ for different P-G stability classes. The standardized wind speeds (u/u_*) increase linearly with the height below $7z_0$. Above $7z_0$, they increase logarithmically with height until they reach the constant values at mixing height. At the same height, standardized wind speeds are greater under more stable stability conditions.

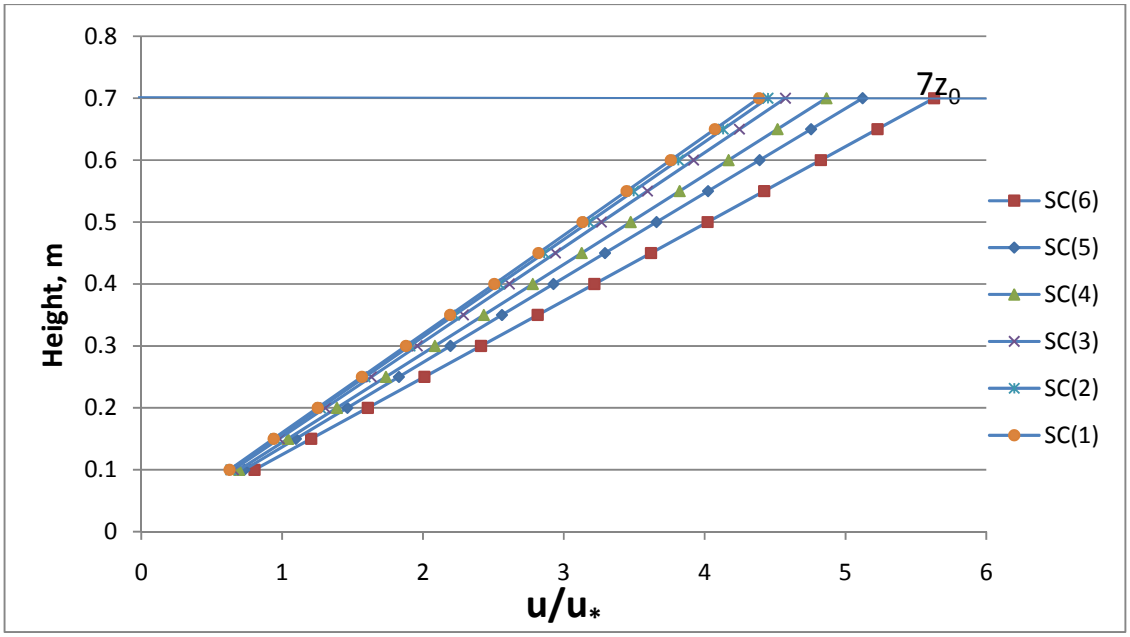

Figure 2.4 Wind profile for each stability class at height less than $7z_0$ (Hereafter, SC(1), SC(2)…SC(6) refer to stability class A, stability class B… stability class F.)

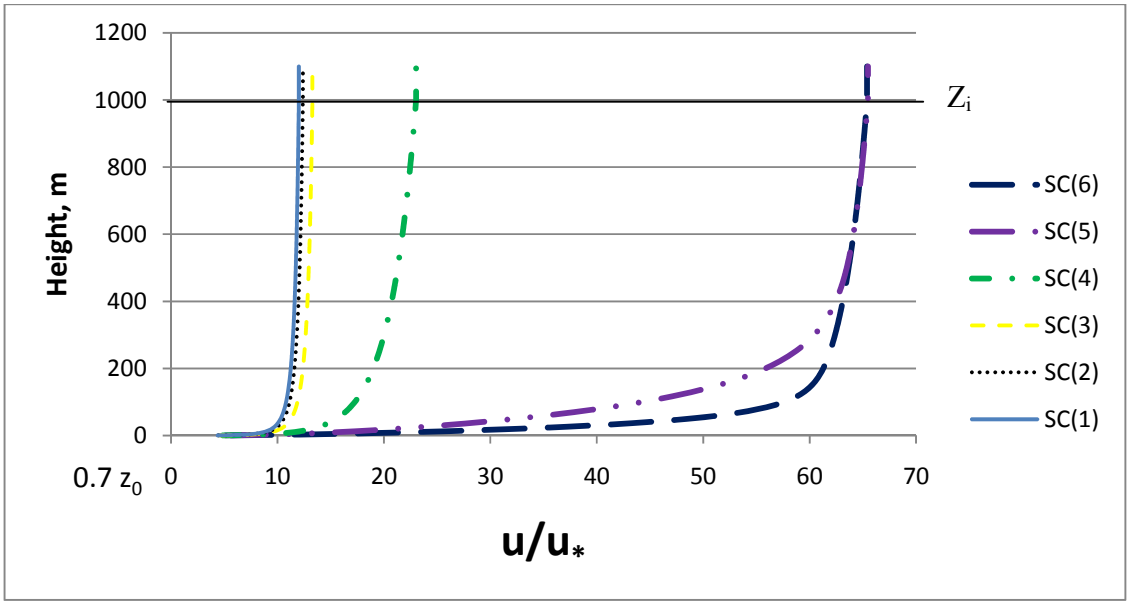

Figure 2.5 Wind profile for each stability class at height greater than $7z_0$

The vertical gradients of potential temperature are shown in Figure 2.6 and 2.7. Below 2 m, the potential temperature gradients are persisted downward from their values of 0.11 and 0.22 k m^{-1} at 2 m for stability E and F respectively. Above 100 m, they are allowed to decay exponentially with height until they reach the minimum value of 0.002 k m^{-1}. The

vertical gradient of potential temperature is larger under more stable conditions (F) than less stable conditions (E) before they reach the minimum value. These values of potential temperature gradient are much lesser than the default values used in ISC models which are 0.02 k m^{-1} for stability class E and 0.035 k m^{-1} for stability class F.

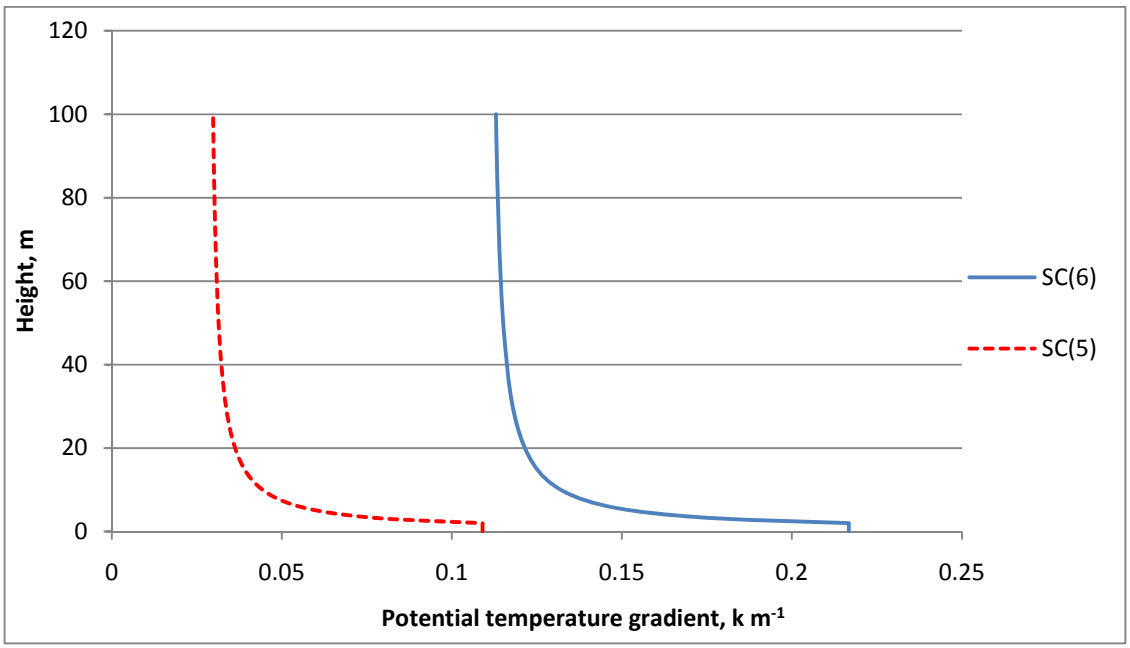

Figure 2.6 Potential temperature gradient profile for each stability class at height less than 100 m

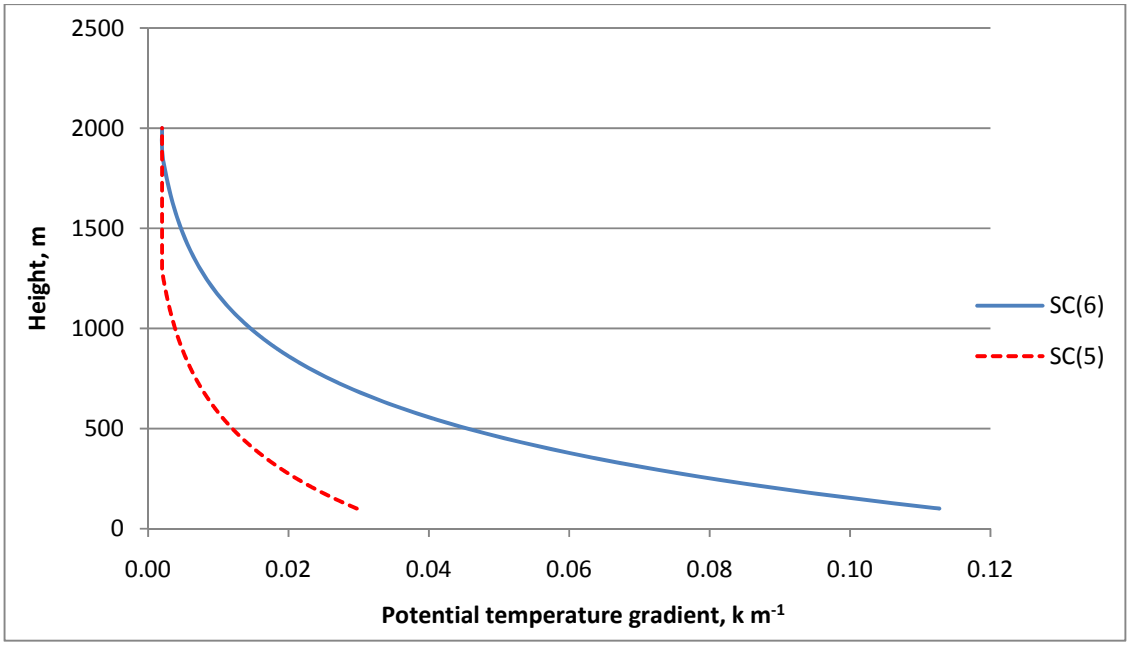

Figure 2.7 Potential temperature gradient profile for each stability class at height greater than 100 m

2.10.2 Effective Plume Height and Hogstrŏm Stability

The Hogstrŏm stability (s) is defined as

$$s = \left(\frac{\partial \theta}{\partial z} \Big/ u_f^2 \right) \cdot 10^5 \tag{2.17}$$

$\frac{\partial \theta}{\partial z}$ is the vertical gradient of potential temperature at the level of the plume centre, k m^{-1},

u_f is the wind speed at the top of friction layer, m s^{-1}.

The top of friction layer is equivalent to the mixing height. Therefore, u_f can be determined by mixing height and wind profile. The vertical gradient of potential temperature at the level of the plume centre varied with the downwind distance, because the effective plume height considering the stack-tip downwash and plume rise varies until it reaches the final plume rise.

For a point source with physical height of 10 m, diameter of 3 m, exit velocity of 5 m s^{-1} and exit temperature of 300 K, during the example hours with different P-G stability

classes. The plume height calculated by the P-G method and the Hogstrŏm method were compared. Results show that the plume heights between two methods are almost identical under unstable and neutral stability conditions (A, B, C, and D). The plume heights under stable conditions (E and F) are shown in Figure 2.8 and Figure 2.9.

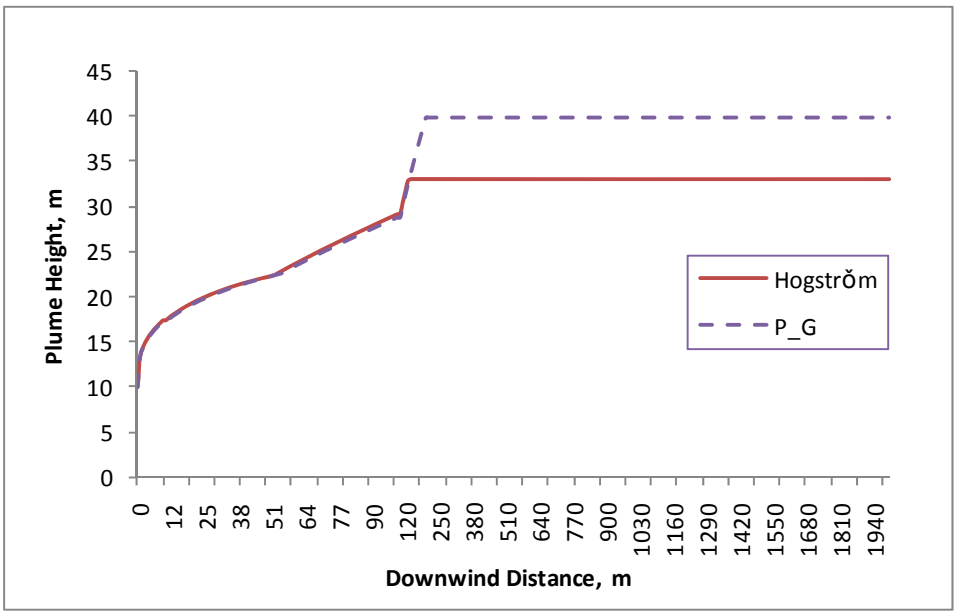

Figure 2.8 Plume height with downwind distance for stability class E

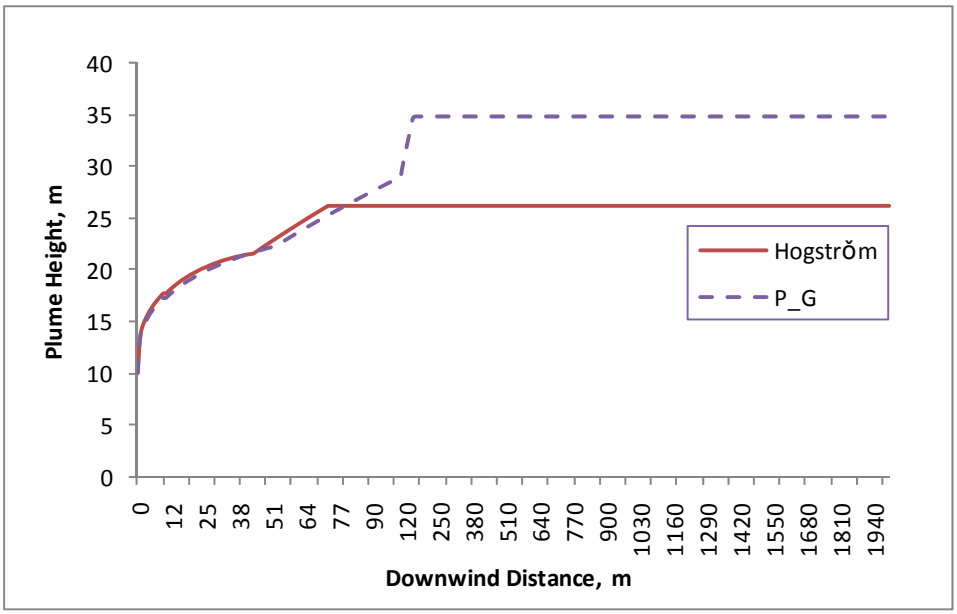

Figure 2.9 Plume height with downwind distance for stability class F

The plume heights calculated by the P-G method are almost as same as those calculated by the Hogstrŏm method before the final plume height reaches under both stability class E and F. The plume heights calculated by the Hogstrŏm method reach the final rise at a closer distance than those calculated by the P-G method, and the final plume heights of Hogstrŏm method are lower than those of the P-G method. The plume heights for stability E are higher than those of stability F for both methods.

The plume height calculated by the Hogstrŏm method and Hogstrŏm stability parameters at different downwind distances (0 m, 10 m, 100 m, and 500 m) for stability class E and F are listed in Table 2.8 and illustrated in Figure 2.10. Hogstrŏm stability for P-G Stability class F is much larger than that of stability class E. The Hogstrŏm stability decreases with downwind distance increase until plume height becomes constant because the gradient of potential temperature decreases with the increase of height of plume center.

Table 2.8 Hogstrŏm stability(s) and the plume height (PH) at different downwind distance for stability class E and F

Stability class	0 m		10 m		100 m		500 m	
	PH, m	Hogstrŏm Stability	PH, m	Hogstrŏm Stability	PH, m	Hogstrŏm Stability	PH, m	Hogstrŏm Stability
E	10	41.68	17.39	35.23	29.14	31.71	33.00	31.09
F	10	285.19	17.72	265.24	26.24	256.87	26.24	256.97

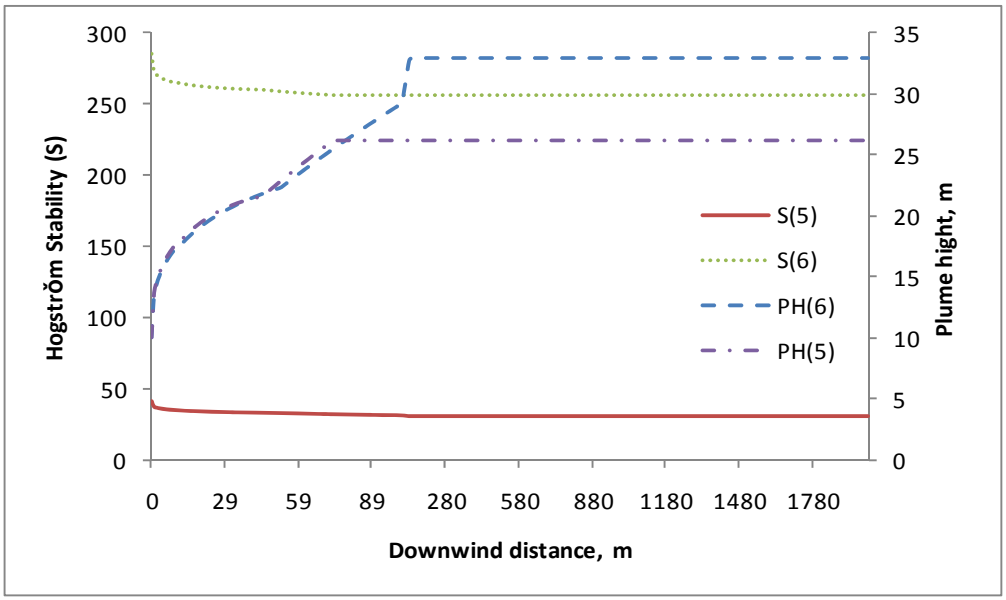

Figure 2.10 Hogstrŏm stability (s) and the plume height (PH) at different downwind distance for stability class E and F

2.10.3 Dispersion Coefficients

The Pasquill-Gifford and Hogstrŏm mean and short time dispersion parameters at both horizontal and vertical directions for the example point source and example hours with different stability classes (from A to F) are shown in Figure 2.11 - 2.18.

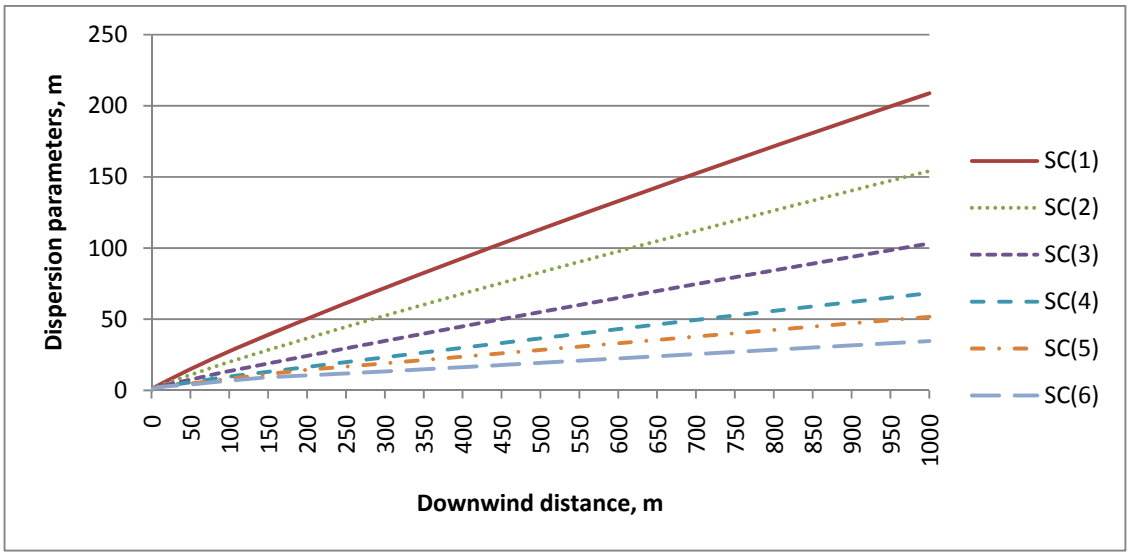

Figure 2.11 Pasquill-Gifford mean horizontal dispersion parameters for different stability classes

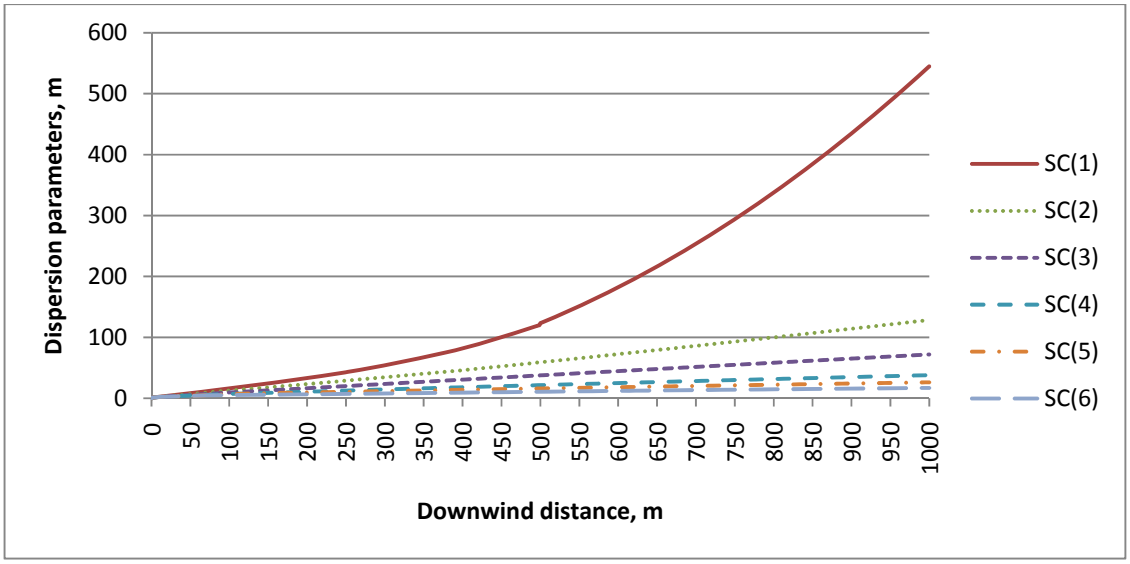

Figure 2.12 Pasquill-Gifford mean vertical dispersion parameters for different stability classes

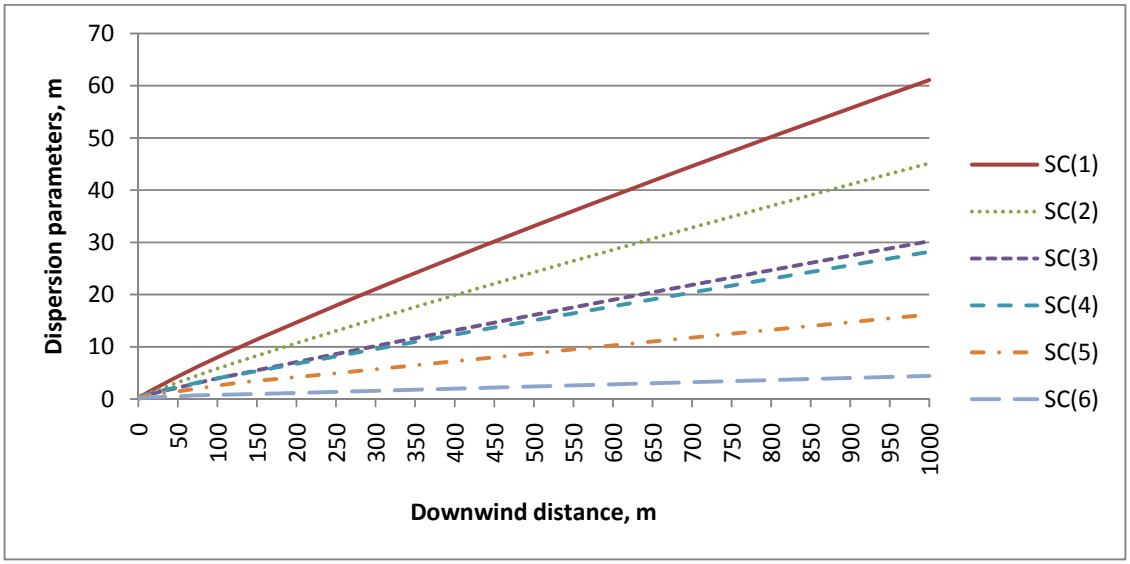

Figure 2.13 Pasquill-Gifford short time horizontal dispersion parameters for different stability classes

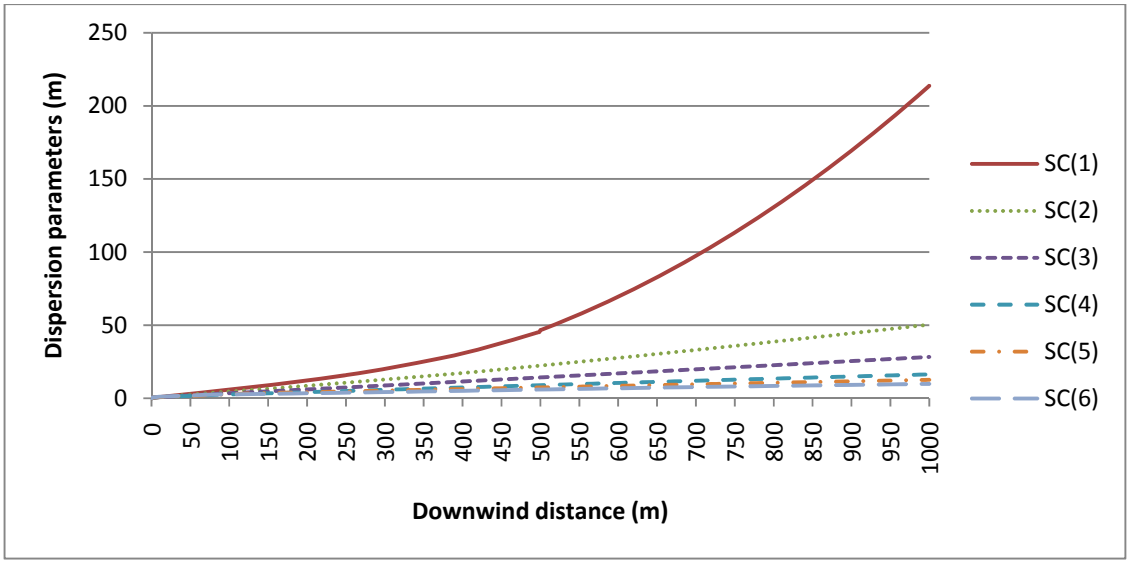

Figure 2.14 Pasquill-Gifford short time vertical dispersion parameters for different stability classes

Pasquill-Gifford dispersion parameters are greater at longer distance. The dispersion parameters for less stable conditions are larger than those of more stable conditions. The vertical dispersion parameters for stability class A are much larger than other stability classes, especially for longer distance.

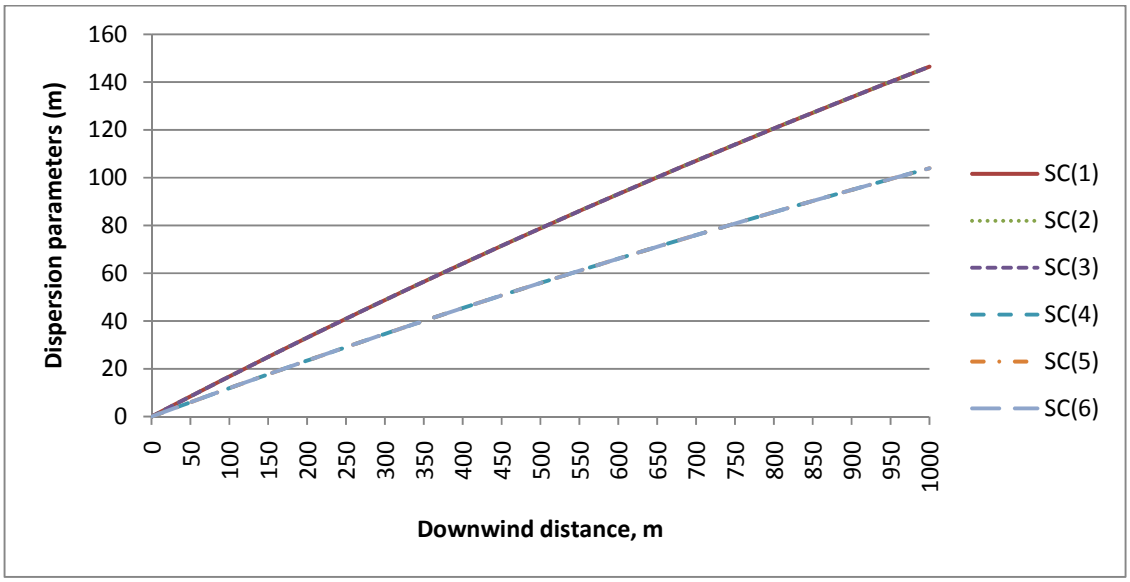

Figure 2.15 Hogstrŏm mean horizontal dispersion parameters for different stability classes

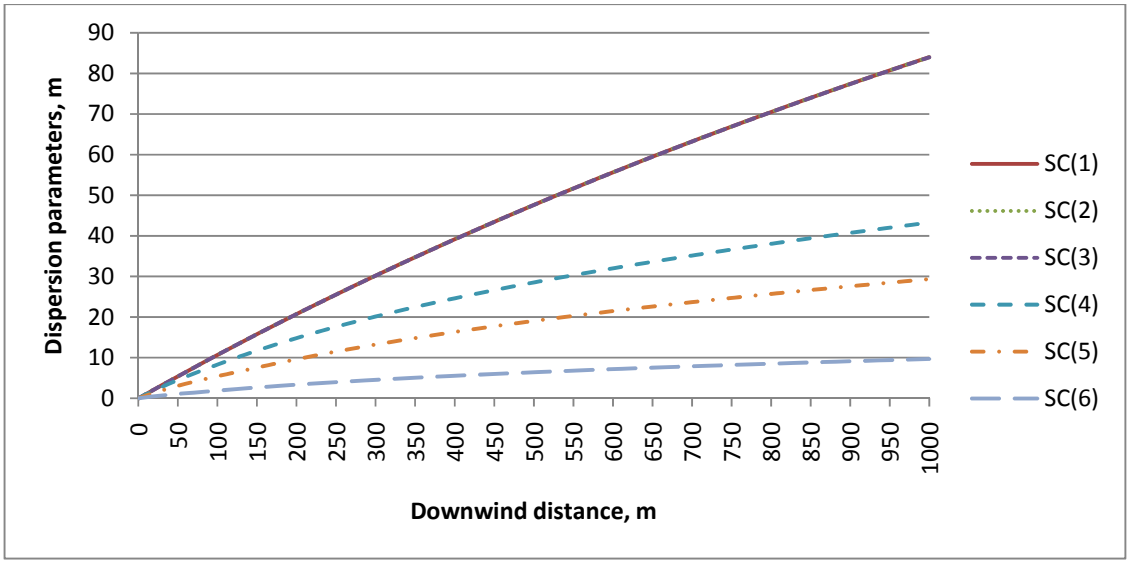

Figure 2.16 Hogstrŏm mean vertical dispersion parameters for different stability classes

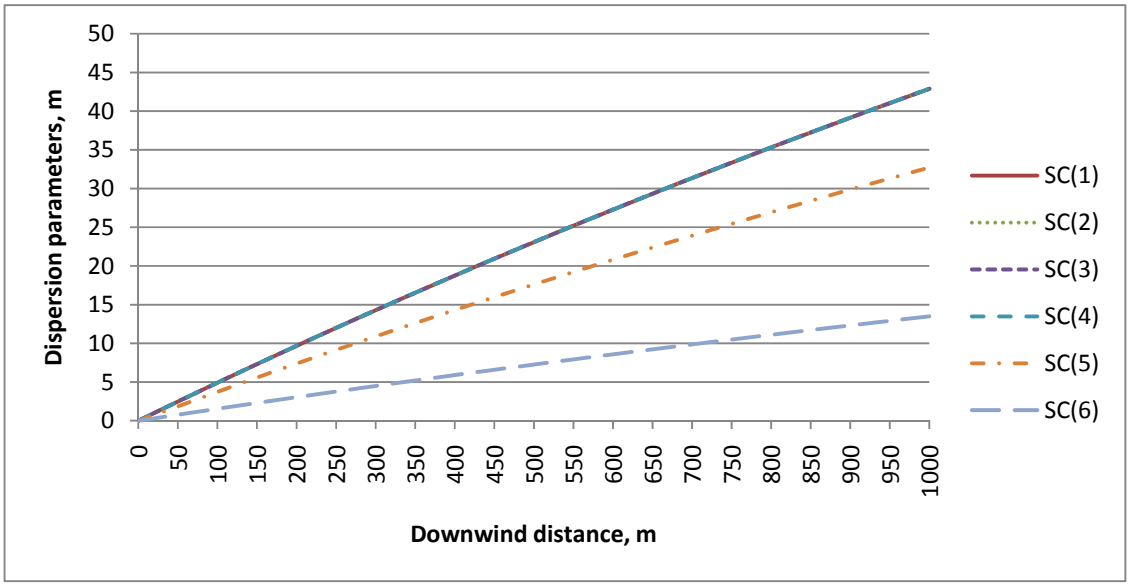

Figure 2.17 Hogstrŏm short time horizontal dispersion parameters for different stability classes

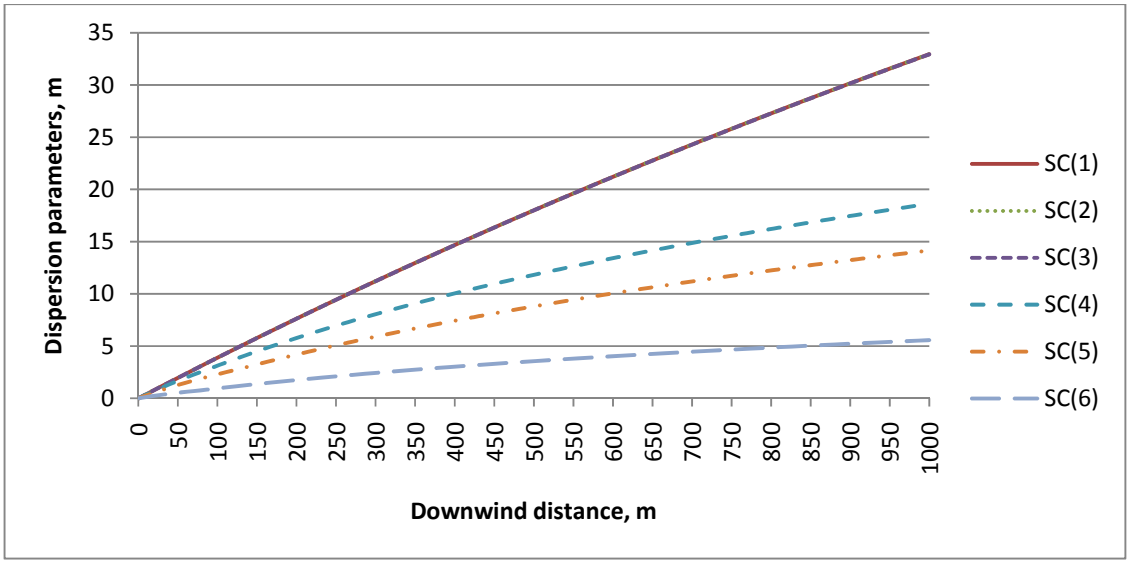

Figure 2.18 Hogstrŏm short time vertical dispersion parameters for different stability classes

Hogstrŏm mean horizontal dispersion parameters only distinguish unstable ($s<0$) and stable or neutral ($s\geq 0$) conditions. Under each condition, Hogstrŏm mean horizontal dispersion parameters are the functions of downwind distance and irrelevant to the stability parameter (s). Hogstrŏm short time horizontal dispersions are related to stability (s). For unstable and neutral conditions ($s\leq 0$), they have the same values at the same distance. For stable conditions, they are larger for less stable conditions. Both the mean and short time vertical dispersion parameters are the functions of stability and downwind distance. For unstable conditions, they remain the same at the same distance. For neutral to stable conditions, they decrease with the increase of stability.

Figure 2.19 shows the comparison between mean and short time horizontal and vertical dispersion parameters for neutral stability (D). The short time dispersion parameters (H_Yinst and H_Zinst) are always smaller than the mean dispersion parameters (H_Ymean and H_Zmean). Sampling time is very important in obtaining the dispersion parameters from experimental data. The longer sampling time (hourly, mean) will result in a larger plume width with larger standard deviations. While shorter sampling time (instantaneous) will produce a narrower plume with small standard deviations. As discussed before, in the fluctuating plume model, the mean dispersion parameters are the sum of contribution from both the relative diffusion within the short time (instantaneous)

plume and the standard deviations of the position of the instantaneous plume centerline. Therefore, the standard deviations of plume meandering can be estimated from the mean and short time dispersion parameters.

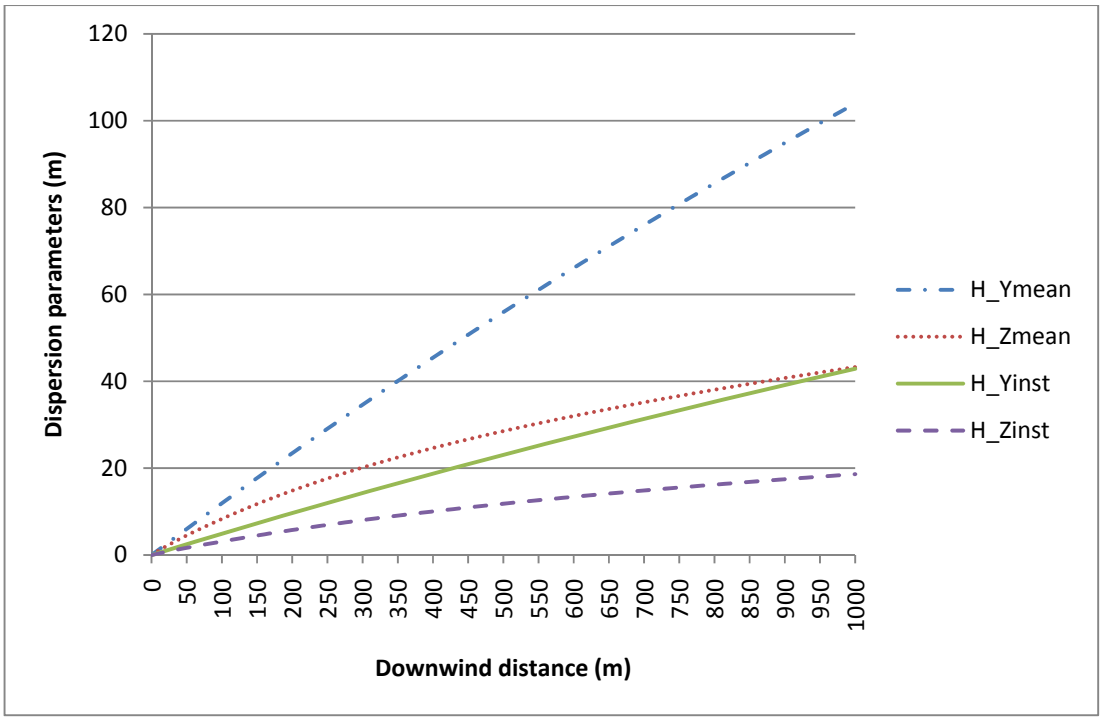

Figure 2.19 Hogstrŏm mean and short time dispersion parameters for stability class D

Comparison between two dispersion coefficients schemes (PG_Ymean and PG_Zmean VS. H_Ymean and H_Zmean) for the example point source and the example hours with different stability classes are shown in Figure 2.20 - 2.25. For stability class A and B, both horizontal and vertical P-G mean dispersion parameters are larger than those of Hogstrŏm. The P-G mean dispersion parameters are much larger than Hogstrŏm's under stability A, especially at vertical direction. However, the gap becomes smaller when the stability class changes to B. From stability class C to F, the Hogstrŏm horizontal dispersion parameters are larger than P-G parameters. The differences are larger for more stable conditions. The Hogstrŏm vertical dispersion parameters are larger than P-G parameters for stability class C to E. However, for stability F, the Hogstrŏm vertical dispersion parameters are smaller than the P-G parameters.

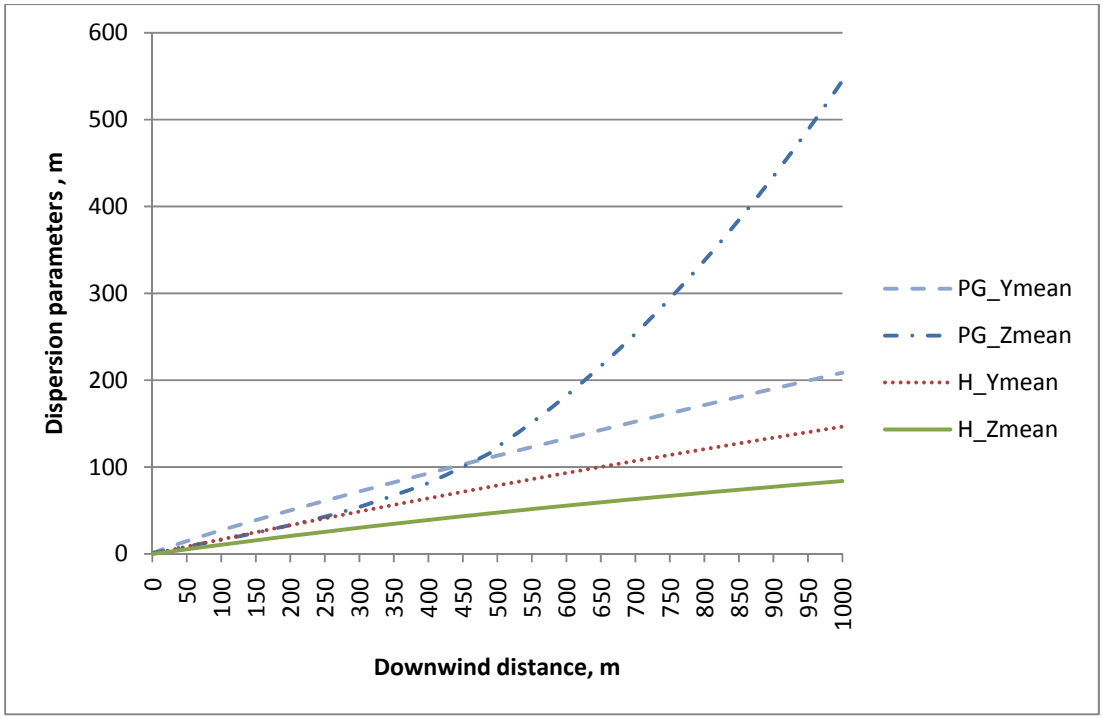

Figure 2.20 Comparisons of mean dispersion coefficients between P-G method and Hogstrŏm method for stability class A

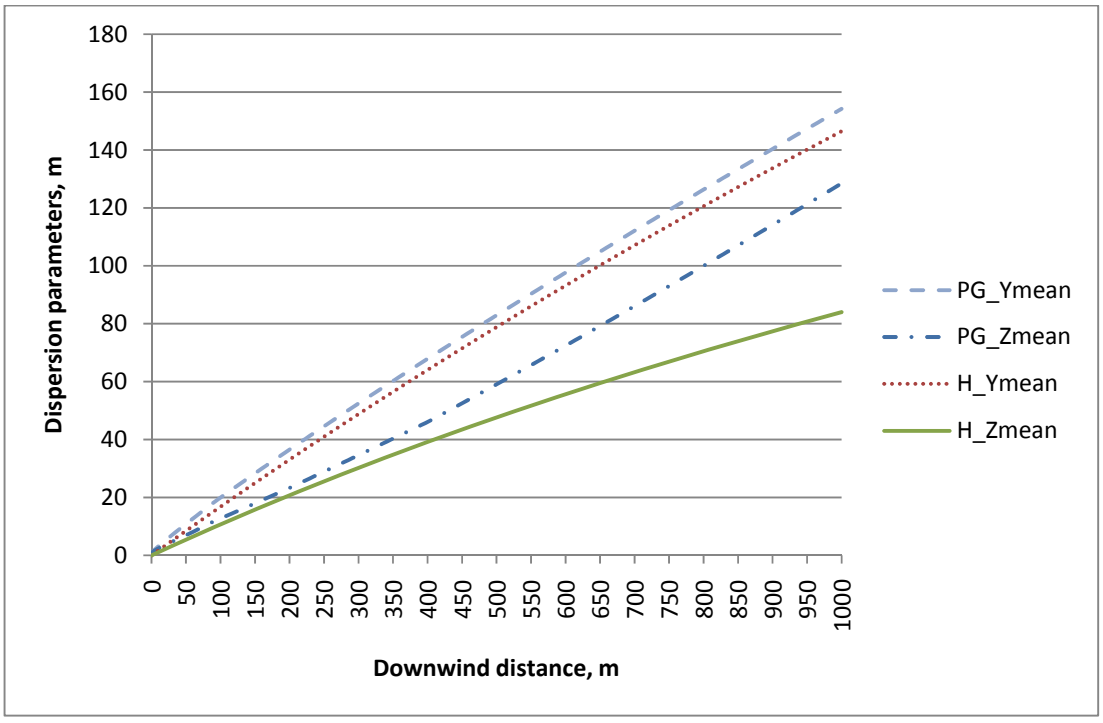

Figure 2.21 Comparisons of mean dispersion coefficients between P-G method and Hogstrŏm method for stability class B

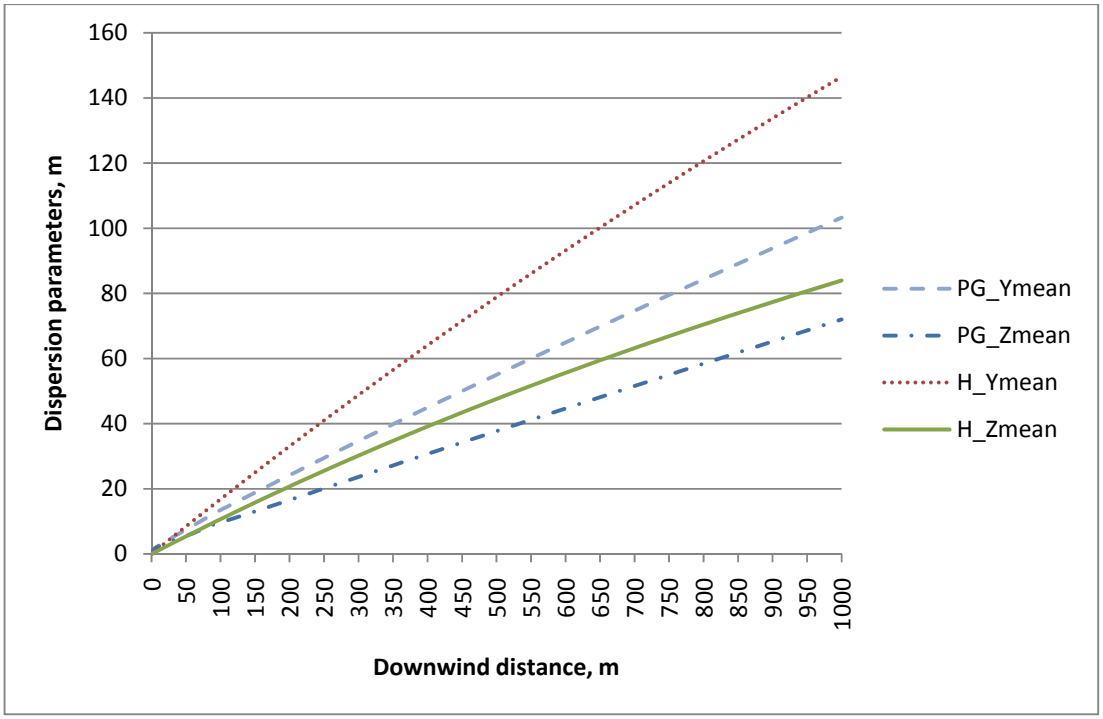

Figure 2.22 Comparisons of mean dispersion coefficients between P-G method and Hogstrŏm method for stability class C

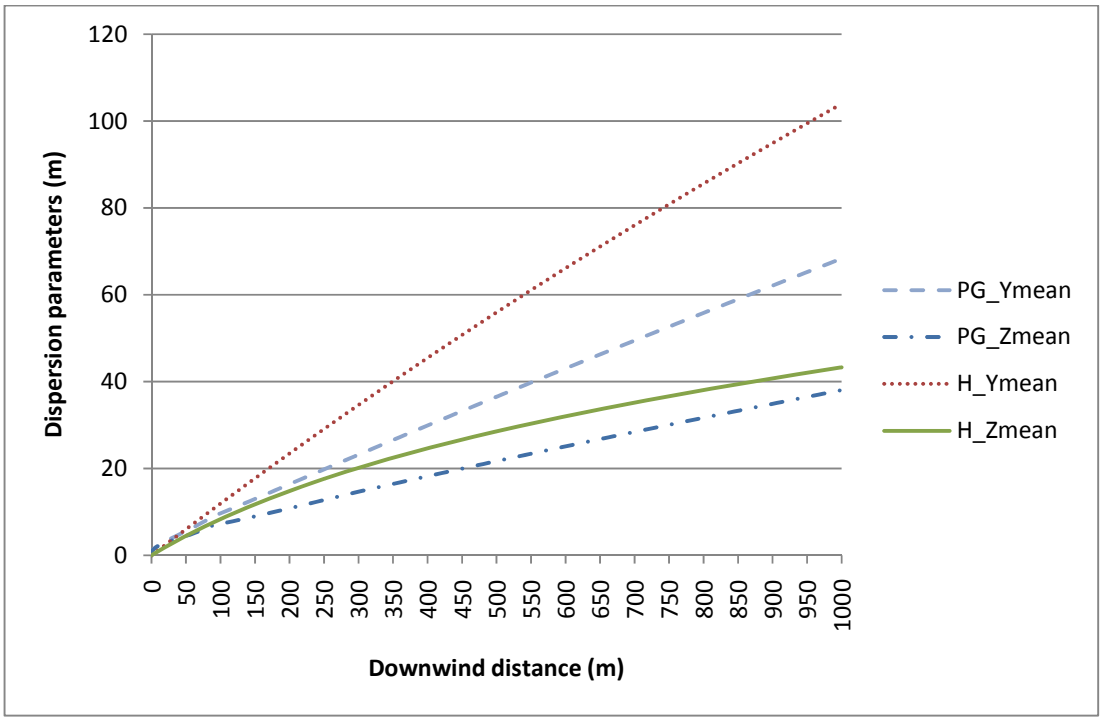

Figure 2.23 Comparisons of mean dispersion coefficients between P-G method and Hogstrŏm method for stability class D

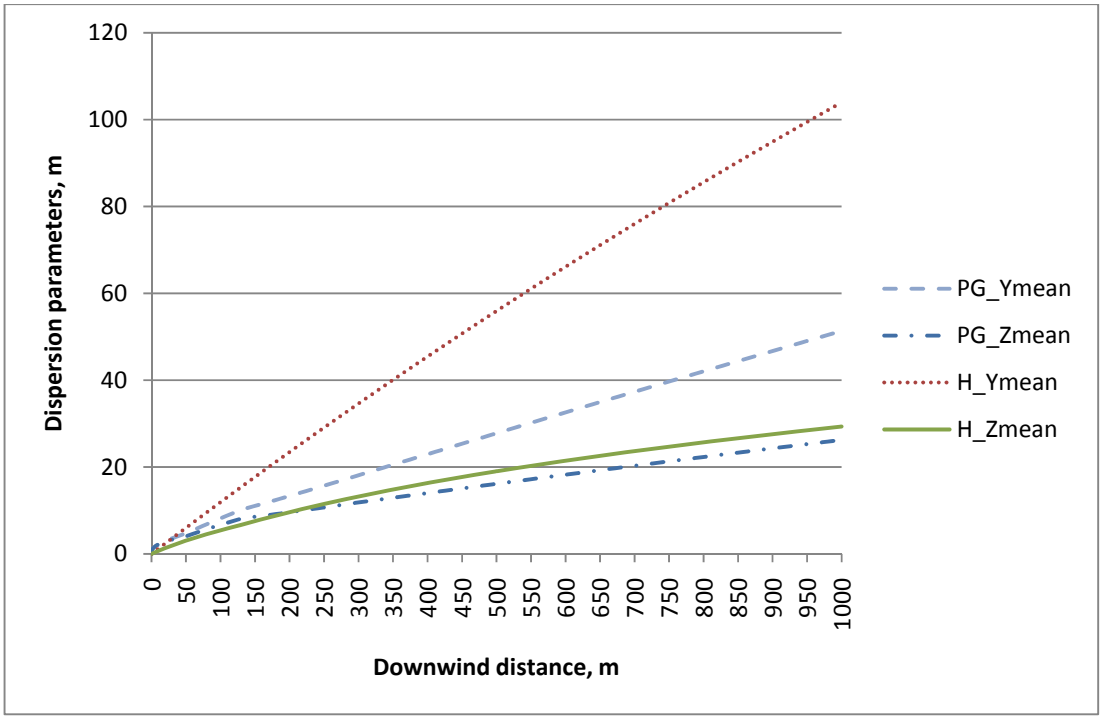

Figure 2.24 Comparisons of mean dispersion coefficients between P-G method and Hogstrŏm method for stability class E

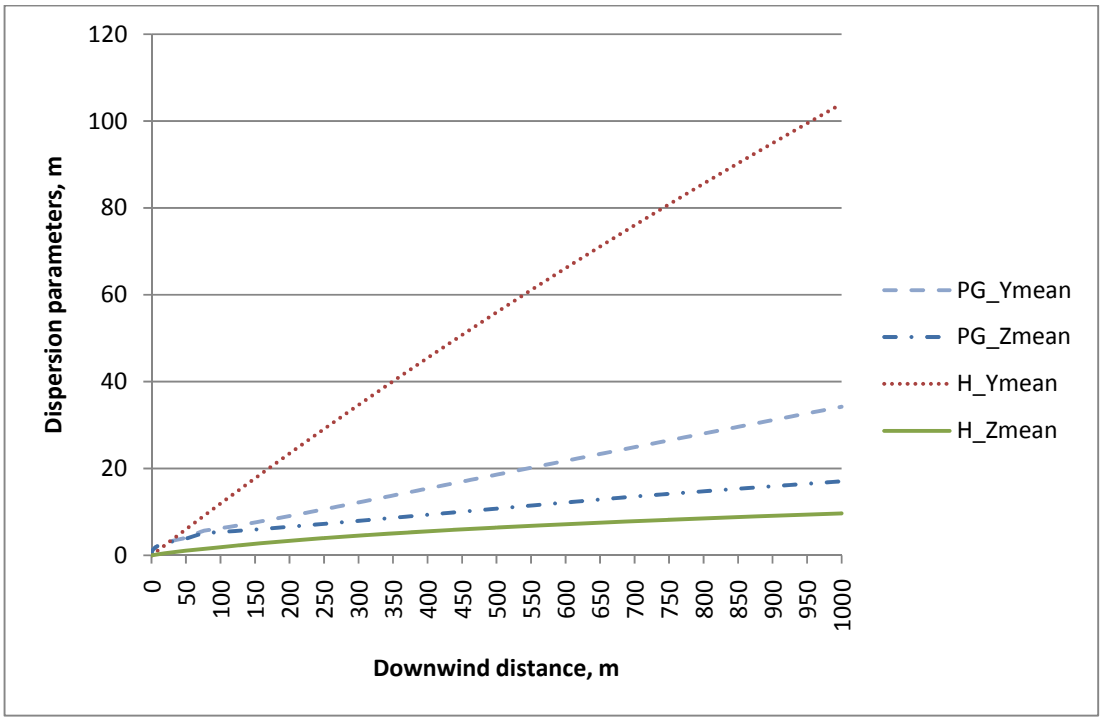

Figure 2.25 Comparisons of mean dispersion coefficients between P-G method and Hogstrŏm method for stability class F

2.10.4 Hogstrŏm Dispersion Coefficients from Ground Release

The Hogstrŏm mean and short time vertical dispersion parameters from ground level release can be estimated from the dispersion parameters that vary with height. Table (2.9) and Table (2.10) list the Hogstrŏm mean and short time vertical dispersion parameters for different heights and ground level for the example hours with stability classes of C and E at downwind distance of 100 m. For stability class C, the ground level mean vertical dispersion coefficient equals to the vertical dispersion coefficient when the plume height is between 6.2 and 6.7. The ground level short time vertical dispersion coefficient is the value of vertical dispersion coefficient when the plume height is between 1.7 and 2.2. For stability class E, the ground level mean and short time vertical dispersion coefficients are the values of vertical dispersion coefficients when the plume heights are between 3.2 and 3.7 and between 1.2 and 1.7 respectively.

Table 2.9 Hogstrŏm mean and short time vertical dispersion parameters for different heights for unstable condition (SC = C)

h	h/0.7	σ_z(mean,H)	σ_z(Inst,H)
1.2	1.71	5.52	2.35
1.7	2.43	6.43	2.68
2.2	3.14	7.10	2.90
2.7	3.86	7.62	3.06
3.2	4.57	8.03	3.19
3.7	5.29	8.35	3.28
4.2	6.00	8.62	3.36
4.7	6.71	8.84	3.42
5.2	7.43	9.02	3.47
5.7	8.14	9.18	3.51
6.2	8.86	9.32	3.55
6.7	9.57	9.44	3.58
7.2	10.29	9.54	3.61
7.7	11.00	9.63	3.63
Ground Level		9.41	2.80

Table 2.10 Hogstrŏm mean and short time vertical dispersion parameters for different heights for stable condition (SC = E)

h	h/0.7	σ_z(mean,H)	σ_z(Inst,H)
0.2	0.29	3.26	1.49
0.7	1.00	3.34	1.56
1.2	1.71	3.64	1.72
1.7	2.43	3.85	1.84
2.2	3.14	4.08	1.95
2.7	3.86	4.35	2.07
3.2	4.57	4.59	2.17
3.7	5.29	4.79	2.25
4.2	6.00	4.96	2.31
Ground Level		4.60	1.72

2.10.5 Odour Concentration and Frequency from an Elevated Point Source

Instantaneous and mean odour concentrations

Instantaneous odour concentrations were calculated for the example hours with different stability classes (A to F) at a receptor of 1.5 m high at wind direction and 1000 m downwind from the example point source defined in section 2.10.2 with the emission rates of $5 \cdot 10^5$ OU s^{-1}. One thousand random values were generated within an hour to get 1000 instantaneous concentrations for each stability class. These values were averaged to obtain a mean concentration, named as computed mean concentration. The frequency of odour concentration that exceeds or equals 1 OU m^{-3} was computed based on the instantaneous odour concentrations, named as computed frequency. The model also calculated the mean odour concentrations for the six cases using Hogstrŏm dispersion coefficients and odour frequencies by weighted exceeding half width method, named as modeled mean concentration and modeled odour frequency respectively.

The instantaneous odour concentrations, computed mean odour concentration, and modeled odour concentration for stability class D are shown in Figure 2.26. The instantaneous concentrations fluctuate around the mean concentration. Both the computed and modeled mean concentrations are below 20 OU m^{-3}. The instantaneous concentrations can be as low as 0 OU m^{-3} and larger than 80 OU m^{-3}.

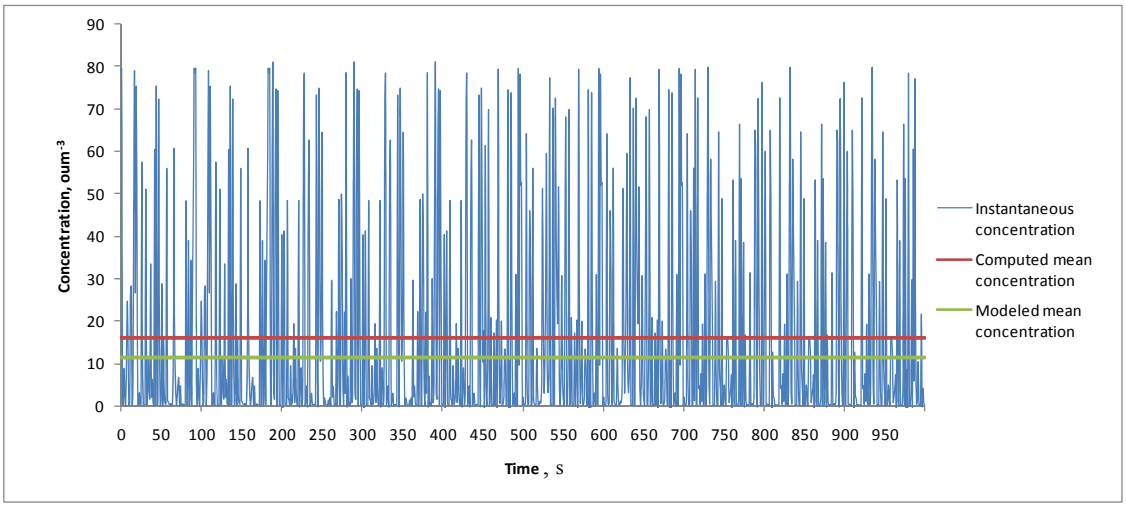

Figure 2.26 The instantaneous odour concentrations, computed mean odour concentration and modeled odour concentration for stability class D at a receptor 1 km downwind of a point source

Mean odour concentration and odour frequency for different stability classes

The computed and modeled mean odour concentration and odour frequency for all six stability classes are listed in Table 2.11. Although the computed and modeled mean odour concentrations have some discrepancies, the computed frequency and modeled frequency are very close. It shows that the weighted exceeding half width method can estimate the odour frequency successfully.

From Table 2.11, the modeled mean concentration and odour frequency for different P-G stability classes can also be examined. The mean concentration and frequency for unstable conditions are almost identical. The reason is that both the mean and short time dispersion parameters under unstable conditions are irrelevant to stability. The slight differences among unstable conditions might be due to the effects of different wind speed profiles. The odour frequency and mean concentration have the largest values under stability D condition and decrease with the increase of stability from D to F. Generally, when the atmospheric stability increases, the dispersion parameters decrease and the odorous pollutant is less dispersing during the transportation and is favoured to transport to longer distance. So the mean odour concentration and odour frequency should be greater when the atmosphere is more stable. One possible reason that the mean odour concentration and odour frequency decrease with the increase of stability is the different

plume heights. Under stable conditions, the plume width is narrow so that the receptor may receive fewer odours because the high concentration plume might not reach the receptor due to the high plume height.

Table 2.11 Modeled and computed mean odour concentration and odour frequency for different P-G stability classes at a receptor 1 km downwind of a point source

Stability class	Modeled		Computed	
	Mean concentration, OU m^{-3}	Frequency	Mean concentration, OU m^{-3}	Frequency
1	4.9	0.41	7.3	0.44
2	4.9	0.41	7.3	0.40
3	4.9	0.41	7.0	0.43
4	11.5	0.60	16.0	0.55
5	11.3	0.42	11.9	0.37
6	0.8	0.03	1.5	0.03

In order to further examine this finding, a point source was placed in ground level with no plume rise, and the mean concentrations and frequencies were modeled and listed in Table 2.12. With the increase of stability, the mean concentrations increase, which is consistent with the common knowledge. However, the frequencies remain the same pattern after the effect of plume height is excluded.

Table 2.12 Modeled mean odour concentrations and odour frequencies for ground level point release without plume rise at a receptor 1 km downwind of a point source

P-G stability Class	Mean odour concentration, OU m^{-3}	Odour frequency
1	6.3	0.28
2	6.3	0.28
3	6.4	0.28
4	34.0	0.65
5	58.6	0.44
6	180.4	0.22

In the fluctuating plume model, the instantaneous plume fluctuates around the centerline of the steady plume. The odour frequency depends on the short time dispersion parameters and the standard deviations of the instantaneous plume fluctuations. With the

increase of stability, decreases of the short time dispersion coefficients result in narrower instantaneous plumes both in horizontal and vertical directions. If the fluctuations of instantaneous plumes remain the same, the chances that a certain receptor can receive a certain level odour will decrease due to the narrower plume width. Only if the standard deviations of the instantaneous plumes centerline decrease at the faster rates than short time dispersion coefficients, the odour frequencies would increase under more stable conditions. However, from Hogstrŏm's formulas of dispersion coefficients, the standard deviations decrease slower than short time dispersion coefficients. Especially, the Hogstrŏm hourly mean horizontal dispersion coefficient is irrelevant to stability, while the short time horizontal dispersion coefficient decreases with the increase of stability. Therefore, the horizontal standard deviation decreases much slower than the short time dispersion coefficient. This explains why odour frequency decreases with the increase of stability from the model theory's point of view.

This finding is also supported by observed odour events from livestock operations. Jacobson et al. (2001) conducted a residents-based field observation of odour in the vicinity (4.8 km x 4.8 km) of livestock buildings. Odour was detected in 71% during neutral to slightly stable conditions and during light winds (<2.5 m/s). Odour episodes occurred predominantly during the warm season and either in the early morning or during evening hours. Their results are consistent with my finding that under neutral or slightly stable conditions, the odour frequencies are the highest. Guo et al. (2005b, 2006a) studied the impact of weather conditions including wind speed and atmospheric stability on odour occurrence with the data reported by resident observers living within 8.6 km from three intensive swine farms in Saskatchewan, Canada. From their study, most odour events (61.7%) were detected under neutral atmospheric stability class D while only 15% were detected under stable atmospheric conditions, which was lower than the total annual occurrence frequency of stability classes of 28.6%. Stable atmospheric conditions occurred the least in the period from May to August, yet this period had the highest number of odour events. Similar results were obtained by Guo et al. (2005c) when monitoring odours downwind of a 5,000-sow farrowing-to-finishing swine operation, located on the Canadian Prairies.

Ranges of odour concentration and frequency under different stability conditions

When dealing with ISC met file, the model converts the P-G stability class into other parameters used in the model, such as friction velocity, sensible heat flux, and Monin-Obukhov length, to obtain the wind speed profile, vertical gradient of potential temperature profile, and Hogstrŏm stability. The model uses the mean radiation or mean cloud cover retrieved from their ranges that differentiate each P-G stability class. The results of the odour frequency and mean concentrations calculated using the maximum, mean, and minimum radiation and cloud cover data of each P-G stability class were presented in Tables 2.13 and 2.14. For unstable conditions, the Hogstrŏm dispersion parameters are irrelevant to stability. Radiation has minor effects on the wind speed profiles, so that it has slight influence on modeled mean odour concentrations and odour frequencies. For stability class E, when the maximum cloud cover of 0.9 is used, Hogstrŏm stability is 15.71. The frequency of odour concentration above 1 OU m^{-3} is 0.47 and the mean odour concentration is 10.4 OU m^{-3}. When the minimum cloud cover of 0.5 is used, the atmosphere is the most stable because the Hogstrŏm stability is as high as 101.66, and the mean concentration and odour frequency are 8.4 OU m^{-3} and 0.22. For stability class F, the maximum and minimum of cloud cover are 0.4 and 0, the modeled mean concentrations are 0.56 and 1.7 OU m^{-3} and the modeled frequencies are 0.02 and 0.05.

Table 2.13 Mean odour concentration and odour frequency ranges for unstable P-G stability class at a receptor 1 km downwind of a point source

P-G Stability class	Radiation, W m^{-2}	Mean odour concentration, OU m^{-3}	Odour frequency (OC ≥1 OU m^{-3})
A	925	4.9	0.41
B	762	4.9	0.41
	718	4.9	0.41
	675	4.9	0.41
C	675	4.9	0.41
	425	4.9	0.41
	175	4.9	0.41

Table 2.14 Mean odour concentration and odour frequency ranges for stable P-G stability class at a receptor 1 km downwind of a point source

P-G stability class	Cloud cover	Hogstrŏm Stability (s)	Mean concentration, OU m^{-3}	Frequency (O.C≥1)
E	0.9	15.71	10.4	0.47
	6/8	31.09	11.3	0.42
	0.5	101.66	8.4	0.22
F	0.4	211.96	1.7	0.05
	3/16	256.87	0.7	0.03
	0	270.58	0.6	0.02

Odour plumes and odour frequency contours

The mean odour concentrations and odour frequencies of 1 OU m^{-3} predicted by LODM at 231 downwind receptors (Figure 2.27) (receptor height = 1.5 m) from the example point source using the example meteorological data for unstable (SC = C), neutral (SC = D) and stable (SC = E) conditions are shown in Figures 2.28- 2.33. Due to the influence of plume height, the maximum odour concentrations occur at a certain distance close to the source. It is obvious that under unstable condition, the odour plume is wider than neutral and stable conditions. But the odour travels to closer distances than neutral and stable conditions.

The frequencies are the highest at the centerline of the odour plume. The frequencies under neutral condition have the largest values. In the close distance to the source, the frequencies are low due to the plume height and the small dispersion coefficients. With the increase of crosswind distance, the frequencies are decreasing. Same as the odour concentrations, under unstable conditions, there is a wider area that can detect odour horizontally than neutral and stable conditions.

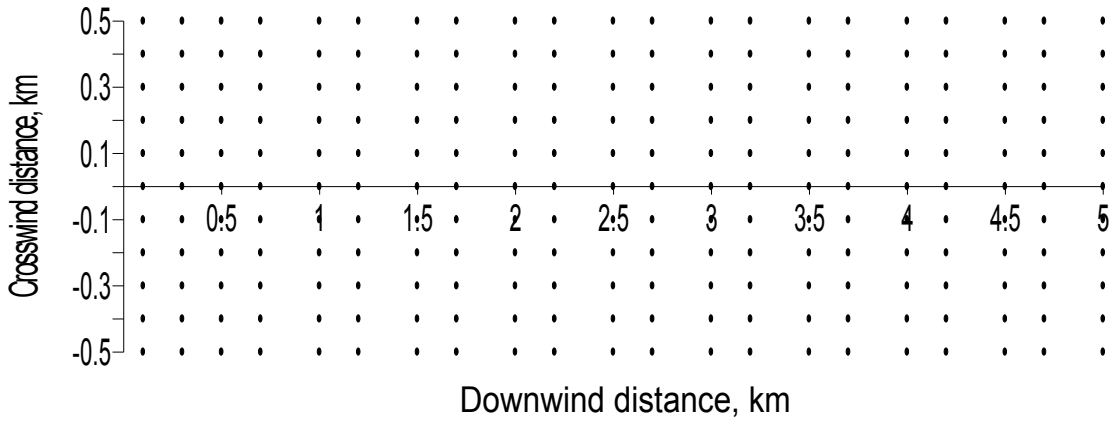

Figure 2.27 Layout of 231 downwind receptors (each symbol represents a receptor with a height of 1.5 m)

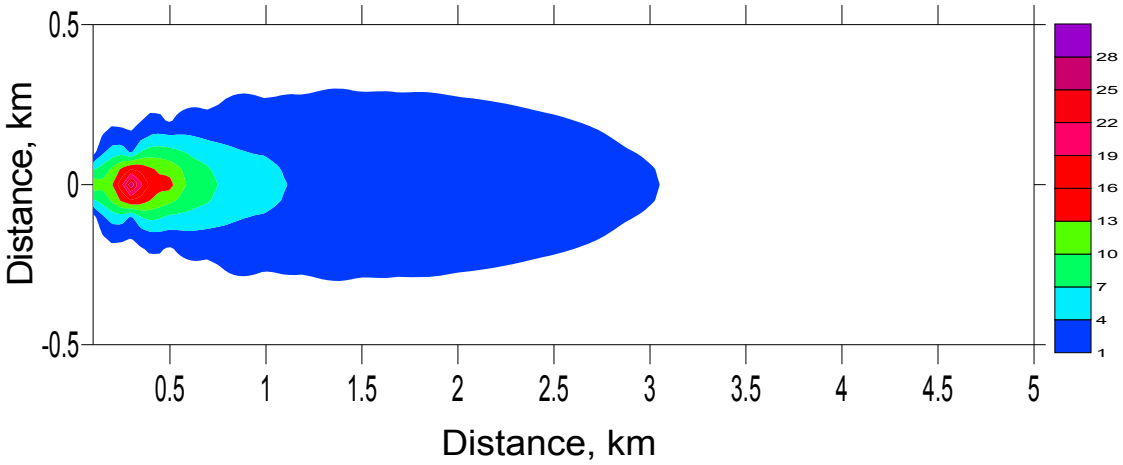

Figure 2.28 Odour plume predicted by the model from an elevated point source for unstable condition

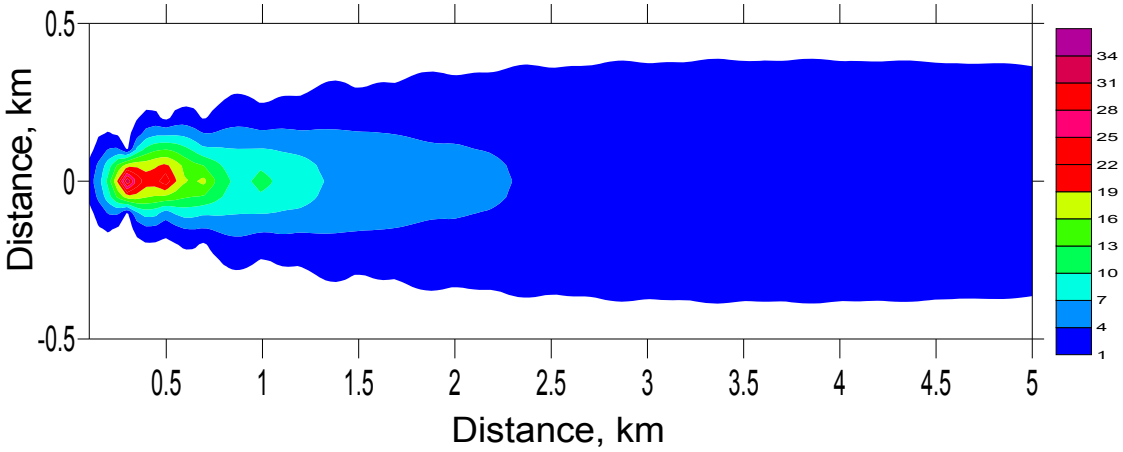

Figure 2.29 Odour plume predicted by the model from an elevated point source for neutral condition

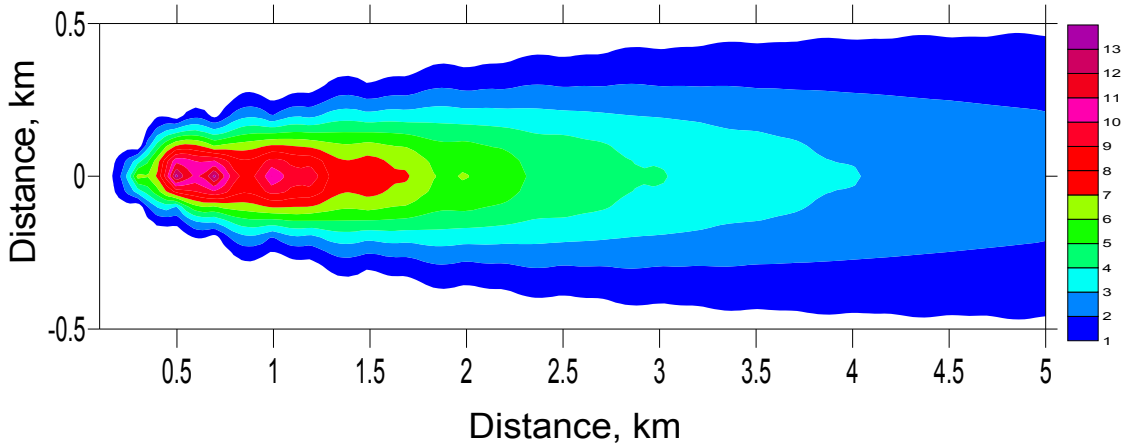

Figure 2.30 Odour plume predicted by the model from an elevated point source for stable condition

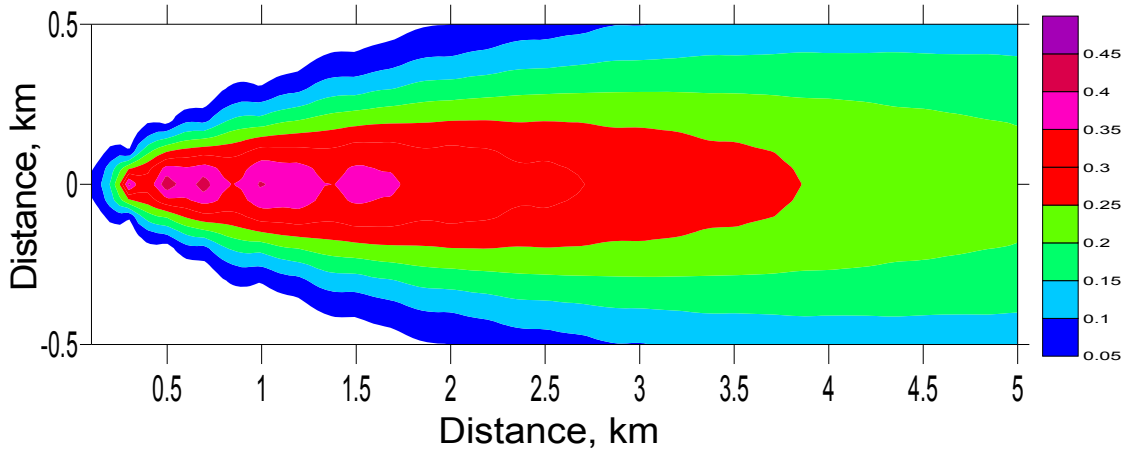

Figure 2.31 Odour frequency predicted by the model from an elevated point source for unstable condition

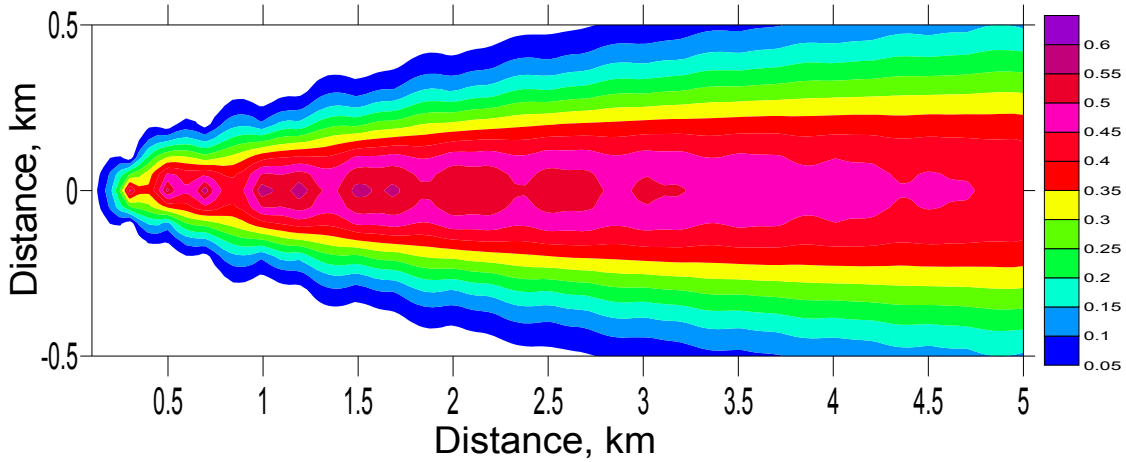

Figure 2.32 Odour frequency predicted by the model from an elevated point source for neutral condition

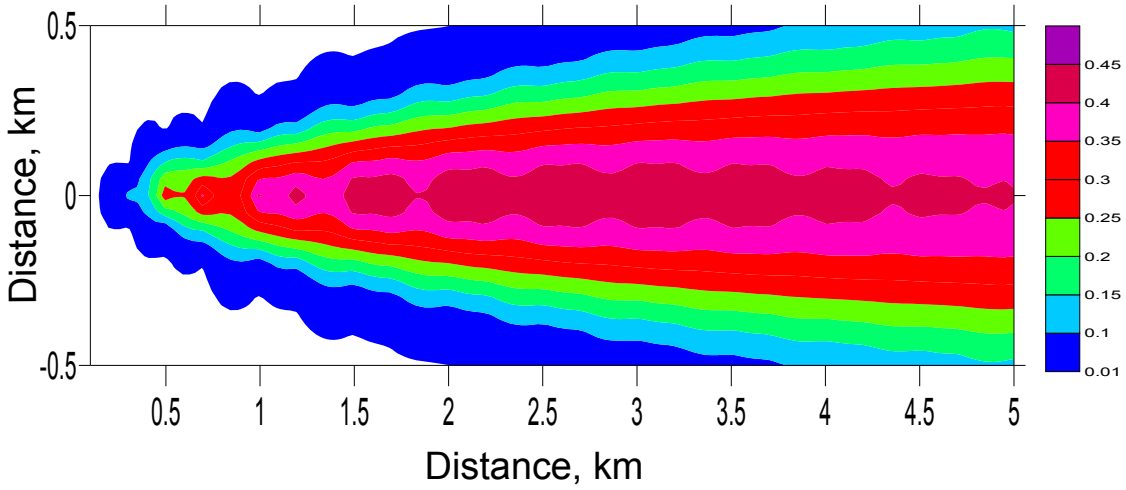

Figure 2.33 Odour frequency predicted by the model from an elevated point source for stable condition

Peak concentrations and peak to mean ratio

The modeled mean odour concentrations and peak concentrations for the example point source and the example meteorological data at the 231 downwind receptors are illustrated in Figure 2.34. Both the mean odour concentrations and peak concentrations decrease along downwind distance. The peak concentrations at the same downwind distance are the same even though the horizontal distances from the receptors to the plume centerline are different. The peak to mean ratios defined as the ratios between the maximum concentrations of fluctuating plume and mean concentrations of steady plume for the example point source at different downwind distances are listed in Table 2.15. The values are very high in near source from 200 to more than thousands. With the increase of downwind distance, the peak to mean ratios decrease. The decrements become less and less, which indicated in far distance, the peak to mean ratio will come to a constant. Ayra (1999) pointed out that the peak to mean ratios have large values near the source and they decrease with the increase of distance or travel time and reach a constant in far distance. The peak to mean ratios calculated demonstrate the same pattern.

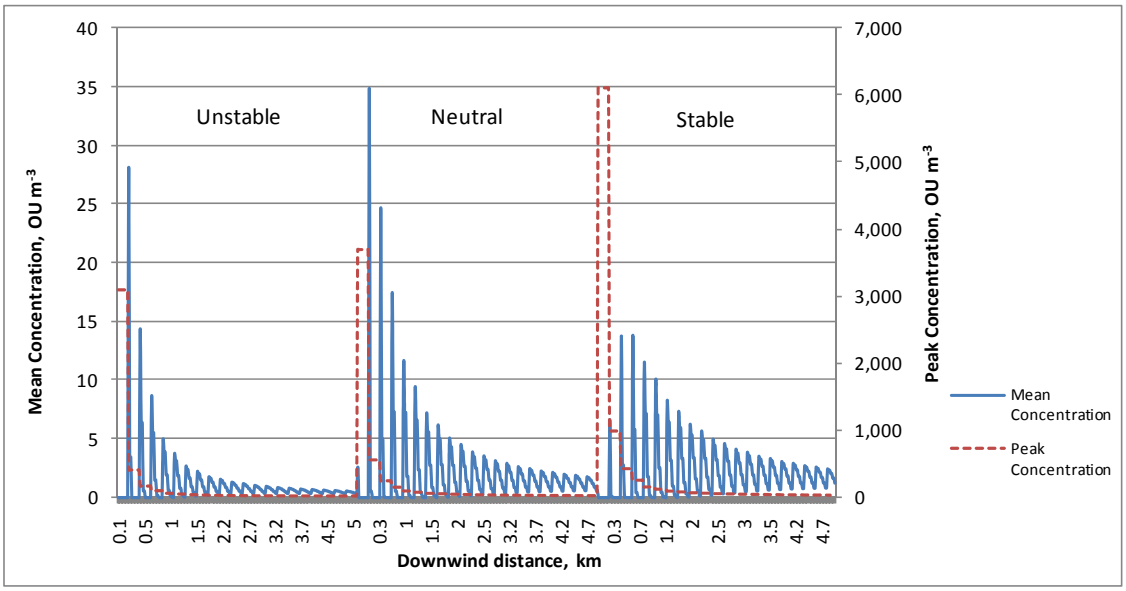

Figure 2.34 Modeled mean odour concentrations and peak concentrations for the example point source

Table 2.15 Peak to mean ratios at different downwind distances

Downwind distance, km	Unstable	Neutral	Stable
0.1	253.9	1426.4	4292442.0
0.5	10.7	9.4	30.0
1	9.2	6.9	12.3
1.5	8.7	6.3	9.6
2	8.5	6.1	8.6
2.5	8.3	5.9	8.0
3	8.2	5.8	7.7
3.5	8.1	5.8	7.5
4	8.0	5.7	7.3
4.5	8.0	5.7	7.2
5	8.0	5.7	7.1

Figure 2-35 shows the peak to mean ratios for the ground level odour released from a ground level point source. At the very close distance to the source, the peak to mean ratios are very small and they decrease when approaching the source. The peak to mean ratios fluctuate but come to a constant at very far distance.

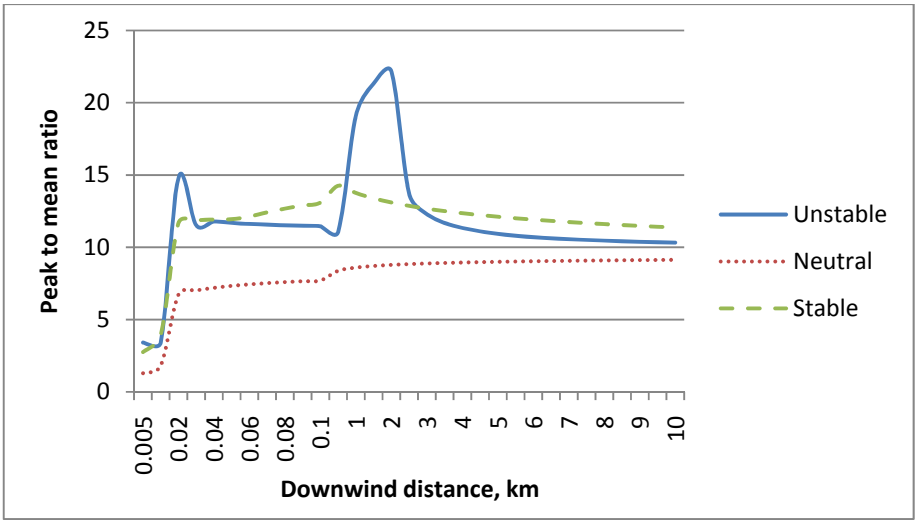

Figure 2.35 Peak to mean ratios with downwind distances from ground level release

2.10.6 Multiple Sources

The frequencies of odour concentration exceeding 1 OU m^{-3} from two point sources at 1 km downwind have been estimated by directly computing from instantaneous concentration (computed method) and from the method used in LODM (modeled method). The two point sources are 10 m away from each other at north-south direction with same characteristics (stack height, stack diameter, exit velocity, exit temperature, and emission rate). The computed odour frequencies from each source and overall odour frequencies from both sources were calculated from the instantaneous concentrations. The odour frequency from the computed method in the Table 2.16 is the averaged values from 100 times of calculations. It indicates that the simplified method used in the model can calculate the odour frequency from multiple sources without large errors (Table 2.16).

Table 2.16 Odour frequencies from computed and modeled methods

Stability class	Computed method			Modeled method		
	P1	P2	P(1+2)	P1	P2	P(1+2)
A	0.42	0.42	0.66	0.41	0.41	0.65
B	0.42	0.42	0.66	0.41	0.41	0.66
C	0.41	0.41	0.65	0.41	0.41	0.65
D	0.53	0.53	0.78	0.60	0.60	0.84
E	0.37	0.37	0.60	0.42	0.42	0.66
F	0.03	0.02	0.05	0.03	0.03	0.05

To further verify modeled method, the odour frequencies from the same two sources for the example hours at the 231 downwind receptors were calculated using the computed method and the modeled method (Figure 2.36). The result indicates that the modeled method to deal with multiple sources is reliable.

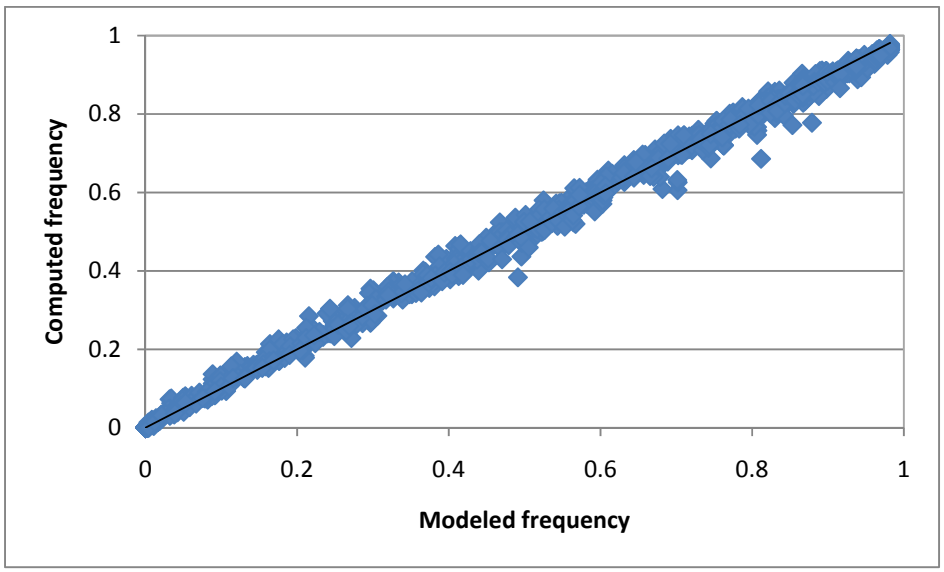

Figure 2.36 Plot of computed odour frequencies and modeled odour frequencies

2.10.7 Odour Concentration and Odour Frequency from an Area Source and an Building Source

Odours from livestock operations are mainly from animal buildings, manure storages units, and land application of manure. When conducting odour dispersion modeling, both manure storages units and land application of manure are often treated as area sources. They are often located on ground level with negligible emitting velocity. No plume rise is considered for area sources. Animal building is treated as a volume source whose dimensions are determined by the building height and the shape of the building. Both area and volume sources are modeled using the virtual point source method.

The odour dispersion from an area source (manure storage) and a volume source (animal building) was analyzed for the example hours with different stability classes at the 231 downwind receptors. The layout of the two sources is shown in Figure 2.37. The building height is 5 m. The odour emission rates for these two sources are both $5 \cdot 10^5$ OU s^{-1}.

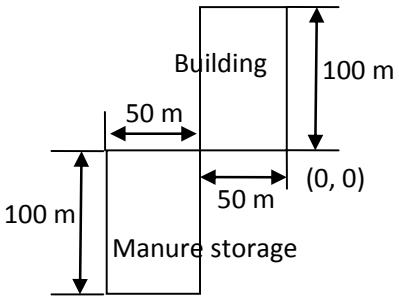

Figure 2.37 Layout of an area source and a volume source

The mean odour concentrations and odour frequencies on the centerline downwind the two sources are shown in Figures 2.38 and 2.39. Mean odour concentrations for 3 unstable hours are almost identical. Mean odour concentrations increase with the increase of stability, but decrease along downwind distance.

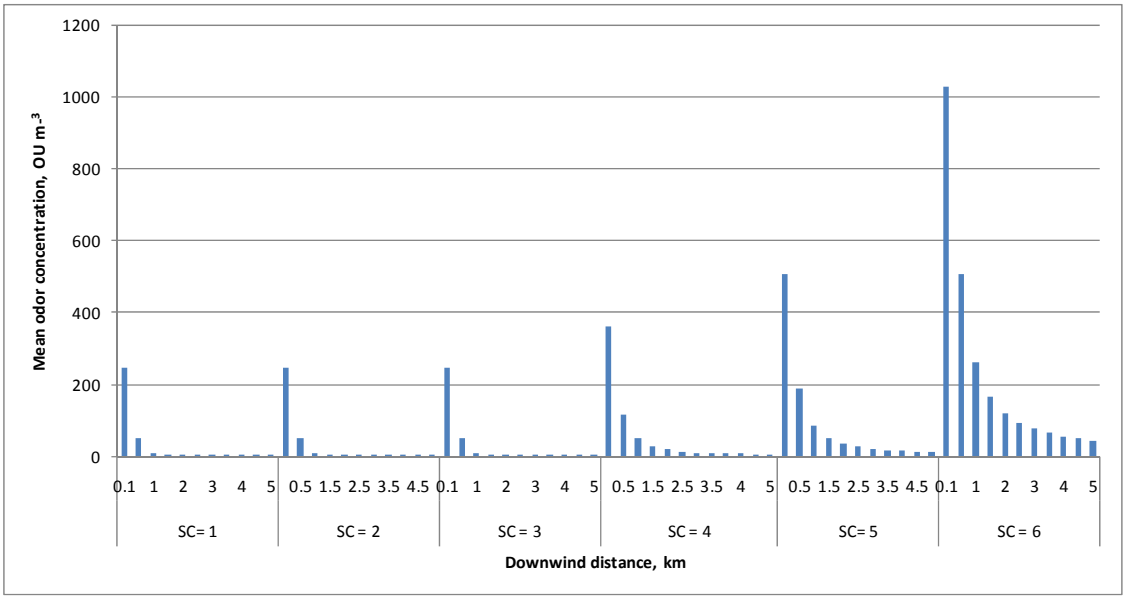

Figure 2.38 Centerline mean odour concentrations from two sources

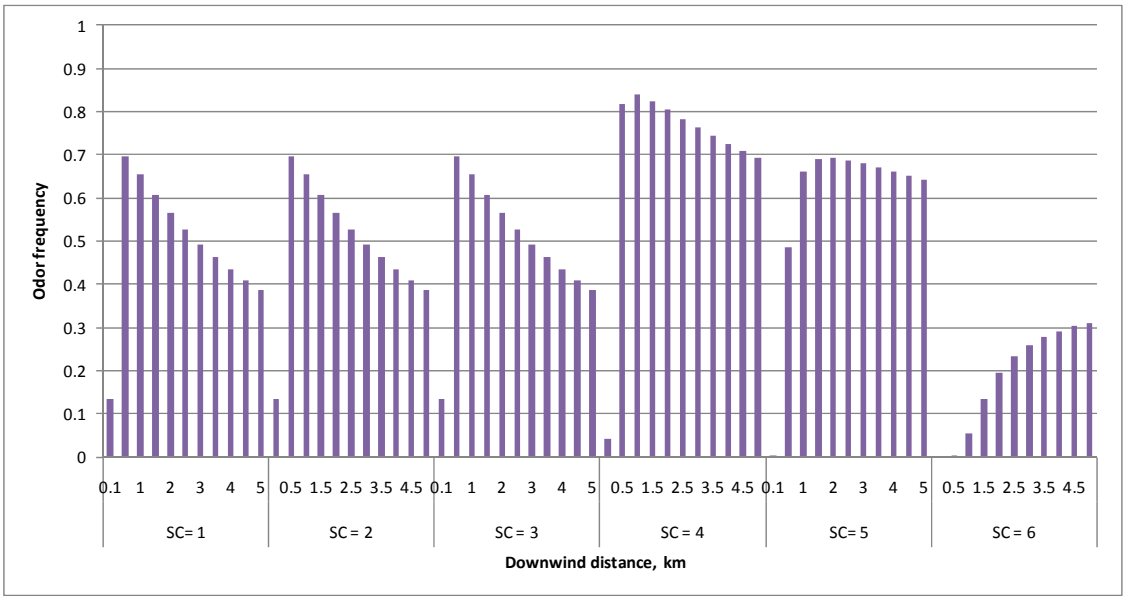

Figure 2.39 Centerline odour frequencies from two sources

The odour frequencies of 1 OU m^{-3} from the two sources for unstable hours are very similar. From a certain distance, the odour frequencies decrease with increase of downwind distance for unstable, neutral, and slight stable conditions (SC = E). However, for stability class F, the odour frequencies increase along downwind distance within the study distances (5 km). However, it is believed that the odour frequencies will go down at even further distance. Odour frequency for neutral stability is the largest. The values of odour frequencies at the same distance decrease with stability changes from neutral to stable.

The mean odour concentration plumes for stability classes 3, 4, and 5 are shown in Figures 2.40 - 2.42. The mean odour concentration plume is no longer wider under unstable condition than neutral and stable conditions, which is probably due to the effects of the superposition of the two sources. However, the odour still travels to longer distance under more stable conditions. The maximum odour concentrations occur at the centerline close to the sources.

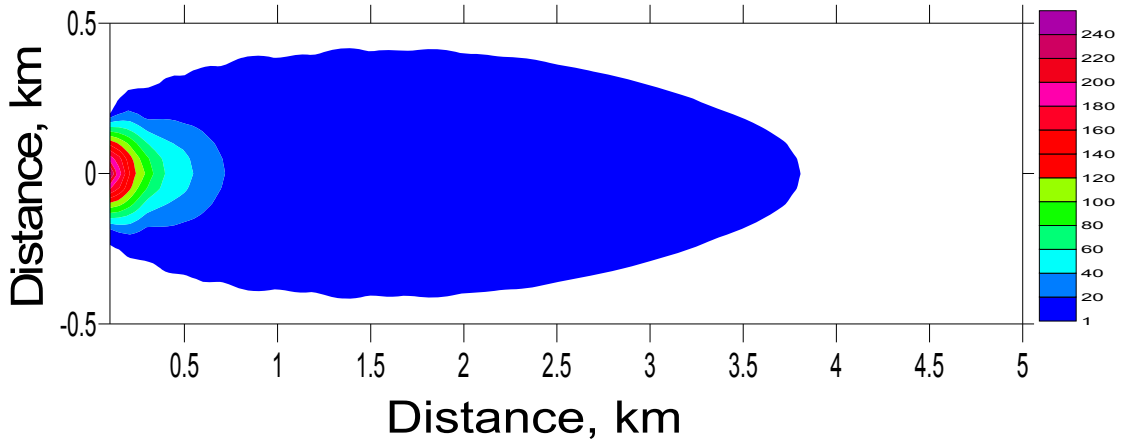

Figure 2.40 Mean odour concentration plume from two sources at unstable condition (SC = C)

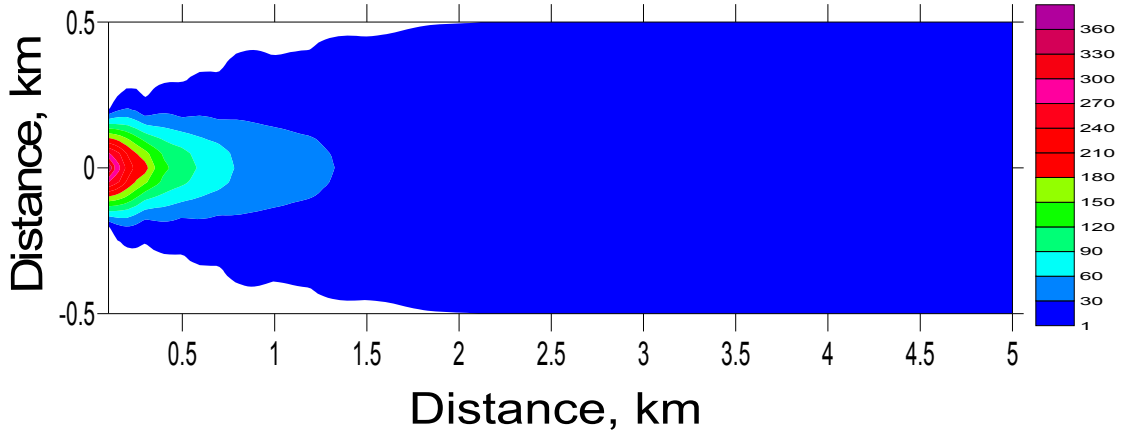

Figure 2.41 Mean odour concentration plume from two sources at neutral condition (SC = D)

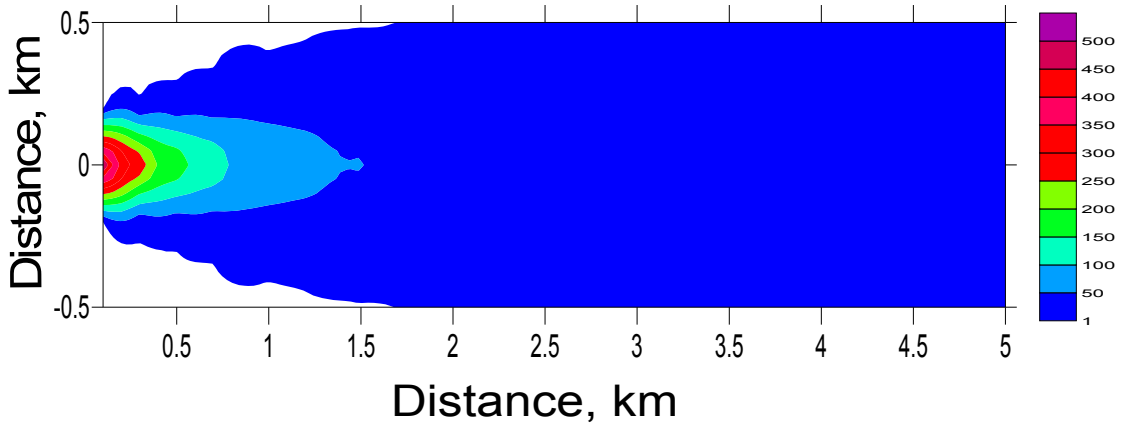

Figure 2.42 Mean odour concentration plume from two sources at stable condition (SC = E)

The odour frequency downwind the two sources for stability classes C, D, and E are illustrated in Figure 2.43 to 2.45. Unlike mean odour concentrations, odour frequencies at the receptors close to sources are low. The maximum odour frequencies occur at the centerline certain distances away from the sources. In close distance, the instantaneous plumes, which fluctuate vertically and horizontally around the steady plume centerline at ground level, are very narrow. The chances that these narrow instantaneous plumes reach the receptor height (1.5 m) are small.

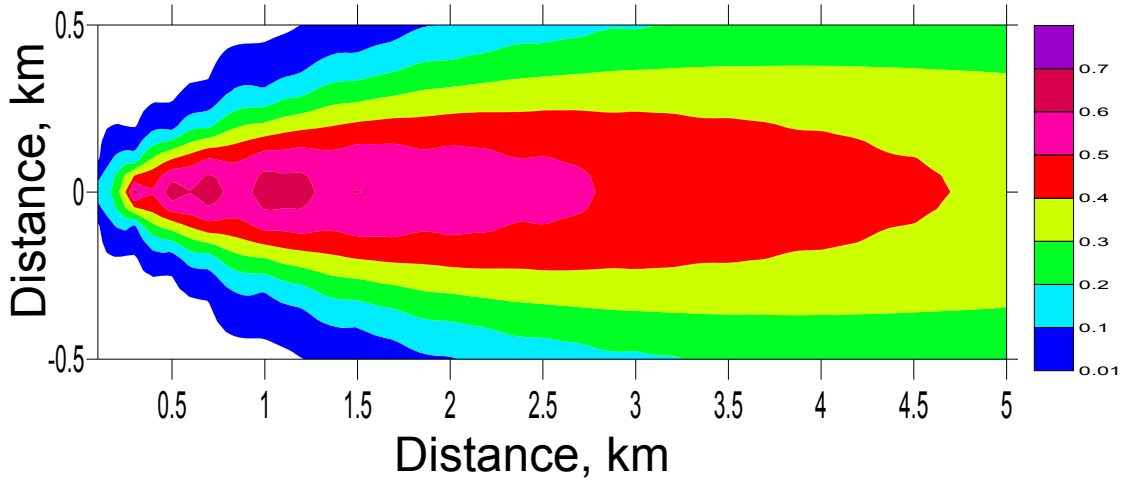

Figure 2.43 Mean odour frequencies from two sources at unstable condition (SC = C)

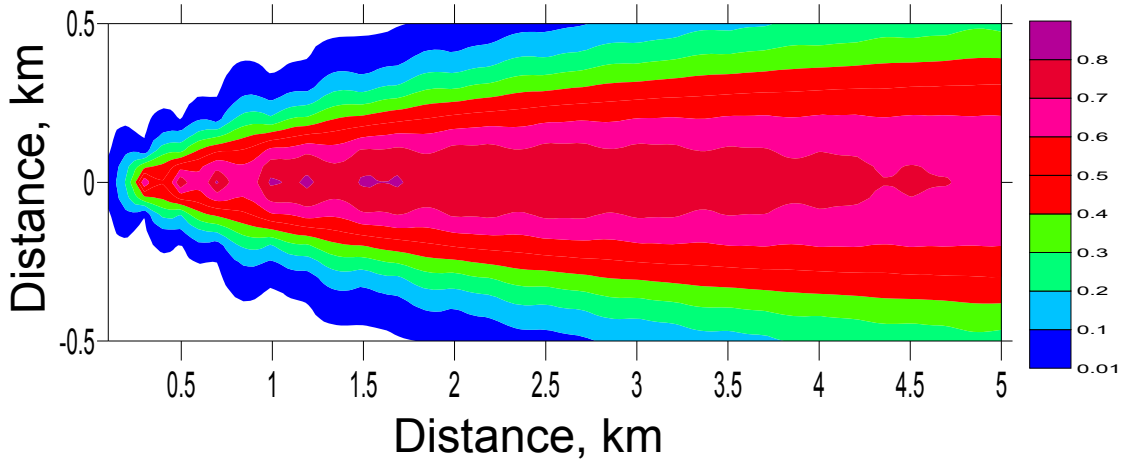

Figure 2.44 Mean odour frequencies from two sources at neutral condition (SC = D)

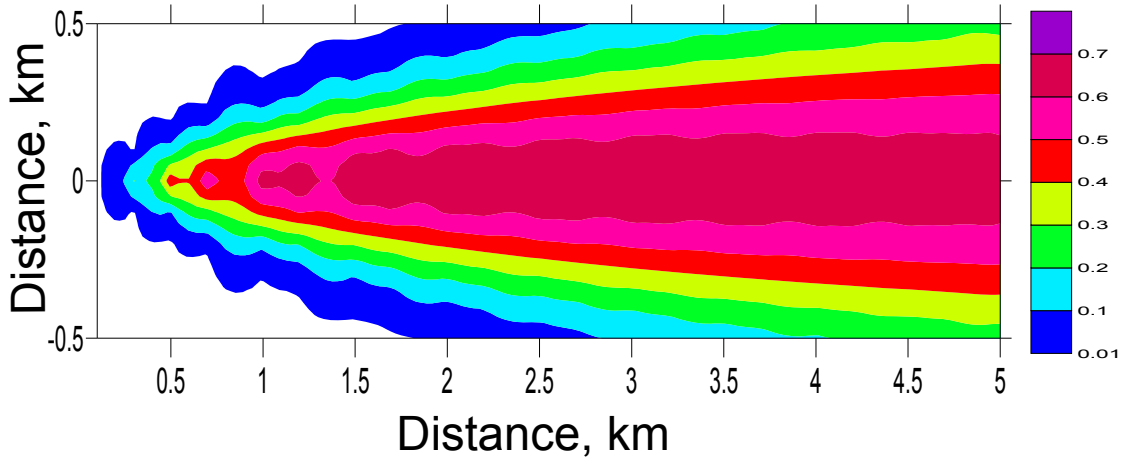

Figure 2.45 Mean odour frequencies from two sources at stable condition (SC = E)

2.10.8 Summary of Case Study

The case study demonstrated that the theories and methods used in LODM can successfully estimate the parameters for characterizing PBL, profiles of wind speed and gradient of potential temperature, Hogstrŏm stability, P-G and Hogstrŏm dispersion coefficients. It also showed that the LODM has the high capability to predict odour concentrations and odour frequencies from an individual point source, area source, and volume source as well as multiple sources. The derived parameters of PBL are close to the values observed in literature. The profiles of wind speed and gradient of potential temperature are reasonable and are able to represent better atmospheric conditions than default values. The Hogstrŏm stability values are considered to be a better indicator of atmospheric stability than P-G stability categories. Both the P-G and Hogstrŏm dispersion coefficients obtained from the case study are within the acceptable ranges and believed to be reliable. The values of odour concentrations and odour frequencies are also within reasonable ranges.

2.11 Summary

In this chapter, the theories and methods that applied in LODM were documented. The fluctuating plume model theory and the weighted odour exceeding half width were underlined. The methods of deriving parameters for PBL and calculating stability and dispersion coefficients were also outlined. The method used to adapt ISC met file was

also emphasized. The approaches to deal with various individual sources and multiple sources were recorded. A case study was conducted to verify the model theories and methods. Results indicated that the theories and methods used in LODM model are reliable and the model functions successfully.

Chapter 3. MODEL DEVELOPMENT PROCEDURE AND MODEL INTRODUCTION

In this chapter, the LODM development procedures that are used to calculate the mean odour concentration, instantaneous odour concentration, peak odour concentration, and odour frequencies were documented. The calculations of downwind distance and crosswind distance were also introduced. Also, a brief introduction of the model interface, functions, and operations was given.

3.1 MODEL DEVELOPMENT PROCEDURES

The fundamental steps in developing the LODM to calculate instantaneous odour concentration, mean odour concentration, peak odour concentration, and odour frequency of certain level odour are:

1) Input source data, meteorological data and receptor locations.
2) Derive parameters involving friction velocity, latent heat flux, and Monin-Obukhov length for PBL.
3) Calculate wind speed profile, vertical gradient of potential temperature, and Hogstrŏm stability parameter.
4) Calculate stack-tip downwash and plume rise for a point source.
5) Calculate long-term plume dispersion coefficient.

Then mean odour concentration can be modeled by the Gaussian plume model for every receptor and every averaging period.

In order to calculate instantaneous odour concentration, the model continues to calculate short time (instantaneous) plume dispersion coefficient, generate random values for location of instantaneous plume centerline, and then calculate the instantaneous odour concentrations by assuming Gaussian distribution of odorous pollutants within the fluctuating plumes.

Peak concentration is calculated by setting fluctuating plume centerline at ground level or receptor height and the horizontal distance to a receptor to be zero. The odour

frequency is calculated by the method of weighted odour exceeding half width which was introduced in detail in previous chapter. The procedures of calculating mean odour concentration, instantaneous odour concentration, peak odour concentration and odour frequency are illustrated in Figures 3.1to 3.4.

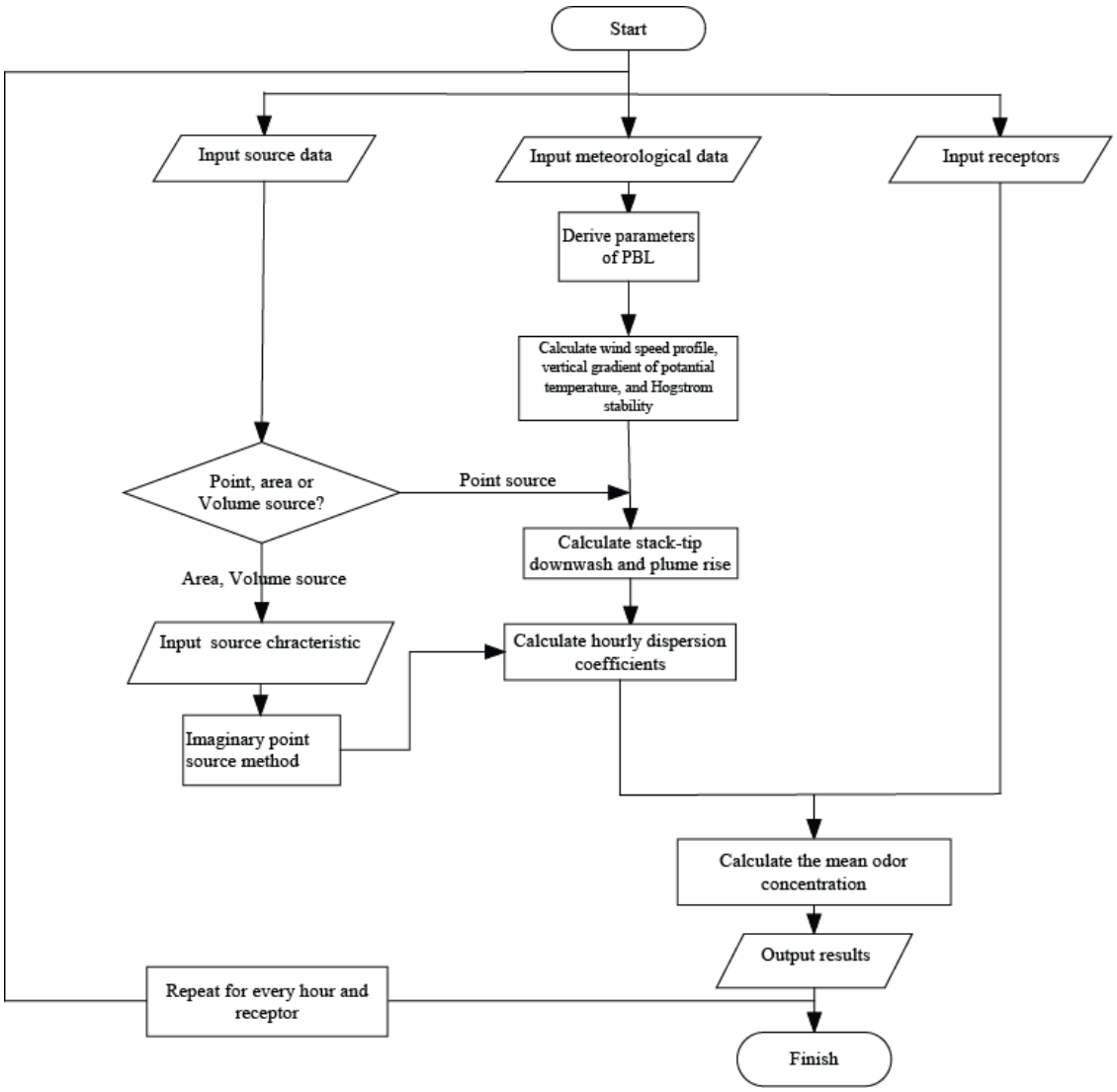

Figure 3.1 Schematic procedure of calculating mean odour concentration by LODM

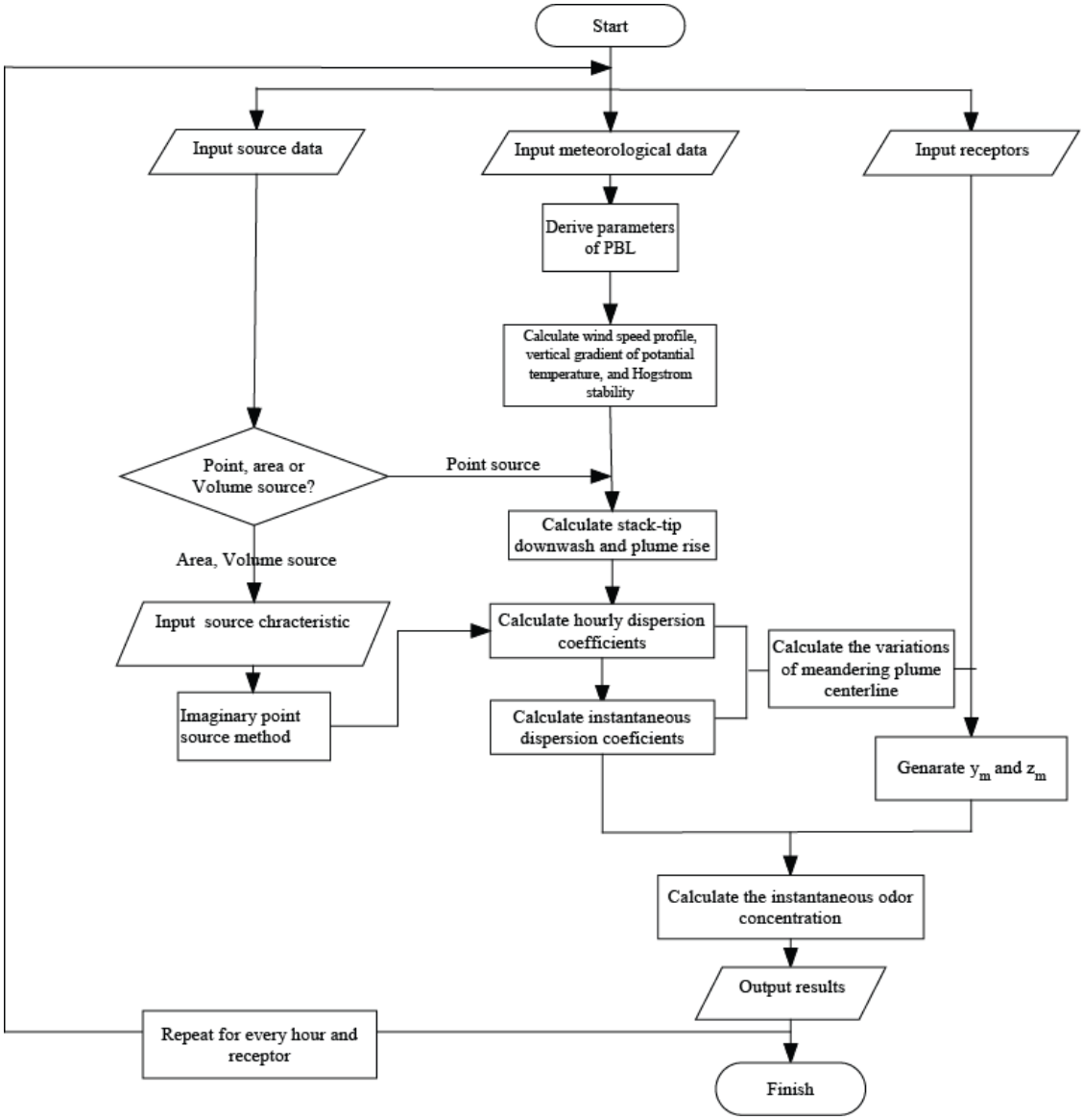

Figure 3.2 Schematic procedure of calculating instantaneous odour concentration by LODM

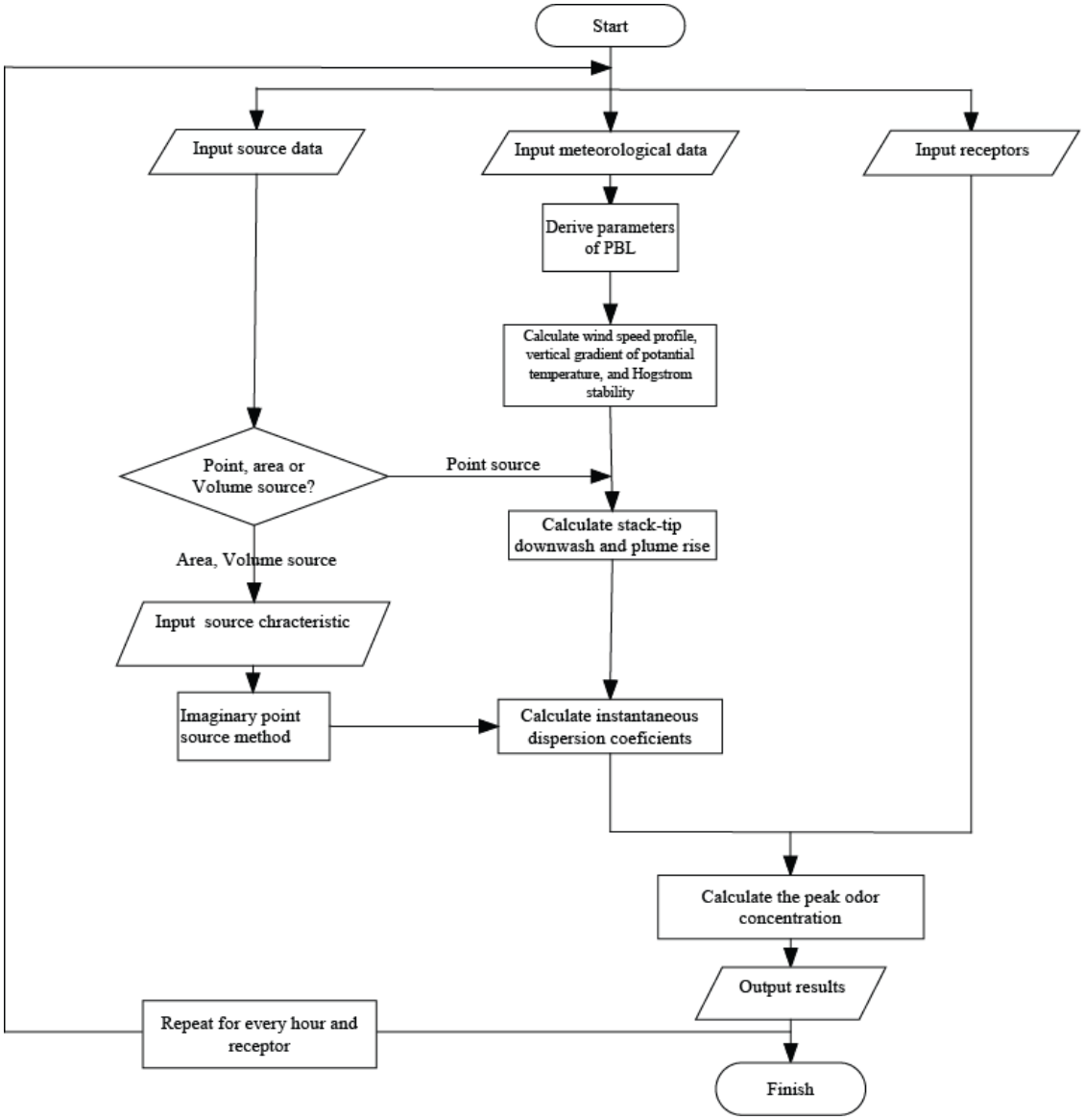

Figure 3.3 Schematic procedure of calculating peak odour concentration by LODM

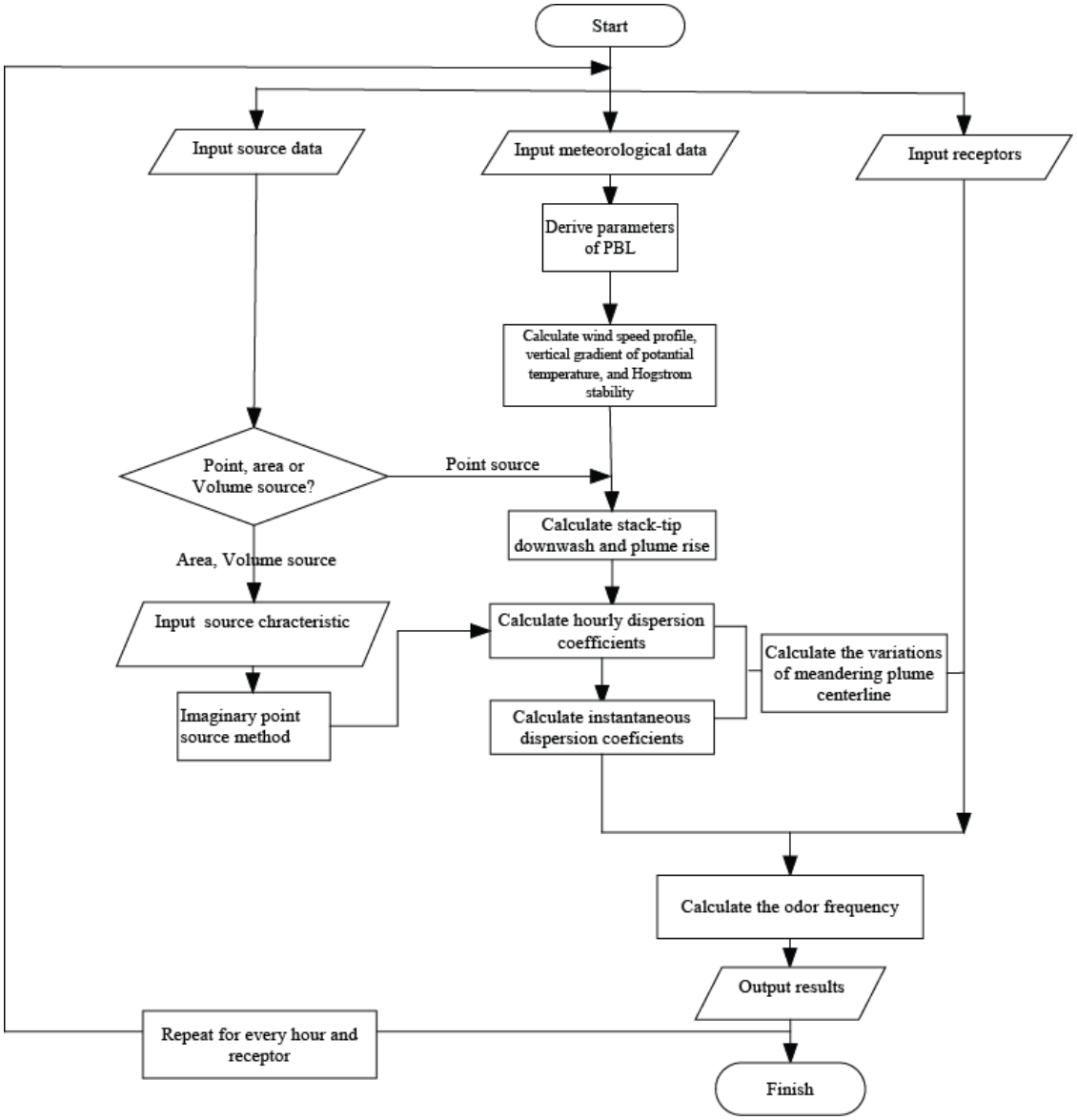

Figure 3.4 Schematic procedure of calculating odour frequency by LODM

3.2 DOWNWIND AND CROSSWIND DISTANCE

LODM uses a Cartesian receptor network as specified by a user. The X axis is positive to east of the user-specified origin and the Y axis is positive to north. The user must define the location of each source with respect to the origin of the grid using Cartesian coordinates.

The downwind distance from a source (x_0,y_0) to the receptor (x_R,y_R) can be determined by (Figure 3.5):

$$X = (x_R - x_0)\sin(WD) + (y_R - y_0)\cos(WD) \quad (3.1)$$

And the crosswind distance can be calculated as:

$$Y = (y_R - y_0)\sin(WD) - (x_R - x_0)\cos(WD) \quad (3.2)$$

In which, WD is the direction to which wind is blowing. This direction is different from the observation of wind direction (WDO) which is the direction wind is blowing from.

If WDO is greater than 180° , then:

$$WD = WDO - 180° \quad (3.3a)$$

In other situations:

$$WD = WDO + 180° \quad (3.3b)$$

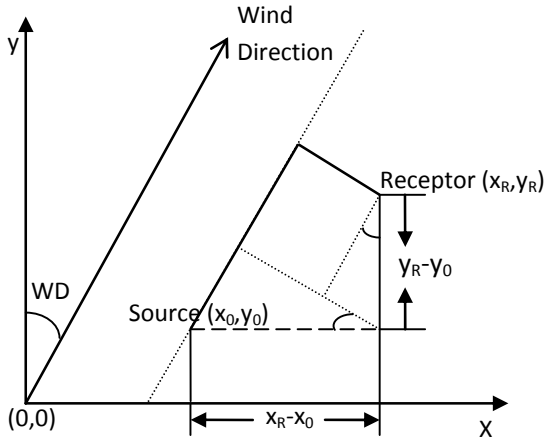

Figure 3.5 Schematic of calculating downwind and crosswind distance

3.3 MODEL INTRODUCTION

The livestock odour dispersion model (LODM) is developed by Visual Basic program. It has a user-friendly interface and is easy to operate. It is very convenient to set up and perform modeling. The following is a brief instruction of the model operation.

3.3.1 Main Interface

The main interface of the model is quite simple (Figure 3.6). It includes five menus (File, Edit, Run, Setup, and Help) and the general setup information of current simulation. "File" menu is used to operate an input file. "Edit" menu is the most important because it includes all necessary inputs that required to be implemented in the model. After setting

up the model, users can simply click “Run” to run it. The “Set up” and “Help” menus can provide some additional information regarding the model configuration. The general setup information includes title, simulation period, source information, and output options. It will help users have an overview of each simulation process.

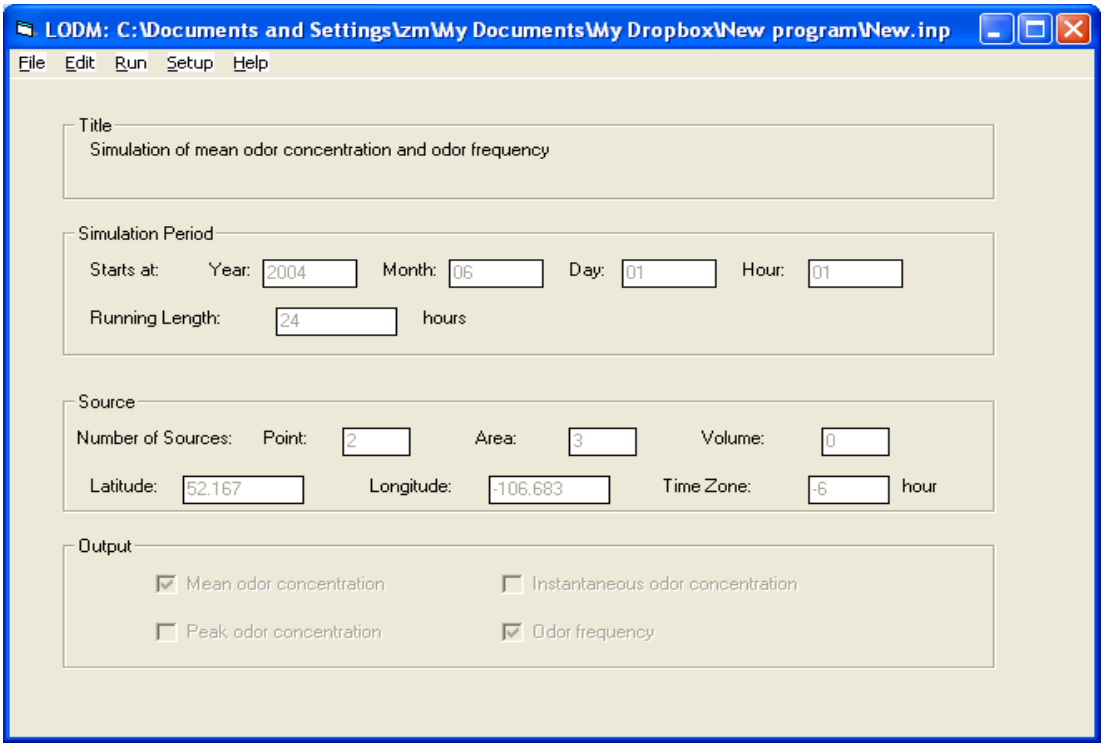

Figure 3.6 Main interface of LODM

3.3.2 “File” Menu

Under “File” menu (Figure 3.7), users can create a new input file, open an existing input file, and save current input file or save it as other files using different sub menus. Users can also click the “exit” menu to exit the model. Recently opened files can be automatically shown at the bottom of the menu. Users can open a recently opened file by simply clicking on it.

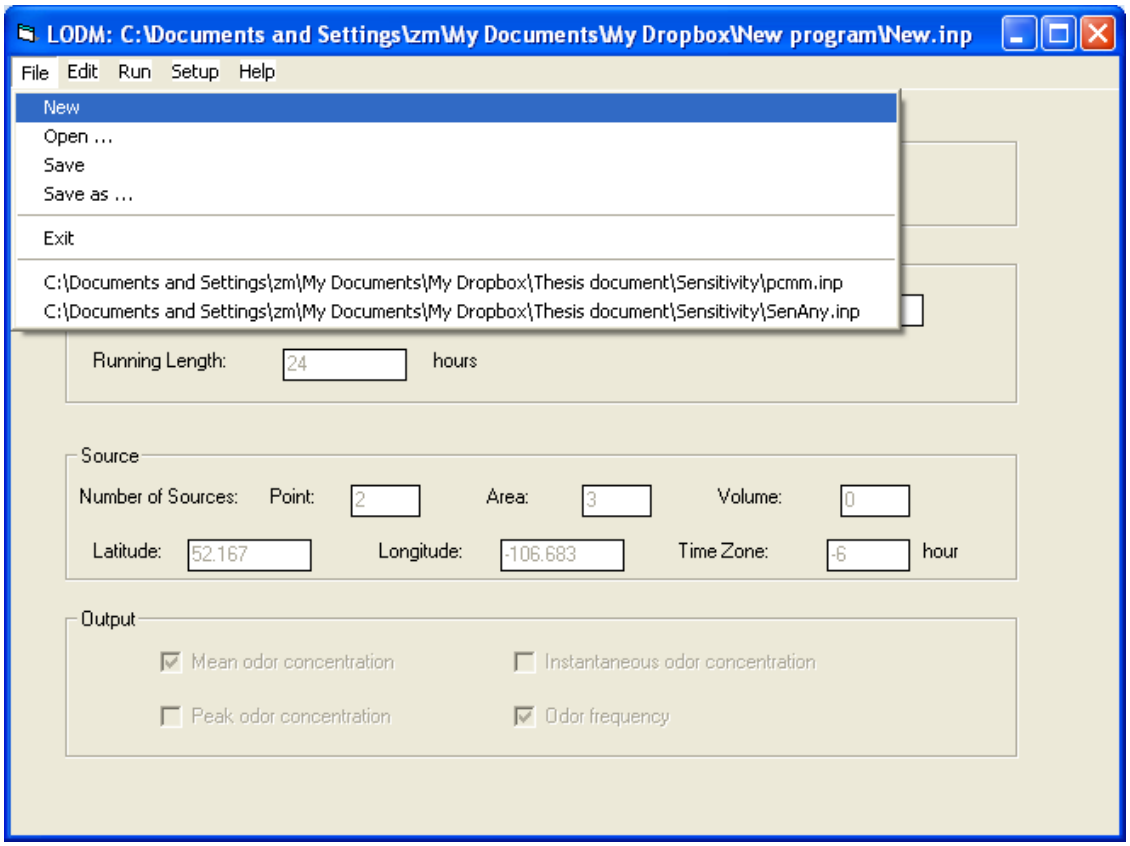

Figure 3.7 File menu of LODM

3.3.3 "Edit" Menu

"Edit" menu (Figure 3.8) is used to input or edit the necessary source information, meteorological and receptor data as well as other parameters to configure a model simulation. All required information to run the model can be set up under this menu. It includes "Simulation", "Source information", "Receptors", "Surface parameters", and "Model output".

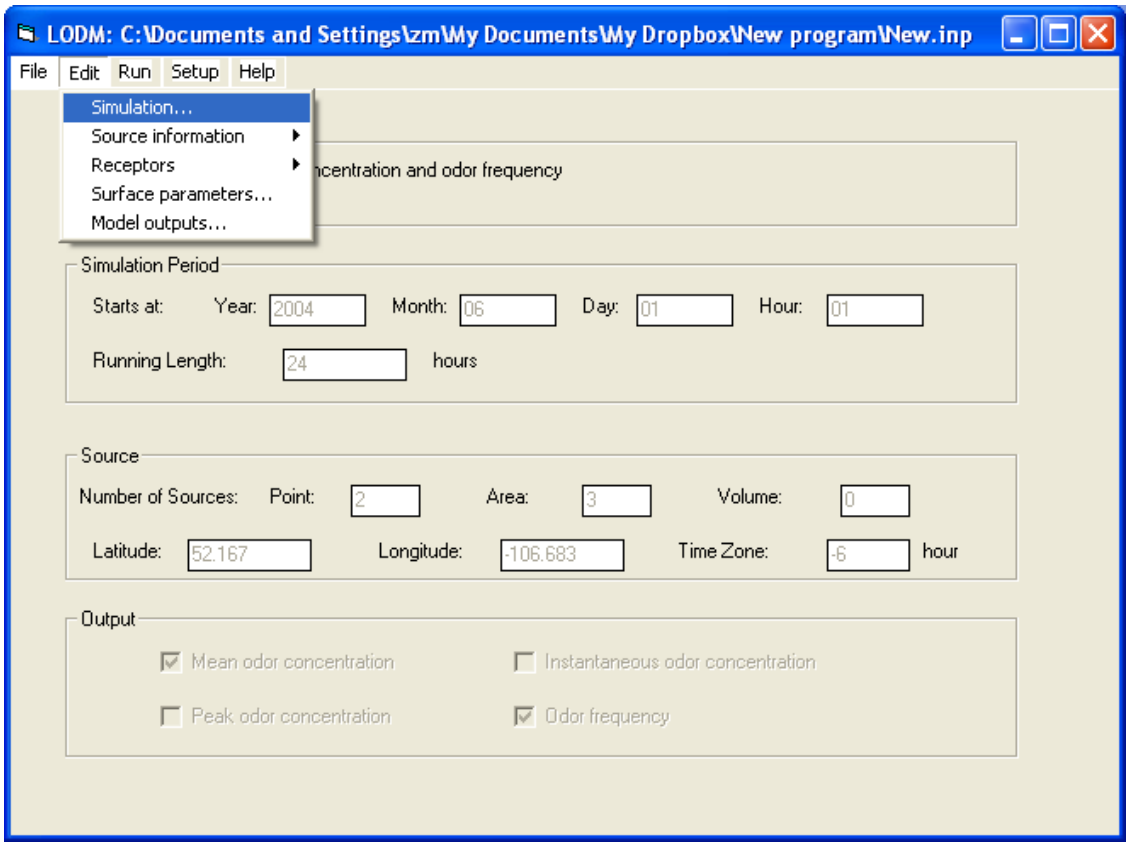

Figure 3.8 Edit menu of LODM

"Simulation"

In this window (Figure 3.9), users can input simulation title and meteorological data and select either Pasquill-Gifford or Hogstrŏm dispersion coefficient to operate a modeling. LODM can only accept the similar met data format as that of ISCST3, in which year, month, day, hour, wind direction, wind speed, temperature, stability class, and mixing height are mandatory while radiation and cloud cover are optional. The format of a met file is shown in Figure 3.10. Before inputting meteorological data, users need to determine the type of a met file to be used. This can be done by selecting the different types of met files listed as ISC met file, ISC met file + cloud cover, ISC met file + radiation, and ISC met file + cloud cover + radiation. If the ISC met file option is selected, the model converts the stability class into either cloud cover or radiation to derive parameters in PBL. If radiation or cloud cover data are available, LODM use these data to derive parameters for characterizing CBL or SBL.

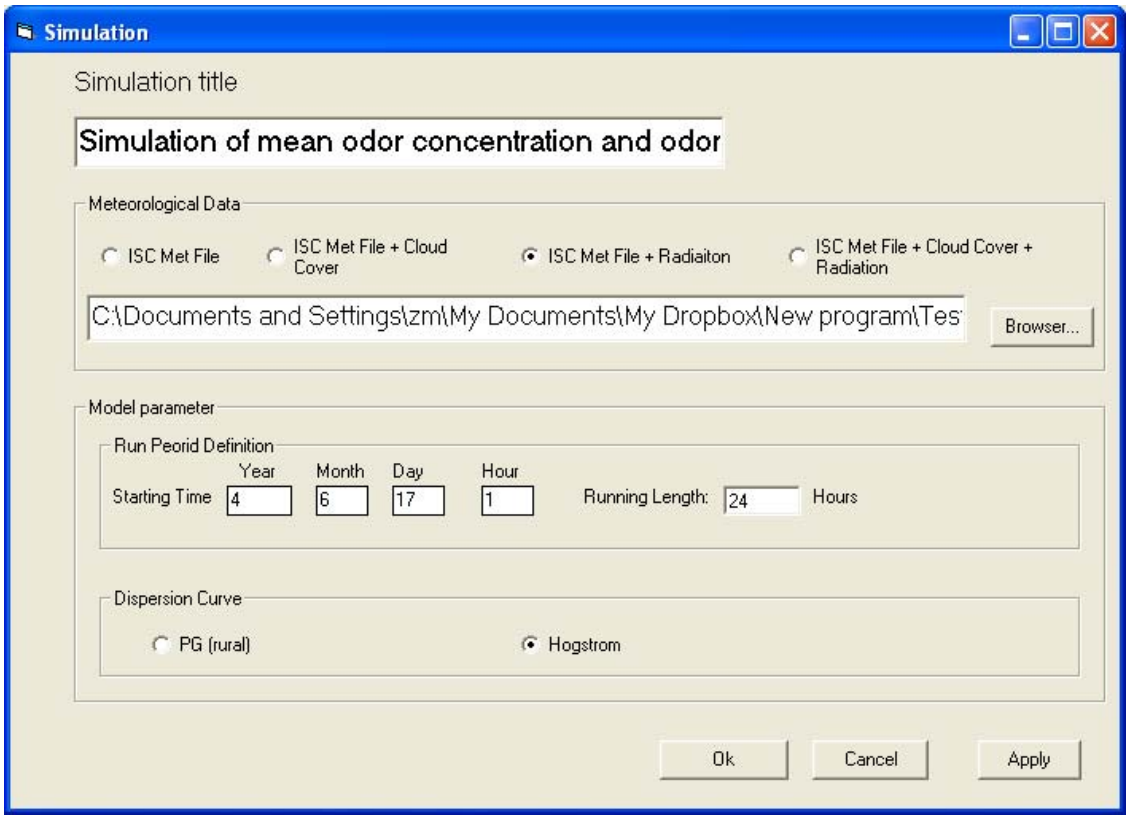

Figure 3.9 Simulation window of LODM

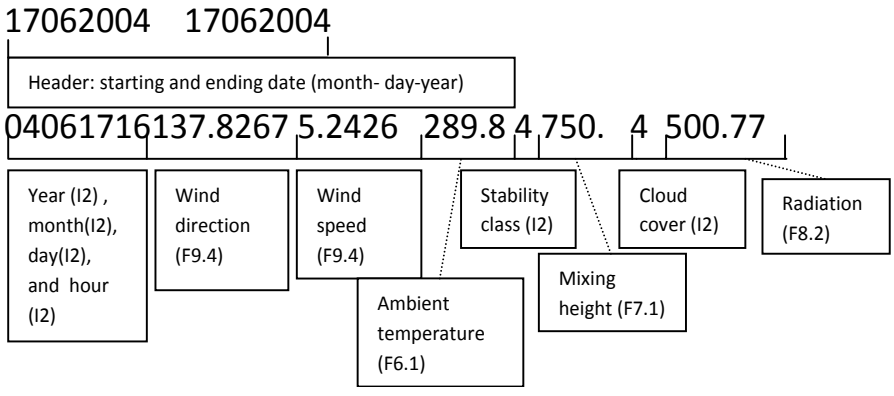

Figure 3.10 Format of input meteorological data file

"Source information"

Point source, area source, and volume source can be modeled in LODM. Odour emitted from an elevated stack can be treated as a point source. A manure storage can be

considered as an area source. Odour emitted from an animal building is not only from fans but also from the openings and leakages. Due to the complicated sources and the effect of building downwash, an animal building can be treated as a volume source. An initial vertical dispersion dimension can be determined from building height.

Point source

As many as 1000 point sources can be added in one modeling (Figure 3.11). Users can easily add, insert, and delete sources. Source name, location, stack height, stack diameter, exit velocity, and exit temperature are needed to calculate plume rise for a point source.

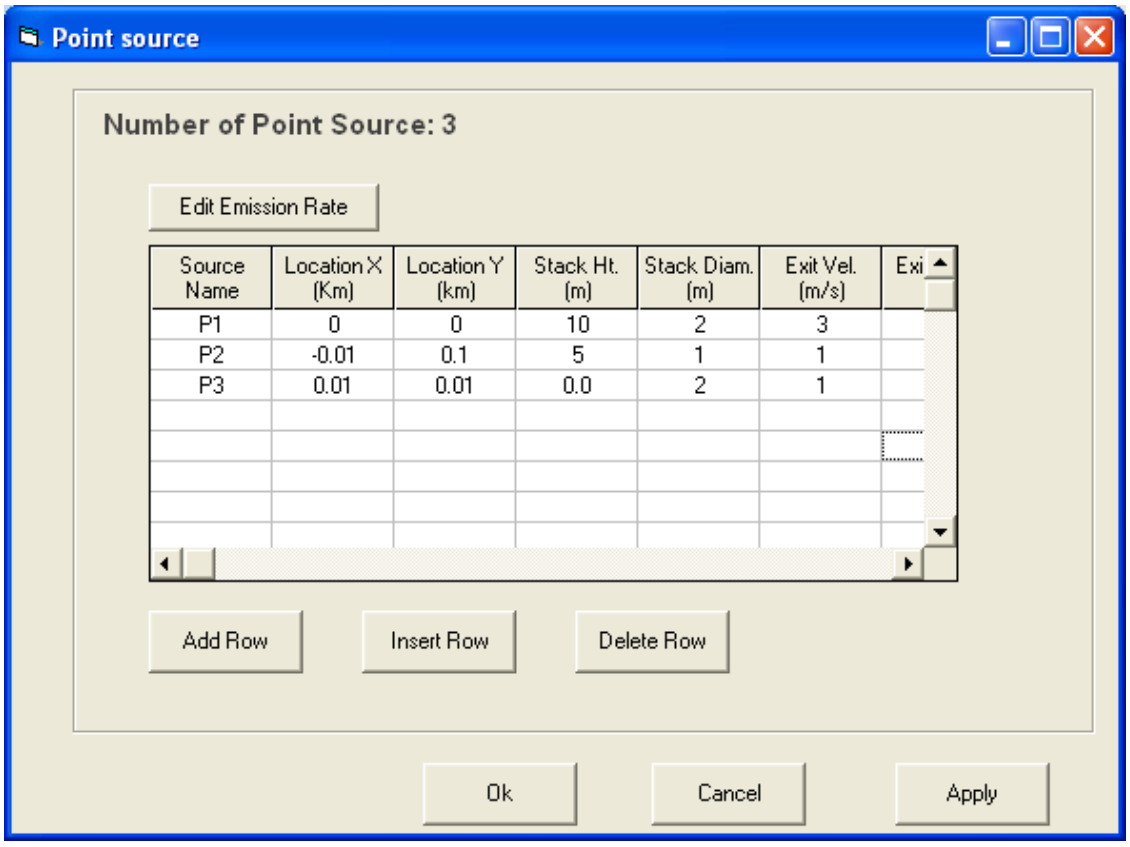

Figure 3.11 Point source window of LODM

Either constant or variable emission rate can be input. For variable emission rate, it can vary hourly, diurnally, monthly, or seasonally as shown in Figure 3.12. When diurnal option is selected, odour emission rate for every hour of the day can be input. When monthly option is selected, odour emission rate can be entered for every month in a year.

When season and hour option is selected, the model provides an input availability of hourly odour emission rate for four seasons.

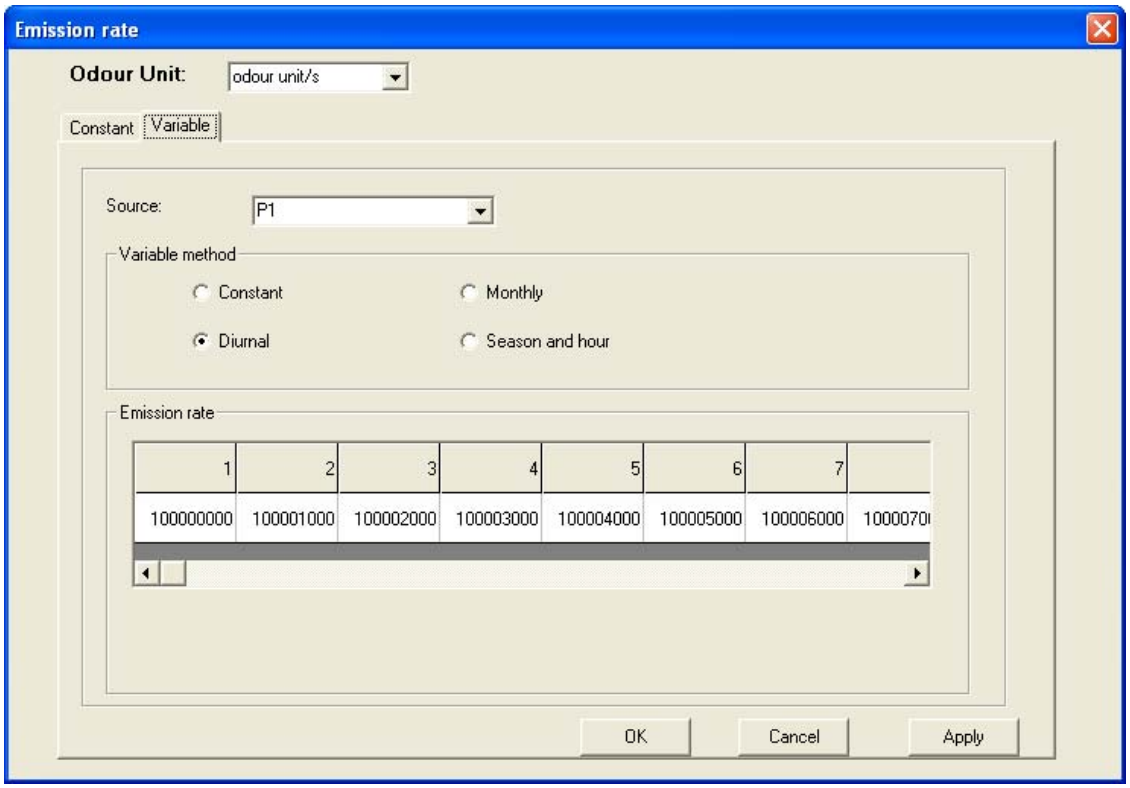

Figure 3.12 Variable emission rate window of LODM

Area source

In the area source window, it is easy to add or delete an area source (Figure 3.13). The location and the area of an area source are determined by user inputted information. LODM can support a simulation of an area source in quadrangle or circular shape. Any non-circular source can be simplified to a certain quadrangle shape by setting up coordinates of its four vertexes. For a circular area, it is very easy to determine the center of source and the maximum projected width of an area source along wind direction.

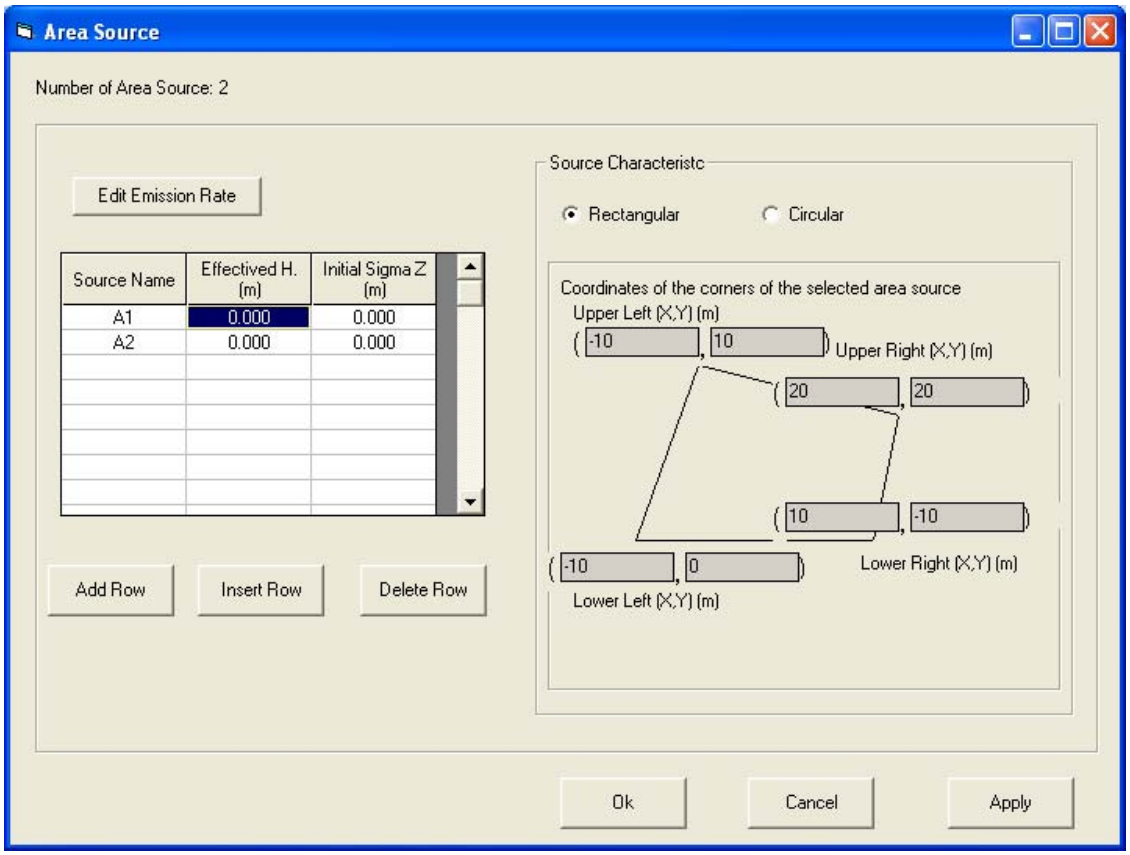

Figure 3.13 Area source window of LODM

In order to consider the shape and area of a quadrangle area source, users need to input coordinates of its four vertexes. As shown in Figure 3.14, the maximum projected width of a source along wind direction, which will be used as the initial dimension of horizontal dispersion, and the center of an area source to determine the location of a virtual point source and downwind and crosswind distances of a receptor can be calculated by the following steps :

1) calculate the maximum and minimum distance from each vertex to the wind direction

For example, for one of the vertex of an area source, $A(x_1,y_1)$, the distance from A to the wind direction will be:

$$Y_1 = (y_1)\sin(WD) - (x_1)\cos(WD) \quad (3.4)$$

Calculate the distance for each vertex, and find out the maximum (Y_{max}) and minimum values (Y_{min})

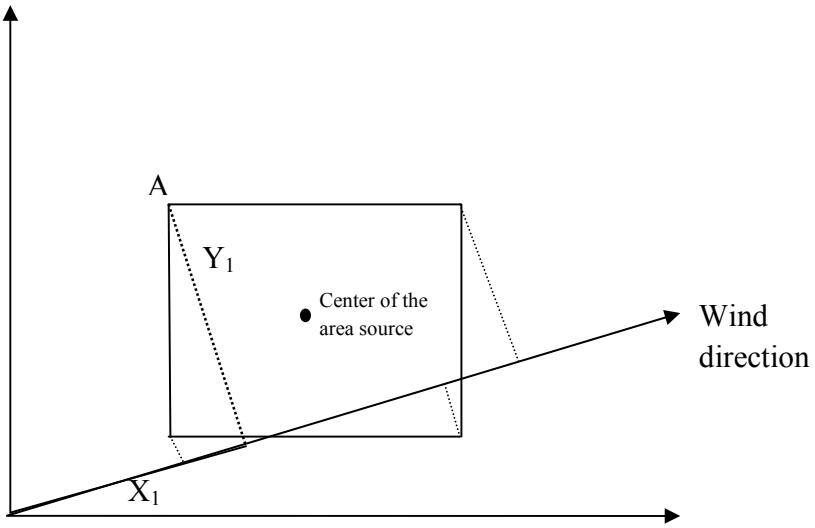

Figure 3.14 Schematic of the treatment of an area source

2) calculate the maximum projected width of an area source along the wind direction

$$P_{wmax} = Y_{max} - Y_{min} \quad (3.5)$$

3) Calculate the maximum and minimum downwind distance of the project of each vertex on the wind direction. For the same example,

$$X_1 = (x_1)\sin(WD) + (y_1)\cos(WD) \quad (3.6)$$

It is easy to get the maximum and minimum distance, X_{max} and X_{min}.

4) The center of the area source (X_c', Y_c') in the new origin using wind direction as x axis:

$$X_c' = X_{min} + (X_{max} - X_{min})/2 \quad (3.7a)$$

$$Y_c' = Y_{min} + (Y_{max} - Y_{min})/2 \quad (3.7b)$$

5) The coordinates of the center of an area source(X_c,Y_c):

$$X_c = (X_c')\sin(WD) - (Y_c')\cos(WD) \quad (3.8a)$$

$$Y_c = (X_c')\cos(WD) + (Y_c')\sin(WD) \quad (3.8b)$$

6) Use the same method described in the section 3.2 to calculate the downwind distance and crosswind distance for the area center to the receptors.

"Volume source"

A volume source is treated almost as same as an area source (Figure 3.15). The initial sigma Z is from the volume source (building) height. The area view of volume source can be determined by the coordinates of four vertexes for quadrangle shape and by the center and diameter for a circular shape.

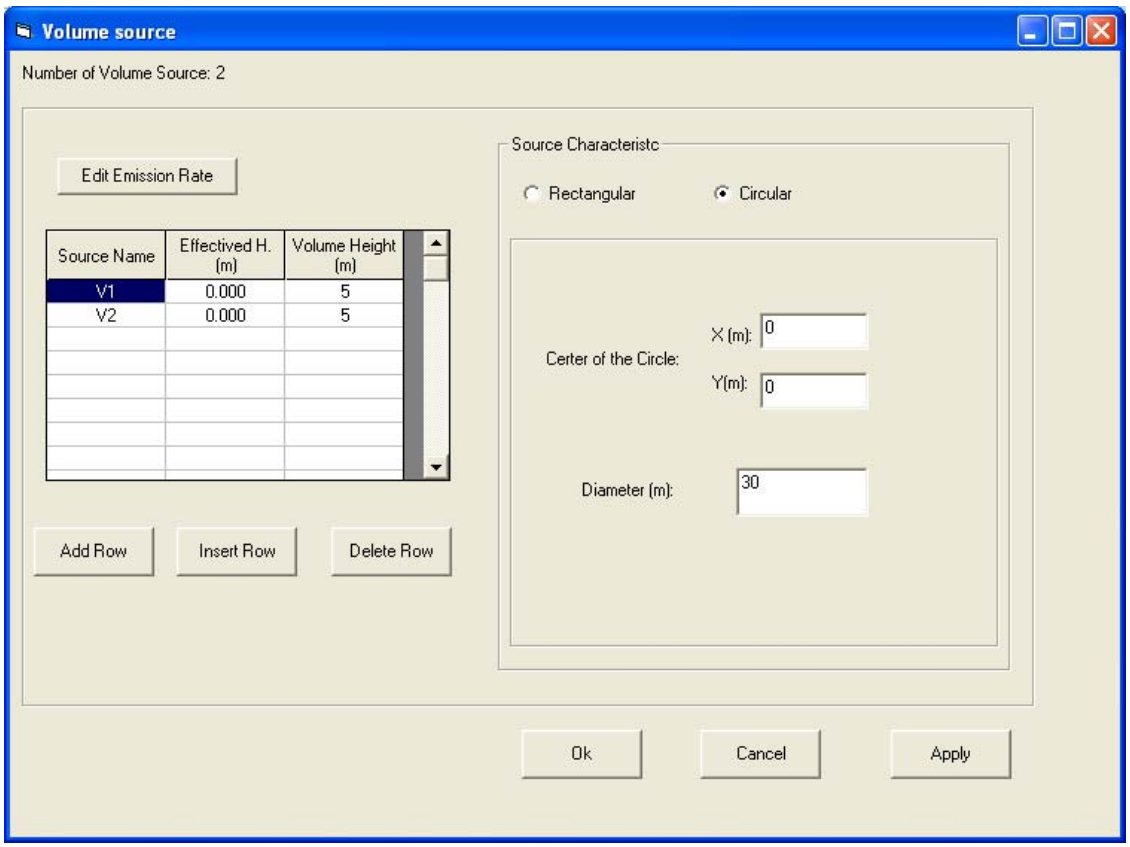

Figure 3.15 Volume source window of LODM

"Receptor"

Grid receptors

A receptor grid can be set up by grid origin, grid number at x and y directions, and grid cell size at x and y directions. As shown in Figure 3.16, the input determines a grid which x direction is from -50 m to 150 m with ten 20 m subgrids and y direction is from -50 m to 250 m with ten 30 m subgrids. The receptors' height is 1.5 m.

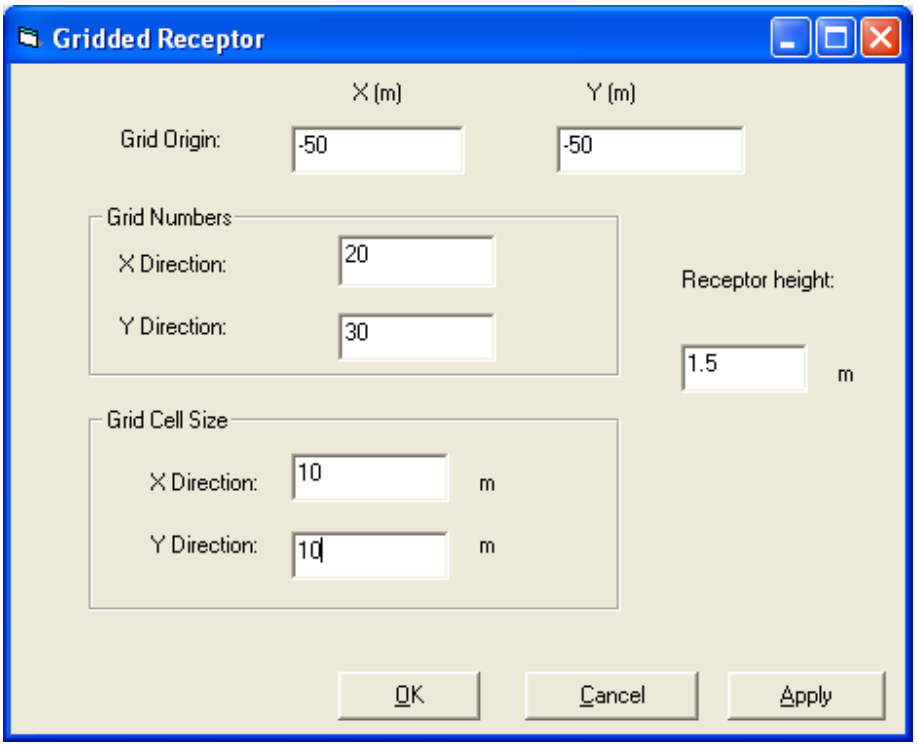

Figure 3.16 Gridded receptors of LODM

Discrete receptors

Receptors can be added one by one, or loaded by file. And the current receptors can be saved into file. The receptor number, location and height should be provided (Figure 3.17).

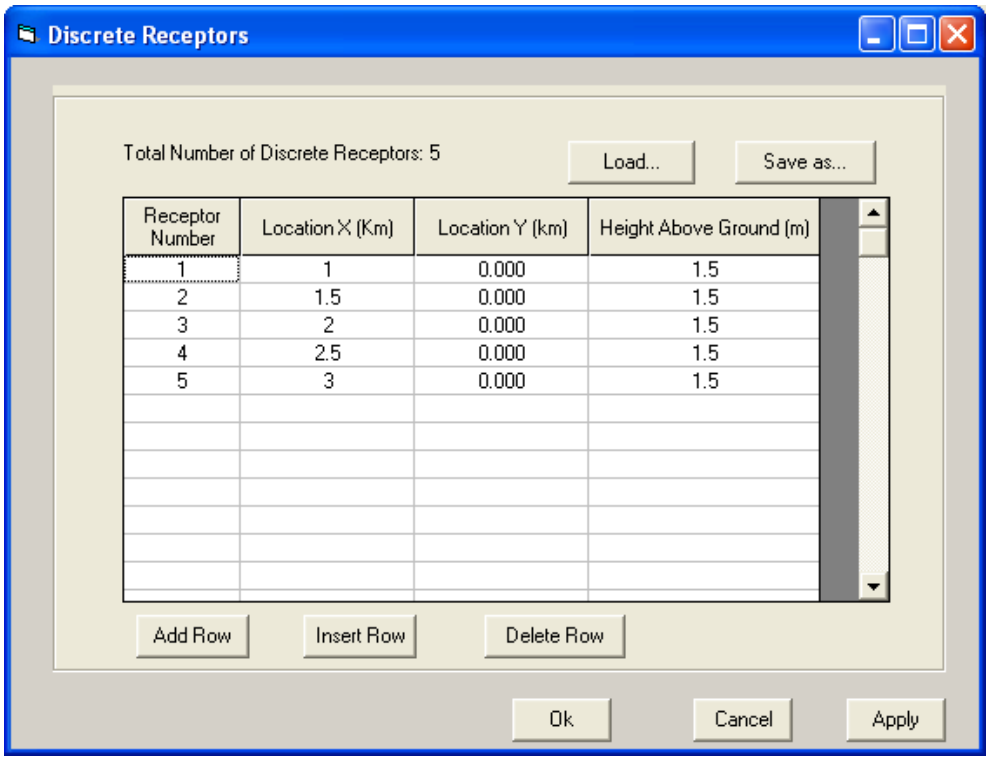

Figure 3.17 Discrete receptors of LODM

"Surface parameter"

In this window, users can input geographic location and time zone of a source as well as surface roughness, albedo, and Bowen ratio that will be used in characterizing PBL (Figure 3.18). The surface roughness length is related to the height of obstacles to wind flow, but also influenced by the shape, flexibility and density of vegetation (Smith et al, 1993; US EPA, 2004). It is, in principle, the height at which mean horizontal wind speed is zero. Values range from less than 0.001 m over a calm water surface to 1 m or higher over a forest. Albedo is the ratio of reflective solar radiation by the surface to incident solar radiation. Typical values range from 0.1 for thick deciduous forests to 0.90 for fresh snow (US EPA, 2004). Daytime Bowen ratio is a ratio of sensible heat flux to latent heat flux, which is an indicator of surface moisture. Midday values of Bowen ratio range from 0.1 over water to 10.0 over desert. The suggested values of these parameters for modeling can refer to US EPA (2004), Paine (1987), and Stull (1998).

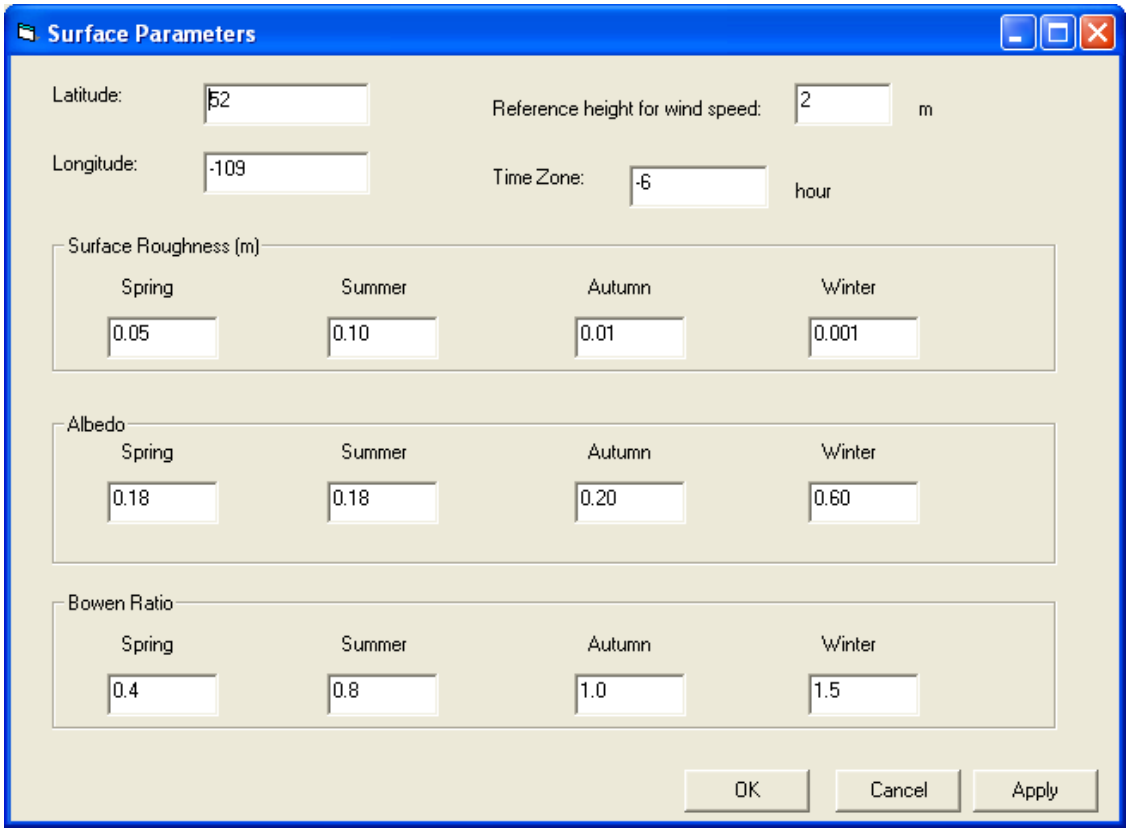

Figure 3.18 Surface parameters of LODM

"Model output"

In the model output window, users can choose different output formats. Either hourly mean odour concentrations, instantaneous odour concentrations, peak odour concentrations, or odour frequencies for certain level odour can be selected. Different files can be selected for various model outputs. Instantaneous odour concentrations can be calculated according to users' requirements regarding how many values would be calculated and output. For example, if 60 s is selected, then the model will calculate 60 instantaneous odour concentrations every hour. If 5 s is selected, then 720 instantaneous odour concentrations will be calculated and output. Also, users can select different odour levels to calculate odour frequency. As shown in Figure 3.19, the model will output odour frequencies of odour concentration exceeding 1 OU m^{-3} into a selected file.

If the intensity button is checked, the model will output odour intensity. In Figure 3.20, three conversion methods are provided including Weber-Fecher law, Steven's power law,

and Beilder model. Users can define specific coefficients or select one of the recommended equations for their purposes. Odour frequency can also be defined by odour intensity level. By selecting a certain intensity level, the model will convert the intensity into concentration by selected conversion equation, and then calculate corresponding odour frequency.

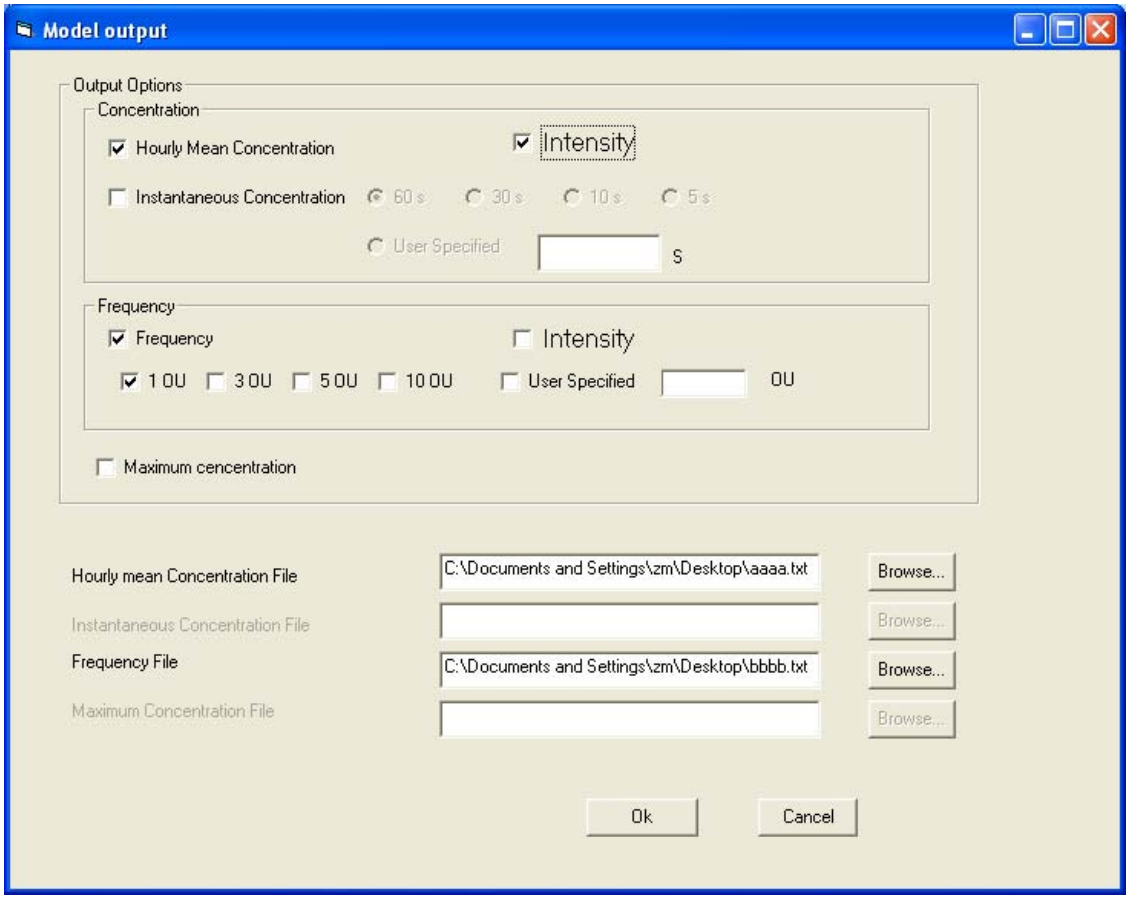

Figure 3.19 Model output window of LODM

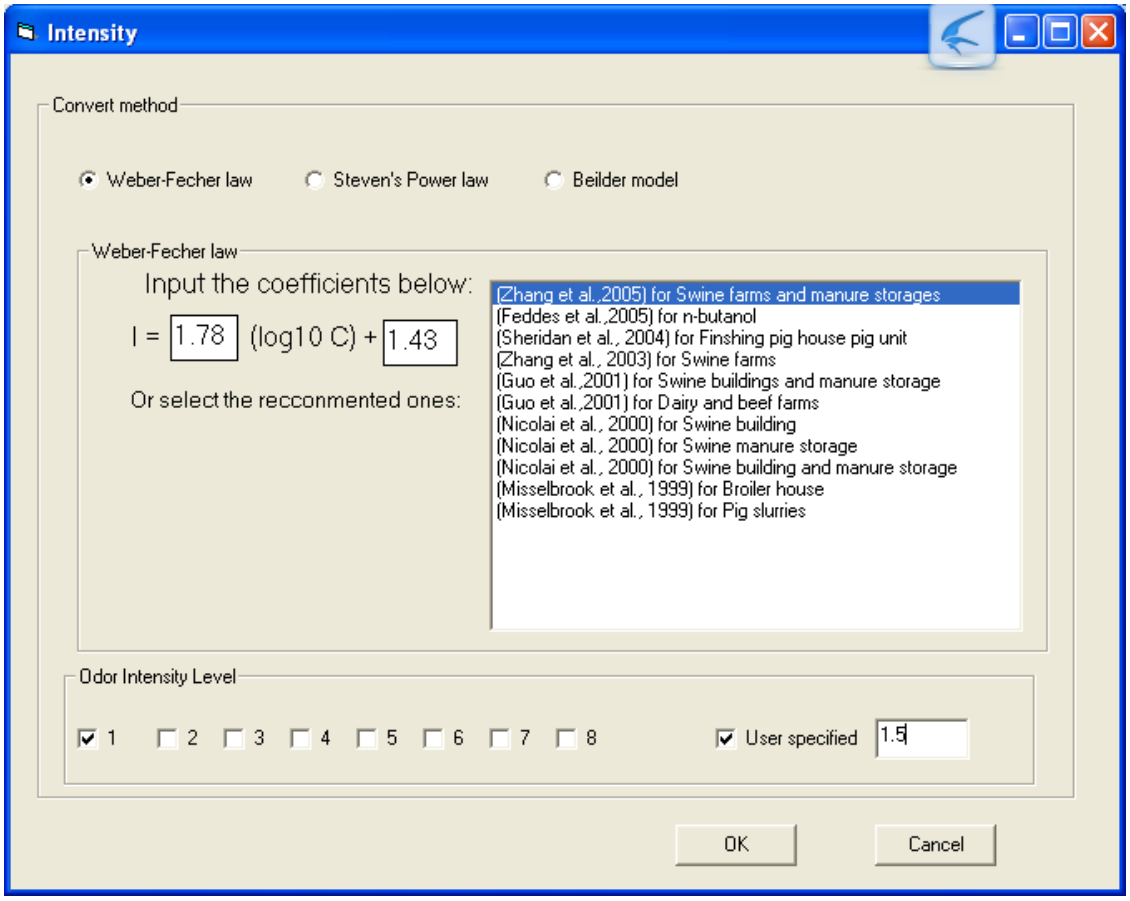

Figure 3.20 Intensity window of LODM

Chapter 4. MODEL EVALUATION AND VALIDATION

Field plume measurement data (data from University of Manitoba and University of Minnesota) were used to evaluate and validate the model developed. Specifically, field measured odour intensities were used to evaluate the LODM predicted odour intensities and odour frequencies. Model predicted odour concentrations based on field measured data from University of Manitoba were also compared to those from ISCST3 and CALPUFF model.

4.1 DATA FROM UNIVERSITY OF MANITOBA

4.1.1 Site Description and Odour Emission Rates

Trained odour sniffers were used to make odour plume measurement around two swine farms (A and B) located in southern Manitoba. The farms were 3000-sow farrowing operations, with identical mechanically ventilated barns. The major difference between the two farms was that Farm A had open single cell earthen manure storage (EMS) whereas Farm B had a two-cell EMS with negative pressure synthetic covers (NPSC). The surroundings of two farms were similar - mostly flat cropland, the roughness length is assumed to be 0.1. Odour emission rate was measured during the period of each odour plume measurement (Zhang et al., 2005). The summary of odour emission rates from the measurement conducted during the odour plume measurement periods are given in Table 4.1.

Table 4.1 Odour emission rates of the farms (Zhang et al., 2005)

	Total Odour Emission (OU s^{-1})					
Farm	Farm A			Farm B		
Date	Building	Storage	Total	Building	Storage	Total
17-Jun-04	115381	571680	687061			
22-Jun-04	186738	118440	305178			
29-Jun-04	94236	501480	595716			
6-Jul-04				145245	1126	146371
8-Jul-04	159819	576720	736539			
13-Jul-04				248161	1674	249835
15-Jul-04	147364	917280	1064644			
20-Jul-04				239651	7408	247059
26-Jul-04				158304	3001	161305
5-Aug-04				267189	5570	272759
12-Aug-04	73261	447120	520381			
17-Aug-04	168944	616320	785264			

4.1.2 Downwind Odour Plume Measurement

Fifteen human odour sniffers were selected and trained for conducting field odour measurements (Zhou et al., 2005). Standard reference n-butanol samples were used to calibrate the sniffers' noses, before they left for the field for each session. A base point was determined by geographical (longitude and latitude) readings from a GPS. It was selected on the edge of the farm. According to the measured wind direction, 15 sniffers were assigned to a three-row grid of 100, 500, and 1000 m downwind from the base point with the assistance of GPS units (GPS 45, Garmin International, Lenexa, Kansas).

Every sniffer followed a central coordinator's instructions to sniff. During each 10 min measurement session, the sniffers put on a carbon filtered air mask to rest his/her nose and sniffed the odour for 10 seconds, and then recorded the odour intensity and odour

description. At the end of each session, 61 observations had been recorded by each sniffer. Normally three measurement sessions were carried out within one hour, with a 10-min break between sessions (Xing, 2006).

Fifty-one field sessions was conducted around the two farms. Only 33 sessions conducted in daytime were used in this study because of insufficient data to determine the stability classes during night time. Weather data including solar radiation, temperature, relative humidity, and wind speed and direction were taken every minute five minutes before and during the plume measurement period by an on-site weather station (WatchDog Model 550, Spectrum Technologies Inc., Plainfield, IL). The weather station was placed at 2 m above the ground to collect weather information during each session.

4.1.3 Model Configuration

Mean odour concentrations predicted by LODM were compared to those from CALPUFF and ISCST3. Both Passquil-Gifford and Hogstrŏm dispersion coefficient schemes were used in LODM to calculate mean odour concentrations. For comparison, configurations of the three models are set up to be same or as close as possible, for example, all three models use the buoyancy-induced dispersion, no exponential decay for rural mode, and no dry/wet depletions. When P-G dispersion coefficients are applied in LODM, default wind profile exponents and default vertical potential temperature gradient same as the other two models were utilized. The barn was treated as a volume source while the manure storage was considered to be an area source in LODM. In ISCST3 and CALPUFF, both barn and manure storage were processed as area sources. When comparisons were made among models, hourly met data obtained by averaging the minute readings within three sessions in one hour was used and one hour simulation was conducted. However, average of 10 minutes session's meteorological data was used to simulate the mean odour concentration and odour frequency for validation of the LODM by field odour plume measurement. The average of wind direction follows the method of Mitsuta (US EPA, 2000), while the other parameters are averaged by taking their arithmetical means.

4.1.4 Relationship between Odour Intensity and Concentration

All the air or odour dispersion models predict concentrations, while the odour intensities are measured in the field plume measurements. This results in a problem to be solved in order to validate odour dispersion models, i.e., the odour detection threshold needs to be converted to the odour intensity in order to compare the field odour plume measurement to the result calculated by an air dispersion model as well as odour frequency.

Odour samples collected in Tedlar bags from swine farms and manure storages were measured in the Olfactometry lab for both odour intensity and concentration in order to establish the relationship between odour intensity and concentration. The conversion equation generated by Zhang et al. (2005), equation (1.16), and Feddes et al. (2005), equation (1.17) (using n-butonal instead of field odour), were used to convert model predicted odour concentration to odour intensity.

4.1.5 Comparison between LODM and ISCST3 and CALPUFF

The mean odour concentration values predicted by LODM were compared with those determined by ISCST3 and CALPUFF models to evaluate LODM. The R square, mean absolute error (MAE) and Root-mean-square error (RMSE) were used to measure the consistency among the three models. MAE and RMSE are defined as followed:

$$MAE = \sum_{i=1}^{n} \left| \frac{I_{ci} - I_{cm}}{n} \right| \tag{4.1}$$

$$RMSE = \left(\frac{\sum_{i=1}^{n} (I_{ci} - I_{cm})^2}{n-2} \right)^{1/2} \tag{4.2}$$

where I_c and I_m are the predicted odour concentration by LODM and ISCST3 (or CALPUFF) respectively, OU m^{-3}; n represents the number of the data points.

As shown in Figure 4.1 and 4.2, when Pasquill-Gifford dispersion coefficients were used, the predicted mean concentrations by LODM have high correlations to those predicted by

ISCST3 and CALPUFF with R square value of 0.860 and 0.969, respectively. Also, their absolute values are very close. The LODM predicted mean odour concentrations are more consistent with results of CALPUFF than ISCST3. It can also be found from the MAE and RMSE values shown in Table 4.2 that the differences between LODM and ISCST3 and CALPUFF are very small. These results demonstrate the credibility of the algorithm used in LODM to calculate the mean odour concentrations. It needs to mention that in LODM the area source is processed by an imaginary point source method which is different from the numerical integration method used in ISCST3 and CALPUFF models. The close mean odour concentration results may verify that the imaginary point source method for treating area source is as accountable as the methods used in other commercial models.

When Hogstrŏm dispersion coefficients were used, the predicted odour concentrations between LODM and other models are still highly correlated (Figure 4.3 and Figure 4.4). However, the LODM predicted odour mean concentrations are much larger than those predicted by ISCST3 and CALPUFF models. According to MAE and RMSE, the differences between LODM and ISCST3 were similar to the difference between LODM and CALPUFF (Table 4.2).

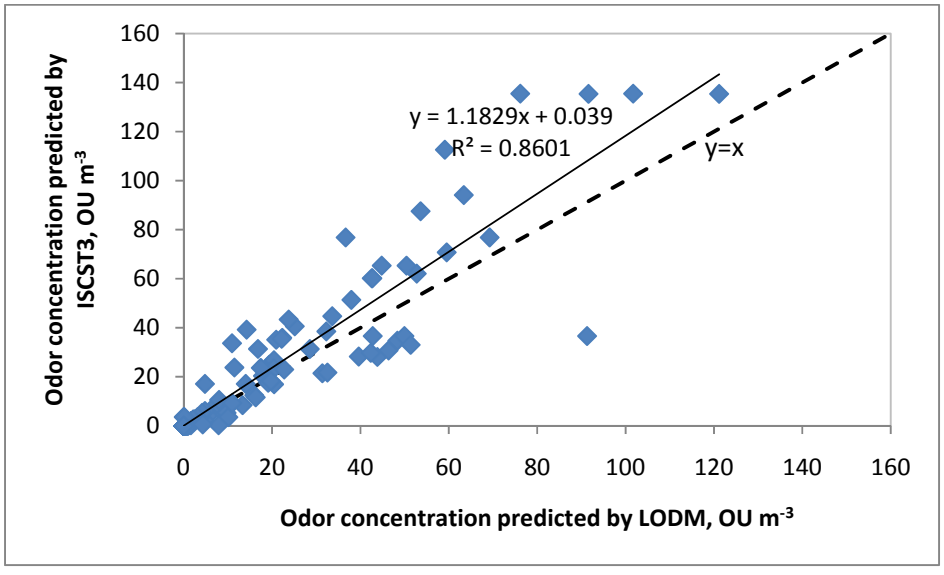

Figure 4.1 Comparisons of the predicted mean odour concentrations by LODM (P-G) and ISTSC3 models

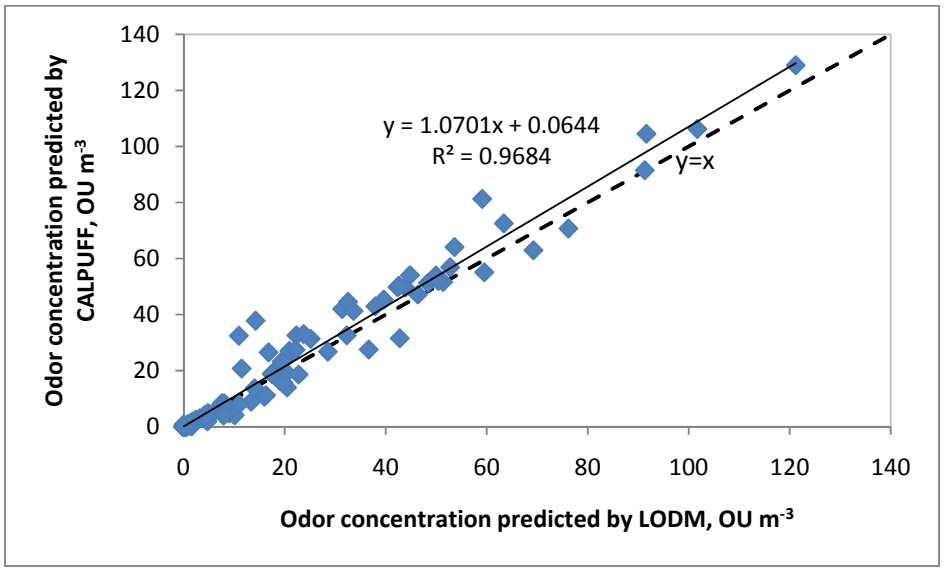

Figure 4.2 Comparisons of the predicted mean odour concentrations by LODM (P-G) and CALPUFF models

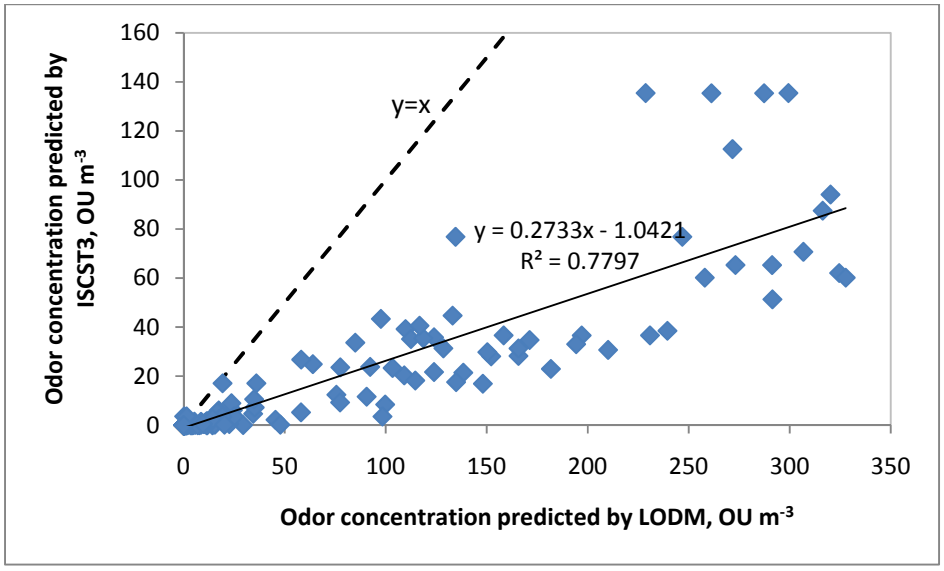

Figure 4.3 Comparisons of the predicted mean odour concentrations by LODM (Hogstrŏm) and ISTSC3 models

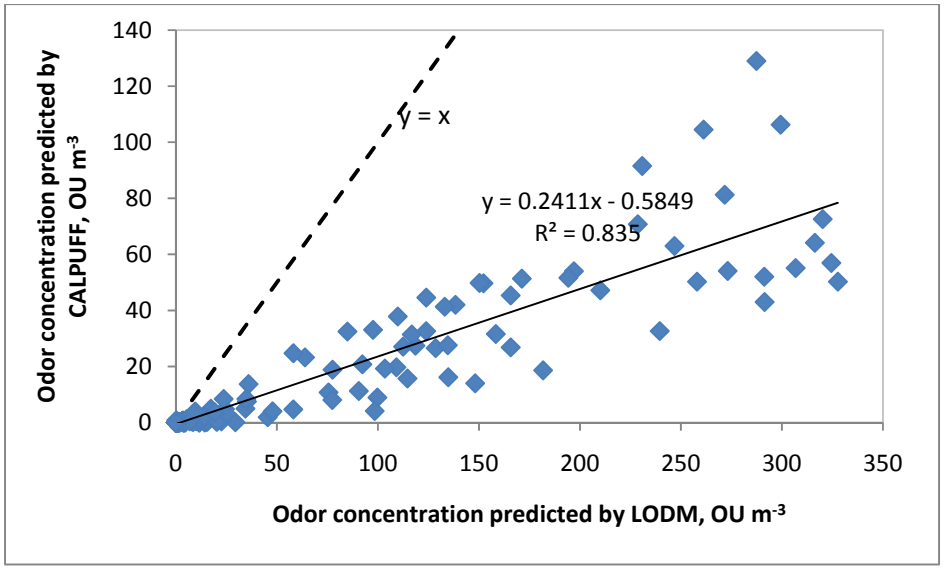

Figure 4.4 Comparisons of the predicted mean odour concentrations by LODM (Hogstrŏm) and CALPUFF models

Table 4.2 Comparisons in odour concentrations between LODM and ISCST3 and CALPUFF

	Use of Pasquill- Gifford dispersion coefficients		Use of Hogstrŏm dispersion coefficients	
	ISCST3	CALPUFF	ISCST3	CALPUFF
R-Square	0.86	0.97	0.78	0.84
MAE	4.7	2.06	40.17	41.39
RMSE	11.17	4.50	76.92	79.50

4.1.6 Comparisons between LODM Predictions and Field Measurements

Comparisons between model predicted and measured mean intensity

Within the 33 sessions, a total of 1444 pairs of data were used to compare the predicted and measured mean odour intensities by agreements. Agreements are defined as the proportion of the predicted intensity values that matched with the experimentally measured ones. The predicted intensity is considered to match with measured intensity if it is within the range of ±0.5 of measured odour intensity (Zhou et al., 2005). For example, if the predicted intensity is 1.3, then it is considered to be matched with measured intensity if measured intensity is between 0.8 and 1.8.

Agreements between predicted and measured mean odour intensities were listed in Table 4.3 and Table 4.4 using the conversion equation (1.16) and (1.17) respectively. The overall agreements between predicted and measured intensities are larger than 40%. At close distance (<250 m) the agreements are smaller than longer distance, which shows that the model has better performance in longer distance (600 to 1200 m). The result is consistent with that predicted by other commercial models with the same data (Zhou et al. 2005; Xing et al. 2006). This relatively longer distance (600 to 1200 m) is where we are interested most because it is likely beyond the properties line of the swine farms. When the no-odour detected periods are excluded, the overall agreements decrease to 30%, which is better than the results from other commercial models (Xing et al. 2006). The overall agreement is enhanced from 41.1% to 46.2 % when equation (1.17) was used instead of equation (1.16). The agreement for only considering non-zero odour periods also has a slight increase from 30% to 33%.

Table 4.3 Agreements between predicted mean odour intensities and measured mean intensities using equation (1.16)

	R	MAE	RMSE	Agreement, %
<250 m	0.22	2.15	2.72	18.9
250-600 m	0.2	1.27	1.86	41.6
600 - 1200 m	0.11	0.78	1.37	62.9
Non-zero	0.46	1.64	2.21	30
Overall	0.5	1.4	2.06	41.1

Table 4.4 Agreements between predicted mean odour intensities and measured mean intensities using equation (1.17)

	R	MAE	RMSE	Agreement, %
<250 m	0.21	2.59	3.3	17.4
250-600 m	0.18	1.16	1.82	47.6
600 - 1200 m	0.13	0.52	1.08	73.5
Non-zero	0.48	1.74	2.48	33
Overall	0.52	1.42	2.26	46.2

Besides agreement, fractional bias (FB) is also used to evaluate the performance of the model. The general expression for the FB is given by:

$$FB = 2\frac{PR - OB}{PR + OB} \tag{4.3}$$

where OB and PR refer to the averages of the observed (OB) and predicted (PR) values. The fractional bias is symmetrical and bounded, which varies from -2.0 (extreme underprediction) to +2.0 (extreme overprediction) and has an ideal value of 0 for an ideal model. A value of -0.67 is equivalent to model underprediction by a factor of two, while +0.67 is equivalent to overprediction by a factor of two. A low variance in FB can be taken as indicating confidence in the model prediction (McHugh et al., 1999).

Figure 4.5 shows the FB values of average and standard deviation of the model regarding mean odour intensity when using equation (1.16) and (1.17). The values of average and stand deviation are 0.53 and 0.29 when using equation (1.16), while they are 0.52 and 0.44 for equation (1.17). All of these values are larger than zero and smaller than 0.67, which shows that the model has relatively good performance and slightly overpredicts the mean odour intensities.

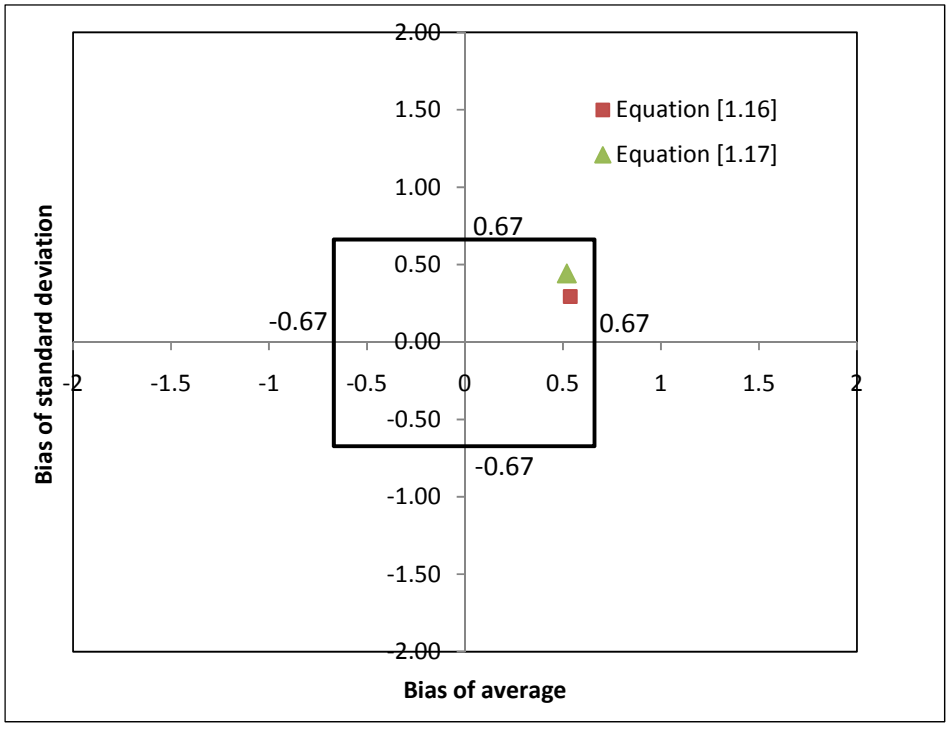

Figure 4.5 Fractial bias (FB) for LODM predicted odour intensities and measured odour intensities

Comparisons between the model predicted and the measured odour frequency

Odour frequency is defined as the percentage of time that the odour exceeds a certain level during the given time period. The odour frequency of 1 OU for each 10-minute session was estimated by LODM. In detail, the frequency of odour concentration that equals or exceeds 1 OU during each 10-minute session was estimated by LODM with input of 10 minute average meteorological data. The observed odour frequency of intensity 1 or greater (≥1) of each 10 minutes session was calculated from the measured intensity data. In total, 1444 pairs of data were used to compare the predicted odour frequency and observed frequency with the aid of FAC2 and FB. FAC2 is defined as the percentage of the predictions within a factor of 2 of the observed values (Chang and Hanna, 2004). It gives an indication of how many predictions are within a factor of 2 of the observed values (Ahuja and Kumar, 1996). In order to further examine the model predicted odour frequencies and measured odour frequencies, another two parameters named Ran0.2 and Ran0.1 are defined as the percentage of the predictions within the range of ±0.2 of the observed values and within the range of ±0.1 of the observed values.

From Table 4.5, the overall Fac2 value is 37 %. It means at least 37% of the predicted frequencies are within a factor of 2 with observed odour frequency. In the relatively closer (<200 m) and longer distance (600-1200 m), the Fac2 value is higher than the value at the middle distance (250-600 m). The overall Ran0.2 and Ran0.1 values are 50.9% and 37.6%, respectively, which means that more than 50% of the LODM predicted odour frequencies are within the range of ±0.2 of observed odour frequencies and more than 37% are within the range of ±0.1 of observed odour frequencies. With the increase of downwind distance, the Ran0.2 and Ran0.1 values are increasing. At the longer distance (600-1200 m), more than 77% and 66% of model predicted odour frequencies are within the range of ±0.2 and ±0.1 of observed odour frequencies. When zero odour periods are excluded, there are still more than 37% and 22% of model predicted odour frequencies within the range of ±0.2 and ±0.1 of observed odour frequencies. The FB value is -0.67, which means that averagely the model under predicts the odour frequency by a factor of two.

Table 4.5 FAC2, Ran0.2, and Ran0.1 of the model predicted odour frequency with observed odour frequency

	Fac2, %	Ran0.2, %	Ran0.1, %
<250 m	44.7	30	13.4
250-600 m	26	45.8	33.6
600 - 1200 m	40.8	77.4	66.2
Non-zero	29.2	37.9	22.1
Overall	37	50.9	37.6

4.2 DATA FROM UNIVERSITY OF MINNESOTA

4.2.1 Site Description and Odour Emission Rates

A total of 28 farm sites were measured in Minnesota, which covered most of the animal species (Zhu et al., 1999). The odour flume measurements were conducted either for animal barns or for earthen manure storages. The surroundings of the farms were all considered as mostly flat cropland free of obstacle. Odour emission rates were measured during the period of each odour plume measurement (Zhu et al., 1999). The summary of average odour concentrations and emission rates from the measurements selected are given in Table 4.6.

Table 4.6 Measured odour emission rates for different farms in Minnesota

Source	Measured time	emission rate, OU m^{-2} s^{-1}	emission rate, OU s^{-1}
EMS, Farm 203	6/3/1998 Morning	41.3	320134
EMS, Farm 203	6/3/1998 Afternoon	26.72	207118
EMS, Farm 217	4/29/1998 Morning	4.44	8106
EMS, Farm 217	4/29/1998 Afternoon	7.73	14102
Barn, Farm 219	4/22/1998 Morning	1.72	998
EMS, Farm 220	6/16/1998	6.52	27747
Barn, Farm 221	4/22/1998 Morning	1.66	298
Barn, Farm 221	4/22/1998 Afternoon	11.85	2125
Barn, Farm 222	6/10/1998	1.73	1327
Barn1, Farm 223	5/20/1998	2.47	4727
Barn2, Farm 223	5/21/1998	2.97	5627
Barn1, Farm 224	6/10/1998	6.89	5286
Barn2,Farm 224	6/10/1998	6.96	5343

4.2.2 Downwind Odour Plume Measurement

According to the experiments descriptions in Zhu et al. (1999), seven trained human sniffers were sent to the field to conduct field odour plume measurements. Jacobson et al. (1998) presented the detailed measurement procedures. Locations of the sniffers were determined based on the centerline of odour plume. Human sniffer scores were taken every 10 s for a period of 10 min session. In this study, a total of 30 sessions of data taken over 8 different days in 1998 were obtained from University of Minnesota. For each of the days, two or three sessions of data were taken in the morning and afternoons, each session at a different short distance (25- 300 meter) downwind of the odour source.

A portable weather station was set up at 2 m above the ground to record weather information including wind speed and direction, solar radiation, temperature, recording time, and relative humidity. The meteorological data were recorded every 10s.

4.2.3 Relationship between Odour Concentration and Odour Intensity

The relationships between odour intensity of 0 to 5 scale and concentration (Equation (1.18)) for swine odour from Guo et al. (2001) was used when comparing the model predicted odour intensities to observed odour intensities.

4.2.4 Comparisons between LODM Predictions and Field Measurements

Because field odour intensity was measured in a 10 s interval within a 10 min session, the average of the measured odour intensity within one session was considered as the one-hour average. The averaged 10 min session meteorological data were obtained and inputted LODM as one-hour average. The EMS were treated as area sources, while the animal barns were treated as volume sources. Because only the centerline of the nasal rangers' layout in the data of 1998 could be ratified, there were 30 pairs of data points that were used to make the comparisons. All the measurements were conducted within the downwind distance of 25 m and 300 m.

Comparisons between the model predicted and measured mean odour intensity

The agreement that defined in the previous section was used to compare the model predicted mean intensity to measured mean intensity. Result shows that more than 34% of the model predicted intensity is within the range of ±0.5 of measured odour intensity. In this case, only receptors at the plume centerline were considered. All the measured odour intensities were non-zeroes, so the agreement obtained is consistent with the result of data from University of Manitoba. The FB value of average intensity is -0.5, which indicates that the model under predicts the mean odour intensity.

Comparisons between the model predicted and measured frequency

The ratios of predicted and measured odour frequencies are shown in Figure 4.6. It shows that most of the model predicted odour frequencies are within a factor of 2 of observed odour frequencies. The Fac2, Ran0.2, Ran0.1 values of the model predicted odour frequency are listed in Table 4.7. The Fac2 value is 79.3%, which indicates that almost 80% of the modeled odour frequencies are in the factor of 2 of observed frequencies. The

Ran0.2 and Ran 0.1 values are 44.8% and 31.0%, respectively. Almost 45% and 30% of the model predicted odour frequencies were within the range of ±0.2 and ±0.1 of the observed odour frequencies.

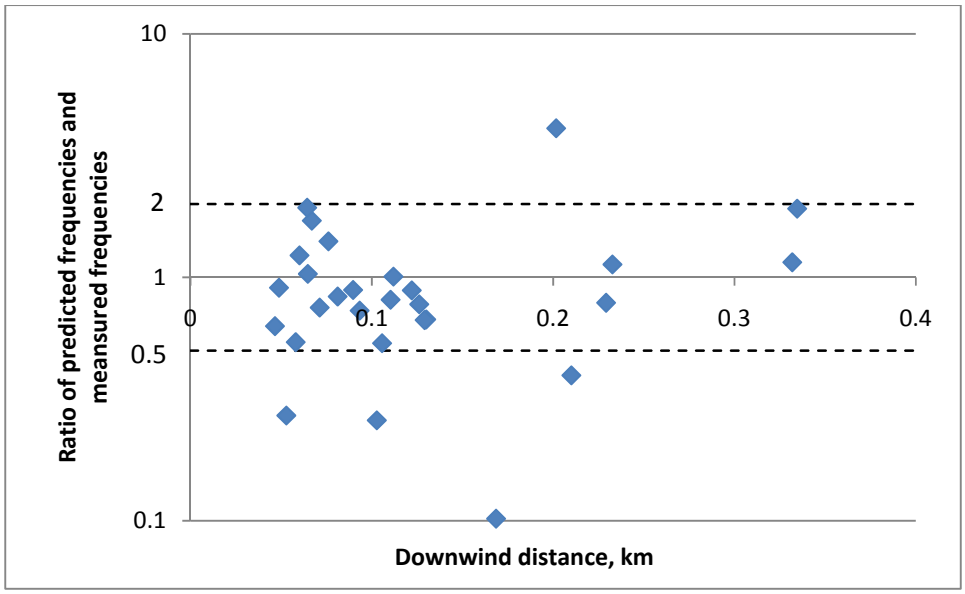

Figure 4.6 Comparisons of the model predicted frequencies and observed odour frequencies

Table 4.7 FAC2, Ran0.2 and Ran0.1 values of the model predicted odour frequency with observed odour frequency

Fac2, %	Ran0.2, %	Ran0.1, %
79.3	44.8	31

4.3 DISCUSSIONS

There are many possible reasons for the discrepancies between the model predicted and measured mean odour intensity and odour frequency. First, LODM was developed with a lot of assumptions, as all the other models. The model assumes that odour can be treated as gas, and there are no chemical and physical reactions during its transportation at atmosphere. The ground level was treated as completely reflected without odour absorption or deposition. The model is based on steady-state meteorological conditions; however, in most of the 10-minute sessions, the wind directions shifted frequently. The short time average vertical dispersion coefficients are functions of plume height, which

varies vertically with the plume fluctuating. However, in this model they are assumed to be the same as the vertical dispersion parameters at the mean plume height. All these assumptions may lower the accuracy of model predictions.

Second, the constant odour emission rates were used in the model simulations. However, diurnal variations of odour emission rate from swine farm were significant (Wang, 2007; Guo et al. 2006b). The measurement of odour concentration used to obtain odour emission rate and the field odour plume were conducted by human sniffers and often exhibited large uncertainties.

Third, the uncertainty of the conversion equation of odour concentration and odour intensity may be another very important effect factor of the model performance. Three different odour intensity and concentration conversion equations from different researchers gave widely varied concentrations, especially at the low intensity levels (Xing, 2006). When analyzing the data from University of Minnesota, both conversion equations of (1.16) and (1.17) were applied to explore the possible effect of different conversion equations. When these equations were used, the agreements of mean odour intensities are around 10%, which are much lower than that of using equation (1.18).

4.4 CONCLUSIONS

After comparing the mean concentration predicted by LODM and ISCST3 and CALPUFF, and comparing LODM predicted concentration (intensity) and odour frequency between model predicted and field measured, some conclusions can be drawn:

1) LODM can predict similar mean odour concentrations as ISCST3 and CALPUFF when using Passiquill-Gifford dispersion parameters. When Hogstrŏm dispersion parameters were used, the LODM predicted odour concentrations are larger than those of ISCST3 and CALPUFF models.
2) Agreements between LODM predicted mean odour intensities and field measured odour intensities are high ($\geq$ 40%) and they are higher at longer distance than close distance.
3) LODM predicted better odour frequency in relatively longer distance than shorter distance. The model under predicted the odour frequency. Several possible reasons,

especially, the effect of conversion equation between odour intensity and odour concentration may contribute to the discrepancy between modeled and observed results.

Chapter 5. SENSITIVITY ANALYSIS

The livestock odour dispersion model (LODM) developed based on the fluctuating plume model has the ability to predict mean odour concentration, peak odour concentration, instantaneous odour concentration, and odour frequency. For livestock odour application, the mean odour concentration and odour frequency are important and commonly used. In this chapter, the sensitivity analysis of the model predicted odour concentration and odour frequency to the input parameters will be conducted.

The sensitivity of estimates of odour concentration and frequency to a particular variable/parameter is the change in the estimate with respect to a change in the value of the parameter while keeping all other parameters constant (Smith, 1993).

The parameters which affect odour concentration and frequency downwind from a source are source parameters, meteorological parameters and surface characteristics, as follows:

1) Source parameters: stack height, stack diameter, exit velocity, exit temperature, and emission rate.
2) Meteorological parameters: wind speed, stability class, ambient temperature, wind direction, mixing height, radiation, and cloud cover.
3) Surface characteristics: surface roughness, albedo, and Bowen ratio.

The source parameters have practical applications because they can be controlled by livestock operators to affect odour dispersion, while the meteorological parameters and surface characteristics are those on which livestock operators have little or no control.

The sensitivity was expressed as an elasticity, S, which is defined as the percentage change in the concentration or frequency for a 1% change in the parameter value. The average sensitivity was determined using the sensitivity index of Ng and Loomis (1984), as cited by Smith (1993).

$$S_{av} = \frac{100}{N\Delta}\sum_{1}^{N}\frac{C_{ni}-C_{ci}}{C_{ci}} \quad (5.1)$$

Where N is the number of points (odour concentration or odour frequency) in the model output; Δ is the absolute change in the parameter value expressed as a percentage of its

control value; C_{ni} is the new value of the concentration or frequency for i_{th} point with a changed value of the input parameter; C_{ci} is the corresponding value at ith point in the control simulation. For example, S = 0.1 would mean that for each percent change of the input parameter, on an average, the output increases by 0.1 %; while S = -0.1 would mean that the output decreases by 0.1 %.

For the sensitive analysis of the stability class:

$$S_{av} = \frac{100}{N}\sum_{1}^{N}\frac{C_{ni}-C_{ci}}{C_{ci}} \tag{5.2}$$

This indicates the average concentration or frequency changes in % for the change in stability class.

For wind direction:

$$S_{av} = \frac{100}{N\Delta'}\sum_{1}^{N}\frac{C_{ni}-C_{ci}}{C_{ci}} \tag{5.3}$$

In which, Δ' is the change of wind direction in angle (°). Therefore, S_{av} is the concentration or frequency change in % for per degree change in wind direction.

The odour concentrations and odour frequency at the 231 downwind receptors that cover the downwind area of 1000 m width and 5000 m length as shown in Figure 2.27 were estimated to conduct the sensitivity analysis. The meteorological parameters or the source parameters that remain unchanged are as same as those used in Chapter 2. The elasticity (S) for every parameter was calculated. The changes in average concentration and frequency with the changing input parameter were also calculated. The changes of centerline odour concentration and odour frequency with the changes of input parameters were plotted to demonstrate the sensitivity of input parameter on centerline odour concentration and odour frequency.

5.1 SOURCE PARAMETERS

For existing livestock operations, once the odour problem occurs, effective ways should be taken to control the odour dispersion and mitigate the odour effect. Producers can control the odour either by enhancing the odour dispersion or reducing odour emissions. Therefore, the model sensitivity to the controllable source parameters by producers such as stack height, exit temperature, stack diameter, exit velocity, as well as emission rate is very important for the odour application.

5.1.1 Stack Height

Stack height is a very important effect parameter for downwind odour concentration. The higher the stack height, the lower is the concentration that can be detected at ground level. As many industries have increased the height of their chimney to control the ground concentrations of pollutants, livestock producers can take the same approach to reduce the odour effect.

From Figure 5.1 and Figure 5.2, the centerline odour concentrations and odour frequencies increase when stack height decreases from 10 m to 5 m, while they decrease when stack height changes from 10 m to 15 m. The changes are larger in the close distance and the changes decrease in larger distance. The effect of stack height on odour concentration and odour frequency under stable conditions is greater than unstable and neutral conditions.

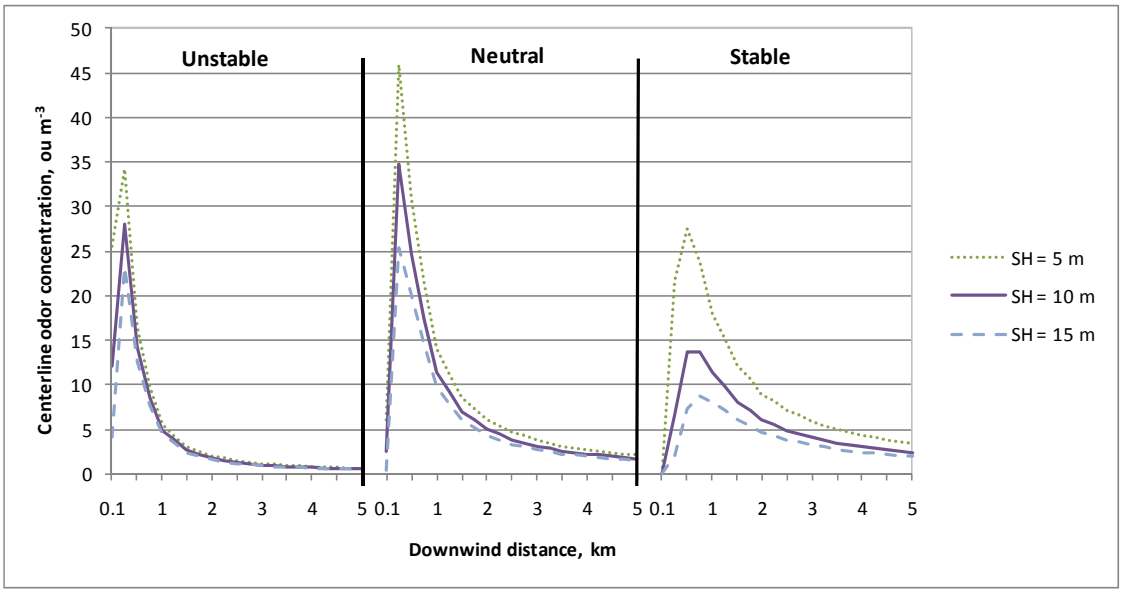

Figure 5.1 Centerline odour concentrations for different stack heights (SH)

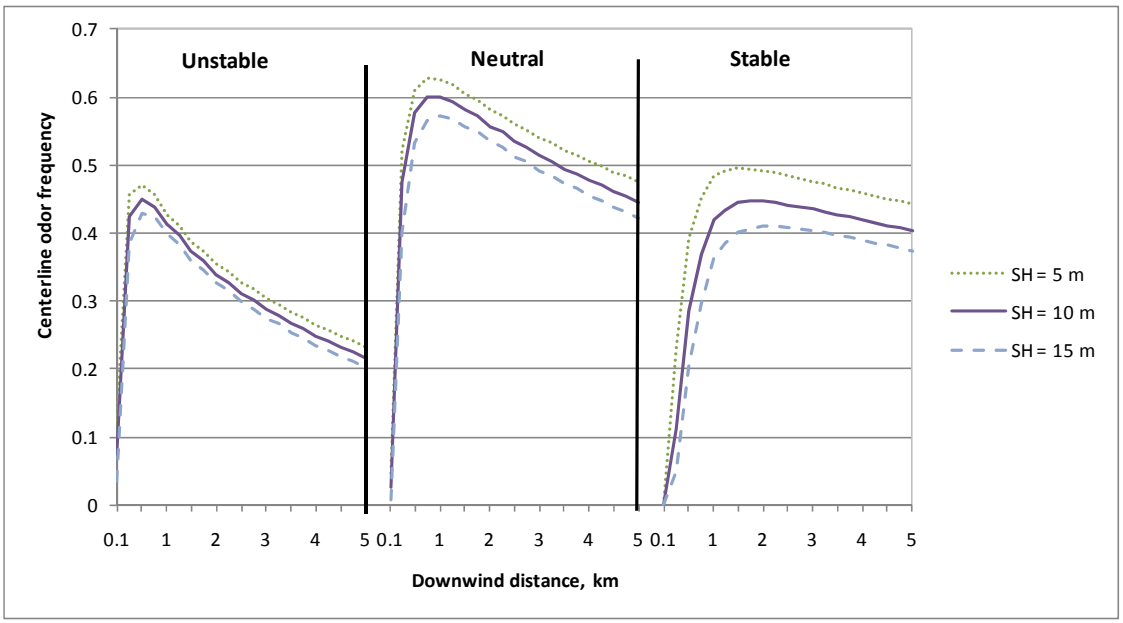

Figure 5.2 Centerline odour frequencies for different stack heights (SH)

The average changes of odour concentrations and odour frequencies with the changes of stack height with a control value of 10 m and the elasticity values at 0.5 km downwind, 5 km downwind, and the average elasticity value are listed in Table 5.1. When stack height increase from 10 m to 15 m, the average odour concentrations decrease from 13.4% to 25.3%, while the average odour frequencies decrease from 5.0% to 8.9%. However, if the stack height decreases from 10 m to 5 m, the odour concentrations and odour frequencies

increase at least 20.1% and 5.8%. The decreasing stack height has greater effect on the odour concentrations and odour frequencies than increasing stack height. The average elasticity values are from -0.2 to -0.5 for odour concentrations and -0.1 to -0.2 for odour frequencies when increasing stack height, while they are from 0.3 to 1.0 for odour concentrations and 0.1 to 0.4 for odour frequency when decreasing stack height. It also shows the effect of changes of stack height on odour frequency is much less than that on odour concentrations. The average changes or elasticity values of odour frequencies are around one third of those of odour concentrations. Generally, the changes of odour concentrations and odour frequencies in short distances are greater than far distance. The changes under stable conditions are more significant than unstable and neutral conditions. Overall, the average changes and elasticity values indicate that stack height has medium sensitivity to the odour concentration and odour frequency.

Table 5.1 Sensitivity analysis of odour concentration and frequency to stack height with a control value of 10 m

Stability	Change, %	Concentration				Frequency			
		Ave. C Change, %	S(0.5)	S(5)	S(ave)	Ave. F Change, %	S(0.5)	S(5)	S(ave)
Unstable	-50	20.1	0.3	0.3	0.3	5.8	0.2	0.2	0.1
	+50	-13.4	-0.2	-0.2	-0.2	-5.0	-0.2	-0.1	-0.1
Neutral	-50	23.6	0.5	0.4	0.4	6.2	0.3	0.1	0.2
	+50	-15.6	-0.4	-0.3	-0.3	-5.3	-0.3	-0.1	-0.1
Stable	-50	52.1	2.0	0.8	1.0	11.9	1.1	0.2	0.4
	+50	-25.3	-0.9	-0.4	-0.5	-8.9	-0.7	-0.2	-0.2

5.1.2 Stack Diameter

Stack diameter is an essential parameter when calculating plume rise. It has great impact on the final plume height. Hence, it has great effect on downwind odour concentration and frequency, as shown in Figure 5.3, Figure 5.4 and Table 5.2. With the decrease of stack diameter, both the odour concentration and odour frequency increase. Especially, at close downwind distance where plume height has great effect on odour concentration and odour frequency, the influence of stack diameter is considerable.

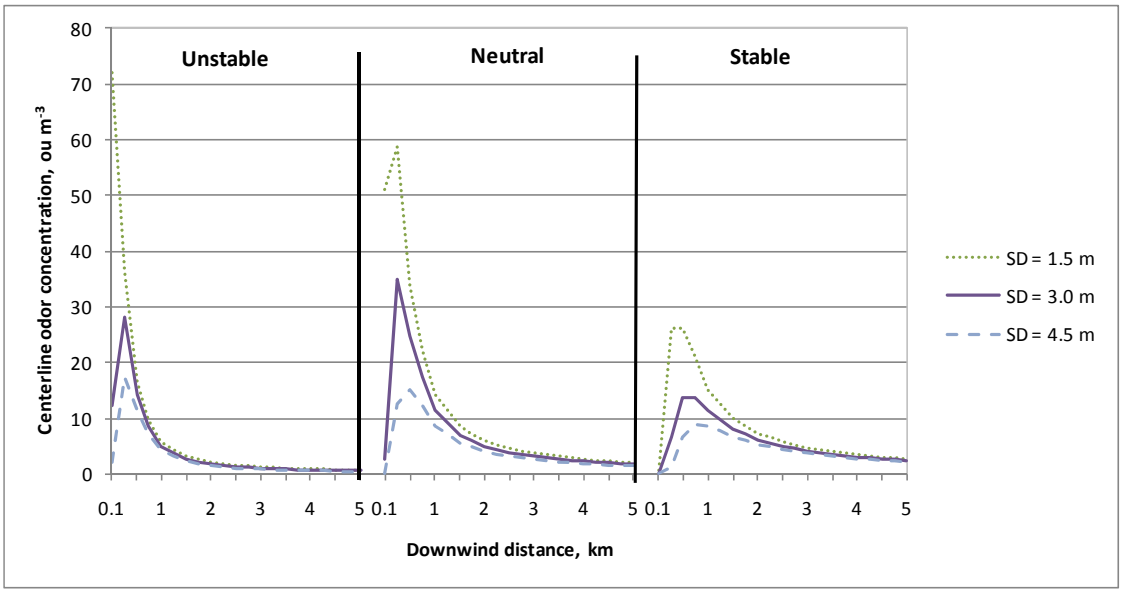

Figure 5.3 Centerline odour concentrations for different stack diameters (SD)

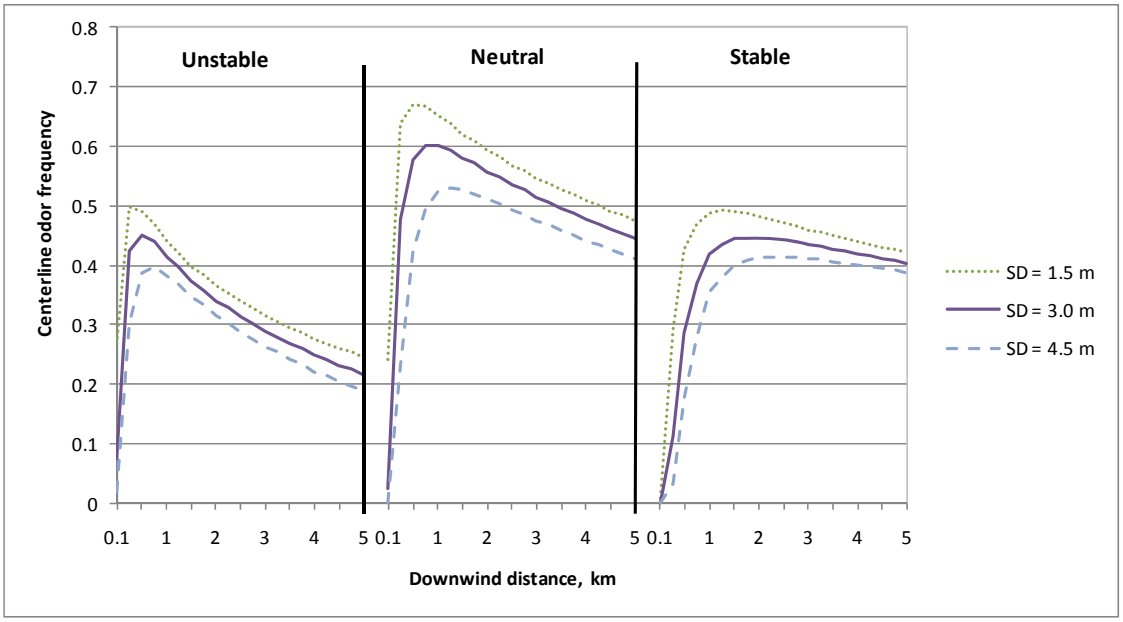

Figure 5.4 Centerline odour frequencies for different stack diameters (SD)

The average changes of odour concentrations and frequencies show that the effect of changes on stack diameter is great for odour concentrations and is fair for odour frequencies. The values of elasticity are similar under different stability conditions. The elasticity values at short distances are greater than long distance, which shows that the diameter has greater effect on odour concentration and odour frequency at near source. Most of the average elasticity values are less than 0.5, which means that with the 1%

changes of stack diameter, the changes of odour concentration and odour frequency are less than 0.5%. It can be concluded that LODM's sensitivity to stack diameter is also medium.

Table 5.2 Sensitivity analysis of odour concentration and frequency to stack diameter with a control value of 3 m

Stability	Change, %	Concentration				Frequency			
		Ave. C Change, %	S(0.5)	S(5)	S(ave)	Ave. F Change, %	S(0.5)	S(5)	S(ave)
Unstable	-50	43.1	0.3	0.3	0.3	10.4	0.2	0.2	0.1
	+50	-21.9	-0.2	-0.2	-0.2	-10.1	-0.2	-0.1	-0.1
Neutral	-50	36.8	0.5	0.4	0.4	8.8	0.3	0.1	0.2
	+50	-25.2	-0.4	-0.3	-0.3	-10.3	-0.3	-0.1	-0.1
Stable	-50	27.4	2.0	0.8	1.0	8.4	1.1	0.2	0.4
	+50	-16.6	-0.9	-0.4	-0.5	-7.3	-0.7	-0.2	-0.2

5.1.3 Exit Velocity

Exit velocity also is an important parameter in determining final plume rise. When exit velocity decreases, the plume rise decreases and the downwind odour concentration and frequency increase. From Figure 5.5, Figure 5.6, and Table 5.3, the decrease of exit velocity has greater effect on odour concentration and odour frequency than the increase of it. For example, when exit velocity increases from 3 m s^{-1} to 4.5 m s^{-1} under neutral conditions, the average elasticity values for odour concentration and odour frequency are -0.3 and -0.2, while the corresponding values are 0.8 and 0.4, when the exit velocity decreases from 3 m s^{-1} to 1.5 m s^{-1}. From Table 5.3, we can also find that most of the values are less than 0.5, which shows that exit velocity has medium sensitivity to the LODM predicted odour concentration and odour frequency.

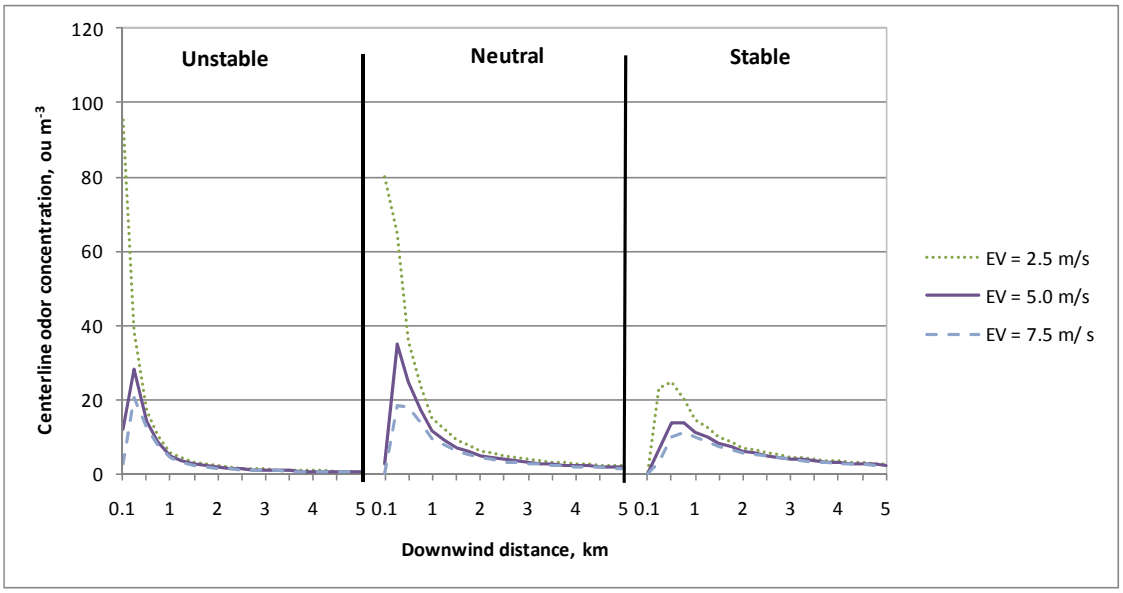

Figure 5.5 Centerline odour concentrations for different exit velocities (EV)

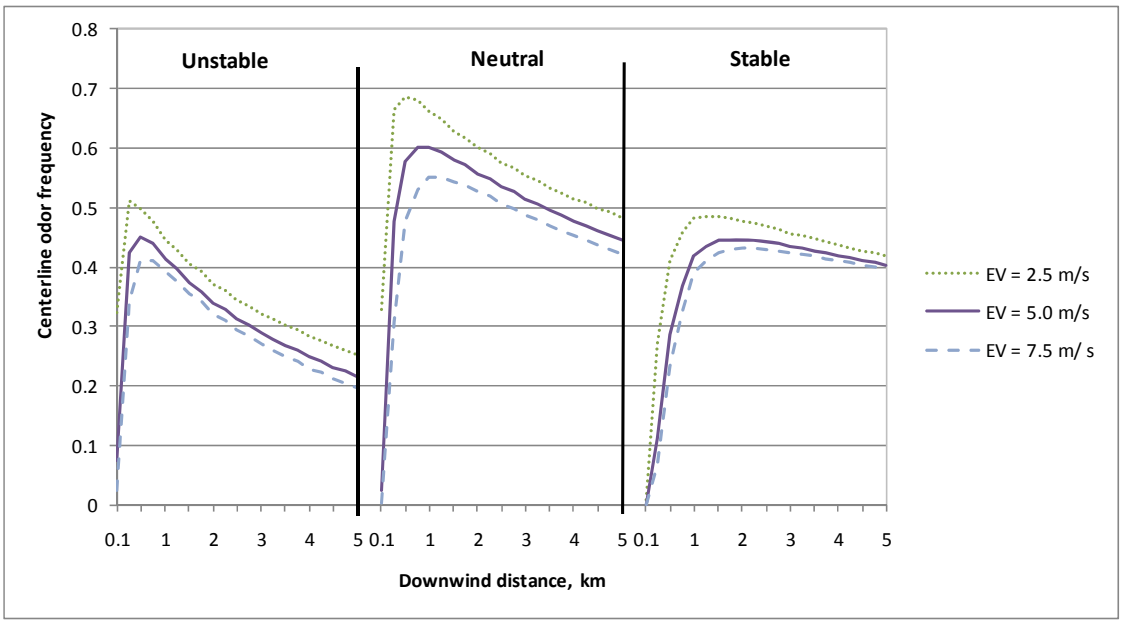

Figure 5.6 Centerline odour frequencies for different exit velocities (EV)

Table 5.3 Sensitivity analysis of odour concentration and frequency to exit velocity with a control value of 3 m s^{-1}

Stability	Change, %	Concentration				Frequency			
		Ave. C Change, %	S(0.5)	S(5)	S(ave)	Ave. F Change, %	S(0.5)	S(5)	S(ave)
Unstable	-50	57.9	0.4	0.6	0.6	13.1	0.4	0.3	0.3
	50	-16.6	-0.3	-0.3	-0.2	-7.2	-0.3	-0.2	-0.2
Neutral	-50	50.3	0.9	0.5	0.8	10.8	1.2	0.2	0.4
	50	-18.3	-0.6	-0.2	-0.3	-7.1	-0.6	-0.1	-0.2
Stable	-50	24.0	1.6	0.2	0.4	7.6	1.4	0.1	0.3
	50	-8.3	-0.5	-0.1	-0.1	-3.4	-0.5	0.0	-0.1

5.1.4 Exit Temperature

Exit temperature is also one of the parameters in the model to determine the plume rise. Under unstable and neutral conditions, the decrease of exit temperature from 300 to 280 K has very slight effects on downwind temperature and frequency. The reason is that when calculating plume rise under stable and neutral conditions, the plume rise is dominated by momentum rise if the exit temperature is close to or less than the ambient temperature. Therefore, the final plume rise remains constant. However, under unstable and neutral conditions, increase of the exit temperature decreases the odour concentrations and frequencies dramatically. Under stable condition, both increasing and decreasing exit temperatures have high effects on downwind odour concentrations and odour frequencies. Overall, the sensitivity of LODM to exit temperature is high (Figure 5.7 and 5.8, Table 5.4).

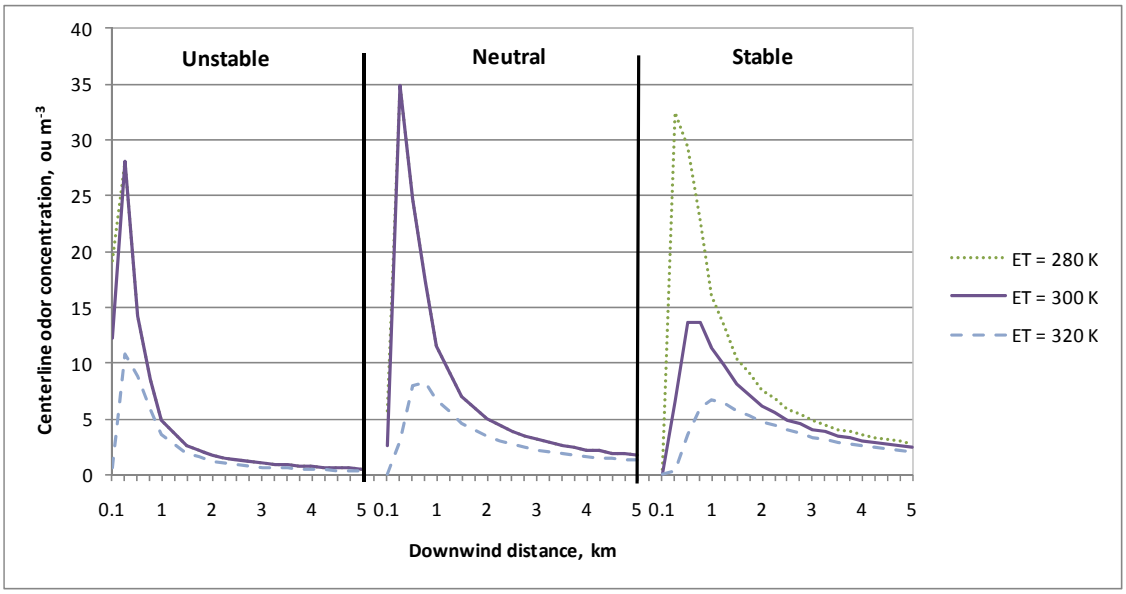

Figure 5.7 Centerline odour concentrations for different exit temperatures (ET)

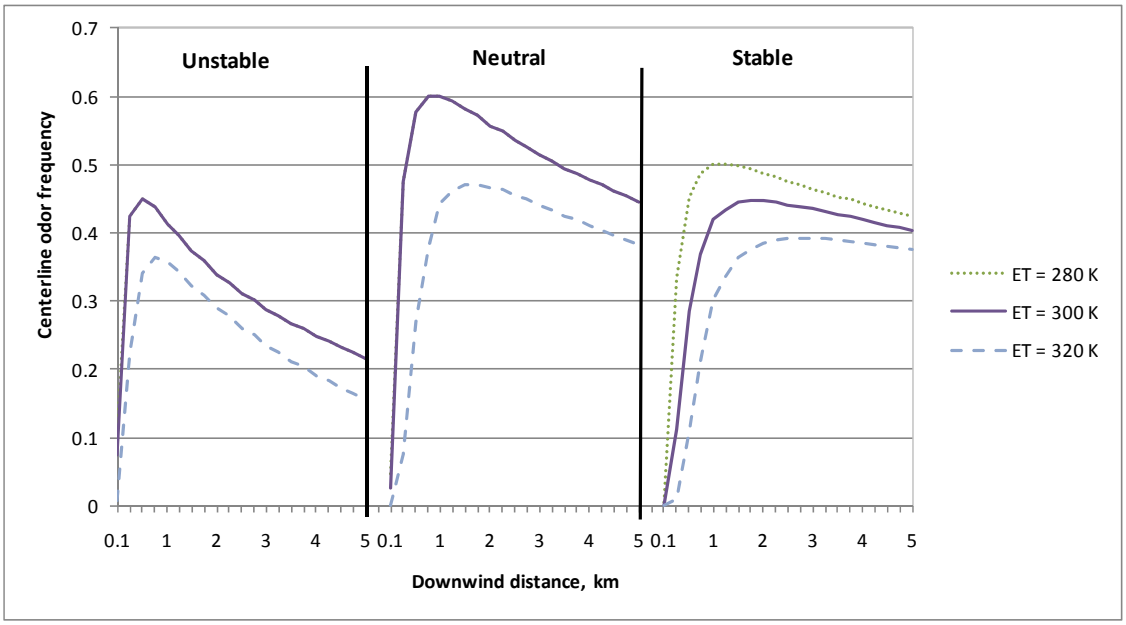

Figure 5.8 Centerline odour frequency for different exit temperatures (ET)

Table 5.4 Sensitivity analysis of odour concentration and frequency to exit temperature with a control value of 300 k

Stability	Change, %	Concentration				Frequency			
		Ave. C Change, %	S(0.5)	S(5)	S(ave)	Ave. F Change, %	S(0.5)	S(5),	S(ave)
Unstable	-6.7	2.8	0.0	0.0	0.0	0.1	0.0	0.0	0.0
	6.7	-38.8	-5.7	-5.3	-4.9	-20.3	-5.2	-4.2	-3.3
Neutral	-6.7	0.7	0.0	0.0	0.1	0.0	0.0	0.0	0.1
	6.7	-41.3	-10.1	-4.1	-5.0	-19.2	-10.4	-2.3	-3.8
Stable	-6.7	34.0	17.1	2.2	30.2	10.0	15.0	0.9	13.0
	6.7	-26.6	-11.1	-2.0	-3.6	-12.8	-10.0	-1.1	-2.9

5.1.5 Emission Rate

The sensitivity of LODM to emission rate is shown in Figure 5.9, Figure 5.10, and Table 5.5. The downwind mean odour concentration has a linear relationship with emission rate. Therefore, the model sensitivity of emission rate is high. However, the change of emission rate does not have the same effect on odour frequency. It is easy to explain considering the odour frequency used here is the odour frequency that odour concentration equals to or exceeds 1 OU m^{-3}. Then even if the emission rate decreases or increases by 50%, the frequency of the occurrence of odour concentrations equal to or exceeding 1 OU m^{-3} will not change at the same extent. Overall, the sensitivity of model predicted odour concentration to emission rate is high, while it is moderate coming to odour frequency.

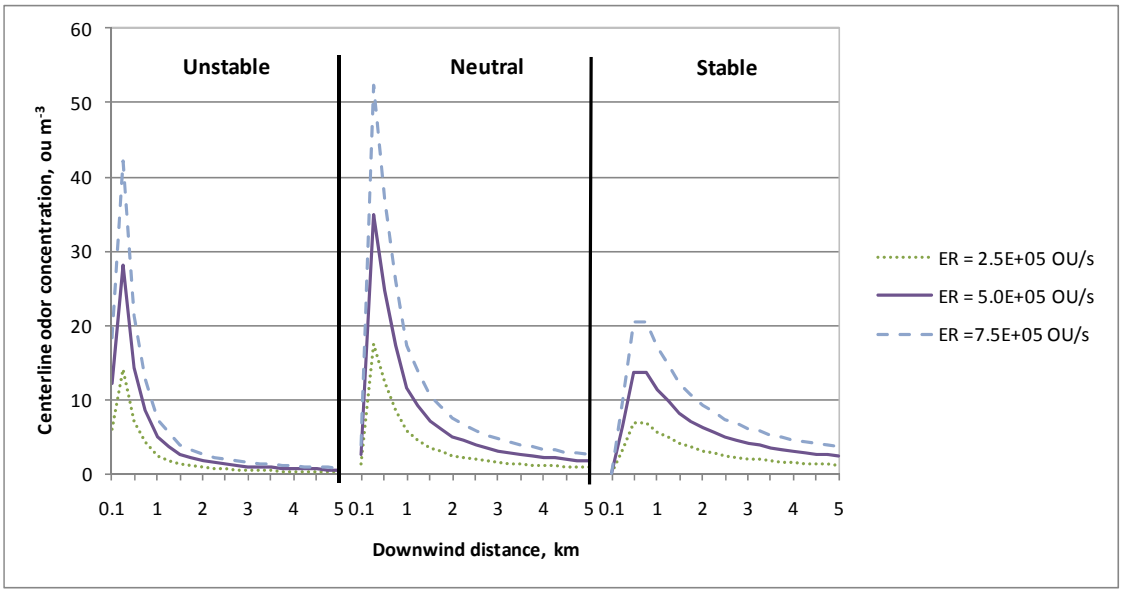

Figure 5.9 Centerline odour Concentrations for different emission rates (ER)

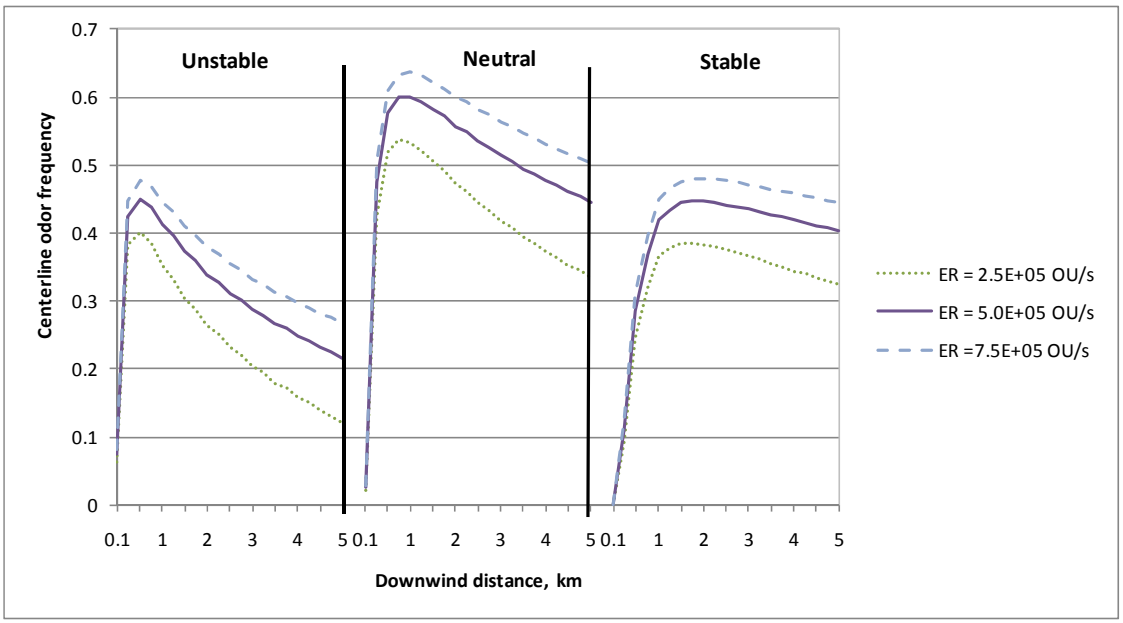

Figure 5.10 Centerline odour frequencies for different emission rates (ER)

Table 5.5 Sensitivity analysis of odour concentration and frequency to emission rate with a control value of 5E5 OU s^{-1}

Stability	Change, %	Concentration				Frequency			
		Ave. C Change, %	S(0.5)	S(5)	S(ave)	Ave. F Change, %	S(0.5)	S(5)	S(ave)
Unstable	-50	-50.0	-1.0	-1.0	-1.0	-28.7	-0.3	-1.2	-0.6
	+50	50.0	1.0	1.0	1.0	16.2	0.2	0.7	0.3
Neutral	-50	-50.0	-1.0	-1.0	-1.0	-15.7	-0.3	-0.4	-0.4
	+50	50.0	1.0	1.0	1.0	8.9	0.2	0.2	0.2
Stable	-50	-50.0	-1.0	-1.0	-1.0	-11.0	-0.2	-0.3	-0.2
	+50	50.0	1.0	1.0	1.0	6.1	0.1	0.1	0.1

5.2 METEOROLOGICAL PARAMETERS

5.2.1 Wind Speed

Effects of wind speed on downwind odour concentration and odour frequency are threefold. First, odour concentration is inversely related to the average wind speed at the stack height which is derived from the reference wind speed. Since, the odour frequency comes from short time odour concentration which has the same relationship with wind speed as mean concentration does, odour frequency is directly related to wind speed as well. Second, the reference wind speed is one of the determining factors of atmospheric stability. Therefore, it is an important factor for the calculation of the dispersion coefficients. Third, the wind speed is also a decisive factor of plume rise, thus it will affect the odour concentrations and odour frequencies downwind.

Under unstable conditions (SC = C), the centerline odour concentrations increase with the increase of wind speed at near source distance. The effect of wind speed on plume rise outweighs its effect on dispersion coefficients' calculation and odour concentration itself at near source distance. After the final plume rise reaches, with the increase of wind speed the odour concentration decrease (Figure 5.11). The centerline frequency increases with the increase of wind speed when the wind speed is larger than 4 m s^{-1} (Figure 5.12).

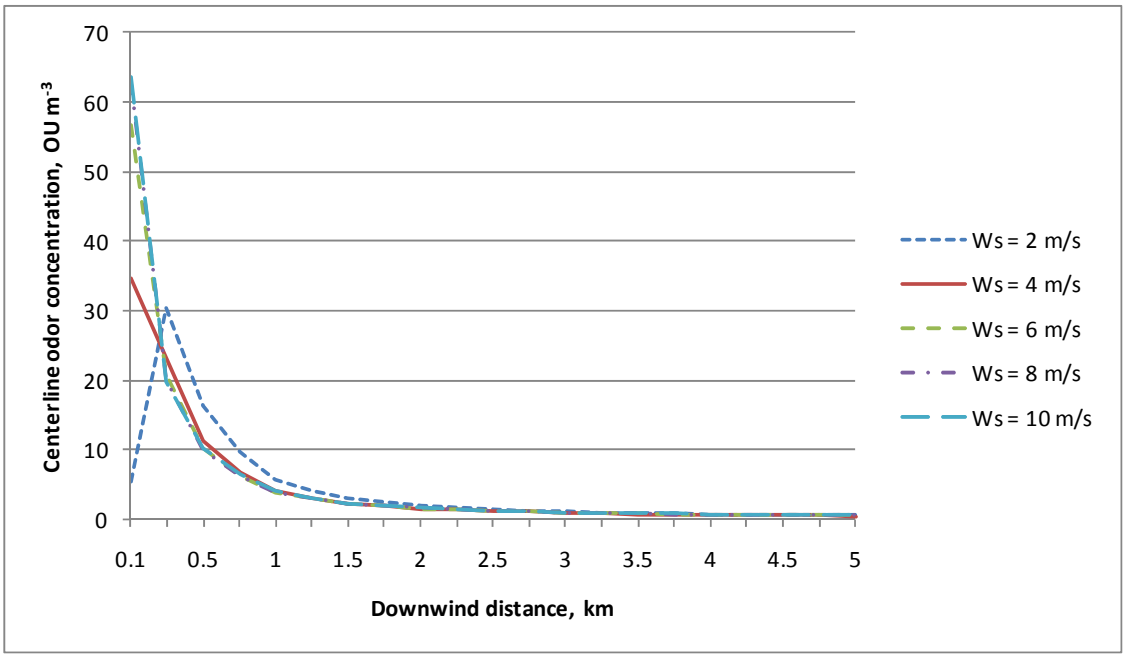

Figure 5.11 Centerline odour concentrations for different wind speeds (Ws) under unstable conditions (SC = C)

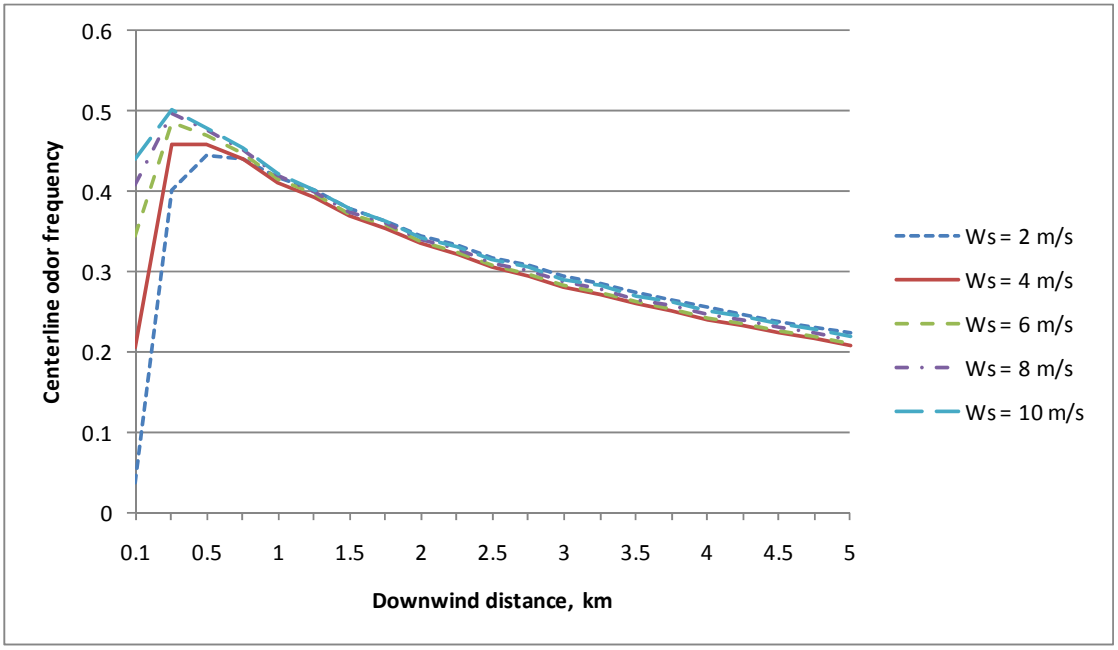

Figure 5.12 Centerline odour frequencies for different wind speeds (Ws) under unstable conditions (SC=C)

Under neutral condition (SC = D), change of the centerline odour concentration with wind speed is as same as those under unstable condition (Figure 5.13). However, the odour frequency increases with wind speed at near source distance. At longer distance,

the odour frequency decreases when wind speed varies from 2 to m s^{-1} to 10 m s^{-1} (Figure 5.14).

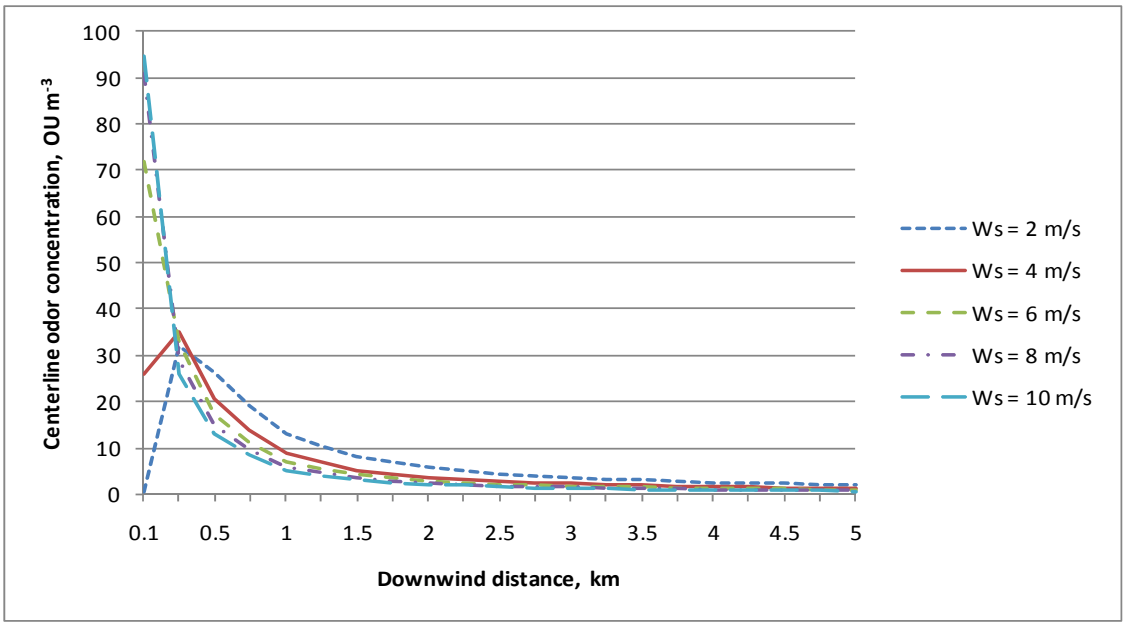

Figure 5.13 Centerline odour concentrations for different wind speeds (Ws) under neutral conditions (SC = D)

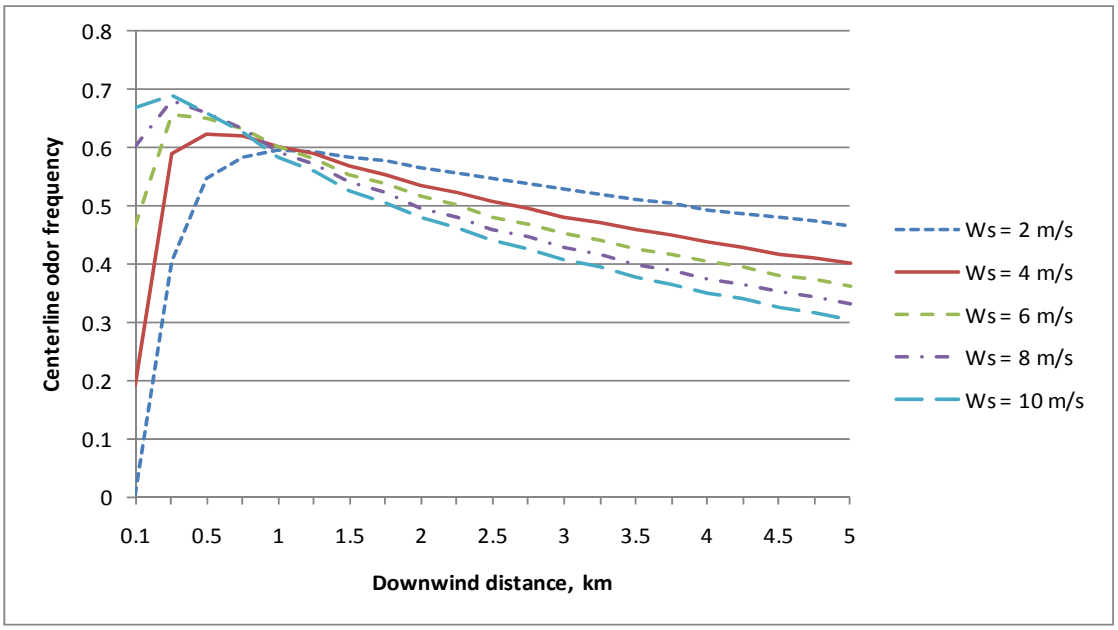

Figure 5.14 Centerline odour frequencies for different wind speeds (Ws) under neutral conditions (SC = D)

Under stable condition (SC = E), the centerline odour concentration demonstrates the same variation trend as those under unstable and neutral conditions, but the magnitude is larger (Figure 5.15). With the increase of wind speed, the centerline odour frequency increase. When wind speed increase from 2 m s^{-1} to 3 m s^{-1}, odour frequency increases dramatically (Figure 5.16).

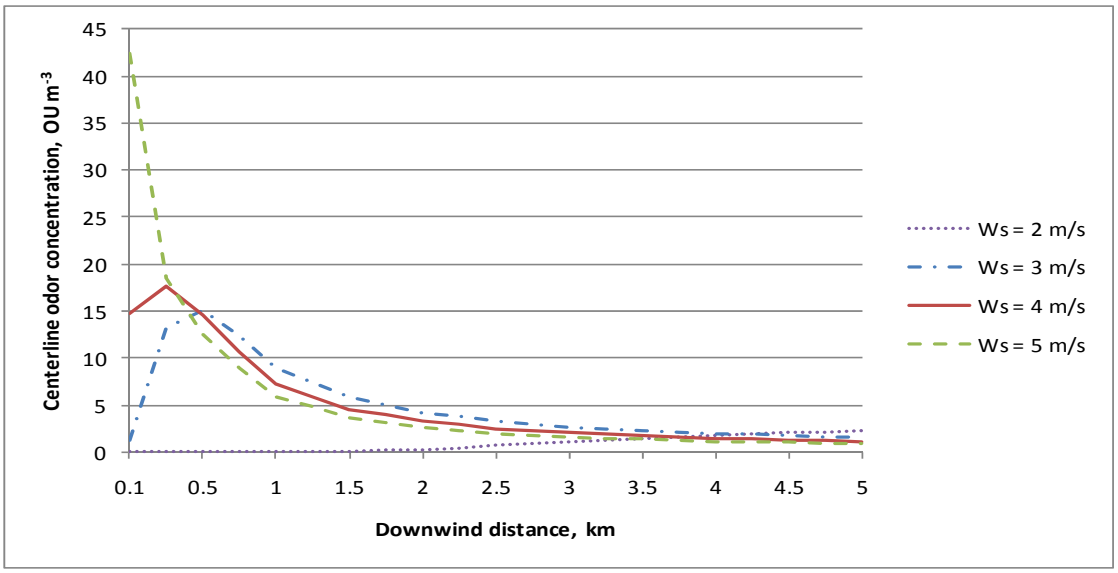

Figure 5.15 Centerline odour concentrations for different wind speeds (Ws) under stable conditions (SC= E)

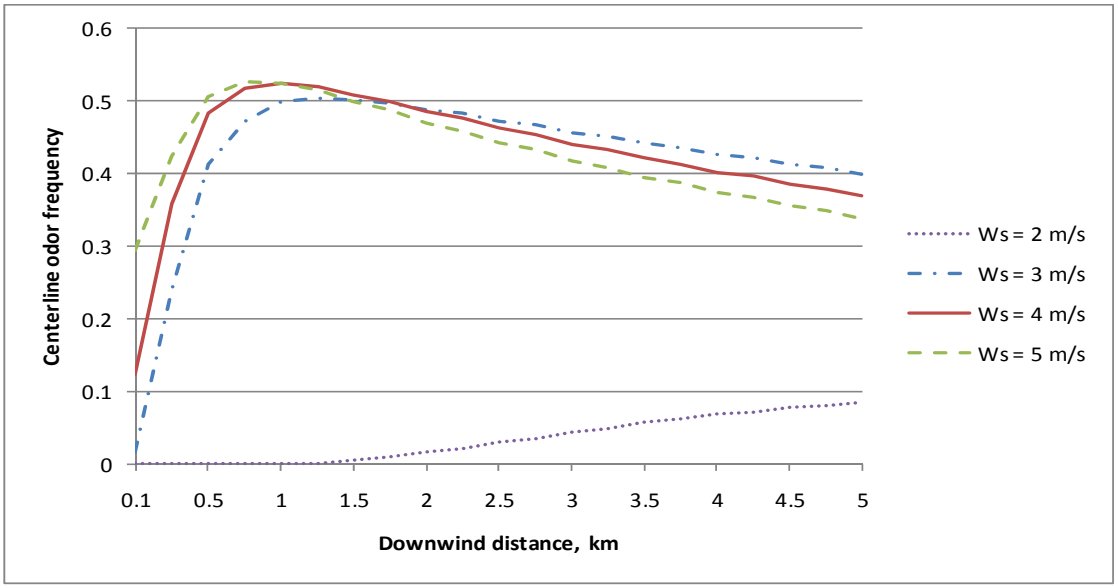

Figure 5.16 Centerline odour frequencies for different wind speeds (Ws) under stable conditions (SC = E)

From the average changes of odour concentrations and odour frequencies and elasticity values shown in Table 5.6, effect of wind speed on odour both concentration and frequency is greater at close distance than further distance. The effect is apparent when wind speed decreases from 4 m s^{-1} to 2 m s^{-1}.

Table 5.6 Sensitivity analysis of odour concentration and frequency to wind speed with a control value of 4 m s^{-1}

Stability	Change, %	Concentration				Frequency			
		Ave. C Change, %	S(0.5)	S(5)	S(ave)	Ave. F Change, %	S(0.5)	S(5)	S(ave)
Unstable	-50	13.2	0.9	0.3	0.5	3.5	-0.1	0.1	0.1
	+50	6.2	-0.2	0.0	0.0	1.5	0.1	0.0	0.0
	+100	9.5	-0.1	0.0	0.0	3.0	0.1	0.0	0.0
	+150	11.8	-0.1	0.1	0.0	4.6	0.1	0.0	0.0
Neutral	-50	36.1	0.6	1.2	1.1	9.0	-0.5	0.4	0.2
	+50	-5.0	-0.3	-0.4	-0.4	-5.3	0.2	-0.2	-0.1
	+100	-11.3	-0.3	-0.3	-0.3	-10.2	0.1	-0.2	-0.1
	+150	-18.3	-0.2	-0.3	-0.3	-14.6	0.1	-0.2	-0.1
Stable	-50	-63.9	-2.0	1.0	-1.0	-98.6	-2.0	-1.6	-1.8
	-25	-14.9	-0.2	-1.0	-0.7	3.3	1.1	-0.4	0.0
	+25	-21.5	-0.7	-1.6	-0.8	-5.1	1.3	-0.7	0.1

5.2.2 Stability class

When solar radiation or cloud cover data are unavailable, the model will convert the stability class into representative solar radiation or cloud cover to derive parameters in the PBL. Under unstable condition, the Hogstrŏm dispersion coefficient is irrelevant to stability. Then the effect of stability class on odour concentration and odour frequency is negligible, which is shown in Figures 5.17 and 5.18. At near distance, the mean odour concentrations are smaller under more stable conditions due to the influence of plume rise. As expected, the mean odour concentrations are larger for more stable conditions at longer distance. The centerline odour frequency decreases when stability changes from neutral to stable and to more stable. The reason has been explained in Chapter 2.

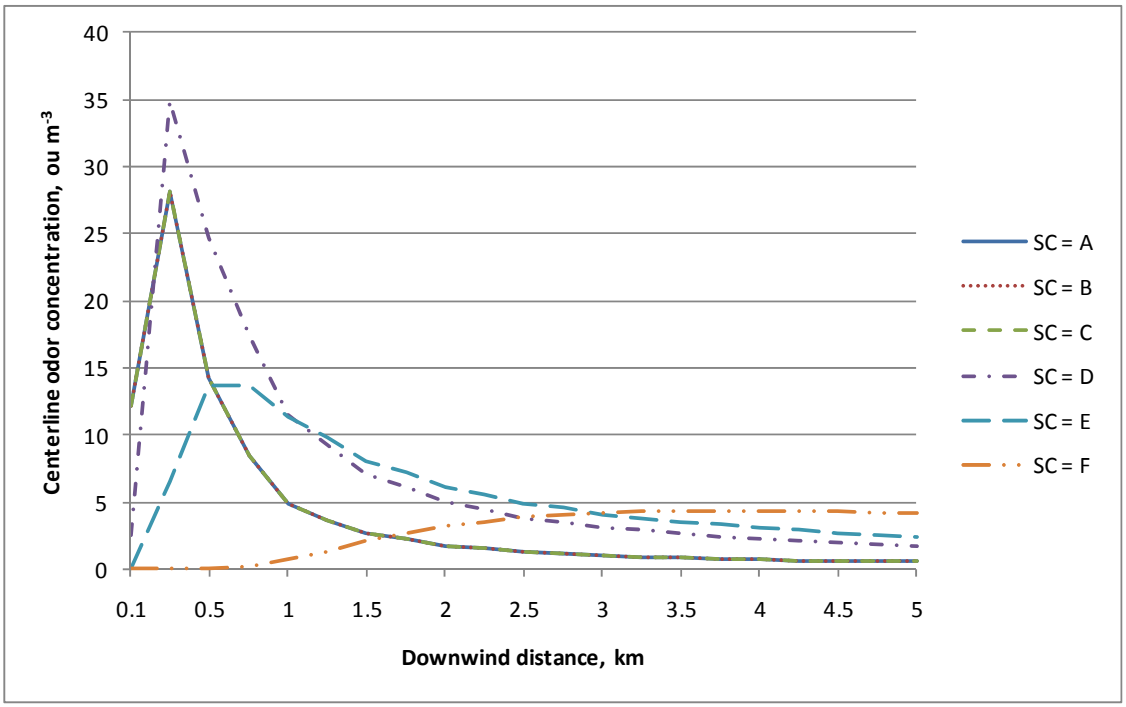

Figure 5.17 Centerline odour concentrations for different stability classes (SC)

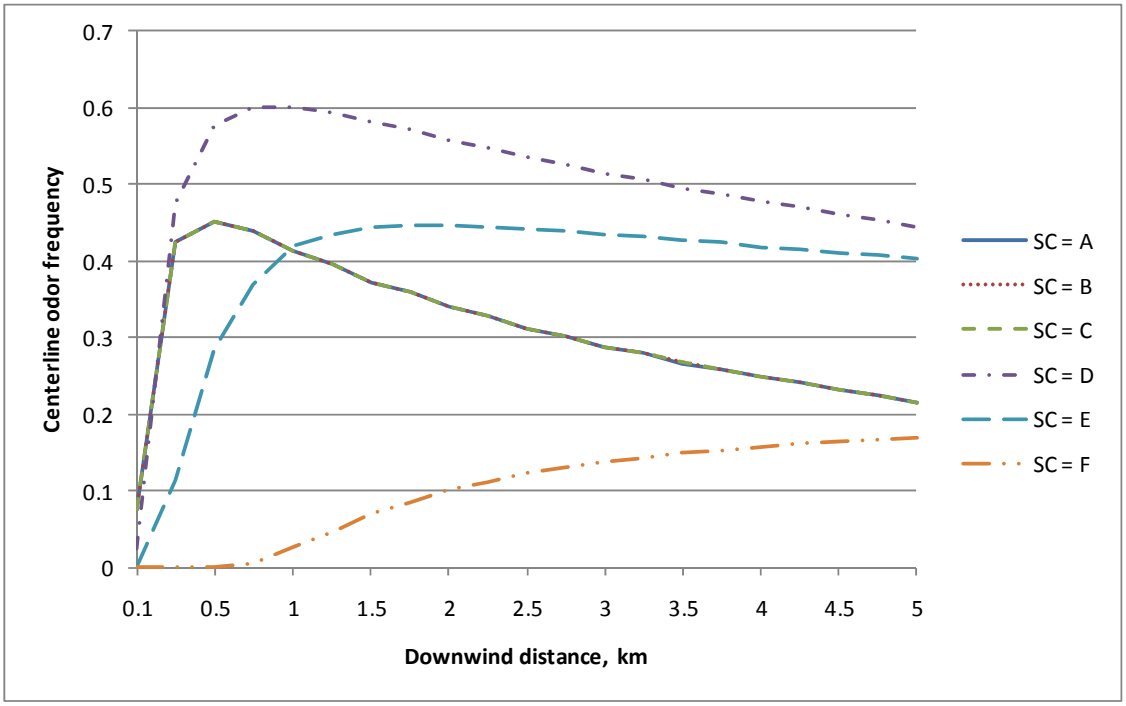

Figure 5.18 Centerline odour frequencies for different stability classes (SC)

The average changes of odour concentrations and odour frequencies, as well as the elasticity values for varying stability class are listed in Table 5.7. When the stability class is varying among unstable conditions, the changes of concentration and frequency can be ignored. When the stability class is varying among unstable, neutral and stable conditions, changing the stability class by one interval involves great changes of odour concentration and odour frequency from 4.6% to more than thousand percents. The sensitivity of stability class is very high.

Table 5.7 Sensitivity analysis of odour concentration and frequency to stability class

Stability class		Concentration				Frequency			
Control	New	Ave. C Change, %	S(0.5)	S(5)	S(ave)	Ave. F Change, %	S(0.5)	S(5)	S(ave)
A	B	0.0	0.0	0.0	0.0	0.0	0.0	-0.1	0.0
B	A	0.0	0.0	0.0	0.0	0.0	0.0	0.1	0.0
B	C	0.0	0.0	0.0	0.0	0.0	0.0	0.0	0.0
C	B	0.0	0.0	0.0	0.0	0.0	0.0	0.0	0.0
C	D	74.6	9.7	163.5	99.0	35.9	-18.4	67.2	20.2
D	C	-42.7	4.6	-60.7	-17.9	-26.4	40.4	-37.7	35.4
D	E	6.3	-44.5	38.1	25.5	-16.7	-54.4	-7.1	-16.2
E	D	-5.9	80.2	-27.6	-18.4	20.0	119.8	7.7	21.6
E	F	-28.2	-176966.6	42.1	-3189.4	-224.2	-51688.7	-136.1	-1275.4
F	E	-22.0	-99.9	72.8	-5.5	-69.2	-99.8	-57.6	-71.6

5.2.3 Wind Direction

Figures 5.19 and 5.20 and Table 5.8 reveal the model sensitivity to wind direction. When changing wind direction, the “centerline” odour concentration and odour frequency are still obtained from the control wind direction. Overall, the sensitivity of wind direction is high. Under unstable condition, the sensibility is smaller than neutral and stable conditions and the sensitivity decreases with the distance.

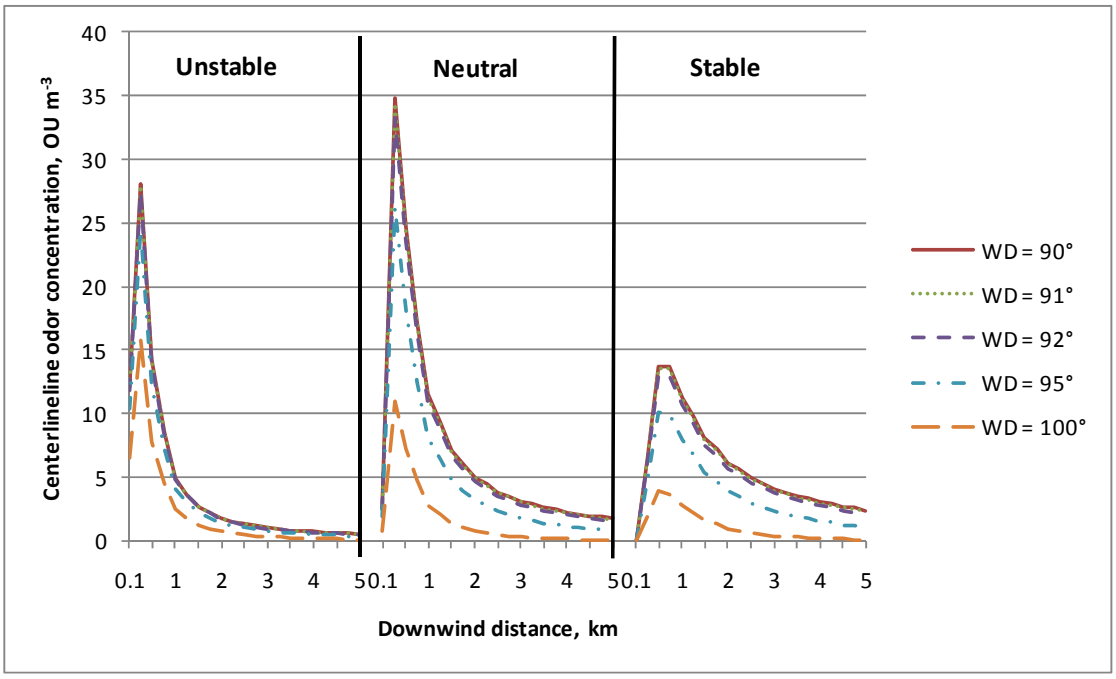

Figure 5.19 "Centerline" odour concentrations for different wind directions (WD)

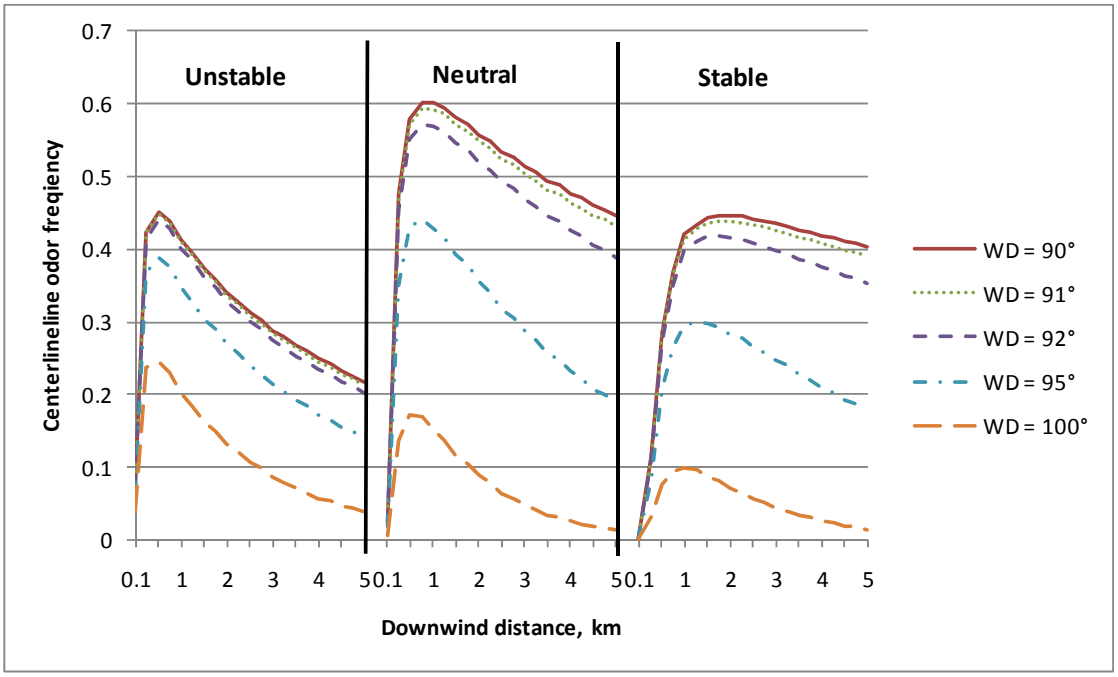

Figure 5.20 "Centerline" odour frequencies for different wind directions (WD)

Table 5.8 Sensitivity analysis of odour concentration and frequency to wind direction with a control value of 90°

Stability	Wind direction change (°)	Concentration				Frequency			
		Ave. C Change, %	S(0.5)	S(5)	S(ave)	Ave. F Change, %	S(0.5)	S(5)	S(ave)
Unstable	1	-0.2	14.9	5.0	-0.9	-0.4	5.2	-0.9	0.8
	2	-0.7	19.4	10.2	-1.8	-1.3	10.7	-1.9	1.6
	5	-4.9	39.9	30.3	-4.3	-9.0	32.2	-4.3	4.7
	10	-14.7	113.7	95.5	-6.4	-27.5	103.9	-6.5	15.4
Neutral	1	0.1	8.2	-0.5	3.1	-0.5	9.0	-0.3	3.4
	2	-1.5	17.1	-1.1	6.3	-1.5	19.0	-0.7	7.0
	5	-7.1	55.3	-3.6	18.7	-10.7	63.6	-3.2	21.2
	10	-21.6	195.4	-7.2	63.9	-35.8	232.1	-7.3	74.7
Stable	1	-0.4	8.5	-0.5	3.1	-0.5	10.1	-0.4	3.3
	2	-1.1	17.7	-1.1	6.4	-1.6	21.3	-1.0	6.8
	5	-7.6	58.0	-3.6	19.0	-11.4	73.6	-3.6	21.0
	10	-25.6	209.4	-7.2	65.8	-37.7	297.2	-7.3	77.5

5.2.4 Ambient Temperature

The effect of ambient temperature on odour concentration and odour frequency is shown on two aspects: plume rise calculation and PBL characterization. Figures 5.21 and 5.22 show the centreline odour concentration and odour frequency of different ambient temperatures and different stability conditions. Table 5.9 lists the average changes of odour concentrations and odour frequencies as well as the elasticity values. Under unstable and neutral conditions, the effect of increasing ambient temperature is negligible. When ambient temperature is close to or larger than the exit temperature, the plume rise is determined by momentum rise. The effect of odour concentration and odour frequency is solely on PBL characterization. It can be concluded that the effect of ambient temperature on plume rise contributes more on concentration and frequency results than on PBL characterization.

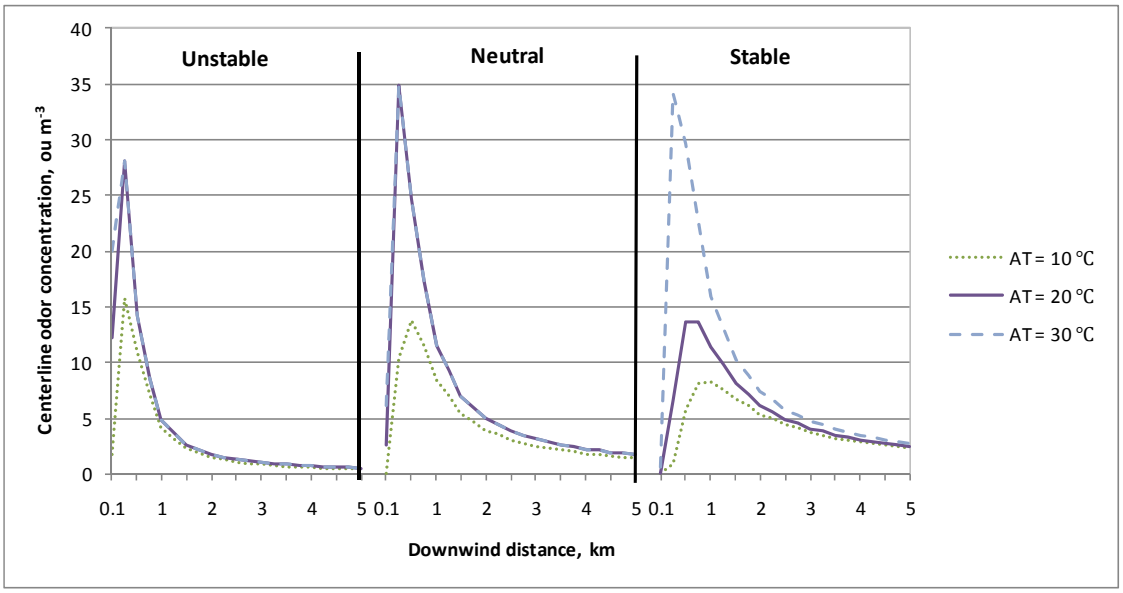

Figure 5.21 Centerline odour concentrations with different ambient temperatures (AT)

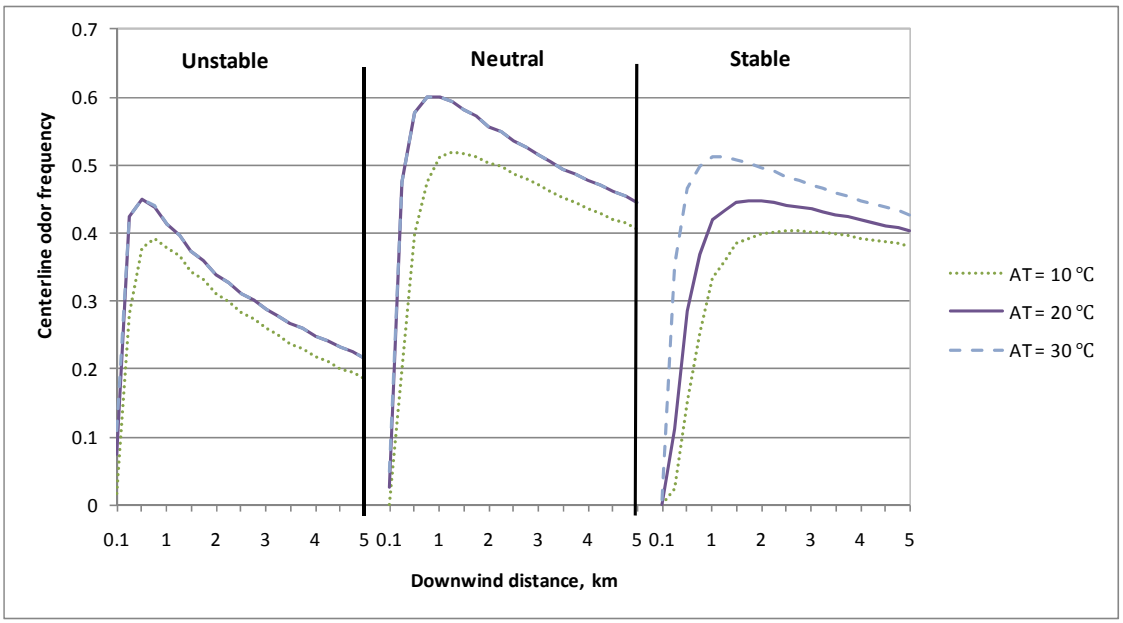

Figure 5.22 Centerline odour frequencies with different ambient temperatures (AT)

Table 5.9 Sensitivity analysis of odour concentration and frequency to ambient temperature with a control value of 20℃

Stability	Change, %	Concentration				Frequency			
		Ave. C Change,%	S(0.5)	S(5)	S(ave)	Ave. F Change,%	S(0.5)	S(5)	S(ave)
Unstable	-50	-24.4	-0.5	-0.4	-0.4	-11.4	-0.5	-0.3	-0.3
	+50	3.1	0.0	0.0	0.0	0.1	0.0	0.0	0.0
Neutral	-50	-28.2	-0.9	-0.4	-0.5	-11.8	-1.0	-0.2	-0.3
	+50	0.8	0.0	0.0	0.0	0.0	0.0	0.0	0.0
Stable	-50	-16.2	-1.2	-0.1	-0.3	-9.7	-1.0	-0.1	-0.3
	+50	32.1	2.3	0.2	5.6	11.5	2.2	0.1	2.2

5.2.5 Mixing Height

The effect of mixing height on concentration and frequency under unstable and neutral conditions comes from the concentration calculation when considering the effects of the restriction on vertical plume growth at the top of the mixing layer as equation (2.1). From Table 5.10, the effect of mixing height in this manner is zero. Under stable conditions, the mixing height is used as the height of friction layer when calculating the Hogstrŏm stability index. From Table 5.10, the effect is negligible.

Table 5.10 Sensitivity analysis of odour concentration and frequency to mixing height with a control value of 1000 m

Stability	Change, %	Concentration				Frequency			
		Ave. C Change, %	S(0.5)	S(5)	S(ave)	Ave. F Change, %	S(0.5)	S(5)	S(ave)
Unstable	-50	0.0	0.0	0.0	0.0	0.0	0.0	0.0	0.0
	+50	0.0	0.0	0.0	0.0	0.0	0.0	0.0	0.0
Neutral	-50	0.0	0.0	0.0	0.0	0.0	0.0	0.0	0.0
	+50	0.0	0.0	0.0	0.0	0.0	0.0	0.0	0.0
Stable	-50	0.5	-0.1	0.0	0.0	-1.2	-0.1	0.0	0.0
	+50	-0.2	0.0	0.0	0.0	0.6	0.0	0.0	0.0

5.2.6 Radiation

At day time, in the convective boundary layer (CBL), the radiation data are used to characterizing the PBL. However, the dispersion parameters are irrelevant to the stability. The effect of solar radiation will be shown on the wind profile. However, the results show that the sensitivity of radiation on odour concentration and odour frequency is very low and can be neglected.

5.2.7 Cloud Cover

In CBL, when solar radiation is not available, LODM use cloud cover to estimate the solar radiation from clear sky solar radiation. Therefore, the sensitivity of cloud cover in CBL is as same as the solar radiation, which is negligible. In SBL, cloud cover is an important factor in determining the Hogstrŏm stability index, and thus it has some effects on odour concentration and odour frequency. However, the effect is very small as shown in Table 5.11.

Table 5.11 Sensitivity analysis of odour concentration and frequency to cloud cover with a control value of 0.5 in SBL (Stable Boundary Layer)

Change, %	Concentration				Frequency			
	Ave. C Change,%	S(0.5)	S(5)	S(ave)	Ave. F Change,%	S(0.5)	S(5)	S(ave)
-100	-0.4	0.0	0.0	0.0	-0.5	0.0	0.0	0.0
-80	-0.4	0.0	0.0	0.0	-0.5	0.0	0.0	0.0
-60	-0.4	0.0	0.0	0.0	-0.4	0.0	0.0	0.0
-40	-0.3	0.0	0.0	0.0	-0.2	-0.1	0.0	0.0
-20	-0.2	0.0	0.0	0.0	0.2	-0.1	0.0	0.0
20	0.2	0.0	0.0	0.0	0.4	0.0	0.0	0.0
40	0.4	0.0	0.0	0.0	0.7	0.0	0.0	0.0
60	0.7	0.1	0.0	0.0	1.1	0.0	0.0	0.0
80	1.0	0.1	0.0	0.0	1.5	0.0	0.0	0.0
100	1.3	0.1	0.0	0.0	0.0	0.0	0.0	0.0

5.3 SURFACE ROUGHNESS, ALBEDO, AND BOWEN RATIO

Surface roughness is an important factor of both characterizing the atmosphere and determining the Hogstrŏm dispersion parameters. The model sensitivity to surface roughness under neutral and unstable conditions is low. Under stable condition, the effect of roughness is significant as shown in Table 5.12. Especially, when roughness changes from 0.1 m to 0.01 m, changes of odour concentration and frequency are great.

Albedo and Bowen ratio are used to derive parameters at day time. Their effects on odour concentration and odour frequency are small. The model sensitivity to them is very low.

Table 5.12 Sensitivity analysis of odour concentration and frequency to surface roughness with a control value of 0.1 m

Stability	Change		Concentration				Frequency			
	%	New value	Ave. C Change,%	S(0.5)	S(5)	S(ave)	Ave. F Change,%	S(0.5)	S(5)	S(ave)
Unstable	-90	0.01	5.9	0.1	0.1	0.1	1.9	-0.1	0.0	0.0
	400	0.5	11.9	0.0	0.0	0.0	6.7	0.0	0.0	0.0
	900	1	17.9	0.0	0.0	0.0	8.7	0.0	0.0	0.0
	1400	1.5	18.6	0.0	0.0	0.0	8.3	0.0	0.0	0.0
Neutral	-90	0.01	8.3	-0.1	0.2	0.1	0.7	-0.3	0.0	0.0
	400	0.5	6.9	0.0	0.0	0.0	1.7	0.0	0.0	0.0
	900	1	8.5	0.0	0.0	0.0	1.9	0.0	0.0	0.0
	1400	1.5	7.9	0.0	0.0	0.0	1.7	0.0	0.0	0.0
Stable	-90	0.01	-100.0	-1.1	-1.1	-1.1	-99.9	-1.1	-1.1	-1.1
	400	0.5	-16.5	0.1	-0.1	6.1	8.7	0.1	0.0	1.5
	900	1	-17.9	0.0	0.0	6.0	9.6	0.1	0.0	1.3
	1400	1.5	-17.9	0.0	0.0	6.1	10.2	0.1	0.0	1.2

5.4 DISCUSSION AND CONCLUSION

In this chapter, the sensitivities of LODM to its input parameters were analyzed using averaged change of odour concentration and odour frequency and a defined elasticity (s). The parameters can be divided into three categories: source parameters, meteorological parameters, and surface parameters. The meteorological parameters have the greatest effects on downwind odour concentrations and odour frequencies. The meteorological parameters in an order of decreasing importance would appear to stability class, wind direction, wind speed, ambient temperature, cloud cover, mixing height, and radiation. The source parameters have the similar medium impact on concentrations and frequencies. Emission rate is linearly related to odour concentrations so it is important to odour concentrations; however, it is much less important to odour frequencies. Among the three surface parameters, LODM is sensitive to surface roughness while its sensitivity to albedo and Bowen ratio is very low.

The controllable source parameters (stack height, diameter, exit velocity, exit temperature, and emission rate) have great practical applications regarding odour issues. When odour problems occur to existing livestock operations, the effective way to control odour dispersion is to modify such parameters. For a livestock building or barn without a chimney, the building exhausts air by openings and fans mounted on the wall or roof. It is unrealistic to modify the source physical characteristics (stack height and stack diameter). Therefore, the best available option is to change emission rate. As an alternate approach, windbreak wall is often built to reduce downwind odour dispersion. It can not only reduce the forward momentum of air flow from exhaust fans, but also provide a sudden vertical dispersion of odour plume, which is equivalent to increasing the emission height. If an exhaust chimney is installed as exhaust outlet for a livestock building, it is very easy to modify the chimney height, exit diameter as well as exit velocity. For an existing manure storage without cover, it is almost impossible to change the source parameters. However, producers can rebuild the manure storage above the ground which will has the same effect as increasing the emission height. When the manure storage is covered and has an exhaust chimney, it is possible to modify the stack height and stack diameter.

By increasing stack height, stack diameter, exit velocity, and exit temperature and by decreasing emission rate, the downwind odour concentrations and odour frequencies will be reduced. When stack height, stack diameter, and exit velocity increase by 50%, the downwind odour concentration and odour frequency decrease by about 20% and 10%, respectively. Among the three parameters, exit velocity has less effect on downwind odour concentration and odour frequency than the other two. When odour emission rate decreases, the downwind odour concentration decrease at the same level; however, the effect on odour frequency is much less. Fifty-percent decrease of odour emission will result in about 20% decrease of odour frequencies. In this analysis, when dealing with one parameter, the other parameters are assumed to be unchanged. However, stack diameter, exit velocity, and emission rate have mutual effects. Emission rate is determined by odour concentration and exhaust air flow rate as shown in Equation 1.2, in which exhaust air flow rate depends on stack diameter and exit velocity. Given the same exhaust odour concentration, when increasing the stack diameter, the odour emission rate will increase if the exit velocity remains unchanged. Therefore, the effect of increasing

emission rate will offset the effect of increasing stack diameter. When increasing exit velocity, the emission rate will also increase given the same stack diameter. Then the effects of increasing exit velocity will be neutralized by increasing of emission rate. In the realistic world, the effects of increasing stack diameter or exit velocity are very small or even negative on reducing odour dispersion. Exit temperature has the greatest effect on odour dispersion. When exit temperature increases only by 6.7% (e.g. from 300 to 320 K), the average downwind odour concentration and odour frequency will decrease by more than 27% and 13%, respectively. In conclusion, in order to reduce the odour effect, the most effective way is to raise the exit temperature, which is not practical, the second effective way is to lessen the emission rate by some approaches such as biofiltration and feed manipulation.

Chapter 6. SUMMARIES AND CONCLUSIONS

Commercial Gaussian models, including the Gaussian plume model (eg. ISCST3 and AERMOD) and the Gaussian puff model (eg. INPUFF2 and CALPUFF), have been originally designed for traditional industrial air pollutant dispersion modeling. These models have also been used for odour dispersion prediction. However, direct application of air dispersion models in livestock odour has been proved unreasonable due to the difference in source characteristics of industry and livestock sources and measurement methods of odour and traditional air pollutant. In addition, most air dispersion models currently applied in livestock odour dispersion can only predict long time average concentration, such as hourly and monthly concentration. In practice, models that can predict odour concentration fluctuations are needed. At the same time, the models should have the ability to account for odour short distance transportation, multiple sources, varied odour emissions, and the conversion between odour concentration and intensity. A livestock odour dispersion model (LODM) with above mentioned abilities therefore was developed. In this chapter, the model's theory, assumption, and function, evaluation and validation, sensitivity analysis, application, advantages and disadvantages, and future direction are summarized.

6.1 THE MODEL THEORY, ASSUMPTION, AND FUNCTION

LODM is developed based on the theory of Gaussian fluctuating plume model that has the ability to account for instantaneous fluctuations. The odour frequency is estimated by a weighted odour exceeding method. When using Hogstrŏm dispersion coefficients, the Hogstrŏm stability index is defined and employed. The parameters that characterize the PBL are retrieved using an advanced method adapted from AERMOD model and routine meteorological data. Also, a simple procedure is utilized to deal with ISC met file without cloud cover or radiation.

As other air dispersion models, development of LODM is based on some assumptions. First, the model assumes that odour transports during PBL as gas, thus its dispersion can be treated as air dispersion. During the odour transportation, it is assumed that there are no chemical and physical reactions and the ground level was treated as completely

reflected surface without odour absorption or deposition. The model is based on steady-state meteorological conditions, even if the wind directions shifted frequently. The short time average vertical dispersion coefficients are assumed to be the same as the vertical dispersion parameters at the mean plume height, although they are actually functions of vertically varied plume height.

LODM is designed specifically for livestock odour. It can predict mean odour concentration, instantaneous odour concentration, peak odour concentration and odour frequency with routine meteorological data. It has the ability to treat individual or multiple sources including elevated point sources, ground level sources, livestock buildings, manure storages, or manure land applications. It also has the ability to deal with constant and varied emission rates. It can deal with odour intensity with several relationships between odour intensity and odour concentrations included. At the same time, it is very easy to use with a friendly interface.

6.2 THE MODEL EVALUATION AND VALIDATION

Mean odour concentrations predicted by LODM and ISCST3 and CALPUFF were compared. Comparisons were also made between LODM predicted and field measured odour concentrations (intensities) and odour frequencies. Conclusions can be drawn:

1) LODM can predict similar mean odour concentrations as ISCST3 and CALPUFF when using Passiquill-Gifford dispersion parameters. LODM predicted odour concentrations are larger than those of ISCST3 and CALPUFF models when Hogstrŏm dispersion parameters were used,
2) Agreements between LODM predicted mean odour intensities and field measured odour intensities are high and they are higher at relatively longer distance than close distance.
3) LODM underestimates odour frequency; however, it has more accurate prediction in relatively longer distance than shorter distance. .

6.3 THE MODEL SENSITIVITY ANALYSIS

The sensitivities of LODM to its input parameters were analyzed. According to the analysis, meteorological parameters in a sequence of importance decrease are stability class, wind direction, wind speed, ambient temperature, cloud cover, mixing height, and radiation. The source parameters have a medium impact on the modeled odour concentrations and frequencies. As for surface parameters, LODM is sensitive to surface roughness while its sensitivity to albedo and Bowen ratio is very low.

6.4 APPLICATION OF THE MODEL

The LODM was developed based on the Gaussian fluctuating plume model that is able to account for odour instantaneous fluctuations. It has the ability to predict mean odour concentration, instantaneous odour concentration, peak odour concentration and the frequency of odour concentration that is equal to or higher than a certain level. Therefore, it can be a great tool for odour dispersion application involving odour impact assessment and setback distance determination. For example, the medium sensitivity of LODM to the controllable source parameters, including stack height, diameter, exit velocity, exit temperature, and emission rate, make it practically applicable in resolving odour issues from existing livestock operations. When odour problems occurs, the most effective way to relieve odour impact is to lessen the emission rate using some approaches, such as biofiltration and feed manipulation.

6.5 ADVANTAGES AND DISADVANTAGES OF THE MODEL

LODM as a specifically designed model for livestock odour has some advantages on theory and methods. It was developed on the basis of Gaussian fluctuating plume model, therefore it has the capability to predict instantaneous odour concentration and frequency. In the model, odour frequency is calculated by a weighted odour exceeding half width method. This method is an improvement of weighted odorous half width method used in de Bree and Harssema (1987) and it has an advantage over that used by Mussio et al. (2001) who calculated the odour frequency from instantaneous odour concentrations. Also, a simple and effective method is created to calculate odour frequency of multiple sources from the odour frequency of an individual source. Both Pasquill-Gifford and

Hogstrŏm dispersion coefficients are applied in the model. When using Hogstrŏm dispersion coefficients, the Hogstrŏm stability index is defined and employed. This index is determined by wind speed at the top of friction layer and the gradient of potential temperature at plume height. Thus, the profiles of wind speed and vertical gradient of potential temperature are calculated based on derived parameters including friction velocity, sensible heat flux, M-O length, and mixing height. The parameters are retrieved using an advanced method adapted from AERMOD model and routine meteorological data. Also, a simple procedure is utilized to deal with ISC met file without cloud cover or radiation, which make it possible for the model to deal with meteorological data as simple as an ISC met file. Hence, even if the simplest met data (ISC met data) are input, the model can also derive parameters of PBL, estimate profiles of wind speed and vertical gradient of potential temperature, and calculate the Hogstrŏm stability parameter.

Besides the theoretical improvements discussed above, LODM, has some other merits. First, it can predict odour frequency which can be a great practical criterion for odour impact assessment. Second, the model accepts and only requires routine meteorological data. Third, the model has the ability to process single or multiple sources which could be elevated point sources, ground level sources, livestock buildings, manure storages, or manure land applications. Fourth, the model has the ability to deal with constant and varied emission rates. Fifth, the model can deal with odour intensity based on several relationships between odour intensity and odour concentrations. Finally, the model is very easy to use with a friendly interface.

LODM is a useful and valuable improvement over other available models for livestock odour dispersion modeling. However, this model only considers the plume fluctuations without considering in-plume fluctuations. This may not reduce the model accuracy as in -plume fluctuations dominate in farther distance than close distance at which odour researchers interest. The biggest concern of this model is that the only available formulas of short time dispersion parameters are those developed by Hogstrŏm under certain conditions in certain area. The uncertainty of application of these parameters in other area and under other conditions is unknown.

6.6 FUTURE DIRECTION

This study solves the problem of predicting odour frequency from livestock operations with hourly routine meteorological data. It has great applications regarding odour impact assessment, evaluation of odour control technology, as well as determination of setback distances. The application of this model should be implemented in the future, whilst there are many issues that remain unsolved and require a lot of future work.

In this research, the model was validated by two sets of filed plume measurement data. However, both of the two filed plume measurements were conducted in relatively short distances (<1200 m) in daytime. No validations were done for farther distances and at nighttime with stable conditions. In the future, more validation works should be done, especially for farther distances and varied meteorological conditions.

When predicting odour from multiple sources, the simple summation method used to deal with odour concentration or the method that proposed in this thesis to account for odour frequency might not be appropriate. If odours are from different sources and having different persistences, after the same dilutions, the strength of each odour is different. In order to assess the odour impact on a receptor from different sources, a method needs to be carried out to consider the different persistences of odours from different sources.

The sampling time of the experiments that used to derive the formulas of calculating short time dispersion coefficients is 30 s. The odour frequency calculated by Gaussian fluctuating plume theory is relevant to the sampling time. Since, the human sensation for odour is in a few seconds, nuisance will be caused by exposing to malodours for a few seconds. Therefore, the frequency predicted by the model will be better reflect the real sensations of receptors if there are short time dispersion coefficients that are obtained for shorter sampling time.

Also, in order to determine a suitable setback distance, an appropriate acceptable odour criterion has to be set up. Different researchers have been using different acceptable odour criteria such as certain level of average odour concentration or certain level of odour concentration combined with its occurrence frequency. More studies need to be done to achieve an acceptable odour criterion.

REFERENCE

Ahuja S. and A. Kumar. 1996. Evaluation of MESOPUFF-II SOx Transport and Deposition in the Great Lakes Region, AWMA Speciality Conference on Atmospheric Deposition to the Great Lakes, VIP-72, pp. 283-299, Oct. 28-30.

Arya, S. 1999. Air pollution meteorology and dispersion. Oxford University Press. New York, N.Y.

ASCE. 1995. Odour control in wastewater treatment plants. Report 82. American Society of Civil Engineers. New York, N.Y.

ASHRAE. 2005. ASHRAE hand book: fundamentals. ASHRAE. Atlanta, GA.

ASTM. 1998. E544-88 Standard practices for referencing suprathreshold odour intensity. American Society for Testing Materials. Philadelphia, PA.

AWMA EE-6. 2002. Subcommittee on the Standardization of Odor Measurement. Guidelines for odor sampling and measurement by dynamic dilution olfactometry. Submitted for Review to: ASTM E18 Sensory Committee—August. American Society for Testing and Materials. West Conshohocken, PA.

Bedogni, M., and R. Sergio. 2004. An applied methodology to evaluate odour impact. 9th int. Conf. on Harmonisation within Atmospheric Dispersion modeling for Regulatory Purposes. 242HNational Environmental Research Institute (Denmark).

Bjerg B., P. Kai, S. Morsing, and H. Takai. 2004. CFD Analysis to Predict Close Range Spreading of Ventilation Air from Livestock Buildings. Agricultural Engineering International: the CIGR Journal of Scientific Research and Development. Manuscript BC 03 014. Vol. VI.

Boeker, P., O. Wallenfang, F. Koster, R. Croce, B. Diekmann, M Griebel, and P.S. Lammers. 2000. The modeling of odour dispersion with time-resolved models. Agrartechnische Forschung, 6 heft 4, S.E 84- E 89.

Bowers, J.F., J.R. Bjorklund, and C.S. Cheney, 1979. Industrial Source Complex (ISC) Dispersion Model User's Guide, Vols. I and II. Report Nos. EPA-450/4-79-030 and 031, U.S. Environmental Protection Agency, Research Triangle Park, NC.

Carney, P. G., and V. A. Dodd. 1989. A comparison between predicted and measured

values for the dispersion of malodours from slurry. J. agric. Engng Res. 44: 67-76.

CEN. 2003. EN13725. Determination of odour concentration by dynamic olfactometry. CEN Central Secretariat: rue de Stassart, 36 B-1050. European Committee for Standardization. Brussels.

CERC. 2004. ADMS: User Guide. Version 3.2, July 2004. Cambridge Environmental Research Consultants Ltd., 3 King's Parade, Cambridge, CB2 1SJ, UK.

Chang, J.C. and S. R. Hanna. 2004. Air quality model performance evaluation. Meteorol Atmos Phys. 87: 167-196 .

Chen, Y., D.S. Bundy, and S.J. Hoff. 1999. Using olfactometry to measure intensity and threshold dilution ratio for evaluating swine odor. J. Air Waste Manag. Assoc., 49, 847–853.

Choinière, D., S. Barrington, C. Foulds. 2007. A validated evaluation protocol for odour reducing additives during swine manure spreading. Proceedings of The International Symposium on Air Quality and Waste Management for Agriculture. ASABE Publication No: 701P0907cd. ASABE St. Joseph, MI.

Curran, T.P., B.A. Sheridan, E.T. Hayes, and V.A. Dodd. 2002. Comparison of two dispersion models for odour nuisance prediction from pig units. ASAE Paper No. 024014. St. Joseph, Mich.

Curtis, S.E. 1983. Environmental management in animal agriculture. Iowa State University Press. Ames, IA.

De Bree, F., and H. Harssema. 1987. Field evaluation of a fluctuating plume model for odours with sniffing teams. In: Grefen, K., Löbel, J.(Eds.), Environmental Meteorology, Proceedings of an International Symposium in Wurzburg, FRG., Dordrecht, Netherlands.

de Haan, P. 2001. Predicting concentration fluctuations with a puff-particle model. Int J Environ Pollut. 16: 49–56.

De Melo Lisboa, H., J. M. Guillot, J .L. Fanlo, and P. L. Cloirec. 2006. Dispersion of odourous gases in the atmosphere—Part I: Modeling approaches to the phenomenon. Sci Total Environ. V361(1-3):220-228.

Deardorff, J.W., and G.E. Willis. 1984. Groundlevel Concentration Fluctuations from a

Buoyant and a Non-buoyant Source within a Laboratory Convectively Mixed Layer. Atmos. Environ. 18, 1297-1309.

Dinar, N., H. Kaplan, and M. Kleiman. 1988. Characterization of Concentration Fluctuations of a Surface Plume in a Neutral Boundary Layer. Boundary-Layer Meteorol. 45, 157-175.

Diosey, P. G., E. H. Maureen, and J. P. Richard. 2000. Modeling odour and VOCs: a comparison of models and modeling techniques. Water Environment Federation Specialty Conference: Odours and VOC Emissions 2000, Cincinnati, OH.

Donham, K. J., and W. J. Popendorf. 1985. Ambient levels of selected gases inside swine confinement buildings. Am Ind Hyg Assoc J. 46(11): 658-61.

Duffee, R.A., M.A. O'Brien, and N. Ostojic, 1991, 'Odour Modeling - Why and How', Recent Developments and Current Practices in Odour Regulations, Controls and Technology. Air & Waste Management Association. Pittsburgh, PA .

Engel, P. L. 1997. Utilizing ISCST to model composting facility odours. Presentation at the Air & Waste Management Association's 90th Annual Meeting & Exhibition, Toronto, Ontario, Canada.

EPA, 2000. AUSPLUME Gaussian Plume Dispersion Model: Technical User Manual, Environment Protection Authority of Victoria, Australia, 243Hhttp://www.epa.vic.gov.au.

Fackrell, J. E., and A.G. Robins. 1982. Concentration fluctuations and fluxes in plumes from points sources in a turbulent boundary layer. J Fluid Mech. 117:1–26.

Feddes. 2006. Development of odour monitoring procedures for Alberta livestock operations: measuring odour with confidence. Project number: 2002A239R. Alberta, Canada.

Franzese, P. 2003. Lagrangian stochastic modeling of a fluctuating plume in the convective boundary layer, Atmos Environ. 37:1691–1701.

Fritz, B.K., G.W. Zwicke, B.W. Shaw, and C.B. Parnell. 1997. A re-examination of the assumptions and parameters of the Gaussian dispersion model. ASAE PaperNo. 974098. St. Joseph, MI.

Gassman, P.W. 1993. Simulation of odour transport: a review. ASAE paper No. 924517.

St. Joseph, MI.

Gifford, F.A. 1959. Statistical properties of a fluctuating plume dispersion model. Adv Geophys. 6:117-137.

Guo, H., W. Dehod, J. Feddes, C. Laguë, and I. Edeogu. 2005b. Monitoring odour occurrence in the vicinity of swine farms by resident observers - Part I: Odour occurrence profiles. Canadian Biosystems Eng. 47: 57-65

Guo, H. , W. Dehod, J. Feddes, C. Laguë, and I. Edeogu. 2006a. Monitoring odour occurrence in the vicinity of swine farms by resident observers- Part II: Impact of weather conditions on odour occurrence. Canadian Biosystems Eng. 48: 23-29

Guo, H., J. Feddes, C. Laguë, W. Dehod and J. Agnew. 2005c. Downwind swine odour monitoring by trained odour assessors - Part I: Downwind odour occurrence as affected by monitoring time and locations. Canadian Biosystems Eng. 47: 6.47-6.55.

Guo, H., L.D. Jacobson, D.R. Schmidt, and R.E. Nicolai. 2001. Calibrating INPUFF-2 model by resident-panelists for long-distance odour dispersion from animal production sites. Applied Eng. In Agric. 17(6): 859-868

Guo, H., L.D. Jacobson, D.R. Schmidt, and R.E. Nicolai. 2003. Evaluation of the influence of atmospheric conditions on odour dispersion from animal production sites. T ASAE. 46(2): 461-466.

Guo, H., L.D. Jacobson, D.R. Schmidt, R.E. Nicolai, J. Zhu, and K.A. Janni. 2005a. Development of the OFFSET model for determination of odour-annoyance-free setback distances from animal production sites: Part II. Model development and evaluations. T ASAE, 48(6):2269-2276

Guo, H., W. Dehod, J. Agnew, C. Laguë, J. R. Feddes, S. Pang. 2006b. Annual odour emission rate from different types of swine production buildings. Tran. of ASABE. 49(2): 517-525.

Guo, H., W. Dehod, J. Agnew, J.Feddes, C. Lague, S. Pang. 2007. Daytime odour emission variations from various swine barns. Tran. of ASABE 50(4): 1365-1372.

Guo. H., L.D. Jacobson, D.R, Schmidt and R.E. Nicolai. 2000. Correlation of Odour Dilution Threshold and H 2 S and NH 3 Concentrations for Animal Feedlots.

ASAE Paper No. 004043. St. Joseph, Mich.

Hanna, S. R., J. C. Weil, and R. J. Paine. 1986. Plume Model Development and Evaluation - Hybrid Approach. EPRI Contract No. RP-1616-27, Electric Power Research Institute, Palo Alto, CA.

Hanna, S.R. 1984. Concentration fluctuations in a smoke plume. Atmos Environ. 18:1091–1106.

Hanna, S.R., P.J. Drivas, and J.C. Chang. 1996. Guidelines for Use of Vapor Cloud Dispersion Models. AIChE/CCPS, 345 East 47th St., New York, NY.

Hartung, E., and T. Jungbluth, 1997. Determination of the odour plume boundaries from animal houses. In Proc. 5th Int. Symp. on Livestock Environment, Bloomington, Minn., 1, 163-139. St. Joseph, Mich.

Hartung, E., and T. Jungbluth. 1997. Determination of the odour plume boundaries from animal houses. In Proc. 5th Int. Symp. on Livestock Environment, Bloomington, Minn., Vol. 1: 163- 169. St. Joseph, Mich.

Hartung, J. and V. R. Phillips. 1994. Control of gaseous emissions from livestock buildings and manure stores. J Agric Engng Res. 57:173-189.

Heber, A.J., D.S. Bundy, T.T. Lim, J. Ni, B.L. Haymore, C.A. Diehl, and R.K. Duggirala. 1998. Odour emission rates from swine finishing buildings. In: Animal Production Systems and the Environment: An International Conference on Odour, Water Quality, Nutrient Management and Socio-economic Issues. Des Moines, Iowa.

Hilderman, T., D.J. Wilson. 2007. Predicting plume meandering and averaging time effects on mean and fluctuating concentrations in atmospheric dispersion simulated in a water channel. Boundary-Layer Meteorol . 122:535–575.

Hilderman, T., D.J. Wilson. 2008. Effect of veritical wind shear on concentration fluctuation statistics in a point source plume. Boundary-Layer Meteorol. 129:65-97.

Hobbs, P. J., T. H. Misselbrook, and B. F. Pain. 1997. Characterisation of odourous compounds and emissions from slurries produced from weaner pigs fed dry feed and liquid diets. J. Sci. Food Agric. 73:437-445.

Högström, U. 1968. A statistical approach to the air pollution problem of chimney emission, Atmos Environ. 2: 251–271.

Högström, U. 1972. A method for predicting odour frequencies from a point source. Atmos Environ. 6: 103-121.

Holtslag, A. A., M. and A. P. van Ulden.1983. A Simple Scheme for Daytime Estimates of the Surface Fluxes from Routine Weather Data. J. Climate Appl. Meteor., 22:517-529.

Jacobson, L. D., C. J. Clanton, D. R. Schmidt, C. Radman, R. E. Nicolai, and K. A. Janni. 1997. Comparison of hydrogen sulfide and odour emissions from animal manure storages. Proceedings of the Ammonia and Odour Control from Animal production Facilities.Vinkeloord, The Netherlands. Rosmalen. The Netherlands.

Jacobson, L. D., H. Guo, D. R. Schmidt, R. E. Nicolai, J. Zhu, and K. A. Janni. 2005. Development of the OFFSET model for determination of odour-annoyance-free setback distances from animal production sites: Part I. Review and experiment. Transactions of the ASAE, 48(6): 2259-2268.

Jacobson, L. D., H. Guo, D. R. Schmidt, R. E. Nicolai, K. A. Janni and J. Zhu. 2000. Development of an odour rating system to estimate setback distances from animal feedlots: Odour from feedlots - setback estimation tool (OFFSET). ASAE Paper No. 004044. St. Joseph, MI.

Jacobson, L.D., R.E. Nicolai, D.R. Schmidt, and J. Zhu. 1998. Odor plume measurements from livestock production sites. AgEng Conference, Paper No. 98-E-038, Oslo, Norway.

Kaye, R., and J. Jiang. 1999. Integration of odour emission measurements from area sources with dispersion modeling analysis of environmental impacts. Research Report No. 136. Sydney, NSW, Australia.

Klarenbeek, J. V. 1985. Odour emissions of Dutch agriculture. In Agricultural Waste Utilization and Management, Proc. 5th International Symposium on Agricultural Wastes, 439-445. ASAE. St. Joseph, MI.

Koerkamp, P. W. G., J. H. M. Metz, G. H. Uenk, V .R. Phillips, M. R. Holden, R. W. Sneath, J. L. Short, R. P. White, J. Hartung, and J. Seedorf. 1998. Concentrations

and emissions of ammonia in livestock buildings in Northern Europe. J Agric Engng Res. 70(1):79-95.

Koppolu, L., D. D. Schulte, S. Lin, M. J. Rinkol, D. P. Billesbach, and S. B. Verma. 2002. Comparison of AERMOD and STINK for Dispersion Modeling of Odourous Compounds. ASAE Paper No. 024015. St. Joseph, MI.

Koppolu, L., D. Schmidt, D.D. Schulte, and L. Jacobson. 2004. Development of Scaling Factors (Peak-to-Mean Ratios) through Dispersion Modeling with AERMOD and Field-based Odour Measurements for Livestock Facilities. ASAE Paper No. 044196. St. Joseph, MI.

Leonardos, G. 1996. Review of odor control regulations in the USA. Odors, Indoor and Environmental Air, Proceedings of a Specialty Conference Air & Waste Management Association, pp. 73-84. Bloomington, MN.

Lewellen, W.S., and R.I. Sykes. 1986. Analysis of Concentration Fluctuations from Lidar Observations of Atmospheric Plumes.J. Clim. Appl. Meteorol. 25, 1145- 1154.

Li, J., D. S. Bundy, S.J. Hoff, and Q. Liu, 1994. Field odour measurement and applications of Gaussian plume model. ASAE Paper No. 94-4054. St. Joseph, Mich.

Li, Y., and H. Guo. 2006. Comparison of odour dispersion predictions between CFD and CALPUFF models. T ASABE. 49(6): 1915−1926.

Li, Y., and H. Guo. 2008. Evaluating the effect of computational time steps on livestock odour dispersion using a Computational Fluid Dynamics model. T ASABE. 50(6): 2199-2204

Lim, T. T., A. J. Heber, and J. Ni. 2000. Odour setback guideline for swine production systems. In Odours and VOC Emissions 2000. Water Environment Federation. Alexandria, Va.

Lim, T. T., A. J. Heber, J. Ni, A.L. Sutton, and D.T. Kelly. 2001. Characteristics and emission rates of odour from commercial swine nurseries. T ASAE. 44(5): 1275-1282.

Luhar, A.K., M.F. Hibberd, M.S. Borgas. 2000. A skewed meandering-plume model for concentration statistics in the convective boundary layer. Atmos Environ.

34:3599–3616.

Mahin, T. D. 1997. Using dispersion modeling of dilutions to threshold (D/T) odour levels to meet regulatory requirements for composting facilities. For presentation at the Air & Waste Management association's 90th annual meeting & exhibition, June 8-13, 1997, Toronto, Ontario, Canada.

Mahin, T. D. 1998. Odour modeling using D/T levels. Water Environment & Technology. 2: 49-53.

McHugh, C. A., Carruthers, D. J., Higson, H., and Dyster, S. J. 1999. Comparison of model evaluation methodologies with application to ADMS 3 and US models, 6th international conference on harmonization within atmospheric dispersion modelling for regulatory purposes, Rouen, France.

McPhail, S. 1991. Modeling the dispersion of agricultural odours. Proceedings of a workshop on agricultural odours, Toowoomba, Queensland, Australia. AMLRDC Report No. DAQ 64/7. Toowoomba, Queensland, Australia.

Mejer, G.J., and K. H. Krause. 1985. Dispersion models for emissions from agricultural sources. In: Nielson, V.C.; J.H. Voorburg; P.L. Hermite (eds). Odour prevention and control of organic sludge and livestock farming. Elsevier. London

Metcalf, A., and A. Eddy, 1991. Wastewater Engineering: Treatment, Disposal, Reuse. McGraw Hill International.

Misselbrook, T. H., C. R. Clarkon, and B. F. Pain. 1993. Relationship between concentration and intensity of odours for pig slurry and broiler houses. J. Agric. Eng. Res. 55: 163-169.

Mole, N., and C.D. Jones. 1994. Concentration fluctuation data from dispersion experiments carried out in stable and unstable conditions. Boundary-Layer Meteorol. 67: 41-74.

Monin, A. S., and A. M. Obukhov, 1954. 'Basic laws of turbulent mixing in the surface layer of the atmosphere', Tr. Akad. Nauk SSSR Geofiz. Inst. 24, 163-187. English translation by John Miller, 1959.

Mussio, P., A. W. Gnyp, and P. F. Henshaw. 2001. A fluctuating plume dispersion model for the prediction of odour-impact frequencies from continuous stationary

sources. Atmos Environ. 35:2955-2962.

Mylne, K.R. 1992. Concentration Fluctuation Measurements in a Plume Dispersing in a Stable Surface Layer. Boundary-Layer Meteorol. 60, 15-48.

Mylne, K.R., and P.J. Mason.1991. Concentration Fluctuation Measurements in a Dispersing Plume at a Range of up to 1000 m. Q.J.R. Meteorol. Soc. 117, 177-206.

Mylne, K.R., K.J. Davidson, and D.J. Thomson. 1996. Concentration fluctuation measurements in tracer plumes using high and low frequency response detectors. Boundary-Layer Meteorol. 79:225-242.

Nicolai, R. E., C. J. Clanton, and H. Guo. 2000. Modeling the relationship between detection threshold and intensity of swine odours. Proceedings of the Second International Conference: Air Pollution from Agricultural Operations. , St. Joseph, MI.

Nimmermark S., L. D. Jacobson, S. W. Gay, and D. R. Schmidt. 2003. Evaluation of OFFSET (Odour Setback Model) using neighborhood monitors. ASAE Paper No. 034024. St. Joseph, MI.

Oke, T.R. 1978. Boundary Layer Climates. John Wiley and Sons, New York..

Ormerod, R. J. 1990. Odours from cattle feedlots – A review of Australian experience. Proceedings of the International Clean Air Conference, Auckland, NZ.

Pain, B. F., C. R. Clarkson, V. R. Phillips, J. V. Klarenbeek, T. H. Misselbrook, and M. Bruins. 1991. Odour emission arising from application of livestock slurries on land: measurements following spreading using a micrometeorological technique and olfactometry. J. agri. Engng. Res. 48: 101-110.

Pain, B. F., and T. H. Misselbrook. 1990. Relationships between odour and ammonia emissions during and following application of slurries to land. In: Proc. Odour and Ammonia Emissions from Livestock Farming. Ed: V.V. Nielsen, J.H. Voorburg and P. L'Hermite. Elsevier Applied Science .New Work.

Pain, B. F., Rees, Y. J. and D. R. Lockyer. 1988. odour and ammonia emissions following the application of pig or cattle slurry to land. In Nelson, V.V., ed, Volatile Emissions from Livestock Farming and Sewage Operations. Elsevier.

Paine, R. J. 1987. User's Guide to the CTDM Meteorological Preprocessor (METPRO) Program. EPA-600/8-88-004, U.S. Environmental Protection Agency, Research Triangle Park, NC. (NTIS No. BP 88-162102).

Paine, R. J. and S. B. Kendall. 1993. Comparison of observed profiles of winds, temperature, and turbulence with theoretical results. Preprints, Joint conference of the American Meteorological Scoiety and Air & Waste Management Association Speciality Conference: The Role of Meteorology in Managing the Environment in the 90s, Scottsdale, AZ. Publication VIP-29, Air & Waste Management Association, Pittsburgh, PA.

Panofsky, H. A. and J. A. Dutton. 1984. Atmospheric Turbulence: Models and Methods for ngineering Applications. John Wiley and Sons, New York.

Patni N. K., and S. P. Clarke. 1991. Transient hazardous conditions in animal buildings due to manure gas released during slurry mixing. Appl Eng Agric. 53:23-50.

Petersen, B. W., and L. G. Lavdas. 1986. Inpuff 2.0 – A multiple source Gaussian puff dispersion algorithm- User's guide. Atmospheric Sciences Research Laboratory. Office of Research and Development, USEPA. Research Triangle Park, N.C.

Piringer, M., E. Petz, I. Groehn, and G. Schauberger. 2007. A sensitivity study of separation distances calculated with the Austrian Odour Dispersion Model (AODM). Atmospheric Environment. 41:1725-1735.

Reynolds, A.M. 2000. Representation of internal plume structure in Gifford's meandering plume model. Atmos Environ. 34:2539–2545.

Schauberger G., M. Piringer, and E. Petz. 2000. Diunal and annual variation of the sensation distance of odour emitted by livestock buildings calculated by the Austrian odour dispersion model (AODM). Atmos Environ. 34:18-28.

Schauberger G., M. Piringer, and E. Petz. 2001. Separation distance to avoid odour nuisance due to livestock calculated by the Austrian odour dispersion model (AODM). Agr Ecosyst Environ. 87: 13–28.

Schauberger G., M. Piringer, and E. Petz. 2006. Odour episodes in the vicinity of livestock buildings: A qualitative comparison of odour complaint statistics with model calculations. Agr Ecosyst Environ. 114: 185-194.

Schiffman, S. S., B. McLaughlin, G. G. Katul, and H. T. Nagle. 2005. Eulerian-Lagrangian model for predicting odour dispersion using instrumental and human measurements. Sensor Actuator. B 106:122-127

Schiffman, S. S., J. L. Bennett, and J. H. Raymer. 2001. Quantification of odours and odourants from swine operations in North Carolina. Agric. Forest Meteor. 108(3): 213−240.

Schiffman, S., C.M. Williams. 2005. Science of odor as a potential health issue. J Environ Qual. 34(1):129-138.

Segura, J. C. and J. J. R. Feddes. 2005. Relationship Between Odour Intensity and Concentration of n-Butanol Paper No. 05-020, CSBE, Winnipeg, MN.

Sheridan B. A., E. T. Hayes, T. P. Curran, and V. A. Dodd. 2004. A dispersion modelling approach to determining the odour impact of intensive pig production units in Ireland. Bioresource Technol. 91:145-152

Skinner, J.A., Lewis, K.A., Bardon, K.S., Tucker, P., Catt, J.A., Chambers, B.J., 1997. An overview of the environmental impact of agriculture in the UK. J. Environ. Manage. 50, 111–128.

Smith, F.B. 1972. A scheme of estimating the vertical dispersion of a plume from a source near ground level. Proceeding of the NATO Expert Panel on Air Pollution Modelling, Oct. 1972. Report NATO-CCMS-14. North Atlantic Treaty Organization, Brussels.

Smith, M.E., 1973. Recommended Guide for the Prediction of the Dispersion of Airborne Effluents. ASME, New York.

Smith, R. J. 1993. Dispersion of odours from ground level agricultural sources. J. agric. Engng Res. 54(3):187-200.

Smith, R. J. 1995. A Gaussian model for estimating odour emissions from area sources. Math Comput Model. 21(9):23-29

Smith, R. J. and N. Hancock. 1992. The prediction of feedlot odour emissions from downwind measurements of odour concentration. ASAE Paper No. 920503. St. Joseph, Mich.

Smith, R.J. and J.P. Kelly. 1996. Comparison of two methods for estimating odour

emissions from area sources. In Proc. International Conference on Air Pollution from Agricultural Operations, 263-269. ASAE. St. Joseph, Mich.

Spoelstra, S .F. 1980. Origin of objectionable odourous components in piggery wastes and the possibility of applying indicator components for studying odour development. In: Agr Environ, Elsevier Science. Amsterdam. The Netherlands.

Stoke, B. 1977. Dispersion of odours in the neighbourhood of pig houses. Agr Environ. 3:287-295.

Stull, R. B. 1988. An Introduction to Boundary Layer Meteorology, Kluwer Academic Publishers, Dordrecht, The Netherlands.

Sun, G., H. Guo, C. Lague. 2008. Diurnal Odour, Ammonia, Hydrogen Sulfide, and Carbon Dioxide emission profiles of confined swine grower/finisher rooms. J. Air & Waste Manage. Assoc. 58: 1434-1448.

Sweeten, J. M., L. D. Jocobson, A.J. Heber, D.R. Schmidt, J.C. Lorimor, P.W. Westerman, J.R. Miner, R.Zhang, C.M. Willianms, and B.W. Auverman. 2001. Chapter 1 in Odour Mitigation for Concentrated Animal Feeding Operations. White paper and recommendations, CD ROM, 58, North Carolina State University, National Center for Manure and Animal Waste Management. Raleigh, N.C.

Turner, D. B., 1970: Workbook of Atmospheric Dispersion Estimates. USEPA Office of Air Programs, 84 pp.

USEPA .2004. AERMOD: DESCRIPTION OF MODEL FORMULATION. EPA-454/R-03-004. Available at: 244Hwww.epa.gov. Accessed September 2005.

USEPA, 2000. Meteorological Monitoring Guidance for Regulatory Modeling Applications. EPA-454/R-99-005. Available at: 245Hwww.epa.gov. Accessed September 2005.

USEPA. 1995a. User's Guide for the Industrial Source Complex (ISC3) Dispersion Models. Volumes I - III. EPA-454/B-95-003a-c. Available at: www.epa.gov. Accessed June 2005.

USEPA. 1995b. A User's Guide for the CALPUFF Dispersion Model. EPA-454/B-95-006. Available at: www.epa.gov. Accessed September 2005.

USEPA. 1998, A Comparison CALPUFF with ISCST3. EPA-454/R-98-020, Available at: www.epa.gov. Accessed September 2005.

Van langenhove, H. and G. Van Broeck .2001. Applicability of sniffing team observations: experience of field measurements. 246HWater Sci Technol. .44(9):65-70.

van Ulden, A. P., and A. A. M. Holtslag. 1985. Estimation of Atmospheric Boundary Layer Parameters for Diffusion Applications. J. Climate Appl. Meteor., 24:1196-1207.

VDI (Verein Deutscher Ingenieure). 1993. VDI 3940: Determination of odorants in ambient air by field inspections. Beuth. Berlin, Germany.

VDI. 2000. Environmental meteorology atmospheric dispersion models, particle model. Beuth. Verlag, Berlin, Germany.

Venkatram, A. 1980. Estimating the Monin-Obukhov Length in the Stable Boundary Layer for Dispersion Calculations. Bound.-Layer Meteor., 19:481-485.

Verdoes, N. and N. W. M. Ogink. 1997. Odour emission from pig houses with low ammonia emission. In Proc. International Symposium on Ammonia and Odour Control from Animal Production Facilities, eds. J.A.M. Voermans and G. Monteny, 317-25. Vinkeloord, The Netherlands, Rosmalen, The Netherlands.

Wang , L. J., D. B. Parker, C. B. Parnell, R. E. Lacey, and B. W. Shaw. 2006. Comparison of CALPUFF and ISCST3 models for predicting downwind odour and source emission rates. Atmos Environ. 40:4663-4669.

Wang, Y. 2007. Monitoring and modeling of diurnal and seasonal odour and gas emissions from different types of swine rooms. MS Thesis. University of Saskatchewan, Department of Agricultural and Bioresource Engineering. Saskatoon, Sk, Canada.

Watts, P.J., and J.M. Sweeten. 1995. Toward a better regulatory model for odour. In: Proceeding of the Feedlot Waste Management Conference, Queensland, Australia.

Williams, M. L. 1985. The effects of weather on odour dispersion from livestock buildings and from fields. In: Nielson, V.C., J.H. Voorburg; P.L' Hermite (eds). Odour Prevention and Control of Organic Sludge and Livestock Farming,

Elsevier. London.

Wood, S. L., D. R. Schmidt, K. A. Janni, L. D. Jacobson, C. J. Clanton, and S. Weisberg. 2001. Odour and air emissions from animal production systems. ASAE Paper No. 014043. St. Joseph Mich.

Xing Y., H. Guo, J. Feddes, and S. Shewchuck. 2006. Evaluation of Air Dispersion Models Using Swine Odour Plume Measurement Data. CSBE paper No. 06-172. Manitoba, Canada.

Yee, E. 2009. Probability law of concentration in plumes dispersing in an urban area. Environ Fluid Mech. 9:389-407.

Yee, E., and C.A. Biltoft, 2004. Concentration fluctuation measurements in a plume dispersing through a regular array of obstacles, Boundary-Layer Meteorol. 111: 363–415.

Yee, E., P.R. Kosteniuk, G.M. Chandler, C.A. Biltoft, , and J.F. Bowers. 1993. Statistical Characteristics of Concentration Fluctuations in Dispersing Plumes in the Atmospheric Surface Layer. Boundary-Layer Meteorol. 65, 69–109.

Yee, E., R. Chan, P.R. Kosteniuk, G.M. Chandler, C.A. Biltoft, , and J.F. Bowers. 1994a. Experimental Measurements of Concentration Fluctuations and Scales in a Dispersing Plume in the Atmospheric Surface Layer Obtained Using a Very Fast Response Concentration Detector. J. Appl. Meteorol. 33, 996–1016.

Yee, E., R. Chan, P.R. Kosteniuk, G.M. Chandler, C.A. Biltoft, , and J.F. Bowers. 1994b, Incorporation of internal fluctuations in a meandering plume model of concentration fluctuations. Boundary-Layer Meteorol. 67: 11-39.

Yee, E., R. Chan, P.R. Kosteniuk, G.M. Chandler, C.A. Biltoft, , and J.F. Bowers. 1995. The Vertical Structure of Concentration Fluctuation Statistics in Plumes Dispersing in the Atmospheric Surface Layer. Boundary-Layer Meteorol. 76, 41–67.

Yu, J. C., C. E. Isaac, R. N. Coleman, J. J. R. Feddes, and B. S. West. 1991. Odorous compounds from treated pig manure. Canadian Agric. Eng. 33(1): 131−136.

Zahn, J. A., J. L. Hatfield, Y. S. Do, A. A. DiSpirito, D. A. Laird, and R. L. Pfeiffer. 1997. Characterization of volatile organic emissions and wastes from a swine

production facility. J. Envir. Qual. 26(6): 1687–1696.

Zhang, Q., J. J. R. Feddes, I. K. Edeogu, and X. J. Zhou. 2003. Correlation between odour intensity assessed by human assessors and odour concentration measured with olfactometers. Canadian Biosystems Eng. 44(6): 27-32.

Zhang, Q., X. J. Zhou, H. Q. Guo, Y. X. Li, and N. Cicek. 2005. Odour and greenhouse gas emissions from hog operations. Project MLMMI 03-HERS-01. Manitoba, Canada.

Zhou, X. and Q. Zhang. 2003. Measurement of odour and hydrogen sulfide emissions from swine barns. Canadian Biosystems Eng. 45: 6.13-6.18.

Zhou, X.J., Q. Zhang, H. Guo, and Y. X. Li. 2005. Evaluation of air dispersion models for livestock odour application. CSAE/SCGR 2005 Meeting, Winnipeg, Manitoba, Paper No. 05-026.

Zhu, J. 1999. The influence of stability class on downwind odour concentration predicted by air dispersion models. J. ENVIRON. SCI. HEALTH. A34(10):1919-1931.

Zhu, J., L. Jacobson, D. Schmidt, and R. Nicolai. 2000b. Daily variations in odour and gas emissions from animal facilities. Transactions of the ASAE 16(2):153-58.

Zhu, J., L.D. Jacobson, D. R. Schmidt, and R. Nicolai. 2000a. Evaluation of INPUFF-2 model for predicting downwind odours from animal production facilities. Applied Engineering in Agriculture 16(2): 159-164.

APPENDIX A: STACK-TIP DOWNWASH AND PLUME RISE

The calculation of stack-tip downwash and plume rise is followed the methods of ISC model. (Bowers et al. 1979)

Stack-tip downwash

When the exit velocity of emitting gas (v_s) is less than 1.5 times of the mean wind speed (u), the stack-tip downwash should be considered. The physical stack hight (h_s) should be modified to h_s', by the following equation:

$$h_s' = h_s + 2d_s\left[\frac{v_s}{u_s} - 1.5\right] \qquad \text{for } v_s < 1.5\ u \qquad \text{(A.1a)}$$

Or

$$h_s' = h_s \qquad \text{for } v_s \geq 1.5\ u \qquad \text{(A.1b)}$$

where h_s is physical stack height, m; and d_s is inside stack top diameter, m.

Plume rise

The plume rise is likely to depend on the following variables: the initial momentum flux parameter (F_m), the initial buoyancy flux parameter (F_b) and the static stability parameter (s).

$$F_m = v_s^2 d_s^2 \frac{T_a}{4T_s} \qquad \text{(A.2)}$$

$$F_b = g v_s d_s^2 \frac{\Delta T}{4T_s} \qquad \text{(A.3)}$$

Where, $\Delta T = T_s - T_a$, T_s is stack gas temperature, K; and T_a is ambient air temperature, K.

$$s = g\frac{\partial\theta/\partial z}{T_a} \qquad \text{(A.4)}$$

The calculation of plume rise will be performed in two atmospheric conditions: unstable or neutral (A, B, C and D) and stable (E, F). For both conditions, it is important to determine that whether momentum or buoyancy dominate the plume rise. The most widely used model to calculate plume rise is Briggs model. In this model, the crossover temperature difference ($(\Delta T)_c$) is used as the parameter to determine whether the plume is dominated by momentum or buoyancy. If the difference between stack gas and ambient temperature (exceeds or equal to $(\Delta T)c$, plume rise is assumed to be buoyancy dominated, otherwise plume rise is assumed to be momentum dominated.

1) Unstable or neutral conditions

The crossover temperature difference is determined by:

For Fb< 55, $$\left(\Delta T\right)_c = 0.0297 T_s \frac{V_s^{1/3}}{d_s^{2/3}} \quad \text{(A.5)}$$

and, for Fb ≥ 55, $$\left(\Delta T\right)_c = 0.00575 T_s \frac{V_s^{2/3}}{d_s^{1/3}} \quad \text{(A.6)}$$

The final rise of the plume for Buoyancy rise is:

$\Delta h = 21.425 * F_b^{3/4} / u_s$, for Fb< 55, (A.7)

and,

$\Delta h = 38.71 * F_b^{3/5} / u_s$, for Fb ≥ 55. (A.8)

For momentum rise, it is:

$$\Delta h = 3 d_s \frac{v_s}{u_s} . \quad \text{(A.9)}$$

2) Stable conditions

The crossover temperature is calculated by:

$$\left(\Delta T\right)_c = 0.019582 T_s v_s \sqrt{s} \quad \text{(A.10)}$$

The final rise of the plume for buoyancy rise can be estimated as:

$$\Delta h = 2.6\left(\frac{F_b}{u_s s}\right)^{1/3} . \qquad \text{(A.11)}$$

For momentum rise, it is

$$\Delta h = 1.5\left(\frac{F_m}{u_s \sqrt{s}}\right)^{1/3} . \qquad \text{(A.12)}$$

3) Distance Less Than Distance to Final Rise.

If the distance downwind from source to receptor, x, is less than the distance to final rise, x_f, the gradual rise is to be estimated for unstable, neutral, or stable conditions. The following equation will be used to calculate the plume rise for buoyancy dominated conditions:

$$\Delta h = 1.60\left(\frac{F_b^{\frac{1}{3}} x^{\frac{2}{3}}}{u_s}\right) \qquad \text{(A.13)}$$

If it exceeds the final rise for the appropriate condition, the final rise is substituted instead.

For momentum dominated conditions, the following equations (Bowers, et al, 1979) are used to calculate a distance dependent momentum plume rise:

a) Unstable conditions:

$$\Delta h = \left(\frac{3F_m x}{\beta_j^2 u_s^2}\right)^{1/3} \qquad \text{(A.14)}$$

where x is the downwind distance, m, with a maximum value defined by x_{max} as follows:

$$x_{max} = \frac{4d_s(v_s+3u_s)^2}{v_s u_s}, \qquad \text{for } F_b = 0 \qquad \text{(A.15a)}$$

$$x_{max} = 49 F_b^{5/8} , \qquad \text{for } 0 \le F_b \le 55 \qquad \text{(A.15b)}$$

$$x_{max} = 119 F_b^{2/5} \quad , \quad \text{for } F_b > 55 \tag{A.15c}$$

b) Stable conditions:

$$\Delta h = \left[3F_m \frac{\sin(x\sqrt{s}/u_s)}{\beta_j^2 u_s \sqrt{s}} \right]^{1/3} \tag{A.16}$$

where x is the downwind distance (meters), with a maximum value defined by x_{max} as follows:

$$x_{max} = 0.5 \frac{\pi u_s}{\sqrt{s}} \tag{A.17}$$

The jet entrainment coefficient, β_j, is given by,

$$\beta_j = \frac{1}{3} + \frac{u_s}{v_s} \tag{A.18}$$

The distance-dependent momentum rise is not allowed to exceed the final rise for the appropriate condition.

APPENDIX B: HOGSTRŎM DISPERSION COEFFICIENTS

Hogstrŏm (1968, 1972) developed a series of general formulas to carry out the calculation of both 1-hour (σ_y and σ_z) and short time (σ_{yp} and σ_{zp}) dispersion parameters from the experiments conducted in Sweden for elevated point continuous release. And a method is proposed for ground level release. These parameters are depended on the distance and the stability condition.

1. 1-hour mean vertical standard deviation σ_z

For neutral conditions,

$$\sigma_z = \frac{i_n}{a_0}\sqrt{\{2[\exp(-a_0 x) + a_0 x - 1]\}} \tag{B.1}$$

In which:

$$i_n = \left(4.31\log\frac{h}{z_0}\right)^{-1} \tag{B.2}$$

$$a_0 = \frac{i_n}{0.4hN_{pa}} \tag{B.3}$$

Here, h is the effective height, m, and z_o is the roughness length, m.

$N_{pa} = 0.5$, when $z_0 > 0.6$; (B.4a)

$N_{pa} = 1$, when $z_0 < 0.1$; (B.4b)

$N_{pa} = -z_0 + 1.1$, when $0.1 \leq z_0 \leq 0.6$. (B.4c)

For stable condition,

$$\sigma_z = \frac{\sigma_{zn}}{1 + as} \tag{B.5}$$

Where σ_{zn} is calculated from equation (B.1) and s is a stability parameter defined as:

$$s = \left(\frac{\partial \theta}{\partial z} \Big/ u_f^2 \right) \cdot 10^5 \tag{B.6}$$

$\frac{\partial \theta}{\partial z}$ is the vertical gradient of potential temperature at the level of the plume centre (k m^{-1}), u_f is the wind speed at the top of friction layer.

a depends on height above ground, h, and on the roughness length z_0:

$$a = (3.6 \cdot 10^{-4} / C_a^2) \cdot 1.675 \cdot 10^{-3} \cdot h^{0.62} \tag{B.7}$$

Where

$$C_a = \frac{0.104}{\log C_a + 2.18 - \log z_0} \tag{B.8}$$

For unstable conditions

$$\sigma_z = \frac{i_u}{b_0} \sqrt{\{2[\exp(-b_0 x) + b_0 x - 1]\}} \tag{B.9}$$

With $i_u = D - \frac{E}{h} (h \geq 50m)$ (B.10a)

$$i_u = D - \frac{E}{50} (h < 50m) \tag{B.10b}$$

in which D and E can be solved by putting h = 50m into $i_u = i_n + 0.03(1 - \frac{\bar{u}}{16})$ and substituting i_u in equation (B.10a), and further putting h = 500 m into $i_u = i_n + 0.03(1 - \frac{\bar{u}}{16})^3$ and substituting i_u in equation (B.10b).

and $b_0 = a_0 \left(\frac{\bar{u}}{16} \right)^{0.8}$, a_0 is defined by equation (B.3).

Hogstrŏm (1968) also proposed that equation (B.9) applies to well developed convection. In high latitudes such conditions occur only during the summer months. He raised a rough method to take account of the reduced convective activity during the other seasons by the introduction of the following formula:

$$\sigma_z = \sigma_{zn}(1-p) + \sigma_{zs}\,p \tag{B.11}$$

Where σ_{zn} is obtained from equation (B.1), σ_{zs} from equation (B.8) and p is a parameter that is equal to unity in summer (May, June, July and August), zero in December and January, 0.25 in February and November, 0.5 in March, October, and 0.75 in April and September.

2. 1-hour mean horizontal standard deviation σ_y

Without considering wind direction shear, the horizontal standard deviation can be written as:

$$\sigma_y = \frac{i_y}{c_0}\sqrt{2[\exp(-c_0 x) + c_0 x - 1]S} \tag{B.12}$$

Where $i_y = 0.122$, $c_0 = 10^{-3}$ and

S = 0.9934 when s≥0 and S = 1.4 when s < 0.

3. Hogstrŏm short time standard deviations

Hogstrŏm (1972) presented a series of formulas to account for short time dispersion parameters from a fairly extensive set of experiments covering a wide range of meteorological conditions. The sampling time was considered to be 30 s, which was equivalent to the time of release of the smoke-puffs in the experiments. The formulas were expressed in the same terms as are used in the 1-hour mean standard deviations with an additional notation “p”.

4. Short time vertical standard deviation σ_{zp}

For neutral and stable conditions

$$\sigma_{zp} = \frac{i_{np}}{a_{0p}} \sqrt{\left\{2\left[\exp(-a_{0p}x) + a_{0p}x - 1\right]\right\}} \cdot \frac{1}{1 + 2.2 \cdot 10^{-2} \cdot \left(\frac{h}{87}\right)^{0.62} \cdot s} \tag{B.13}$$

With $i_{np} = 0.36 i_n$ and $a_{0p} = 0.65 a_0$, in which in and a_0 has the same meaning as in the 1-hour mean vertical standard deviation calculation, and s = 0 in neutral condition.

For unstable conditions

$$\sigma_{zp} = \frac{i_{up}}{b_{0p}} \cdot \sqrt{2\left[\exp(-b_{0p}x) + b_{0p}x - 1\right]} \tag{B.14}$$

where:

$$i_{up} = 0.36 i_u \tag{B.15}$$

and

$$b_{0p} = 0.65 b_0 \tag{B.16}$$

i_u and b_0 have the same meaning as defined above. Equation (B.11) also applied here with σ_{zn} obtained from equation (B.13) with s = 0, σ_{zs} from equation (B.14).

5. Short time horizontal standard deviation σ_{yp}

For the horizontal standard deviation at short time, no variation with height and a rather weak variation with stability are suggested.

$$\sigma_{yp} = 50\sqrt{2\exp(-10^{-3}x + 10^{-3}x - 1)} \cdot \frac{1}{1 + 10^{-2}s} \tag{B.17}$$

with s=0 for neutral and unstable conditions.

6. Hogstrŏm vertical standard deviation for ground level release σ_{gz}

Hogstrŏm (1964) proposed a method to account for the vertical standard deviation for ground level release.

$$\begin{cases} \sigma_{gz}(x) = \sigma_z(h) \\ 0.7\sigma_z(h) = h \end{cases} \tag{B.18}$$

In which $\sigma_z(h)$ is determined from the formulas used for the elevated point source either for the hourly or short time plume.

APPENDIX C: SOLAR ELEVATION ANGLE

φ is the solar elevation angle, which can be estimated by the following procedure:

First, the fractional year (γ) is calculated, in radians:

$$\gamma = \frac{2\pi}{365} * \left(\text{Julianday} - 1 + \frac{\text{hour}-12}{24}\right) \quad \text{(C.1)}$$

The equation of time can be estimated, in minutes:

$$\text{eqtime} = 229.18 * (0.000075 + 0.001868\cos\gamma - 0.032077\sin\gamma - 0.014615\cos 2\gamma - 0.040849\sin 2\gamma \quad \text{(C.2)}$$

And the solar declination angle, in radians:

$$\text{decl} = 0.006918 - 0.399912\cos\gamma + 0.070257\sin\gamma - 0.006758\cos 2\gamma + 0.000907\sin 2\gamma - 0.002697\cos 3\gamma + 0.00148\sin 3\gamma \quad \text{(C.3)}$$

Then the time offset is found in minutes:

$$\text{time\_offset} = \text{eqtime} - 4 * \text{longitude} + 60 * \text{timezone} \quad \text{(C.4)}$$

Where, longitude is in degree and time zone is in hour from UTC.

The true solar time in minutes can be estimated:

$$\text{tst} = \text{hr} * 60 + \text{mn} + \frac{\text{sc}}{60} + \text{time\_offset} \quad \text{(C.5)}$$

Where, hr is the hour (0-23), mn is the minute (0-60), sc is the second (0-60).

The solar hour angle, in degrees, is;

$$\text{ha} = \left(\frac{\text{tst}}{4}\right) - 180 \quad \text{(C.6)}$$

The solar elevation angle (φ) can then be calculated from the following equation:

$$\sin\varphi = \sin(\text{lat})\sin(\text{decl}) + \cos(\text{lat})\cos(\text{decl})\cos(\text{ha}) \quad \text{(C.7)}$$

In which, lat is the latitude of the source.

(Available online: http://www.srrb.noaa.gov/highlights/sunrise/solareqns.PDF)